



Utilisation of Deep Eutectic Solvents for Post-Combustion Carbon Capture Processes

Mohaned Aboshatta

**A thesis submitted to the Chemical and Process Engineering
Department at the**

University of Strathclyde

in accordance with the requirements for the degree of

Doctor of Philosophy

September, 2024

Declaration of Authenticity and Author's Rights

'This thesis is the result of the author's original research. It has been composed by the author and has not been previously submitted for examination, which has led to the award of a degree.'

'The copyright of this thesis belongs to the author under the terms of the United Kingdom Copyright Acts as qualified by University of Strathclyde Regulation 3.50. Due acknowledgement must always be made of the use of any material contained in, or derived from, this thesis.'

Signed:.....M.ABOSHATTA.....

Date:.....01/09/2024.....

Acknowledgements

I would like to express my profound appreciation to my PhD supervisor, Dr Vitor Magueijo. The person who four years ago agreed to take responsibility for my personal and scientific growth and that every day is supporting, directing and co-existing with my passion. I am grateful for his patience, compassion, and dedication. He has always had a thoughtful and efficient way of clarifying difficult concepts and delivering valuable and effective feedback.

I would like to express my gratitude to the administrative staff in the department of chemical and process engineering. The laboratory technicians were very supportive as well, special thanks to Michael W., Chris J., Ian A., and Cameron G. They were always there for me, helping out during my inter-departmental laboratory experiments, and I appreciate them for this. I also would like to acknowledge all my PhD colleagues, for their support, sharing experiences, and guidance during the process.

Also, I would not apprehend to recognise the words of inspiration from my beloved parents, siblings, aunts, uncles, and friends, who in one way or another, were always present, even at a distance. They have been very supportive and always reassured me that all will end in glory despite my research challenges. I would like to express my gratitude to my closest friends, M. Salim, A. Ibrahim, I. Musa, A. Ibrahim, G. Hussien, M. Juili, M. Ameen, I. Kilani, Naseeruddin, I. Awad, M. Baseery, M. Jelili, Imad, Jihad, Mujahid, Musab, Osama, Migdad, Shoan D., Tom C., Christine T., J. Edet., P. Eweka, S. Ottobini, C. Martin, L. Gallager, L. Messi, M. Hota, M. Mathers and many others for their ultimate support, they constantly had the accurate words to inspire me in the process.

Finally, and not less important, I would like to express my gratitude to my wife Remaz, for her tremendous inspiration, patience, and mostly for making me happy and motivated all the time.

Abstract

The rising carbon dioxide (CO₂) emissions across the globe, and the resulting negative impact on the environment, have become the focus of a multitude of scientific studies in recent times. Despite the recent technological advancements in the scientific area of carbon capture, reducing and managing CO₂ emissions has persisted as a huge challenge to researchers working in this area of research. Conventional carbon capture typically uses amine absorption methods/processes, and while the latest technologies indicate an enhancement of conventional CO₂ absorption methods, there is a necessity to investigate options to replace the currently used sorbents with more benign alternatives.

This work investigates the viability of using deep eutectic solvents (DESs) from a specific DES system, as novel absorbents for carbon capture absorption processes. The study was divided into two parts, firstly, mixtures/DESs composed of choline chloride (ChCl) and levulinic acid (LvAc) were prepared at different compositions and fully characterised. Secondly, the performance of the prepared compositions in terms of CO₂ absorption and desorption, was assessed at different operational conditions.

To ensure the suitability of these sorbents for carbon capture processes, the prepared DESs were extensively characterised to identify their nature. ChCl:LvAc DESs were described in terms of their physicochemical properties, including their density, viscosity, thermal stability, and chemical fingerprint (FTIR spectra). These properties have been compared to those of other DESs that have been described in literature.

It was essential to identify the nature of ChCl:LvAc mixtures before jumping to the application domain. For the first time in the literature, the phase behaviour plot (solid-liquid equilibrium) of binary mixtures of choline chloride and levulinic acid was developed and described. According to the phase behaviour plot, ChCl:LvAc mixtures can only be defined as DESs when the mole percentage of levulinic acid (HBD) is equal or higher than 66.7%.

ChCl:LvAc DESs were found to be highly thermally stable at temperatures up to 196 °C. The density and viscosity of the characterised DESs decrease with increasing temperature. These figures make ChCl:LvAc DESs suitable for many engineering applications including carbon capture processes.

The corrosivity of the prepared ChCl:LvAc DESs was found to be lower by 92% as compared to the corrosivity of monoethanolamine under the same conditions. The corrosivity of ChCl:LvAc DESs increases with the concentration of levulinic acid, stirring speed, and CO₂ concentration, simultaneously, and decreases with increasing the water content in the system.

The CO₂ absorption capacity of ChCl:LvAc DESs was measured at different conditions using a vapour–liquid equilibrium rig. The experimental results showed that the CO₂ absorption capacity of the ChCl:LvAc DESs is strongly affected by the operating pressure and stirring speed, moderately affected by the temperature, and minimally affected by the Hydrogen bond donor (HBD): Hydrogen bond acceptor (HBA) molar ratio as well as water content.

A maximum CO₂ absorption capacity of 1.58 moles of CO₂ per kg of DES (1.58 mol kg⁻¹) was measured at 25 °C, 6 bar and stirring speed of 250 rpm for a DES with HBA:HBD molar ratio of 1:3 and a water/HBA molar ratio (water content) of 2.5. The regeneration of the DESs was performed at different temperatures, and an optimal regeneration temperature of 60 °C was obtained. All DESs exhibited good recyclability and moderate CO₂/N₂ selectivity, with a maximum selectivity value of 5.63 obtained for a mixture of gases containing 50% CO₂ and 50% N₂.

Dedication

I would like to dedicate this work to the innocent souls of the Sudanese people who lost their lives since the spark of the non-violent, pro-democratic movement for only seeking freedom, peace and justice for their country. This work is also dedicated to the souls of people who lost their lives since the outbreak of the COVID-19 global pandemic crisis.

Table of Contents

1. Chapter 1: Introduction.....	22
1.1 Preface.....	22
1.2 CO ₂ characteristics	22
1.3 CO ₂ as a principal greenhouse gas	23
1.4 Energy supply and CO ₂ emission sources	24
1.5 CO ₂ capture systems.....	28
1.5.1 Pre-combustion capture systems.....	29
1.5.2 Oxy-fuel combustion before CO ₂ capture.....	30
1.5.3 Post-combustion capture processes	32
1.5.4 Direct air capture	33
1.6 CO ₂ capture methods based on PCC strategies	34
1.6.1 CO ₂ post-combustion capture by adsorption.....	34
Activated Carbon.....	36
Zeolites	37
Amine functionalised Metal-Organic Frameworks (MOFs).....	38
Comparing the Efficiency of Adsorbents for Carbon Capture.....	39
1.6.2 Cryogenic separation.....	39
1.6.3 Membrane processes for CO ₂ capture.....	41
1.6.4 Microbial CO ₂ post-combustion capture.....	43
1.6.5 CO ₂ post-combustion capture by absorption.....	44
CO ₂ absorption capture via amines	45
CO ₂ absorption capture via potassium carbonate	50

Selexol process.....	51
Novel absorbents: Ionic Liquids.....	52
Novel sorbents: deep eutectic solvents	53
Choline chloride	55
Levulinic Acid	55
1.7 Conclusion	55
1.8 Thesis Aims and Structure	57
2. Chapter 2: Utilization of Deep Eutectic Solvents in Carbon Capture: State of the Art Review	60
2.1 Overview	60
2.2 Summary.....	60
2.3 Introduction	61
2.4 Classification and preparation DESs	63
2.4.1 Classification of DESs.....	63
2.4.2 Preparation of type III DESs	64
2.5 Environmental profile and corrosivity of DESs	65
2.5.1 Toxicity of DES systems	65
2.5.2 Biodegradability of DESs	66
2.5.3 Corrosivity of DESs systems	67
2.5.3.1 The electrochemical method	67
2.5.3.2 Weight loss method	68
2.6 Thermodynamics and properties of DESs	70
2.6.1 Phase behaviour (definition of type III DES)	70
2.6.2 Viscosity and Density.....	72

2.6.3 Thermal stability.....	75
2.6.4 Refractive Index.....	76
2.6.5 Contact Angle.....	77
2.7 CO ₂ absorption and desorption measurements for DESs.....	78
2.7.1 Weight-gain method.....	78
2.7.2 High-pressure cell method.....	79
2.7.3 Measurements using a vapour-liquid equilibrium absorption rig.....	79
2.7.4 Sorbent regeneration.....	81
2.7.5 Sorbent selectivity.....	82
2.8 Review of CO ₂ absorption and desorption using DESs.....	83
2.8.1 Thermodynamic properties of CO ₂ absorption using DESs.....	86
2.8.2 The compositional and operating parameters that affect CO ₂ solubility in DESs.....	88
2.8.2.1 HBD to HBA Molar Ratio.....	88
2.8.2.2 Operating Pressure.....	88
2.8.2.3 Operating Temperature.....	89
2.8.2.4 Water Content.....	89
2.9 Conclusion.....	91
3. Chapter 3: Characterisation of Choline Chloride:Levulinic Acid-Based Deep Eutectic Solvents.....	93
3.1 Overview.....	93
3.2 Summary.....	93
3.3 Introduction.....	94
3.2 Experimental Methodology.....	96

3.2.1	Materials.....	96
3.2.2	Preparation method	96
3.2.3	Construction of the phase diagram for the choline chloride: levulinic acid binary system	97
3.2.4	FTIR measurements of the DES.....	99
3.2.5	Density measurements	100
3.2.6	Viscosity measurements.....	100
3.2.7	Thermal stability	101
3.2.8	Corrosivity measurements	101
	Corrosion measurements procedure and method using the weight-loss method according to the standard practice for laboratory immersion corrosion testing of metals ²²¹	104
3.2.8.1	Apparatus	104
3.2.8.2	Test specimen.....	105
3.2.8.3	Specimen support.....	106
3.2.8.4	Control specimen	106
3.2.8.5	Duration of test.....	106
3.2.8.6	Cleaning coupons after the test.....	107
3.2.8.7	Calculating Corrosion Rates.....	107
3.3	Results and discussion	108
3.3.1	Preparation of ChCl:LvAc DESs compositions.....	108
3.3.2	Choline chloride: levulinic acid binary phase diagram	110
3.3.3	Phase behaviour plot of ChCl:LvAc mixtures	111
3.3.4	FTIR measurements of ChCl:LvAc DESs	113
3.3.5	The effect of water on FTIR transmittance of ChCl:LvAc DESs	114

3.3.6	Density measurements	116
3.3.7	Viscosity measurements.....	118
3.3.7.1	Effect of water content, HBD and temperature on viscosity	118
3.3.7.2	The effect of CO ₂ on viscosity	121
3.3.7.3	Steady shear flow behaviour	122
3.3.8	TGA measurements of ChCl: LvAc DESs	123
3.3.9	The corrosivity of ChCl:LvAc DESs.....	125
3.3.9.1	Calculation of the corrosion penetration rate (CPR)	127
3.4	Conclusion.....	130
4.	Chapter 4: Experimental study of CO ₂ absorption and desorption by choline chloride levulinic acid-based deep eutectic solvents	133
4.1	Overview	133
4.2	Summary	133
4.3	Introduction.....	134
4.4	Materials and methods	137
4.4.1	Preparation of the DESs	137
4.4.2	CO ₂ absorption measurements	137
4.4.3	Thermodynamics analysis of CO ₂ absorption.....	140
4.4.4	Sorbent regeneration measurements.....	141
4.4.5	FTIR spectra measurements.....	141
4.4.6	Recyclability of the DESs	142
4.4.7	Selectivity of the DESs towards CO ₂	142
4.5	Results and discussion	144
4.5.1	CO ₂ absorption.....	144

4.5.2 Thermodynamics analysis of CO ₂ absorption.....	146
4.5.3 The effect of stirring speed on the CO ₂ absorption capacity of the DESs	148
4.5.4 Statistical analysis of CO ₂ absorption results.....	151
4.5.5 The effect of water content on the CO ₂ absorption by DESs	157
4.5.6 CO ₂ desorption results	159
4.5.7 Total CO ₂ released	163
4.5.8 The recyclability of the DESs	164
4.5.9 The selectivity of the DESs towards CO ₂	167
4.6 Conclusion.....	170
5. Chapter 5 : Conclusions.....	172
5.1 Overview	172
5.2 Overall conclusions	173
5.3 Research limitations	178
6. Chapter 6: Future Work.....	181
6.1 Overview	181
7. Appendix A.....	186
8. Appendix B.....	188

Table of Figures

Figure 1-1 Total energy supply (TES) between the years1990-2020 by source ¹⁵	25
Figure 1-2 CO ₂ Concentration at Muana Loa Observatory ²	25
Figure 1-3 CO ₂ emissions by sector ¹⁵	27
Figure 1-4 CO ₂ emissions by fuel type ¹⁷	27
Figure 1-5 CO ₂ pathways (taken from ²²)	29
Figure 1-6 Types of CO ₂ capture systems	29
Figure 1-7 Schematic diagram of the pre-combustion capture with IGCC (adapted from ³³)	30
Figure 1-8 Solar integrated chemical looping oxyfuel combustion system proposed by Hong <i>et al.</i> ³⁷	32
Figure 1-9 PCC processes/technologies	34
Figure 1-10 Schematic diagram of CO ₂ cryogenic separation unit (adapted from ⁵⁹)	40
Figure 1-11 Schematic diagram of membrane separation for CO ₂ from flue gas (adapted from ⁶⁵)	42
Figure 1-12 A typical layout of CO ₂ post-combustion capture via amines (adapted from ⁸⁵)	46
Figure 2-1 Number of publications containing “deep eutectic solvents for carbon capture” generated from Science direct database February 2023 ³ ..	61
Figure 2-2 Types of deep eutectic solvents (DESS)	63

Figure 2-3 The most important milestones of the development of deep eutectic solvents ^{5, 7, 8, 9, 10}	64
Figure 2-4 Schematic representation of the formation of the DES [choline chloride:urea] with HBA:HBD molar ratio 1:2. Figure modified from reference ¹²	64
Figure 2-5 Most common hydrogen bond acceptors and hydrogen bond donors used to prepare deep eutectic solvents (adapted from Achkar . ⁶)	65
Figure 2-6 Generic phase behaviour plot for a DES system	71
Figure 2-7 The contact angle between DESs and selected metals	78
Figure 2-8 VLE rig components (adapted from Mirza . ⁴⁵)	81
Figure 3-1 Generic binary phase diagram for DES formation	97
Figure 3-2 ChCl:LvAc DESs prepared at HBA:HBD molar ratios of (1:2) (left) and (1:3) (right)	109
Figure 3-3 Unsuccessful preparation of ChCl:LvAc DESs at the HBA:HBD molar ratio of (1:1)	109
Figure 3-4 DSC plots showing the glass transition temperature of ChCl: LvAc mixtures	110
Figure 3-5 Phase behaviour plot of ChCl:LvAc binary mixtures	112
Figure 3-6 FTIR spectra of ChCl:LvAc DESs (1:2:0 and 1:3:0) at 25 °C	114
Figure 3-7 FTIR spectra of ChCl:LvAc DESs (1:2) with different water contents at 25 °C	115
Figure 3-8 FTIR spectra of ChCl:LvAc DESs (1:3) with different water contents at 25 °C	116

Figure 3-9 Density of ChCl:LvAc DESs (1:2) as a function of temperature .	117
Figure 3-10 Density of ChCl:LvAc DES systems as a function of temperature, water content and HBA:HBD molar ratio 1:2 (left) and 1:3 (right)	117
Figure 3-11 Viscosity of ChCl: LvAc DESs as a function of water content and temperature. Measurements carried out at a constant shear rate of 100 s ⁻¹	119
Figure 3-12 Viscosity of ChCl: LvAc DESs as a function of water content and temperature. Measurements carried out at a constant shear rate of 100 s ⁻¹	120
Figure 3-13 Steady shear flow curves of ChCl:LvAc DESs at 25 °C with Newtonian and non-Newtonian regions.....	123
Figure 3-14 Thermal gravimetric analysis of ChCl:LvAc DESs with HBA:HBD molar ratio (1:2) (left) and (1:3) (right).....	124
Figure 3-15 Thermal gravimetric analysis of ChCl:LvAc DESs and pure individual components	124
Figure 3-16 (A) Weight-loss of control specimen Vs. weight-loss of experimented specimen	126
Figure 3-17 (B) Weight-loss of control specimen Vs. weight-loss of experimented specimen	126
Figure 3-18 CPR values of ChCl:LvAc DESs and MEA on coupons at 25 °C at stagnant conditions	129
Figure 3-19 Average CPR values of ChCl:LvAc DESs on coupons at stagnant conditions Vs. stirring conditions of 100 rpm and in the presence of CO ₂ at. All measurements carried out at 25 °C.....	129

Figure 4-1 Schematic diagram of the VLE absorption rig to measure CO ₂ absorption by DES systems. Adopted with modification from ²⁵	140
Figure 4-2 CO ₂ absorption capacity of ChCl:LvAc DESs with different compositions at temperatures ranging from 25 °C to 45 °C at a stirring speed of 250 rpm: A – 1:2:0; B – 1:2:2.5; C – 1:2:5; D – 1:3:0; E – 1:3:2.5; F – 1:3:5.	146
Figure 4-3 The CO ₂ absorption capacity of ChCl: LvAc Vs. MEA 30% wt. at 25 °C	146
Figure 4-4 Arrhenius plot of Henry's law constant for the absorption of CO ₂ in ChCl:LvAc (1:3:5)	148
Figure 4-5 CO ₂ absorption capacity of ChCl: LvAc (1:2:0) at 0 ,50, 100 & 250 rpm at 25 °C	149
Figure 4-6 CO ₂ absorption capacity of ChCl:LvAc DESs compositions at stagnant conditions	151
Figure 4-7 Residual plots for response	153
Figure 4-8 Main effects plot for CO ₂ absorption in ChCl:LvAc DESs	154
Figure 4-9 The second-order interactions plots.....	156
Figure 4-10 Optimization of controlled parameters.....	157
Figure 4-11 Water content (mole %) in different ChCl:LvAc DES compositions	158
Figure 4-12 The effect of water content on the CO ₂ absorption capacity of ChCl: LvAc DESs (1:2) (left) and (1:3) (right) at 6 bar and different temperatures	159

Figure 4-13 Weight gained by ChCl:LvAc (1:3:0) after CO₂ absorption at 25 °C, 35 °C and 45 °C and lost by CO₂ released spontaneously after depressurisation 160

Figure 4-14 The FTIR spectra of ChCl:LvAc (1:3:0) before and after CO₂ absorption at 25 °C and CO₂ desorption at different temperatures..... 161

Figure 4-15 Regeneration of ChCl:LvAc (1:3:0) after CO₂ absorption at 25 °C. A) Reduction in FTIR transmittance peak associated with the double carbonyl group with increasing regeneration temperature; B) residual CO₂ after depressurisation, CO₂ released by heat treatment and weight loss after regeneration at different temperatures..... 162

Figure 4-16 Regeneration of ChCl:LvAc (1:3:0) after CO₂ absorption at 35 °C. A) Reduction in FTIR transmittance peak associated with the double carbonyl group with increasing regeneration temperature; B) residual CO₂ after depressurisation, CO₂ released by heat treatment and weight loss after regeneration at different temperatures..... 163

Figure 4-17 Regeneration of ChCl:LvAc (1:3:0) after CO₂ absorption at 45 °C. A) Reduction in FTIR transmittance peak associated with the double carbonyl group with increasing regeneration temperature; B) residual CO₂ after depressurisation, CO₂ released by heat treatment and weight loss after regeneration at different temperatures. 163

Figure 4-18 The total CO₂ released from ChCl:LvAc (1:3:0) samples absorbed CO₂ at 25 °C, 35 °C & 45 °C and released CO₂ at 60 °C, 80 °C & 100 °C.. 164

Figure 4-19 Variation of the CO₂ absorption capacity of ChCl:LvAc (1:2:0) over five consecutive absorption/desorption cycles: values measured at 25 °C and 250 rpm..... 165

Figure 4-20 Weight gained through CO ₂ absorption for 5 cycles at 25 °C and CO ₂ released spontaneously after depressurisation. Experiments carried out with ChCl:LvAc (1:2:0) at 25 °C and 250 rpm.....	166
Figure 4-21 Absorption capacity of ChCl:LvAc (1:3:2.5) for different gas mixtures of CO ₂ and N ₂ . Experiments carried out at 25 °C and 250 rpm.....	167
Figure 4-22 Weight gained by ChCl:LvAc (1:3:2.5) after gas absorption at 25 °C and 250 rpm, and lost by the spontaneous release of gas after depressurisation	169
Figure 4-23 CO ₂ selectivity based on the absorption of pure gases by ChCl:LvAc (1:3:2.5) at 25 °C and 250 rpm.....	169
Figure 6-1 Ternary Phase Diagram of ChCl:LvAc:Water.....	184

List of Tables

Table 1-1 A comparison between commercial adsorbents.....	39
Table 1-2 Comparison of absorption-based CO ₂ capture using various sorbents	56
Table 2-1 Key properties of sorbents (adopted from Martinez <i>et al.</i> ⁴).....	62
Table 2-2 Corrosion rates of some selected DESs.....	68
Table 2-3 Density of choline chloride-based DESs as a function of temperature and water	72
Table 2-4 Viscosity of choline chloride-based DESs as a function of temperature and water	73
Table 3-1 Materials used in the characterisation work.....	96
Table 3-2 Experimental design of the viscosity measurements under different compositional conditions	100
Table 3-3 DESs used in corrosion tests, test methods, metals used, standard protocols and specimen areas from the literature	103
Table 3-4 Factorial design of corrosivity tests	104
Table 3-5 Chemical composition of mild steel specimen ²⁶	105
Table 3-6 Clarke solution formula, cleaning duration, the temperature of the test according to the ASTM G1.03 - C.3.5 ²⁷	107
Table 3-7 The water content of ChCl:LvAc DESs compositions	110
Table 3-8 Melting the glass transition temperatures of ChCl:LvAc mixtures	111

Table 3-9 Temperature depression of the DES compositions from ideality.	113
Table 3-10 FTIR peaks for ChCl:LvAc DESs and its pure components.....	113
Table 3-11 The calculated values of the activation energy and the pre-exponential constant	121
Figure 3-12 Viscosity of ChCl: LvAc DESs as a function of temperature and in the absence or presence of residual CO ₂ . Measurements carried out at constant shear rate of 100 S ⁻¹	122
Table 3-13 Thermal Stability of DESs at a heating rate of 5 °C ·min ⁻¹ , P = 0.1 MPa	125
Table 4-1 Partial pressures of CO ₂ and N ₂ and the total pressure applied in the selectivity tests.....	143
Table 4-2 Calculated values of Henry's law constant, changes in enthalpy, entropy and Gibbs free energy of CO ₂ -DESs at 1 bar.	147
Table 4-3 Factorial design factors, levels and values	152
Table 4-4 The selectivity of some adsorbents at 100 kPa and 25 °C.....	170
Table B-8-1 Calculated correction factors at 318.15 K	194
Table 8-2 Factors and levels of the factorial design at different temperatures	196
Table 8-3 The effect of stirring speed on CO ₂ absorption capacity of ChCl:LvAc (1:2:0) at 298.15 K.....	199
Table 8-4 Analysis of variance	202
Table B-8-5 Factorial design array	205

List of Equations

Equation 1-1 Carbamate formation via the Zwitterion mechanism (modified from ⁸⁶)	47
Equation (3-1)	98
Equation (3-2)	98
Equation (3-3)	99
Equation (3-4)	99
Equation (3-5)	106
Equation (3-6)	107
Equation (3-7)	108
Equation (3-8)	120
Equation (4-1)	139
Equation (4-2)	139
Equation 4-3	141
Equation 4-4	143
Equation 4-5	143
Equation (4-6)	152
Equation (8-1) HLC	199
Equation (8-2) VLE.....	200

Equation (8-3) HLC based on mass fraction.....	200
Equation (B-8-4) HLCx	200
Equation (B-8-5) Changes in Gibbs free energy	201
Equation (8-6) Changes in Enthalpy	201
Equation (B-8-7) Changes in Entropy	201
Equation B-8 Refined model equation	204

Chapter 1: Introduction

1.1 Preface

According to the Intergovernmental Panel on Climate Change (IPCC), the global average temperature has now increased between 0.2 and 1.0 °C above pre-industrial levels ¹. This increase is linked to the dramatic rise in the concentration of carbon dioxide (CO₂) in the atmosphere over the last 60 years, reaching a value of approximately 424.23 ppm in June 2024 ². Therefore, a substantial reduction in the anthropogenic emissions of greenhouse gases (GHG), and in particular carbon dioxide, is compulsory to stop the increase of the global average temperature. Fossil fuels are the world's principal energy sources (about 83% of global energy production), and burning them is responsible for releasing up to approximately 35 billion tons of CO₂ annually. As a result, there is an imperative necessity to reduce CO₂ emissions by developing energy-efficient alternatives with less CO₂ emissions such as renewables energy.

Given the current trend of the CO₂ emissions associated with utilising fossil fuels, the natural sinking for carbon capture such as forestation has a significant role in reducing CO₂ levels in the atmosphere, while carbon capture and storage (CCS) pathways provide a promising mitigation measure to reduce the levels of CO₂ emissions from industrial applications.

1.2 CO₂ characteristics

Carbon dioxide was discovered by Joseph Black, a Scottish physicist (1728–1799) and was identified as colourless, odourless, acidic and non-flammable gas³. In nature, CO₂ can exist in various forms of matter as extensively reported in literature ^{4,5}.

The triple point temperature and pressure of CO₂ are 216.6 K and 0.52 MPa respectively. CO₂ in the solid state is known as (dry ice) which has a wide range of cooling applications such as the Pfizer supporting softbox which is used for distributing COVID-19 vaccines ⁶. At moderate temperatures and pressures (temperatures above 304.25 K and pressures above 7.38 MPa) CO₂ exists in a form of a supercritical liquid and can be used as a solvent in supercritical fluid extraction, a unit operation involved in the production of cosmetics, food and pharmaceuticals ^{7,4}

1.3 CO₂ as a principal greenhouse gas

The greenhouse effect is a natural mechanism by which the Earth adjusts its temperature. However, after the industrial revolution, the atmospheric radiation balance has been adversely affected due to uncontrolled human activities and the excessive emissions of GHGs ⁸. CO₂ is a principal GHG responsible for 50-60% of global warming while methane contributes with 16% to these figures followed by nitrous oxide with 6% ⁹.

The CO₂ molecule is non-polar due to its linear symmetry, this symmetry makes the CO₂ molecule interacts with the infrared radiation ¹⁰. Therefore, CO₂ has the highest effective radiative force (ERF) among the greenhouse gases (GHGs) ¹⁰. The ERF concept has been used by IPCC to evaluate, assess and compare the strength of different GHGs. The ERF is mainly composed: a) positive forcings caused by GHGs such as CO₂ (1.85 W.m⁻²), CH₄ (0.71 W.m⁻²), and halocarbons (0.30 W.m⁻²) and b) negative forcing due to the total aerosols (- 1.22 W.m⁻²). The positive figures of the ERFs of the GHGs trap emitted radiation and affect the radiation balance of the earth and lead to global warming ¹¹. While the negative ERFs figures due to aerosol-reduce

the amount of sunlight reaching the Earth's surface, leading to a cooling effect however, it does not fully offset the positive ERFs caused by GHGs such as CO₂.

In 1896, Svante Arrhenius, a Swedish chemist, suggested a strong connection between global warming and CO₂ emissions for the first time in the literature ¹². His conclusion at that time was based on assuming that, the average surface temperature of the Earth is ≥ 15 °C, because of the infrared radiation absorption by CO₂ and water vapours, which might increase in proportion with the concentration of these gases in the atmosphere ¹². His views faced many denunciations from the scientific community at the time as some other scientists suggested that ocean circulation and solar activity as another natural phenomenon may have the ability to neutralize the pollution caused by CO₂ emissions ¹². In 1931, Hulburt in his paper titled "*The temperature of the lower atmosphere of the Earth*" ¹³, experimentally proved the impact of CO₂ on global warming using radiative equilibrium calculations. Hulburt concluded that doubling the concentration of CO₂ in the atmosphere rises the average temperature of the sea by 4 °C, thus proving Arrhenius's theory ¹³.

The prominence of CO₂ as a principal greenhouse gas discussed in this section underscores the critical link to its sources, particularly in energy supply and other sectors (section 1.4), where CO₂ emissions have a significant impact on global warming as demonstrated in the following section.

1.4 Energy supply and CO₂ emission sources

The total energy supply (TES) is the energy supplied by different fuel sources in their principal form before any conversion such as oil to electricity ¹⁴. The global energy demand has been increasing since the last century except in the year 2020 when the

overall energy demand decreased by 4.5% as a result of the lockdown caused by the outbreak of the COVID-19 pandemic ¹⁴ as per Figure 1-1.

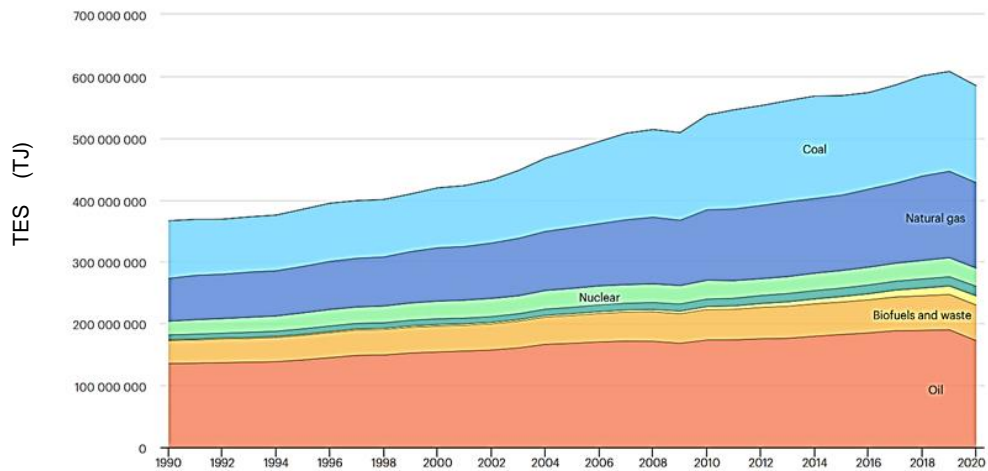


Figure 1-1 Total energy supply (TES) between the years 1990-2020 by source ¹⁵

Considering the fact that, the global average temperature has now increased up to 1.0 °C above pre-industrial levels. This increase is linked with the dramatic rise of the concentration of carbon dioxide in the atmosphere over the last 60 years, reaching a value of approximately 424.23 ppm in June 2024 as can be seen in Figure 1-2 ². Therefore, a substantial reduction in the anthropogenic emissions of carbon dioxide is compulsory to stop the increase in the global average temperature.

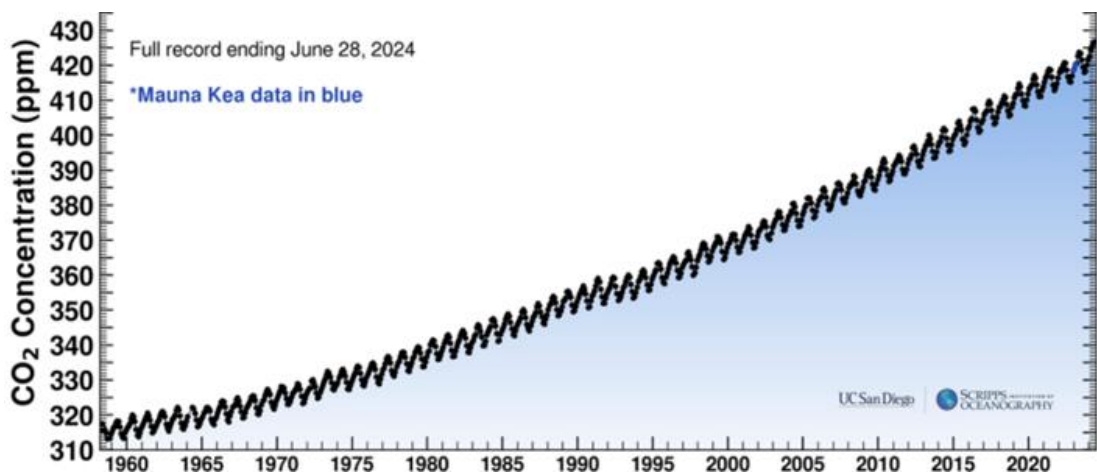


Figure 1-2 CO₂ Concentration at Muana Loa Observatory ²

The energy production sector is responsible for more than 80 % of the CO₂ emissions as of 2020 ^{14, 16}. The contribution of each fuel type and energy sector to CO₂ emissions has been changing significantly since the last century as shown in Figure 1-3 and Figure 1-4.

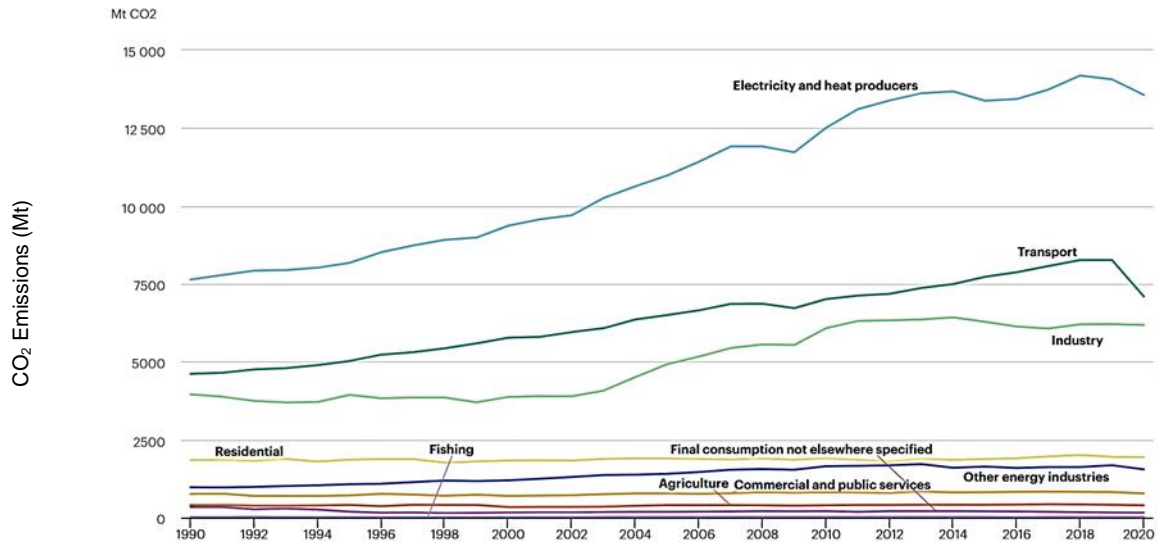


Figure 1-3 CO₂ emissions by sector ¹⁵

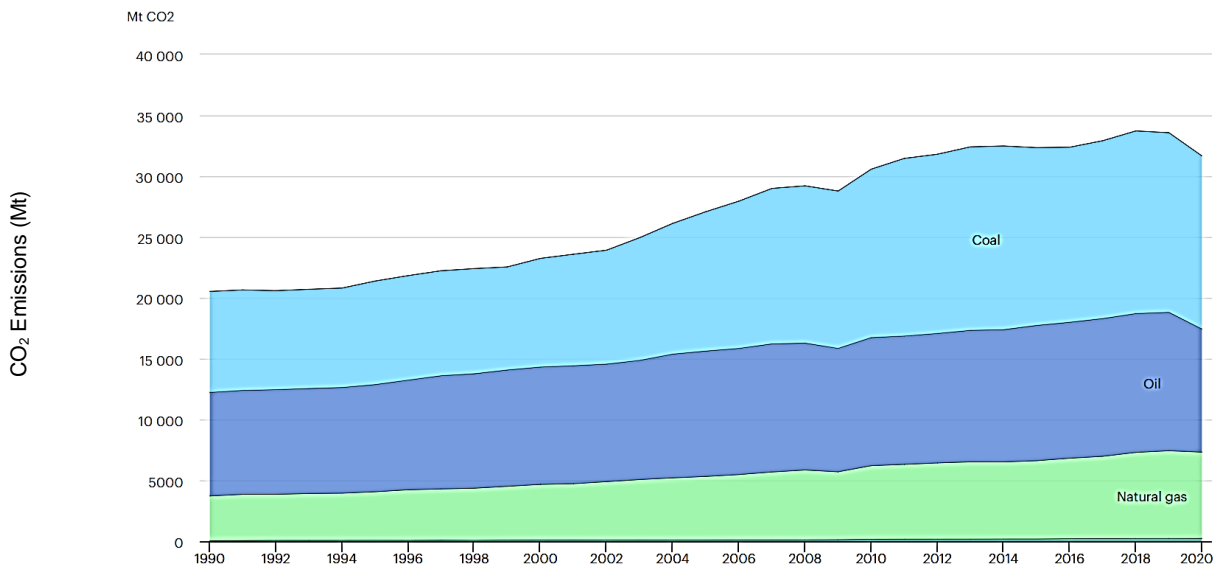


Figure 1-4 CO₂ emissions by fuel type¹⁷

According to the BP statistical review of world energy 2022 ¹⁸, carbon dioxide emissions associated with the energy sector have increased in 2021 by 5.9% to 33.9 Giga tonnes of CO₂ ¹⁶ as compared with the previous year, which implies the current mitigation measures are unsatisfactory to comply with the objectives of the Paris

agreement ¹⁹. Therefore, any efforts to decrease CO₂ emissions must be centred on the energy production sector to meet the climate objectives.

Some important efforts have focused on improving clean power generation and increasing energy efficiency ²⁰, however, regardless of the accelerated advances in the production of renewable electricity, state-of-the-art “renewable” production methods are still not an alternative to burning fossil fuels for now. Therefore, all estimates indicate that power generation plants based on fossil fuels will continue to play a dominant role in energy production in the coming years. Concomitantly, anthropogenic carbon dioxide emissions are expected to continue increasing in the coming decades, hence, carbon capture and storage (CCS) techniques are expected to play a principal role in the mitigation of CO₂ emissions.

1.5 CO₂ capture systems

In industry, CO₂ emissions from different energy-related applications can be captured by different means depending on the activity. The CO₂ captured can then either be utilised as a pure gas or in a mixture of gases, or it can be converted into valuable chemicals or fuels ^{21, 22} as per Figure 1-5.

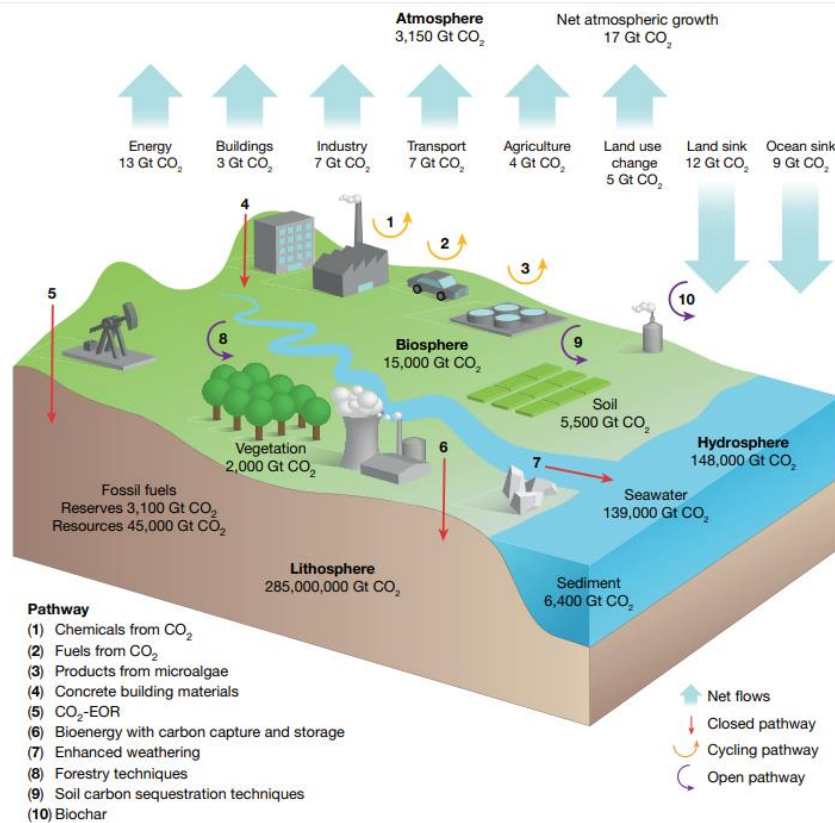


Figure 1-5 CO₂ pathways (taken from ²²)

There are three main types of CO₂ capture systems named according to the stage at which CO₂ is captured. These have been extensively reviewed in the literature ^{23,24,25} and presented in Figure 1-6.

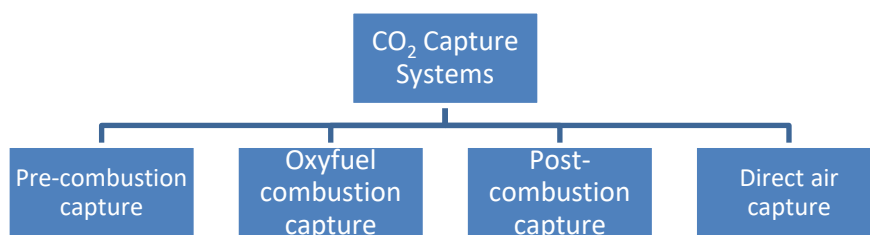


Figure 1-6 Types of CO₂ capture systems

1.5.1 Pre-combustion capture systems

These systems remove the CO₂ before the burning process is initiated ^{24,26}. Firstly, the primary fuel is converted into a synthesis gas (composed mostly of hydrogen and

carbon monoxide), then the syngas stream reacts with steam to shift the CO to CO₂ prior to the separation of CO₂. The synthesis gas is used to generate power via the integrated gasification combined cycle (IGCC) as per Figure 1-7 follows. This method is capable of capturing 85% of the CO₂ (volume basis) with relatively low energy and water consumption as compared to other techniques²⁷. However, the capital cost of the IGCC system is higher than the cost of the coal power plant, which is considered to be a major disadvantage. Currently, many projects are aiming to increase the efficiency of the pre-combustion capture systems by reducing the energy requirements of the process, besides developing more efficient catalysts for improved CO₂ and hydrogen production²⁴.

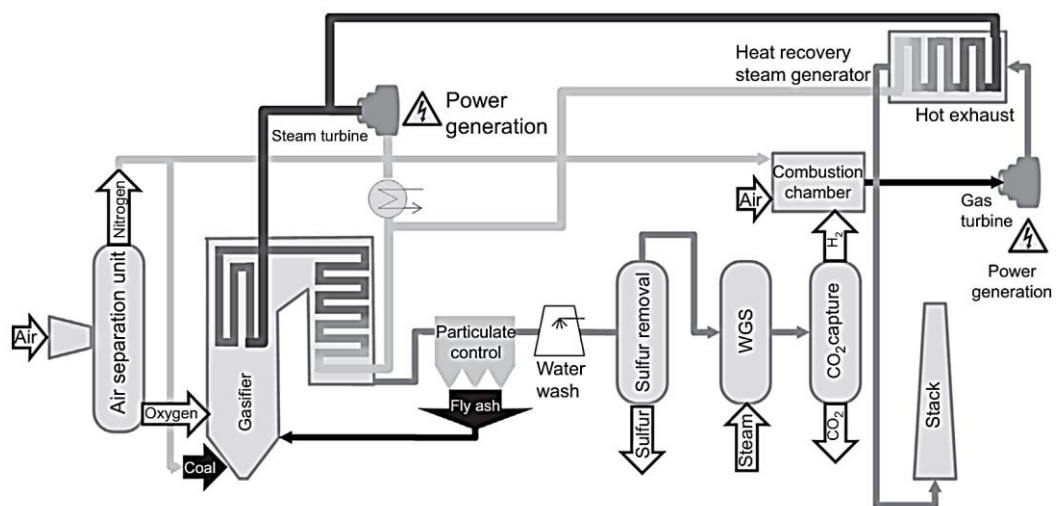


Figure 1-7 Schematic diagram of the pre-combustion capture with IGCC (adapted from²⁸)

1.5.2 Oxy-fuel combustion before CO₂ capture

In this strategy, pure oxygen is used to burn the fuel instead of air. Therefore, the concentration of the CO₂ in the flue gas is maximised, which makes the separation of CO₂ from the exhaust gas much easier due to the absence of N₂ in the exhaust gas²⁹. Oxy-fuel combustion systems are more environmentally friendly when compared

with other systems ⁸. However, they require an air separation unit (ASU) to produce the oxygen along with an integrated cooling system required to remove condensable vapours from the exhaust stream. These two additional units reduce the overall net efficiency of the process by 10 % which explains why there are only five capture systems utilising this strategy ⁸. To reduce the energy requirements of oxyfuel processes, Ishida *et al.* proposed an integrated chemical looping oxyfuel combustion process for carbon capture ³⁰. This innovative process is carried out in two successive reactions: firstly, the preheated hydrocarbon fuel reacts with the solid NiO in the reduction reactor releasing CO₂ from upstream of the reduction reactor. Then, Ni produced reacts with the compressed air in the oxidation reactor ^{30, 31}. Further modification of this integrated process was proposed and experimentally done by Hong *et al.* ³² in 2005 by utilising solar thermal energy (Q_{soltth}) in the reduction step that reduced the energy penalty of this strategy as compared to conventional post-combustion carbon capture technologies as shown in Figure 1-8.

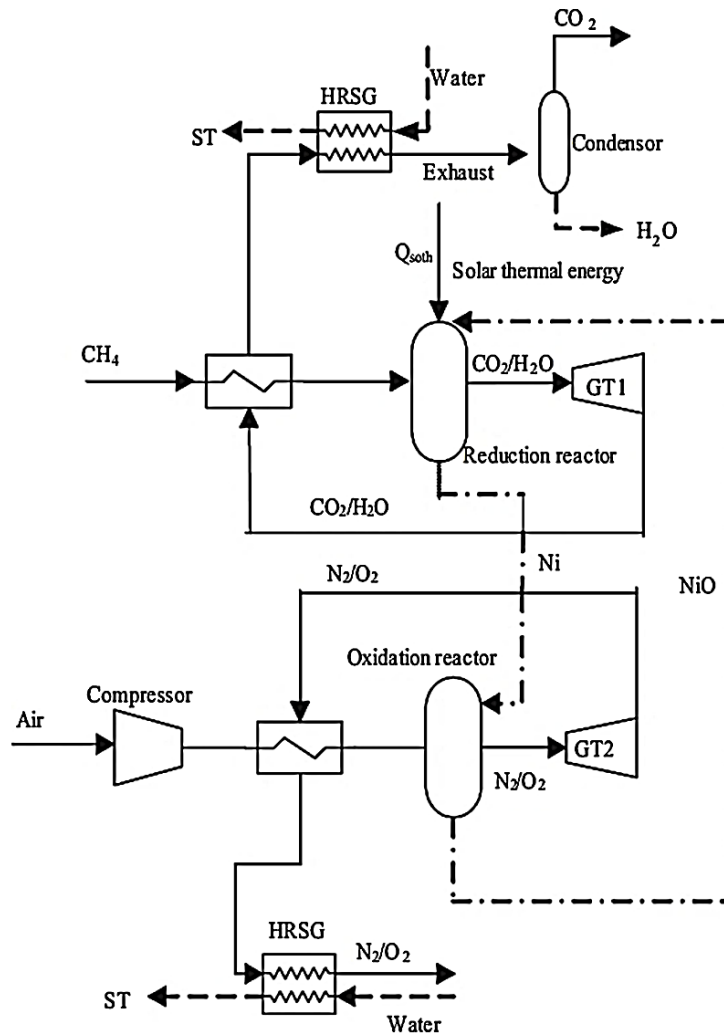


Figure 1-8 Solar integrated chemical looping oxyfuel combustion system proposed by Hong *et al.*³²

1.5.3 Post-combustion capture processes

In post-combustion capture (PCC) processes, CO₂ is captured from the flue gas stream after burning the fossil fuel^{24,26}. Today, PCC is the most established CCS strategy utilised in large-scale applications including power generation plants, industrial furnaces, and cement kilns where the concentration of CO₂ in the flue gas is around 15% (volume)²³. PCC can capture up to 90% of the CO₂ from the flue gas stream using sorbents, membranes, and other techniques discussed in the following sections. The capital cost of PCC processes is lower than the capital cost of pre-

combustion and oxyfuel combustion processes. Nowadays, PCC also has a great economic potential in CO₂-enhanced oil recovery (EOR) ²⁵. Furthermore, PCC have a more flexible design, which makes PCC the most accessible option for the retrofitting of existing systems ²¹. Most PCC processes require the pre-removal of the acidic gases incorporated in the flue gas such as NO_x and SO_x. These pre-treatments reduce the overall efficiency of PCC by 11% ³³. It is worth mentioning that, the energy penalty of a typical amine PCC unit is up to 40% of the plant efficiency ³⁴.

1.5.4 Direct air capture

While most industrial plants can only capture their CO₂ emissions with up to 94% ³⁵, the uncaptured CO₂ escapes to the atmosphere. Direct air capture (DAC) is a relatively new capture strategy targeting carbon capture from the atmosphere (in which the CO₂ concentration is above 420 ppm ²) regardless of the CO₂ emission origin ³⁵. Therefore, the target concentration of CO₂ of DAC is quite low as compared to capture systems such as the PCC processes in which the targeted concentration of CO₂ is around 15% (v/v).

A typical DAC is composed of : a) air contacting medium containing the sorbent and, b) Sorbent regeneration system ³⁶. To achieve this task, DAC mainly utilises a wide range of absorbents such as alkaline solvents, aqueous amines ³⁷ and adsorbents such as solid-supported alkalines and amines ³⁸.

For DAC applications, absorbents will continue to be a compelling option to solid adsorbents since they have a number of advantages over solid adsorbents, including ease of handling and scaling up, the ability to take advantage of economies of scale, favourable heat transmission, and cheaper cost and maintenance ³⁷. In general, DAC facilities have certain advantages: a) they offer scalability, enabling them to produce the precise amount of CO₂ needed by consumers, and b) their size, location and mobility can be tailored to be in close proximity to CO₂ consumers, eliminating the expenses associated with transporting CO₂ ³⁹. On the other hand, DAC facilities are at a cost disadvantage in comparison to capturing emissions from point sources or natural sources because the later options have advanced further in terms of development and efficiency as explained in the following sections ³⁶. Recent studies

have shown that, the DAC systems would be more cost-effective and preferable when it run on a decarbonised grid or renewables energy resources ^{40,41}.

1.6 CO₂ capture methods based on PCC strategies

This work focuses on CO₂ absorption but is worthwhile presenting other strategies and methods (Figure 1-9) based on adsorption, cryogenic, membrane and others will be briefly presented and more focus will be given to absorption later as highlighted in Figure 1-9.

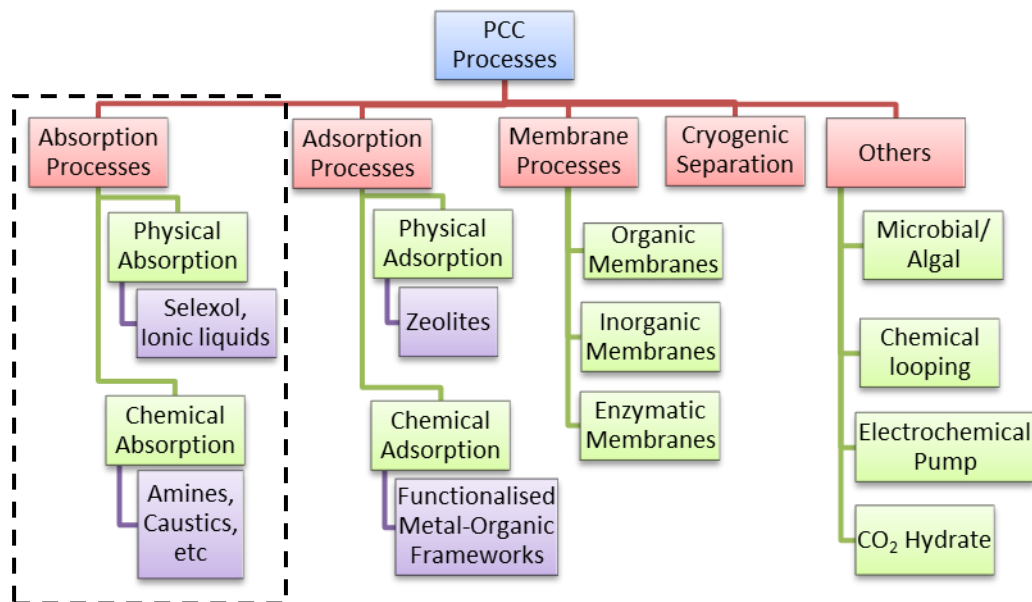


Figure 1-9 PCC processes/technologies

1.6.1 CO₂ post-combustion capture by adsorption

This PCC method utilises a solid adsorbent for CO₂ capture via physical or chemical mechanisms. In both cases, firstly CO₂ is captured (adsorbed) in the adsorber followed by a stripping process to regenerate the sorbent ⁴². CO₂ adsorption offers three main advantages: firstly, adsorbents have a high selectivity towards CO₂ among other acidic gases such as NO_x and SO₂. Secondly, it does not require water or any liquid sorbent therefore, no liquid waste is produced from adsorption processes ⁴³.

Finally, solid adsorbents have less heat capacity as compared to liquid sorbents, therefore the regeneration energy requirement of the adsorption process is less than the absorption one ³³.

In physical adsorption, CO₂ is adsorbed on the surface of the solid sorbent via weak Van Der Waals intermolecular forces. It can take place in layers, with subsequent layers building on top of one another. Up to saturation, each layer increases the surface coverage. On the other hand, chemical adsorption includes forming a chemical bond between CO₂ and the adsorbent. A monolayer of the adsorbate molecules typically forms on the surface. This is so that bonds can form in chemical processes that call for specific places on the surface.

Physical or chemical adsorption of CO₂ is dependent on a number of variables, including the type of adsorbent material, temperature, pressure, and the particulars of the system. However, compared to physical adsorption, chemical adsorption often has a higher capacity for CO₂ ⁴⁴.

The major technical difficulty associated with adsorption is that typically adsorbents have a high affinity towards water vapour. Therefore, the flue gas must be dried before adsorption. Also, the technology shows low selectivity as compared to other PCC alternatives, and currently, used adsorbents are difficult to regenerate ²⁷.

Adsorption processes can also be categorised into two main methods according to the sorbent regeneration process. CO₂ can be desorbed either by increasing the temperature or decreasing the pressure, commonly known as temperature-swing adsorption (TSA) and pressure-swing adsorption (PSA) respectively ²³. TSA is usually preferred at low concentrations of CO₂, while the PSA is more commonly used for high

concentrations of CO₂. PSA is also much faster than TSA²⁴. The most common physical and chemical adsorbents are discussed in the following section.

1.6.1.1 Physical Adsorbents

Activated Carbon

Activated carbon (AC) is considered one of the conventional adsorbents utilised in many applications such as the separation of liquid mixtures and medical applications. AC is cheap, safe, and available from various biomass waste such as straws, shells and bark⁴⁵. In industry, AC is synthesised in two steps, carbonisation and activation utilising physical and chemical processes. The physical process includes pyrolysis of biomass to produce char at temperatures below 800 °C under inert conditions, resulting in a porous material. To increase the surface area of AC, chemical activation process follows the carbonisation step by using oxidants such as KOH and H₃PO₄ at temperatures up to 1000 °C. Under these conditions, the carbon body is activated by enlarging the size of the pores without producing tar⁴⁵.

As a char material with high porosity, the CO₂ adsorption capacity of the AC reaches up to 15% (by weight) and can easily be recycled up to 10 cycles with low energy for regeneration^{46,47}. It is also convenient for low-temperature applications however, the AC have low selectivity towards CO₂ over N₂ as compared to other adsorbents such as zeolite, which is considered the major drawback of utilising the AC for adsorption processes⁴⁵. Furthermore, there are other serious challenges associated with the high energy consumption during the AC synthesis thermal processes along with the uniformity of the pores produced. Some recent work in the literature suggested utilising one-step activation could reduce the energy requirements of this process⁴⁸. Some other works focused on enhancing the CO₂ adsorption capacity of the AC by

functionalisation via potassium ⁴⁸ and metal oxides ⁴⁹, although the CO₂ adsorption intake increased with functionalisation via electrostatic interaction physical adsorption processes, however, the porosity of the AC reduced along with a heterogeneous dispersion of the activation agents on the surface of the AC ⁴⁹.

Zeolites

Zeolites are crystalline aluminosilicates microporous compounds produced from alkali metals ⁴⁶. Zeolites are a three-dimensional framework in structure, containing interconnected cavities through which molecules such as CO₂ reside ⁵⁰. The size of the zeolite cavity depends on the exchange cation type, whereas the mechanism of CO₂ adsorption by zeolite is affected by the cation (e.g. Al, Si, and Li) and the number of oxygen atoms. Zeolites have high CO₂ adsorption capacity and selectivities (up to 10 for CO₂/ N₂ selectivity) when compared to activated carbon. Zeolites are suitable for low temperature applications; however hydrophilic zeolites have low CO₂ intake when dealing with wet flue gases. For example, zeolite 13X has a higher selectivity for water vapour over CO₂. Zeolite 13X is the most common/utilised physical adsorbent and is used as a benchmark to evaluate newly developed adsorbents ²⁶. A similar issue has been reported with NaX, one the most recently developed adsorbent in which the CO₂ adsorption capacity decreased by 60% in the presence of moisture in the flue gas ⁵¹. Hence, a flue gas must be completely dehydrated when utilising physical adsorbents for CO₂ capture processes ^{26,51}. Also, a high regeneration temperature is needed -up to 300 °C- to expel the water and CO₂ from the zeolite which reduces the overall energy efficiency of the adsorption capture systems using zeolites.

1.6.1.2 Chemical Adsorbents

Amine functionalised Metal-Organic Frameworks (MOFs)

Utilising MOFs in CO₂ capture was first proposed by Yaghi *et al.*⁵². MOFs are porous compounds with a three-dimensional structure formed by metallic cations and ligands which are organic linkers that contain oxygen and hydrogen. MOFs offer a large surface area for CO₂ adsorption with higher selectivity of CO₂ over N₂ as compared to conventional physical sorbents. The structure of the MOFs can be tuned during the preparation process to increase the porosity and maximise functionality. Moreover, MOFs are chemically functionalised via amines to enhance the CO₂ adsorption capacity, Lin *et al.*⁵³ synthesised the first amine-functionalised MOF for in the literature named MIL-101(Cr) which was obtained from a direct reaction between 2-aminoterephthalic acid (ATPA) and chromic nitrate at 150 °C. In general, the unfunctionalized MOFs have been reported to have a lower pore volume and surface area as compared its unfunctionalized counterparts due to the presence of amino groups⁵³. For example, the overall pore volume of the NH₂-MIL-101(Cr) and MIL-101(Al) have frequently been lower as compared the unfunctionalized material of MOF^{53, 54}.

MIL-101(Cr) are thermally stable, and the maximised CO₂ adsorption intake by MOFs can be achieved at room temperature and high pressures up to 10 bar⁵². However, the adsorption efficiency decreases with the presence of moisture and impurities which usually exists during the preparation phase of the MOFs⁴⁶. Moreover, the presence of moisture in the flue gas stream reduces the durability and the mechanical strength of the MOFs over time, with high costs of preparation and utilisation of their applications in post-combustion carbon capture being limited^{46,44}.

Comparing the Efficiency of Adsorbents for Carbon Capture

Highly efficient adsorbents should show several fundamental properties including high adsorption capacity, high selectivity for CO₂, cheap and available raw materials, low heat capacity, fast adsorption kinetics, as well as chemical, and mechanical stability during the adsorption and desorption cycles⁵⁵. Several adsorbents meet some of the abovementioned requirements these are summarised in Table 1-1.

Table 1-1 A comparison between commercial adsorbents

Parameter	Adsorbent			References
	AC	Zeolite (13X)	MOFs	
CO ₂ capacity	15% (wt.%)	6.9 mmol. g ⁻¹	15 mmol. g ⁻¹	46,47,55
Selectivity (CO ₂ /N ₂)	5.1	10	770	56, 26,53
Advantages	Cheap and available	High adsorption capacity	High selectivity	46,44,57
Disadvantages	High energy demand for AC synthesis	Highly hygroscopic	Synthesis cost is high. Limited to laboratory scale	26, 53, 58

1.6.2 Cryogenic separation

The cryogenic separation method involves a series of compression operations at high pressure and sub-ambient temperatures to separate the CO₂ from flue gas streams containing high concentrations of CO₂ (more than 50%)⁵⁹. This method has been widely used in producing high-purity liquid CO₂ for food application processes⁴⁶. The CO₂ capture efficiency via cryogenic processes depends on the operation conditions, up to 99% of CO₂ can be recovered at a pressure below 1 bar and a temperature of – 135 °C⁶⁰. Firstly, the flue gas is cooled and compressed to low temperatures where the CO₂ in the gas form is solidified followed by an expansion process to liquefy the

CO₂ which is finally separated from N₂ gas via a distillation process as shown in Figure 1-10.

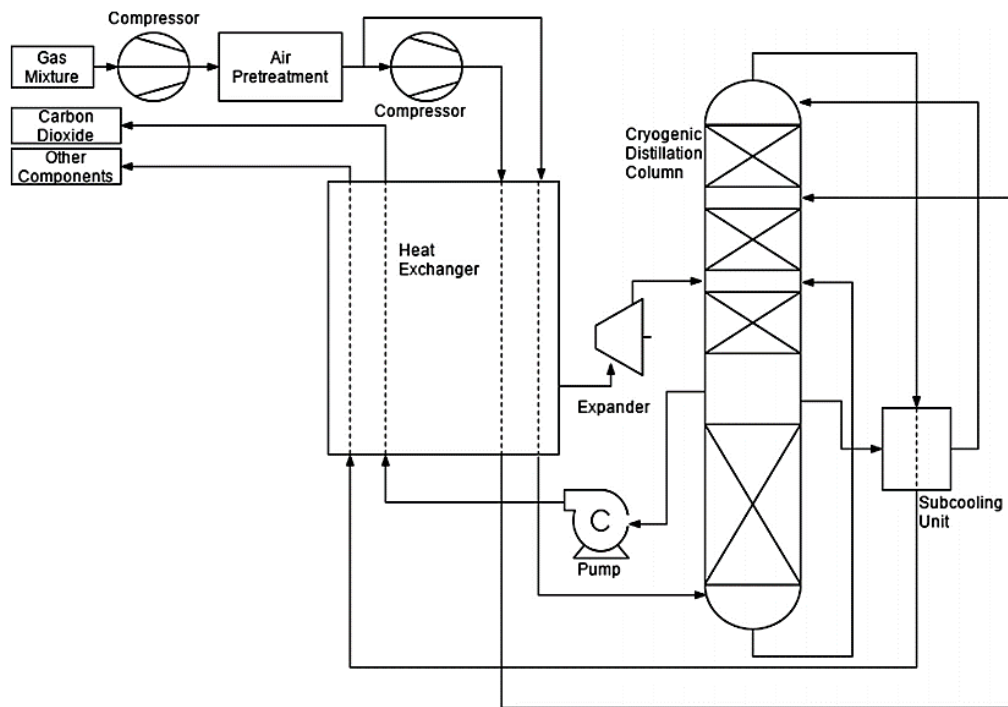


Figure 1-10 Schematic diagram of CO₂ cryogenic separation unit (adapted from ⁶¹)

Cryogenic separation systems have major advantages because they consume less water than absorption systems, are less corrosive and require no chemical agents to recover the CO₂. Also, cryogenic processes do not produce waste liquids, liquefied CO₂ is recovered at ambient pressure and is ready for transportation ⁵⁹.

Despite being one of the well-established CO₂ capture technologies, cryogenic separation has many disadvantages. Firstly, it is very energy intensive as CO₂ is captured at very low temperatures, it consumes up to 6 MJ per kg of recovered CO₂, resulting in high operation costs ⁶². Lin *et al.* ⁶³ were capable of increasing the efficiency of the cryogenic process by reducing the energy consumption down to 0.4

MJ per kg CO₂. They managed this via the synergetic integration of the cryogenic CO₂ recovery unit with a hydrogen production process with 99% CO₂ capture efficiency.

More importantly, there are major safety issues associated with the extreme pressure drop during the liquefaction process due to the blockage of pipes by the formation of ice when dealing with a wet flue gas ⁶⁴. Therefore, an additional dehydration process to remove the moisture from the flue gas is needed which adds to the capital cost and operational costs of the cryogenic separation plant. In addition, the efficiency of the heat exchangers used in cryogenic processes decreases during operation due to the accumulation of frost (CO₂ and moisture) on the surface of the heat exchanger resulting in an additional undesirable insulation layer ⁶⁴. To eliminate the moisture from the flue gas stream, some efforts were done by Tuinier *et al.* ⁶⁵ via utilising the liquified natural gas as a source of energy to cool the flue gas, separating the moisture from the flue gas, thus resolving the technical issues of pressure drop and blockage of pipes.

1.6.3 Membrane processes for CO₂ capture

Membrane separation is widely employed for CCS applications, it is the most efficient method to separate CO₂ from the natural gas stream where partial pressures of CO₂ are high. In pre-combustion capture systems, membranes are used to separate CO₂ from H₂, whereas it separates CO₂ from N₂ in post-combustion capture processes ⁶⁶. There are two main pre-treatments of flue gases before membrane separation: firstly, the flue gas must be cooled down to the operating temperature of the membrane, then this is followed by a compression step of the flue gas to increase the total pressure and then the partial pressure of the CO₂ to provide enough driving force allowing CO₂ to pass through the membrane. Other flue gas components are retained as demonstrated in Figure 1-11.

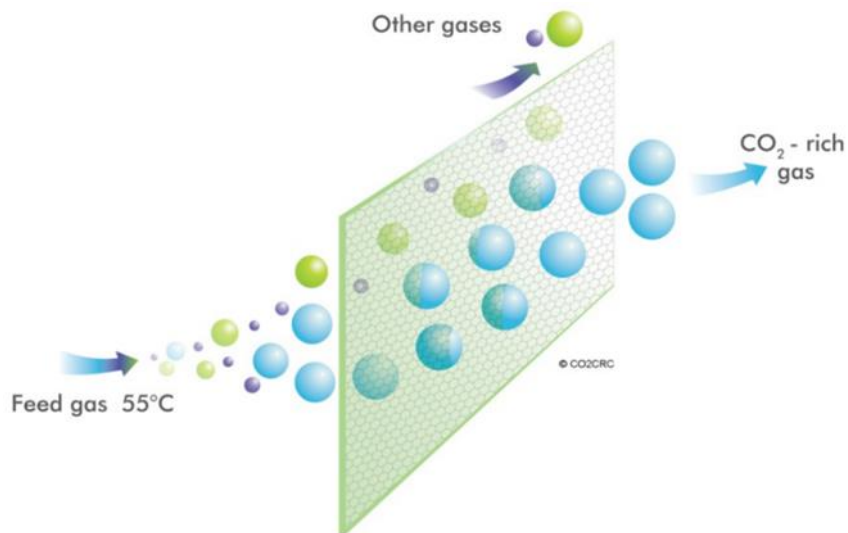


Figure 1-11 Schematic diagram of membrane separation for CO₂ from flue gas (adapted from ⁶⁷)

The selectivity of a membrane depends on the pore size of the membrane relative to the molecular size of the targeted gas along with the gas affinity towards membrane material ⁶⁶.

Currently, there are many types of membranes utilised in CO₂ capture processes such as organic, inorganic, enzymatic ⁶⁸ and dense (non-porous) membranes ⁶⁶. Organic membranes are basically utilised for the gas separation process ⁶⁹, whereas the inorganic ones are employed in highly selective membrane separations ⁶⁶. Mixed matrix membranes (MMM) are newly developed types of membranes made up of a polymeric matrix filled with dispersed particles such as silica, zeolites or carbon xerogels ^{70, 71}. The MMM have many advantages over the conventional membranes such as more stability and mechanical strength, higher permeability and lower operation cost ²⁴.

When discussing membranes, the term “end of life” can apply to both their operating duration and their eventual disposal and environmental impact. The operational lifespan of membranes is mainly depends on several factors, such as the type of

membrane, operating conditions, its quality, and maintenance ⁷². While organic and polymeric membranes are recyclable, some other types of inorganic membranes are disposed by the end of their life-span ^{72,73}. One area of study and innovation is the creation of more environmentally friendly membrane materials and recycling techniques. The environmental impact of disposing of membranes at the end of their useful lives may be lessened through improvements in membrane design, material selection, and recycling techniques.

In CO₂ capture using membrane technology, there is no regeneration step required which is considered the major merit of this method. The main demerits include that the selectivity and the permeability of membranes are directly affected by impurities present in the flue gas stream which decreases the CO₂ permeation with time during operation. Therefore, filtration of particulates is necessary before membrane separation ⁶⁶. Also, this technology is limited to low volumetric flow rates, and fouling issues associated with high pressure and temperature operations have been reported ⁷⁴. As a result, an additional recycling system might be needed which increases the operating costs of the membrane separation unit ⁶⁶.

1.6.4 Microbial CO₂ post-combustion capture

PCC via microbial technologies is based on the bio-fixation of CO₂ by microalgae. Microalgae are microscopic organisms with a high capability to utilise CO₂ as a source to produce biomass. Bioelectrochemical systems (BESs) are systems utilised for the simultaneous carbon capture and production of value-added products ⁷⁵. There are many BESs such as the microbial carbon capture cells (MCCs) in which microalgae such as *Tetraselmis suecica* and *Chlorella sp.* are employed to capture CO₂ from flue gases ^{76,77}. The major merits of utilising microbial technology are high selectivity towards CO₂ in flue gases with a low concentration of CO₂, availability of raw

materials, use of solar energy, cost-effectiveness and the fact that it is an environmentally friendly technology converting CO₂ into valuable biomass⁷⁷. The biomass produced from the cultivation process contains useful compounds such as carbohydrates, proteins, and lipids that can be easily converted to more valuable products such as other chemicals and biofuels^{28,78,79}. Also, the microbial technology can be utilised for CO₂ capture integrated with wastewater treatment processes in industrial processes as has been proved experimentally by Lu *et al.*⁸⁰. However, microalgae can be easily damaged by other acidic gases that existed in the flue gas stream apart from CO₂, the application of BESs in large-scale is still limited as the microorganism used in BESs have a low CO₂ absorption rate⁷⁷. BESs are not energy-efficient systems as they require using electrical energy to capture CO₂ via the cultivation process which reduces the power efficiency of the whole unit. In addition, the heat integration of this unit is limited to producing fuel cells, whereas the integration of microbial CO₂ capture with thermal power units has not been thoroughly investigated⁸¹.

1.6.5 CO₂ post-combustion capture by absorption

This work is mainly focused on post-combustion carbon capture via the absorption process. Therefore, it is essential to discuss this technology thoroughly. PCC absorption processes can be divided into two main types: physical and chemical absorption. Physical absorption is defined as CO₂ absorption from the flue gas stream according to Henry's law without any chemical reaction involved^{27, 46}. The CO₂ absorption capacity of the sorbent in this case depends on the partial pressure of the CO₂ in the flue gas stream. Generally, physical absorption is less efficient for CO₂ capture than chemical absorption, but sorbent regeneration is much easier in the case of physical absorption^{26,42}.

The chemical absorption of CO₂ involves physical absorption along with a chemical reaction between the CO₂ and the absorbent, forming labile compounds. Chemical Absorption is widely utilised in large-scale energy applications as it can capture up to 98% CO₂ from the flue gas stream ⁴³. The major advantages of the absorption process are: higher CO₂ absorption capacity than adsorption, less energy-intensive than cryogenic separation, and allow more flexible designs than membrane processes ⁴³.

More details about the advantages and disadvantages of physical and chemical absorption processes are discussed in the following section.

1.6.5.1 Chemical Absorption

CO₂ absorption capture via amines

Amine absorption is the most well-established method for CO₂ post-combustion capture in large-scale applications such as industrial furnaces, cement kilns, and boilers ²³. Typically, CO₂ absorption using amines is accomplished in two different steps as per Figure 1-12. Firstly, the flue gas containing CO₂ enters the absorber at temperatures ranging between 40 and 60 °C, where the CO₂ is chemically absorbed. Secondly, the CO₂-rich stream is transferred to the stripping unit where the solvent is regenerated at temperatures up to 120 °C, thus releasing the CO₂ ⁸².

Primary, secondary and tertiary amines are used for carbon capture. Monoethanolamine (MEA), diethanolamine (DEA) and tertiary methyldiethanolamine (MDEA) are respective examples of primary, secondary and tertiary amines used in PCC processes. All amines contain an amine functional group along with a minimum of one hydroxyl group ⁴⁴. Tertiary amines have the highest CO₂ absorption capacity, while primary amines have the lowest. However, in terms of CO₂ affinity, amines follow the order: tertiary < secondary < primary ⁸³. Monoethanolamine (MEA) is considered

the benchmark to evaluate the performance of any developed absorbent for carbon capture processes ⁸⁴. The CO₂ absorption capacity of MEA 30% (wt/wt) is 453 g of CO₂ per kg of MEA as extensively reported in literature ^{85, 86}.

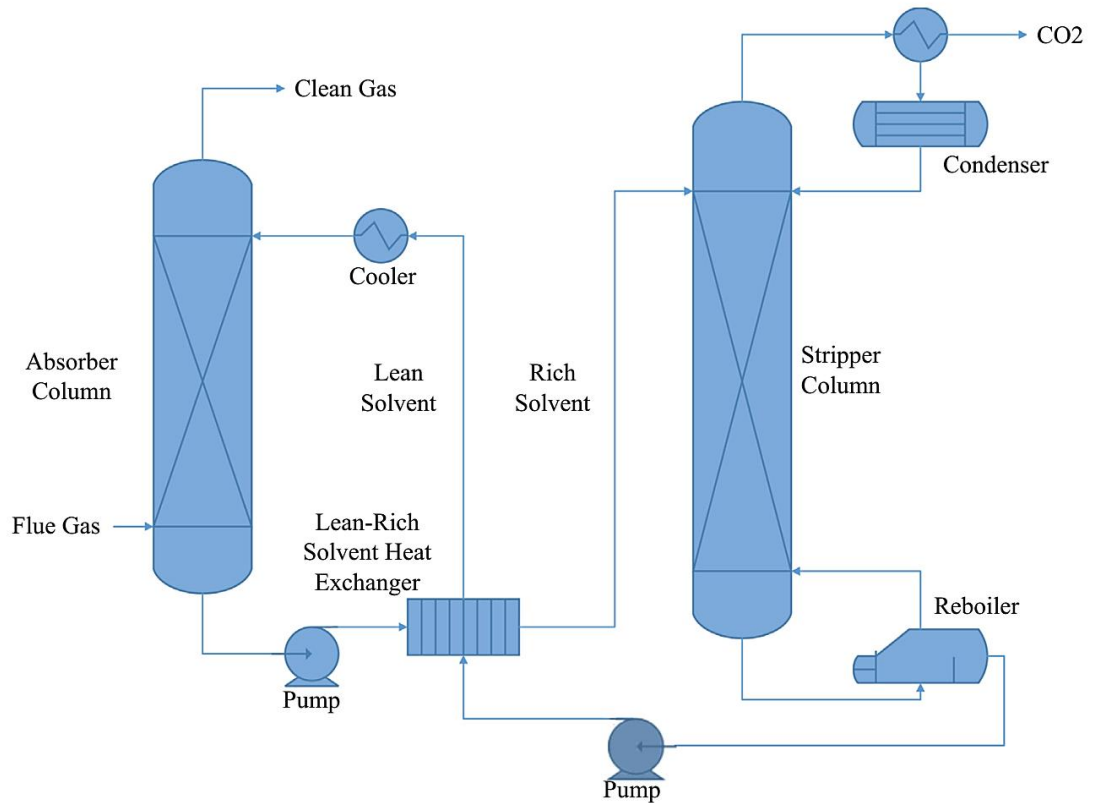
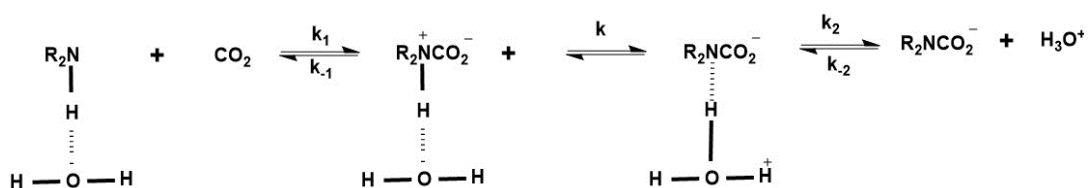


Figure 1-12 A typical layout of CO₂ post-combustion capture via amines (adapted from ⁸⁷)

As strong bases, amines donate pair of electrons from the amine or hydroxyl groups to the CO₂ molecule, forming stable carbamate. Carbamate formation is a key reaction in CO₂ absorption by amines. Regarding the reaction mechanism of carbamate formation, the zwitterion mechanism proposed by Caplow in 1968 ⁸⁸ is described in Equation 1-1. In this mechanism, an amine molecule interacts with water forming a hydrogen bond before interacting with CO₂. Then, the aqueous amine bonds with CO₂ forming an unstable intermediate known as the zwitterion. In the third

step, the zwitterion is deprotonated while the amine molecule acts as a base molecule forming carbamate.



Equation 1-1 Carbamate formation via the Zwitterion mechanism (modified from ⁸⁸)

Additionally, amines that are sterically inhibited have been suggested as potential CO₂ absorbents. Any primary or secondary amine with the amino group connected to a tertiary carbon is classified as a sterically hindered amine by Sartori and Savage ⁸⁸. 2-amino-2-methyl-1-propanol (AMP) is one such example. Numerous research teams have looked into several sterically hindered amines and found that, on average, these amines are more effective at absorbing CO₂ than MEA. These amines only created unstable carbamates due to the presence of a bulky tertiary carbon next to the amino functional group. This allowed for a faster reaction with CO₂ than tertiary amines and a lower solvent regeneration cost.

In 1989, Crooks *et al.* in their work in ⁸⁹ proposed another mechanism for carbamate formation known as a termolecular mechanism. In this mechanism, the proton transfer and the bond formation with CO₂ occur simultaneously in a single step. In other terms, Caplow's mechanism approaches the termolecular mechanism if the lifetime of the zwitterion is very short ⁸⁹. Although both mechanisms can be used to represent the experimental data, model calculations done by Silva *et al.* ⁹⁰ showed that the termolecular reaction with a single step is more likely to happen than the zwitterion mechanism. Recently, a new mechanism suggested by Said *et al.* ⁹¹ showed that the formation of the zwitterion intermediate is highly improbable for two reasons: firstly

the existence of the zwitterion is inconsistent with the orbital symmetry necessities to complete the reaction, and secondly, zwitterion formation is an energetically unfavoured reaction ⁹¹.

There are many advantages of utilising amine solutions in post-combustion carbon capture, amine absorption system is capable of capturing up to 99.99% of CO₂ from a flue via two simple processes ²⁸. Therefore, this technology is considered the most mature method and sets a benchmark in terms of evaluating the newly developed sorbents or CO₂ capture processes ⁹².

The major drawbacks of the amine absorption systems are: the high energy penalty required to regenerate the sorbent of approximately 60-80% of the overall energy consumption of the plant ⁹³. Amine absorption utilises large quantities of water as compared to other PCC strategies. Also, amine solutions are highly corrosive to the process units and pipes ^{43,94}.

Amine degradation is defined as an irreversible chemical reaction between amines and the flue gas components producing undesirable products ⁹⁵. The degradation products are highly viscous and directly responsible for many operation faults such as foaming, corrosion and fouling ⁹⁶. Furthermore, there are several health and environmental complications when dealing with emissions and disposal of the degradation products.

Several amine degradation scenarios have been reported such as oxidative, thermal, and polymerisation of the carbamate. Oxidation occurs when the amine reacts with oxygen present in the flue gas, producing oxidation products such as hydroxyethyl formamide and oxalate ⁹⁷. Thermal degradation of amines occurs due to the high-temperature operation during the regeneration process, resulting in the formation of

by-products of amines such as tetraethylenepentamine (TEP)⁹⁶. Finally, carbamate polymerisation occurs in the desorber unit, where carbamate forms long-chain products of hydroxyethyl ethylenediamine⁹⁸.

Ongoing research has been directed to resolve the degradation challenge, and different degradation inhibitors have been developed. For example, it is technically impracticable to separate oxygen from the flue gas, however, some inhibitors such as chelating agents and heavy metal salts can be utilised as O₂ scavengers, reducing the oxidative degradation reactions^{99,100}. The addition of stable salts in the system is another method used to prevent the oxidation degradation of amines during stripping, as salts reduce the solubility of oxygen in the system¹⁰⁰. Chelating agents such as ethylenediaminetetraacetic acid (EDTA) showed high efficiency in reducing oxidation degradation. It is worth mentioning that, most of the oxidation degradation inhibitors are unstable at high temperatures⁹⁹.

Similar to the degradation inhibitors, there are many corrosion inhibitors used in large-scale amine-based PCC processes. Corrosion inhibitors reduce the high corrosivity of amine solutions. Corrosion inhibitors can be classified as organic and inorganic, with the first type being preferable to the second due to the environmental concerns associated with using the inorganic inhibitors⁹⁹.

Therefore, future work in the optimisation of amine absorption systems should mainly focus on reducing the high energy demand of the regeneration process, on resolving the degradation issues, and on minimising corrosion concerns.

CO₂ absorption capture via potassium carbonate

Due to the attributes of low cost, low toxicity, ease of regeneration, slow corrosion, low degradation, high stability, and CO₂ absorption capacity, potassium carbonate (PC) solution is an important chemical absorbent to minimise CO₂ emissions. Since then, the PC method has been used in more than 700 plants across the globe to remove CO₂ and hydrogen sulphide from streams such ammonia synthesis gas, crude hydrogen, natural gas and municipal gas ¹⁰¹.

The "Hot Potassium Carbonate (Benfield) Process" was the name given to the method of CO₂ absorption utilising potassium carbonate solutions ¹⁰². Similar to the amines CO₂ capture system described above, the absorber and desorber are the two key components of this process. For CO₂ absorption, the flue gas is supplied into the absorber in the opposite direction of the absorbent. The loaded absorbent is then introduced into a desorber, where CO₂ is removed from the solvent by raising or lowering the desorber's temperature or pressure. The absorbent can then be routed back to the absorber for use in the absorber ¹⁰³.

Compared with the amines CO₂ absorption systems such as MEA, PC solutions are easier to regenerate as the CO₂ absorption process is carried out at elevated temperatures (up to 140 °C) ¹⁰⁴. Also, PC solutions are cheaper and more thermally stable than amines ¹⁰¹. Furthermore, PC solutions are less corrosive to carbon steel as compared to the amines ¹⁰⁵. On the other hand, the major limitations of utilising PC in carbon capture are: a) slow reaction rate, which leads to limited mass transfer of CO₂ in the liquid phase. By employing some promoters such as ethylenediaminetetraacetic acid (EDTA) into the PC solution to speed up the reaction,

this flaw can be eliminated ¹⁰³. Also, in the process' reboilers and pipeline, the solvent precipitates as crystal accumulations and fouling ¹⁰⁶.

1.6.5.2 Physical Absorption

Selexol process

This physical absorption method is mainly used to capture acidic gases such as SO₂ and CO₂ from a flue gas stream with high concentrations of these gases. The dimethyl ethers of polyethylene glycol (DEPG) is a thermally and chemically stable compound usually utilised as a solvent for this type of process which is known as a hydrophilic weak base with low volatility that can remove the moisture from the flue gas stream with high selectivity towards the acidic gases ^{46,107}.

DEPG is highly efficient in capturing acidic gases in a wide range of temperatures ¹⁰⁸. CO₂ capture processes occur in two main steps, firstly, the flue gas enters the absorber where H₂S is separated by the DEPG at the ambient temperature. Then, a second absorber is used to capture CO₂ followed by a regeneration process ¹⁰⁸. Alternatively, the residual CO₂ can be removed from the sorbent by a depressurising process in which CO₂ has low solubility at low pressures.

The capital and the operation costs of this method are minimal as compared to other physical absorption processes which are considered the major advantages of this approach. On the other hand, this technique is only suitable for CO₂ capture if the concentration of CO₂ in the flue gas is higher than the other acidic gases such as H₂S. Also, DEPG is viscous at low temperatures which reduces the CO₂ absorption capacity and mass transfer rate ^{46,109}. Because of the high viscosity of DEPG, there is a push for research in novel physical absorbents to overcome such limitations.

Novel absorbents: Ionic Liquids

Ionic liquids (ILs) are molten salts having a melting point up to 100 °C when it was first reported in 1914 by Walden *et al.* in ¹¹⁰. ILs are now defined as compounds (salts) composed solely of ions with melting points below 100 °C ¹¹¹. ILs have some unique properties as compared with conventional liquids such as high thermal and chemical stability, non-volatility, and low vapour pressure ¹¹² which make them favourable in the application of many industrial as well as research works. Due to several attractive properties of ILs, they have different applications including solvent extraction and CO₂ capture processes. In 1999, ILs composed of [BMIM][PF₆] were reported to have high CO₂ absorption capacity for the first time in the literature ¹¹³. Consequently, a large number of studies focused on the utilisation of ILs for CO₂ capture processes.

ILs have been investigated as potential “green chemicals” for CO₂ absorption due to their distinctive characteristics, which include low vapour pressure, high thermal stability, non-flammability, and tuneable physicochemical characteristics, as compared to conventional amines ¹¹⁴. The characteristics and applications of ILs for carbon capture have been thoroughly reviewed ^{115, 116, 117, 118, 119}. Ramdin *et al.* ¹²⁰ reviewed the carbon capture performance of ILs such as their CO₂ absorption, diffusivity, selectivity and CO₂ solubility dependence on the constituent ions and functional groups.

The CO₂ absorption by ILs can either be physical or chemical, depending on the composition of ILs. Physical absorption is limited to the traditional ILs employed for CO₂ separation where CO₂ partial pressure is high ⁴³. While chemisorption (in addition to physical absorption) occurs when ILs are functionalised. Functionalisation of ILs is adding functional groups such as amines, phenols and hydroxyl groups to the

traditional ILs ^{112, 121}. In general, functionalised ILs have higher CO₂ absorption capacity than the traditional ones, ILs of imidazolium ion associated one amine group with showed a similar absorption capacity to the monoethanolamine (MEA) ¹²². While amino acid-based ILs which contain multiple amine groups proven to have higher CO₂ absorption capacity than ILs functionalised with one amine group. Furthermore, functionalised ILs have a faster absorption rate as compared to the traditional ones, however, they are more complex in structure with high viscosity which increases the energy requirements for the regeneration process and limits their large-scale applications ¹²³. Water can significantly reduce the high viscosity of ILs resulting in increasing the CO₂ absorption capacity of ILs as extensively reported in the literature ¹²⁴.

Utilising ILs as an alternative absorbent for CO₂ separation processes have considerable advantages. For example, the energy consumption of CO₂ capture via [Bmim][PF₆] ILs is lower by 26.7% than that in amines PCC processes ¹²⁵. On the other hand, many ILs have intrinsic disadvantages, such as high vulnerability to contamination, poor biodegradability, high toxicity, high cost, and complex manufacturing processes ^{126, 119, 127}.

Novel sorbents: deep eutectic solvents

A deep eutectic solvent (DES) is defined as a mixture of pure chemicals whose eutectic point temperature is lower than the temperature of an ideal liquid mixture¹²⁸. The green industrial revolution requires developing and utilising green chemicals in several application domains. Deep eutectic solvents are now recognised as green chemicals and as an alternative to ionic liquids (ILs) with more interesting characteristics ¹¹⁹. DESs are defined as DESs have some unique properties which

make them favourable in the application of many industrial as well as research works such as solvent extraction ¹²⁹, biocatalysts, oil shale processing, separation of petrochemicals products ⁴⁶, electrochemistry solvent ¹³⁰, chemical and biochemical transformation, and nuclear-based separation ¹³¹. To overcome limitations associated with employing ILs for CO₂ separation processes, an alternative class of ILs called deep eutectic solvents was pioneered by Abbott *et al.* ¹³². Generally, DESs are synthesized from raw materials with desirable characteristics such as biodegradability, biocompatibility, non-toxic and cheap materials ^{133, 134}. The most recent review ¹²⁹ highlighted the advantages of DESs over ILs: the synthesis methods, DESs are prepared by simple heating and mixing processes, without generating any waste and no further refining steps are required, the preparation of ILs is much more complex and expensive. Unlike ILs, DES are formed via hydrogen bond formation between the hydrogen bond acceptor (HBA) and the hydrogen bond donator (HBD), choline chloride (ChCl) has been used as the HBA in most DES reported in the literature. DESs are known as natural deep eutectic solvents (NADES) when the components forming the DESs are primary metabolites such as organic acids, sugars, or amino acids associated with choline derivatives ¹³⁵. ILs and DESs capture CO₂ via hydrogen bonds instead of alkaline, therefore the corrosion rate of process units is much lower than MEA ¹³⁶.

The approach of using DESs for CO₂ capture processes is relatively new compared to conventional sorbents including ILs, yet it provides a promising method for large-scale CO₂ applications. Chapter 2 provides a critical literature review on the utilisation of DESs for PCC processes.

Choline chloride

Choline chloride (ChCl) is an organic compound related to quaternary ammonium salts. ChCl can be produced in the laboratory via a methylation reaction between dimethylethanolamine with methyl chloride. While in industry, ChCl is produced via the Davy process in which trimethylamine, hydrochloric acid, and ethylene oxide react to form ChCl¹³⁷. ChCl is a benign chemical that has been used as a primary chemical for producing choline hydroxide which is commonly used as an intermediate for organic synthesis in the area of biochemical research¹³⁸. It is also been used as an additive ingredient in poultry food¹³⁹. Furthermore, ChCl is a cheap, non-toxic, and biodegradable compound which means it has a perfect environmental profile with low negative impact¹⁴⁰. ChCl is considered the most famous HBA that has been used to produce DESs. In this work, ChCl was used as an HBA to prepare ChCl:LvAc DES compositions.

Levulinic Acid

Levulinic acid (LvAc) is an organic compound (carboxylic acid) that is produced from biomass waste such as lignin and cellulose¹⁴¹. It is considered one of the top value-added compounds derived from biomass waste. LvAc has been widely used in a wide range of applications including DES preparations^{141, 142}. In this work, LvAc was used as the HBD to form a hydrogen bond with the HBA (ChCl).

1.7 Conclusion

This chapter presented the challenges facing the global community regarding global warming caused by CO₂ and other GHGs emissions. The main CO₂ capture methods that have been developed to avoid CO₂ emissions have been reviewed. Among these

methods, absorption-based processes are widely considered to be the most reliable methods due to the high absorption capacity of the sorbents used and due to economic considerations (minimisation of expenditures). This chapter ended up by describing various absorption processes, it summarized the CO₂ absorption capacity, mechanisms and performance of sorbents used along with the advantages and disadvantages of newly developed sorbents as compared with amines (benchmark). The most relevant information is summarized in Table 1-2.

Table 1-2 Comparison of absorption-based CO₂ capture using various sorbents

Absorbent	Advantages	Disadvantages	Improvement Pathways	Ref.
Amine Solutions	Most well-established method (benchmark). High absorption capacity. Fast reaction rate.	Highly corrosive. High energy consumption for regeneration. Easily degraded and oxidized.	Corrosion inhibitors. Amine-based blends. Amine-based solid adsorbents.	95,28,43 , 94, 99,100
ILs	Low vapour pressure and volatility. Properties can be tailored depending on the application. Less corrosive than amines.	Highly complex synthesis process associated with high costs. Highly viscous. High regeneration energy.	Increased performance by functionalization. Using promoters and additives like amines.	126,119, 127, 123,118, 119
DESs	Availability of biodegradable raw materials. Low vapour pressure. Low toxicity.	High viscosity. Application is still limited to the laboratory scale.	Using promoters and additives like amines.	119,103, 104, 133, 134,136,

As shown in Table 1-2, the various sorbents that have been utilised for CO₂ capture processes at different scales, have their associated advantages and disadvantages. Therefore, the optimisation of currently used sorbents along with developing alternative ones is essential to satisfy the requirements of large-scale carbon capture processes used to capture CO₂ from major emission sources such as fossil fuel power plants. Developed sorbents must meet the criteria of high CO₂ capture performance such as high CO₂ absorption capacity and selectivity towards CO₂ from the flue gas streams. Such sorbents need to be “green” compounds, with chemical and thermal stability such that these are capable of absorbing CO₂ at elevated temperatures and can be easily regenerated simultaneously considering the overall energy costs associated with the CO₂ capture unit.

1.8 Thesis Aims and Structure

DESs are among the most promising options to overcome these ILs problems while retaining their positive properties and the ability to tune their behaviour, DESs are greener solvents and more benign solvents for CO₂ separation than conventional ILs due to the former’s biodegradability and nontoxicity^{135, 140}. This research program investigated the viability of ChCh:LvAc DES for post-combustion carbon capture processes. This project will attempt to achieve the following objectives/answering the following research questions:

1. Can choline chloride:levulinic acid-based mixtures be considered DESs or another type of mixture?
2. What are the key thermophysical properties of the proposed ChCh:LvAc DESs?
3. What is the corrosivity of the proposed ChCh:LvAc DESs as compared to the corrosivity of amines (benchmark sorbents) in different corrosion scenarios?

4. What is the CO₂ absorption and desorption performance of the proposed ChCh:LvAc DESs as compared to MEA (benchmark)?
5. What are the mechanisms of CO₂ absorption by ChCh:LvAc DESs?
6. What are the optimal key operating parameters for CO₂ absorption and desorption using ChCl:LvAc DESs?
7. What is the selectivity of ChCl:LvAc DESs towards CO₂?
8. To which extent ChCh:LvAc DESs are recyclable?

In the following chapter (chapter 2), this work focuses on investigating the viability of DESs as an ideal sorbent for CO₂ capture, reviewing the key thermophysical and transport properties that are affecting CO₂ absorption and desorption in DESs along with the environmental profile of DESs. Chapter 2 starts with addressing the gaps in the literature on utilizing ChCh:LvAc DESs for CO₂ capture purposes and the methods of CO₂ absorption and desorption in DES along with some aspects associated with these processes such as the corrosivity of DES-CO₂ systems. The last section of Chapter 2 reviews the compositional and operating parameters affecting CO₂ absorption in DESs. Chapter 2 represents the bulk of a review paper which will be published in the literature.

Chapter 3 provides the preparation and characterization techniques employed in this work to evaluate choline chloride levulinic acid-based DESs as an alternative green sorbent for CCS. It describes the methodology for the experimental methods used for CO₂ absorption and desorption these have been discussed extensively in chapter 2 along with their limitations and assumptions to justify their use in this work. Chapter 3 provides a comprehensive characterisation of the ChCl:LvAc DESs investigated in this work and contains the bulk of a research paper to be published.

Chapter 4 presents the experimental results and discussion. In detail, it provides the results of the performance of proposed ChCl:LvAc DESs in the application domain of this work of CO₂ absorption and desorption. Chapter 4 starts by highlighting the gaps in the literature related to the application of ChCl:LvAc DESs carbon capture processes and how this knowledge gap is going to be filled by this work. Chapter 4 is mainly composed of a peer-reviewed paper that was published in September 2021. The paper is titled (*A Comprehensive Study of CO₂ Absorption and Desorption by Choline-Chloride/Levulinic-Acid-Based Deep Eutectic Solvents*). Furthermore, chapter 4 includes some additional statistical analysis of the carbon capture absorption by ChCl:LvAc DESs besides a detailed discussion about the findings of the experimental results in light of the literature.

Chapter 5 critically discusses and summarizes the key findings of the research of this work. It highlights and presents the answers to the research questions presented in this section and addressed in chapters 3 and 4. Chapter 5 also addresses the theoretical and experimental implications faced during this work. It reveals the important research gaps in the literature as summarised these were filled by this work.

Finally, chapter 6 focuses on the limitations of the research and on recommended future work that addresses such limitations. Chapter 6 represents a guideline for future researchers who will be working on the area of the utilisation of DESs for post-combustion carbon capture processes. These guidelines are essential to evaluate the viability of any candidate DESs for this application domain.

Chapter 2: Utilization of Deep Eutectic Solvents in Carbon Capture: State of the Art Review

2.1 Overview

Chapter 1 presented the challenges facing the global community regarding global warming caused by CO₂ and other GHG emissions. It also summarized the CO₂ absorption capacity, mechanisms and performance of sorbents used, along with the advantages and disadvantages of the newly developed sorbents.

This chapter reviews the previous studies on the utilisation of deep eutectic solvents for carbon capture processes, and the operational and compositional parameters affecting the CO₂ absorption and desorption by deep eutectic solvents.

2.2 Summary

Two decades ago, deep eutectic solvents were developed to share similar features to ionic liquids but with advantages in terms of thermo-physical and transport properties, “green” and sustainability credentials, preparation cost, and efficiency for CO₂ capture via absorption¹⁴³. The review presented in this chapter focuses on the preparation methods, solvent selection and design criteria for CO₂ capture using deep eutectic solvents. In particular, the review presents an up-to-date review of methods used to characterize DES, and in particular, on techniques employed to study CO₂ absorption and desorption in DES-based systems.

This review shows that the compositional and operating parameters that affect CO₂ solubility in DESs are: hydrogen bond donor (HBD) to hydrogen bond acceptor (HBA) molar ratio, pressure, temperature, water content and viscosity. Also, according to

this review, instead of focusing on the use of ionic liquids as substitutes to amine systems, it is highly recommended to develop more sustainable and efficient CO₂ capture processes based on DES/NADES systems.

2.3 Introduction

The research in the field of deep eutectic solvents for carbon capture increased dramatically in the past two decades as shown in Figure 2-1. Although the area of research on the utilisation of DESs for carbon capture is still young, choline chloride-based DESs are the most efficient DESs so far among the different DESs utilised for carbon capture according to recent investigations ^{143, 144}.

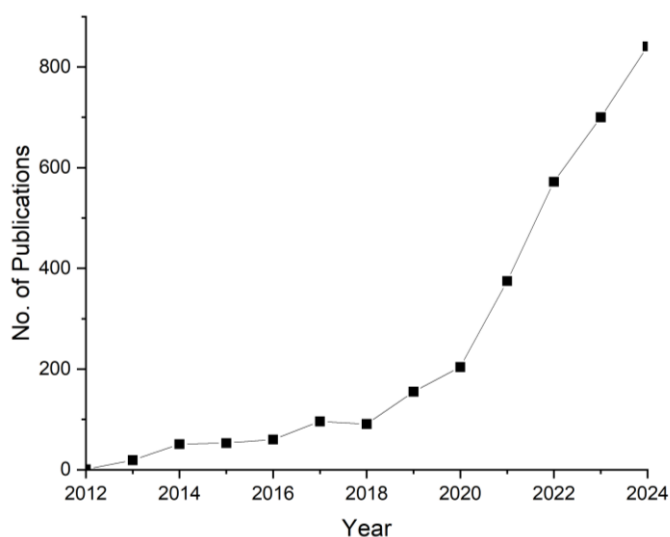


Figure 2-1 Number of publications containing “deep eutectic solvents for carbon capture” generated from Science direct database July 2024 ¹⁴⁵

Martinez *et al.* ¹⁴⁶ identified a minimum set of properties/factors (Table 2-1) which must be testified to validate the claim of suitability as a new alternative solvent for CO₂ capture, in particular, for gas absorption processes.

Table 2-1 Key properties of sorbents (adopted from Martinez *et al.* ¹⁴⁶)

Property	Effect on:
<ul style="list-style-type: none"> • Viscosity • Contact angle 	<ul style="list-style-type: none"> • CO₂ absorption capacity • Process design • Process efficiency
<ul style="list-style-type: none"> • Thermal stability • Density • Heat of reaction • Refractive index 	<ul style="list-style-type: none"> • Capital cost • Operation cost

The ideal sorbent should have good transport, rheological and thermo-physical properties along with a “green” environmental profile. The sorbent should be environmentally friendly, sustainable, biodegradable, non-toxic, non-corrosive, non-flammable and recyclable.

In this critical review chapter, we are going to investigate the viability of DESs as sorbents for CO₂ capture. Section 2-4 focuses on the classification and preparation of DESs. Section 2-5 highlights the environmental profile of DESs along with the corrosivity of DES-CO₂ systems as important parameters associated with CO₂ sorption processes in DESs. Section 2-6 explores the key thermophysical and transport properties that affect CO₂ absorption and desorption in DESs. Section 2-7 reviews the methods employed to measure CO₂ absorption and desorption in DESs. Section 2-8 critically summarises the data available in the literature CO₂ absorption and desorption some selected DESs and reviews the compositional and operating parameters that affect CO₂ absorption in DESs. The last section, section 2-9, presents the conclusions of this review along with future recommendations.

2.4 Classification and preparation DESs

2.4.1 Classification of DESs

DESs are categorised into four types according to the general formula $\text{Cat}^+ \text{X}^- z\text{Y}$ (Figure 2-2). Cat^+ represents a cation in a form of phosphonium, ammonium or sulfonium salt, X^- is usually a halide anion or a Lewis base, Y is generally a Brønsted or a Lewis acid, and z represents the number of molecules of Y ¹⁴⁷.

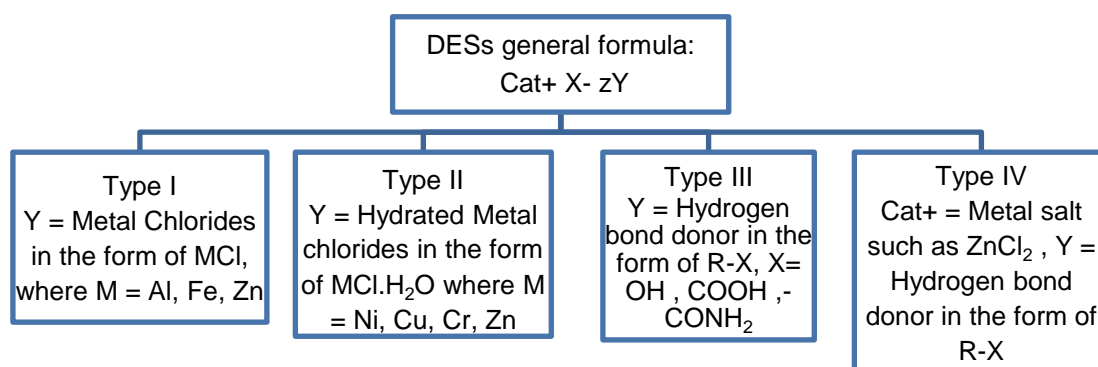


Figure 2-2 Types of deep eutectic solvents (DESs)

Type III DES systems are the most researched in the literature. They are generally composed of choline chloride as the hydrogen bond acceptor (HBA) combined with one or more hydrogen bond donors (HBDs) that interact through hydrogen bonds ¹⁴⁸.

The most important milestones in the development of deep eutectic solvents are presented in Figure 2-3.

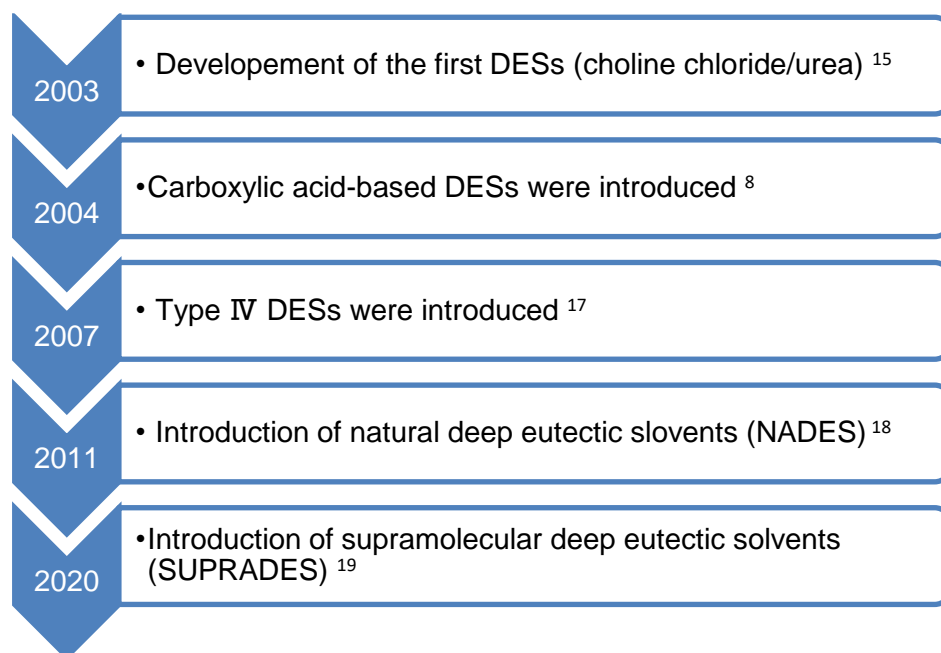


Figure 2-3 The most important milestones of the development of deep eutectic solvents ^{147, 132, 149, 150, 151}

2.4.2 Preparation of type III DESs

DESs are prepared by the combination of quaternary ammonium or phosphonium salts such as choline chloride with other HBDs such as carboxylic acids and amines at a specific temperature and mixing speeds. The melting point of a DES is below the melting points of each component of the mixture and lower than that of an ideal mixture ¹⁵². An example of the formation of a DES using choline chloride as the HBA and urea as the HBD is shown in Figure 2-4.

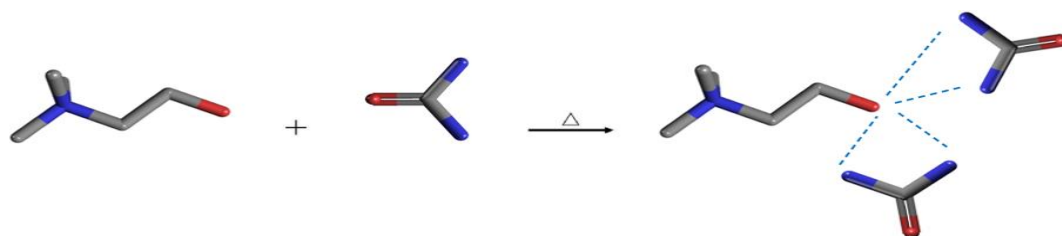


Figure 2-4 Schematic representation of the formation of the DES [choline chloride:urea] with HBA:HBD molar ratio 1:2. Figure modified from reference

153

DES systems can be synthesized by two main methods: a) the heating method and b) the grinding method ¹⁵⁴. The heating method is the most frequently used ^{155, 156, 157, 154, 134, 158, 159, 160}. It is based on mixing the two components (the HBA and the HBD), which are then heated at around 100 °C under a constant stirring rate until a homogeneous liquid is formed. The less-used grinding method has been used in the preparation of DESs in the pharmaceutical industry. It involves mixing and grinding the components at room temperature to produce a homogeneous DES. The most common HBAs and HBDs used to prepare DESs are summarised in Figure 2-5.

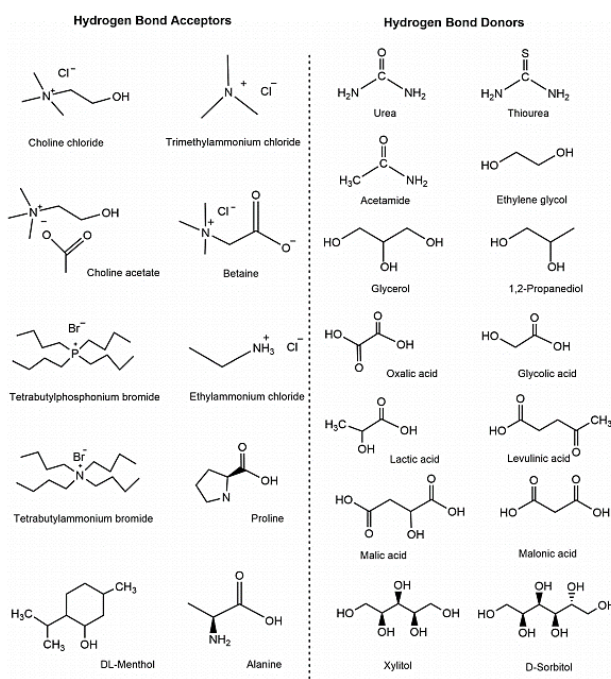


Figure 2-5 Most common hydrogen bond acceptors and hydrogen bond donors used to prepare deep eutectic solvents (adapted from Achkar . ¹⁴⁸)

2.5 Environmental profile and corrosivity of DESs

2.5.1 Toxicity of DES systems

DESs have been employed in many areas of research including, extraction methods, enzymatic reactions, and electrochemistry. Furthermore, DESs seem to be a less

toxic substitute for ILs. Since ILs exhibited high levels of toxicity against organisms of different trophic levels ¹⁶¹. In the same way, NADES are less toxic and environmentally friendly making them suitable for several many applications as new green technology media in cosmetic, pharmaceutical and food industries ¹⁶².

Wen *et al.* ¹⁶³ studied the toxicity of cholinium-based DESs consisting of choline chloride and acetate as HBA and glycerol, acetamide, ethylene and glycol urea as the HBDs against different microorganisms such as *hydra*, *allium sativum* (*garlic*, a plant) and *Escherichia coli*. Investigated systems showed inhibitory impacts on the microorganisms due to their interaction with the cellular membranes according to the molar ratios of DES components.

Cholinium and phosphonium-based DESs exhibited a toxic effect on shrimps that was greater than the components (HBD/HBA) of the DESs individually ^{139,164}. On the other hand cholinium-based, DES associated with glycerol, oxalic acid and glucose has low to medium toxicity in cell lines of humans and fish ¹⁶⁵. Furthermore, NADES are prepared by natural principal metabolites that are cheap, available and much greener as compared to ILs ¹³⁵.

2.5.2 Biodegradability of DESs

The biodegradability of eight different DESs was assessed by Wen *et al.* in their work in ¹⁶³ choline acetate and choline chloride-based as HBAs associated with four HBDs acetamide, urea, ethylene glycol and glycerol at molar ratios of (1:1, 1:2 and 2:1). The biodegradability of investigated DESs was experimented with using “the closed bottle test” to determine a ratio between the experimental value of biochemical oxygen demand (BOD) and the theoretical biochemical oxygen demand (ThOD). In Wen *et al.* in ¹⁶³ only two DES systems (reline and ChCl: acetamide) showed a biodegradable level lower than the IL system composed of [BMIm] [PF6] ¹⁶³.

In another biodegradability study, Radosevic .¹⁶⁵ defined choline chloride-based DES systems namely (ChCl:glycerol, ChCl:glucose and ChCl:oxalic) as “readily biodegradable DES systems” since they showed much lower biodegradability indices as compared to values obtained by Wen *et al.*¹⁶³.

From a preliminary simple scientific interest, DESs are now considered the next generation of sorbents; therefore, many studies are yet to be tracked. DESs as a new class of sorbents, being more biodegradable than ILs make them more viable for carbon capture processes.

2.5.3 Corrosivity of DESs systems

Corrosivity analysis for the DESs or any sorbent used for CO₂ capture purposes is important because corrosion is accounted for severe risk for processing units and the overall plant, where metallic plumbing, absorber columns, and other utilities are in direct contact with the absorbent.

Currently, two main corrosion measuring methods are used to measure the corrosivity of DES: the electrochemical method and the weight loss method.

2.5.3.1 The electrochemical method

The electrochemical method is widely used by many studies i.e.^{129, 166} to prepare the polarization values that indicate the corrosion resistance of the material in a corrosive environment. In this method, corrosion rate i is calculated based on the polarisation curve. Table below shows the corrosion rates of some selected DESs.

Table 2-2 Corrosion rates of some selected DESs and amines (benchmark sorbents)

DESs/Amine	Molar ratio/Concentration	corrosion potentials (V)	Corrosion rate (mm.year ⁻¹)	Reference
Choline chloride : Phenylacetic acid	1:2	-0.633	0.022	167
	1:3	-0.511	0.118	
	1:4	-0.521	0.278	
Choline chloride : Phenylacetic acid + CO ₂	1:2	-0.49	0.044	
	1:3	-0.493	0.267	
	1:4	-0.488	0.916	
Choline chloride: Levulinic acid	1:2	-0.43	0.027	166
Monoethanolamine	30%	-0.75	0.54	166
Diethanolamine	30%	-	0.24	168
Methyldiethanolamine	99%	-	0.35	169

In Altamash *et al.* work, Corrosion rates were calculated at different conditions of temperature, HBA:HBD molar ratio, and CO₂ concentration. However, the effect of water content in the system on the CR values was not taken into consideration ¹⁶⁷.

The same method was also used to study the corrosivity of choline chloride:levulinic acid -based DESs ¹⁶⁶. Results clearly show that choline chloride:levulinic acid -based DESs showed much less corrosivity than amines. However, the effects of water content, temperature, HBA:HBD molar ratio on the corrosion rate were not considered in Ullah *et al.* work ¹⁶⁶.

2.5.3.2 Weight loss method

Weight loss method is the second less-used corrosion measurement technique. Carbon steel, stainless steel, and mild steel are currently used in designing CO₂

capture absorption plants including the absorber and storage tank according to the CO₂ capture and storage VGB report ¹⁷⁰. Therefore, it is important to stress that the CRs and CPRs of DESs with these particular metals should be prepared in different scenarios of HBA: HDB molar ratios, water contents, CO₂ concentrations and temperatures to optimise the corresponding parameters on corrosion resistance rates.

An example of study of the corrosivity of a DES system under different conditions was published by Traviedi *et al.* ¹³³. In this work, metallic samples were weighted before and after the immersion on [MEA·Cl][Ethanoldiamine (EDA)] DES, based on the weight difference, the corrosion penetration rate (CPR) in millimetre per year was calculated after being immersed in the DES solution for 10 days along with 20% CO₂ loading. The CPRs of the EDA, MEA and DES solutions were 0.448, 0.385, and 0.124 mm.year⁻¹ in sequence, signifying that [MEA·Cl]: [EDA] = (1: 3) has high corrosion resistance and is thus anticipated to be more maintainable under actual industrial conditions.

On the other hand, several DESs exhibited high efficiency as corrosion inhibitors of mild steel ^{171, 172, 173} similarly, DESs were investigated as potential marine lubricants, surprisingly some DESs exhibited a very low corrosion rate with mild steel, nickel, and aluminium ¹⁷⁴.

In general, DESs showed lower corrosivities as compared with conventional amines; this significant difference has the benefits of decreasing capital costs and the operating costs of the absorption vessel and its auxiliary units in a CO₂ absorption system.

2.6 Thermodynamics and properties of DESs

2.6.1 Phase behaviour (definition of type III DES)

Nowadays there is a huge misconception about the definition of DES according to the most recent review by Martins *et al.* ¹²⁸. Most researchers limit their studies to the applications of DES in different domains rather than understanding the nature of the mixtures used whether it is DES or conventional mixtures. Only a few studies in the literature studied the nature of the interaction between the HBA and the HBD in the liquid phase using phase behaviour plots such as Rodriguez *et al.* work in ¹⁷⁵. The definition of the DES is based on hydrogen bond formation between the HBA and the HBD only is limited according to the recent reviews ^{132,128}. DES formation must only be defined according to the difference in freezing point of the prepared mixture to that of the theoretical ideal binary mixture of the HBA and the HBD. Therefore, we would like to introduce a more accurate definition of the DES based on “*eutecticity*” which defines the DES as a mixture between the HBA and the HBD at which $\Delta T_f > 0$ the larger the freezing point difference ΔT_f the stronger the interactions between the individual components as shown in Figure 2-6.

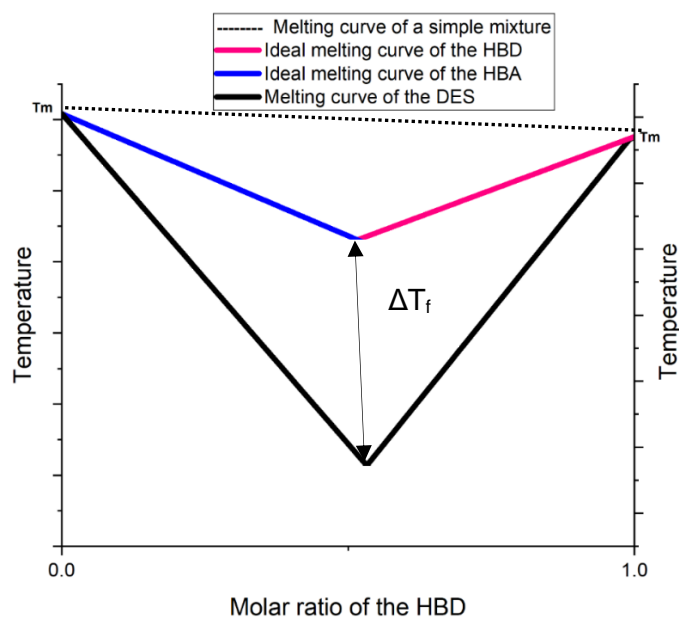


Figure 2-6 Generic phase behaviour plot for a DES system

The ideal melting curves of the individual components could be prepared experimentally by studying the fusion properties of a simple eutectic mixture of the individual components or could be estimated using thermodynamic models as per Fernandez *et al.* work ¹⁷⁶. Many researchers in the literature such as Abbott *et al.* in their work in ^{147, 132} reported the melting curves of the DESs without comparing them with the ideal ones. The most recent review on DES thermodynamics by Zhang *et al.* ¹⁴⁰ compared the freezing points of DESs with their components. However, to satisfy the definition of the DES stated above, the comparison must be made based on the ΔT_f by providing the solid-liquid equilibria phase diagram of each DES by plotting the ideal melting curves of the individual components against the ones of the DES. Hence, only ΔT_f determines whether the mixture is a simple mixture ($\Delta T_f < 0$) or eutectic mixture or deep eutectic mixture ($\Delta T_f > 0$), it is very important to understand the nature of the mixture, which is crucial for efficient selection, and design of the optimal DES for any proposed application.

2.6.2 Viscosity and Density

Density and viscosity are crucial properties to characterize any kind of absorbent including DESs. Density and viscosity are important properties used in the calculation of further thermodynamic properties using suitable equations of state (EOS) for these exotic mixtures. In the industrial development of chemical processes, EOS play a dominant role, especially in gas sorption processes that involve unique absorbent alternatives for conventional amines. Choline chloride-based DESs investigated in the literature have density values ranging between 0.98 –1.2 g.cm⁻³ at 298 K ¹⁶⁶. The density of some choline chloride-based DESs is summarised in Table 2-3.

Table 2-3 Density of selected DESs and amines (benchmark sorbents) as a function of temperature and water

HBA:HBD	Molar ratio	T (K)	Density (kg.m ⁻³)	Density of hydrated absorbent (kg.m ⁻³)	Water mass fraction	Ref.
ChCl:Urea	1:2	298-373	1.951-1.163	1.121-1.05	0.1-0.9	177,178
ChCl:Glycol	1:2	293-363	1.26-1.18	1.202–1.062	0.1-0.9	156
ChCl:Ethylene glycol	1:2	298-323	1.132-1.103	1.131-1.031	0.1-0.6	119
ChCl:Levulinic acid	1:2	298-363	1.137-1.09	-	-	166
Betaine:Lactic acid	1:2	293-363	1.21-1.17	-	-	179
Alanine:Malic acid	1:2	293-363	1.41-1.36	-	-	179
Monoethanolamine	99%	298-363	1.016-1.0	1.0-0.995	0.1-0.7	180
Diethanolamine	99%	313-333	1.085-1.07	-	-	181
Methyldiethanolamine	50%	283-353	1.051-1.004	-	-	182

Density and viscosity of DESs found to decrease with increasing temperature and water content simultaneously according to ^{156,158,183, 184}. The density of DESs is generally declining linearly with increasing temperature at temperatures lower than 333 K for carboxylic acid-based DES ¹⁵⁴ and up to 343 K for imidazole-tailored DESs ¹⁵⁸. It is worth mentioning that density dependency on the temperature of any DES is subjected to the range of temperature at which density is measured. For example, Leron *et al.* in ¹⁷⁷ reported a linear dependency of density on temperature for reline and its aqueous mixtures at 323 K. However, Anita *et al.* in ¹⁷⁸ reported a quadratic relation between density at the temperature of reline at higher temperatures up to 363 K. Therefore, the range of temperature at which density is measured determines its behavioural model whether it is linear or quadratic or another model.

The viscosity of DESs is a very important feature that has been investigated by many researchers ^{156,158,183,184}. The viscosity of some choline chloride-based DESs is summarised in Table 2-4. The gas solubility performance is enhanced at low-temperature levels, however, viscosity increases with decreasing the temperature which might bring major concerns regarding increasing the transportation (pump requirements) for any fluid.

Table 2-4 Viscosity of choline chloride-based DESs and amines (benchmark sorbents) as a function of temperature and water

HBA:HBD	Molar ratio	T (K)	Viscosity (mPa.s)	Viscosity of hydrated absorbent (mPa.s)	Water mass fraction	Ref
ChCl:Urea	1:2	293-363	1371-19.9	73.3-6.18	0.1-0.9	^{119,127}
ChCl:Glycol	1:2	293-363	1000-19.6	669-0.4	0.1-0.9	^{119,127}

ChCl:Ethylene glycol	1:2	298-323	40-8.6	1.9- 1.3	0.6-0.9	119,127
ChCl:Levulinic acid	1:2	298-348	171.3-16.1	-	-	166
ChCl:Xylose	1:1	293-373	10 ⁵ – 922	220 - 140	0.1-0.9	185
Betaine:Lactic acid	1:2	293-363	10 ⁴ -10 ³	-	-	179
Alanine:Malic acid	1:2	293-363	10 ⁶ -10 ²	-	-	179
Monoethanolamine	99%	293-423	24.0-0.806	2.9- 0.77	0.1-0.7	186
Diethanolamine	99%	283-333	655-22	21.44-2.8	0.8	180
Methyldiethanolamine	99%	283-353	77.19-7.15	32.11-3.26	0.75	180,182

As can be seen in Table 2-4, the viscosity of DESs/NADES decreases considerably with both temperature and water content with Newtonian behaviour as reported by Paiva *et al.* in ¹⁸⁵. The high viscosity of the investigated NADES system might be considered a major disadvantage of such systems since it will increase the capital and operation costs subsequently.

The viscosity of the classical ILs is much higher as compared to glycerol-based DESs as reported by Sarmad *et al.* in their work in ¹²⁷. Tetraethylammonium chloride (1:2) and tetrapropylammonium chloride (1:4) exhibited a higher CO₂ absorption capacity and reduced viscosity when functionalised by adding ethanolamine. By functionalization, the CO₂ absorption capacity of DESs improved from 1400 to 3200 mmol.kg⁻¹ DES for TPAC/ EA with a molar ratio of (1:4), enhancing the performance of NADES as compared with that of the ILs. The results also demonstrated that adding traces of water to BTMA/GLY (1:2) decreases the viscosity from 0.716 to 0.020 Pa.s.

on the other hand, the solubility of CO₂ increased from 260 to 330 mmol/kg correspondingly. The CO₂ absorption decreased beyond that limit, due to the reduced CO₂ solubility in water.

This important finding was also reported by Ren . in their work in ¹⁵⁶, adding traces of water to NADES of glycerol (Gly) and hydrophilic L-arginine (L-Arg) systems leads to a high reduction in the viscosity from 1.6 to 0.05 Pa.s. Again, adding water remarkably enriched the solubility of CO₂ consequently as compared with concentrated DES. The dynamics phase transfer behaviour exposed the correspondence of CO₂ solubility on viscosity and temperature that fit with the Arrhenius model equation. Altamash *et al.* in their work in ¹⁶⁷ reported another non-Newtonian behaviour of phenylacetic acid-based DES; both Herschel-Bulkley and the Bingham plastic models well define the behaviour of the flow of ChCl:PhoAc DESs at molar ratios (1:2 -1:4).

As we can see here the viscosity of the DESs is ranging from high to low, some DESs showed a Newtonian behaviour while others exhibited a non-Newtonian behaviour with different rheological models. The high viscosities and the non-Newtonian behaviours might be considered major disadvantages of some DES systems since they will increase the capital and operation costs subsequently. It is worth-mentioning that, the effect of water content on density and viscosity of ChCl:LvAc DESs was not taken into consideration in previous studies. Therefore, it is highly recommended to study the effect of water content on ChCl:LvAc DESs, also the rheological properties of ChCl:LvAc DESs must be known for a proper selection and design.

2.6.3 Thermal stability

Thermal stability is a very important factor associated with the absorbents utilised for capturing CO₂ from the flue gas at high temperatures. Many studies in the literature ^{155, 157, 159, 167} investigated the thermal stability of DESs using thermo-gravimetric

analysis (TGA). In most studied DESs compositions, single-step degradation behaviour with different slopes was observed. For example, choline chloride: Levulinic acid DES with (1:2) HBA:HBD molar ratio and no added water exhibited high thermal stability at temperatures up to 180 °C as reported by Mellado *et al.*¹⁸⁷ and Ullah *et al.*¹⁶⁶ respectively. Similarly, Altamash . (39) studied the thermal stability of phenylacetic acid-based ChCl: PhoAc with molar ratios of (1:2, 1:3 and 1:4), investigated DESs showed high thermal stabilities to temperatures up to 127 °C without having any decomposition issues.

Currently, CO₂ absorption and desorption by monoethanolamine (MEA) take place at temperatures from 40 °C and 120 °C respectively at the atmospheric pressure in most of the industrial and pilot plants^{188, 189, 170, 190, 191, 34}. Since DESs are stable at this range of temperature, this makes investigated DES systems that exhibited high thermal stability more convenient for post-combustion CO₂ absorption processes.

On the other hand, choline chloride and carboxylic acid-based DESs are degraded with time and temperature due to self-esterification reaction between the hydroxyl group of choline chloride and carboxylic acids regardless of preparation method according to Rodriguez *et al.* in¹⁷⁵. Self-esterification of these DESs reached up to 35 mol % when they are stored for a couple of months. Therefore, the shelf life of this family of DESs is questionable, more studies on the degradation of DESs are highly recommended for all families of DESs at which such degradation reactions might occur.

2.6.4 Refractive Index

Refractive index (RI) is the measure of the electronic polarization molecules that can give important indications to identify the behaviour of molecules in solution according to the forces between them¹⁵⁴. DESs composed of choline chloride and carboxylic

acids have larger RI values as compared with other ILs. DES follow a linear trend in the range of temperature with RI values of 1.47 –1.^{53, 154, 192, 132}.

2.6.5 Contact Angle

The contact angle is a significant tool to describe the wettability or adherence of a liquid droplet on a metal surface ¹⁹³. The contact angles of ILs with some selected metals have been studied by many researchers ^{194, 195, 196, 171}. Whereas, only a few studies ^{167,174} have investigated contact angles of DESs with selected metals as summarized in Figure 2-7. In Altamash . study ¹⁶⁷ –red bars in Figure 2-7 - contact angle between phenylacetic acid: choline chloride (1:2) DESs and copper, brass, carbon steel and stainless steel were studied at 20 °C.

The copper surface exhibited the lowest contact angle of 36.71° while the contact angle between copper and reline (1:2) is the smallest contact angle value reported in the literature of 28.7° at 25 °C as per Abbott . in ¹⁷⁴.

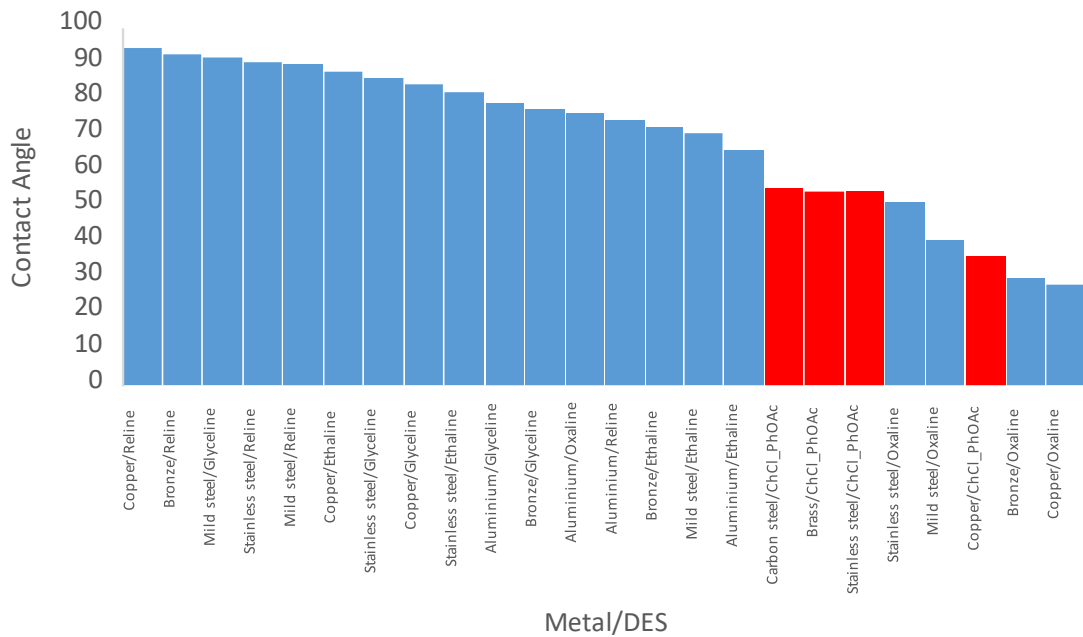


Figure 2-7 The contact angle between DESs and selected metals

2.7 CO₂ absorption and desorption measurements for DESs

Currently, there are three main techniques used to measure the solubility of CO₂ in DESs and sorbent regeneration as well, these are:

2.7.1 Weight-gain method

In this method, the absorption of CO₂ in the DES is measured using a thermogravimetric pressure balance that is incorporated with a control system for monitoring and controlling real-time data i.e. pressure, temperature, and weight. High precision balance is used in this set, which is designed to operate at pressures up to 109 bar^{127, 155, 197}. The CO₂ desorption tests cannot be done on this set which is considered the main limitation of this technique.

2.7.2 High-pressure cell method

Many researchers used this method such as ^{155, 156,157, 134, 158, 133, 198}. In this method, a known mass of DES is placed in the absorption bottle (inner radius around 10 mm) while CO₂ gas is bubbled inside the bottle. Absorption equilibrium is reached once the mass of the absorption bottle remains constant for more than 2 hours. The main limitation of this absorption system is that it does not provide real-time data to study the absorption/desorption dynamics. Also, this method does not provide any data about the residual amount of CO₂ after depressurising, hence, it does not allow to study CO₂ regeneration process and does not give any information about the nature of CO₂ absorption whether it is chemical or physical absorption.

2.7.3 Measurements using a vapour-liquid equilibrium absorption rig

The vapour-liquid equilibrium absorption rig (VLE) is one of the common techniques used for this purpose in which, CO₂ is absorbed by direct contact with a liquid phase DES system. In this system, CO₂ is injected into a pressure vessel containing the DESs at a certain temperature and pressure. The VLE absorption rig has been widely used to measure the CO₂ absorption capacity of different absorbents at different conditions of temperature and pressure as per Figure 2-8.

The VLE rig consists of a buffer tank, which could be smaller in volume as compared to the VLE vessel ¹¹⁹. Both vessels are fitted with pressure gauges and valves to monitor, and control applied absorption pressure. An incubation heater with high accuracy is normally used to maintain the temperature of the system at a certain point.

The VLE absorber is a typical stainless-steel pressure vessel that is provided with pressure valves to control the flow of the gas on the inlet -from the buffer tank- and the outlet towards the release valve. To perform the test, N₂ gas is used to purge the VLE vessel and then incubated at the desired experimental temperature through a

thermally controlled setup until thermal equilibrium is reached. DES of known mass is then loaded into the VLE absorber. The system must be satisfactorily stirred to confirm that the temperature distribution inside the absorber is uniform. After thermal equilibrium –normally within 2 hours - CO₂ is pressurised from the buffer tank into the VLE vessel to the desired test level. The system is maintained under test conditions (temperature, pressure and stirring rate) until equilibrium is reached. Equilibrium is the thermodynamic state at which the pressure inside the VLE vessel remains constant for a while ¹¹⁹.

To ensure the validity of results generated from the VLE rig, baseline conditions of the systems must be determined before conducting any absorption measurements, to ensure that the absolute pressure drop in the system is only due to the absorption by the DESs and it is not due to leakage or any other reason. Baselines can be obtained by running blank runs of CO₂ at constant temperatures and monitoring pressure drop in the system until it reaches equilibrium. Absorption isotherms must be compared to baseline conditions before calculating the absorption capacity of the DES or any sorbent in general. Mirza *et al.* in their work in ¹¹⁹ validated obtained results from the VLE rig in Figure 2-8 by measuring CO₂ absorption capacity in water at 40 °C. However, this approach does not give enough information about all the reasons behind the pressure drop in the system i.e. leakage in the system and not limited only to CO₂ absorption. On the other hand, this set allows studying the effect of stirring on CO₂ absorption unlike the other methods below, it might also help to nature of the reaction between CO₂ and the sorbent whether it is physisorption or chemisorption as the amounts of residual CO₂ and spontaneously released can be calculated from the weight gained during CO₂ absorption and the weight lost during depressurising.

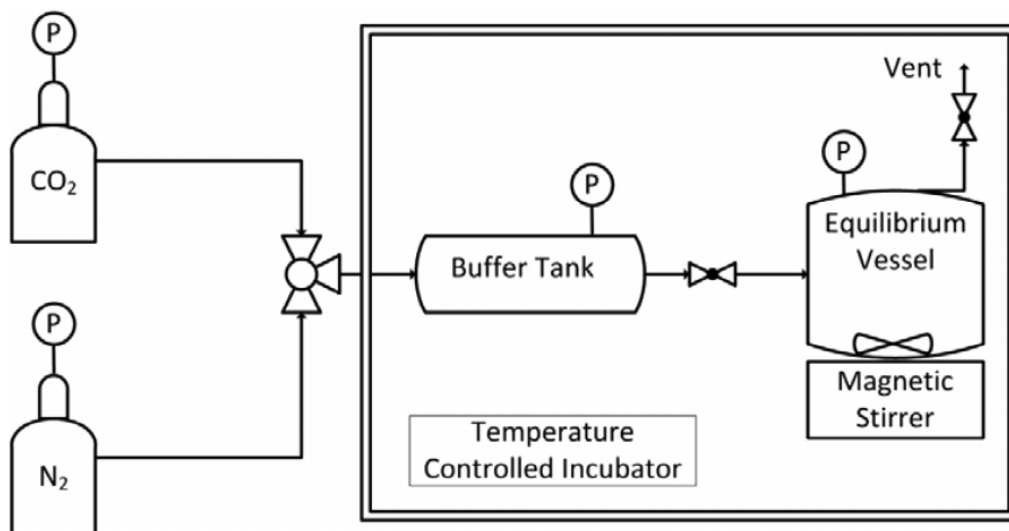


Figure 2-8 VLE rig components (adapted from Mirza . ¹¹⁹)

2.7.4 Sorbent regeneration

The reversibility of the sorption processes (CO₂ absorption and desorption) of sorbents used for CO₂ capture is a very significant parameter that determines the suitability of selected solvents ¹⁹⁹. In industrial absorption processes i.e. CO₂ absorption using MEA, the rich amines stream that contains CO₂ is taken to the desorber which usually operates at pressures ranging between 1.5 – 1.8 atm and generates steam from the reboiler at the bottom of the column at temperatures between 100 – 120 °C ²⁰⁰. Generated steam comes in counter-direction contact with the rich amines stream, which enters from the top. After the mass transfer takes place in the desorber, CO₂ is diverted to the steam stream that exits at the upstream part of the desorber. However, on the laboratory scale, a nitrogen stream at high temperatures was used for CO₂ desorption. Chemat . ¹³⁰ studied the regeneration process of L-arginine -based DESs L-arginine (L-Arg) and glycerol of (1:6) molar ratio. The CO₂ desorption tests were performed by bubbling nitrogen current at 100 °C for 80 min to release CO₂. The molar ratio of CO₂ has slightly decreased from 0.36 to

0.32 mol CO₂/mol DES using five different sets of the system under investigation. However, in this set, the weight reduction might be due to water vaporisation as well and not limited to releasing CO₂. Apparently, during the five-sequential absorption/desorption sets the solubility of CO₂ and the rapid sorption rates were well sustained, indicating that such a DES system could be recycled for the CO₂ capture with high rates since the absorption/desorption kinetics of CO₂ absorption by glycerol /L- arginine DES system was extremely reversible.

Only a few studies have considered and investigated the regeneration of DES systems utilised for CO₂ absorption so far, more research is highly needed in this area using both quantitative and qualitative approaches to assess the viability of each DESs for CO₂ capture purposes.

2.7.5 Sorbent selectivity

Selectivity is a significant property when screening and suggesting DESs for carbon capture purposes where the flue gas is composed of a mixture of gases. According to the recent review ¹⁴³, there are only 2 published works that reported the selectivity of DESs towards CO₂ over other gases. Deng . in their work in ²⁰¹ reported a selectivity value of 97 (NH₃/CO₂) of Guanidine isothiocyanate: Acetamide (1:4) DESs at 5.768 bar and 303.15 K. While Yan *et al.* in their work in ²⁰² reported a selectivity value of 20 (CO₂/ NH₄) of a “DESs” composed of choline chloride:MEA (1:5) at 12.7 bar and 313.15 K. It is worth mentioning that, the selectivity of DESs towards CO₂ over N₂ has not been considered in most of the published work in literature. Therefore, this aspect is considered one of the most important research questions that were investigated thoroughly in chapter 4 of this work. More extensive research is highly needed in this important aspect of assessing the potential DESs for carbon capture processes.

2.8 Review of CO₂ absorption and desorption using DESs

The CO₂ absorption capacity of 29 choline chloride-based DESs is ranging between 0.002 – 0.4 (mole fraction) at 100 kPa and 25 °C which is higher than CO₂ solubility values of ILs as summarised by Marcus . in their review in ²⁰³. Similar findings were reported by many other researchers, i.e. in Leron *et al.* work ¹⁵⁵ CO₂ absorption capacity in choline chloride and ethylene glycol (1:3) DESs were examined at pressures up to 60 bar and a temperature range between 30 – 70 °C. Prepared solubility values of this system are falling in the range of the absorption of CO₂ in [Emim] and [Bmim] based ILs.

Task-specific ternary DESs systems including choline chloride and glycerol associated with three different super bases as potential sorbents for carbon capture processes were investigated by Sze *et al.* in ¹³⁴. It found that the DES system is composed of choline chloride (ChCl), glycerol (Gly) and 1, 5-diazabicyclo [4.3.0]-non-5-ene (DBN) ChCl:Gly:DBN of (1:2:6) have the highest absorption capacity among many other DESs. The CO₂ absorption capacity of this system is 103 mg of CO₂ per gram of sorbent. More importantly, the desorption process was easy to be performed by bubbling N₂ at mild heat. On the other hand, the system has some limitations related to its rheological characteristics; the non-Newtonian behaviour has been observed which limits the mass-transfer coefficient and rates by the Stokes–Einstein–Debye model. In addition, the effect of water content on the CO₂ absorption capacity of this DES family was not taken into consideration. Finally, 35 minutes was the time assumed for the system to reach equilibrium which is the state at which the weight of the sample inside the pressure cell remains constant. The authors claimed that 35 minutes is sufficient to reach equilibrium, however, according to their results -in which CO₂ uptake continued increasing with time- the system did

not reach the equilibrium. However, these disadvantages did not avoid exceptional CO₂ absorption capacity as high as 2.4 mmol. gram⁻¹, these absorption rates beyond most branded ILs.

Several DESs composed of monoethanolamine MEA associated with of molar ratio (4:1) were examined for their absorption performance of CO₂ at 25 °C and 1 atm in Cao *et al.* work in ¹⁵⁸. CO₂ absorption uptake was up to 21.4 wt. % that is larger by 13% than that of the % MEA (30 wt. %). DES acts as an intermediate to enhance CO₂ absorption through the formation of hydrogen bonds through the hydrogen bond mechanism. The overall heat of CO₂ solubility is marginally greater than that of 30 wt. % MEA, due to hydrogen bonds between DESs and ILs that are also responsible for the overall heat of absorption. In addition, the CO₂ absorption test for the 30% MEA was performed for less than 4 minutes only while the test lasts for up to 50 minutes for the DESs. To make a fair comparison between the CO₂ absorption capacity between the MEA and prepared DESs the equilibrium time should be similar in both cases, furthermore, according to the absorption curves, it can be seen that the VLE equilibrium was not reached in both cases. Finally, the baseline conditions were not identified or reported in their work.

Statistical and experimental analysis of the solubility of CO₂ in allyl triphenylphosphonium bromide-trimethylene glycol DES system in a predictive quadratic regression model was studied by Ghaedi . ¹⁶⁰. DESs were prepared in different molar ratios of (1:4, 1:10 and 1:16) with different water contents. The test was designed by adopting the Taguchi-L18 design of experiment (DOE) method, the input factors were molar ratios, temperature, pressure and water content in the system. While the main yield factor was a mole fraction of absorbed CO₂ (X_{CO_2}) on a molality basis. The pressure was the most important factor in the solubility of the CO₂

in the DESs, while temperature had the lowest weight on X_{CO_2} according to the analysis of variance ANOVA results. Again, the absolute pressure drop calculations were not precise since the pressure drop in the system was assumed to be only due to the CO_2 absorption. Without determining the leakage rate in the system, this assumption is not precise.

Magugeri *et al.* in ²⁰⁴ studied choline chloride (ChCl):levulinic acid (LvAc) DESs system, LvAc as HBD found to be non-toxic fully and biodegradable, that may be prepared from biomass at cheap prices. While Ullah *et al.* ¹⁶⁶ utilised ChCl:LvAc DES of (1:2) molar ratio system for CO_2 absorption purposes. The DES system under investigation showed favourable solubility of approximately $2.25 \text{ mmol. gram}^{-1}$ of DES sample at $20 \text{ }^\circ\text{C}$ that achieved at 30 bar. The solubility of CO_2 in ChCl:LvAc DES increases with pressure and decreases with temperature. Whereas, Lu *et al.* in their work in ²⁰⁵ studied ChCl: LvAc DES but with an increased molar ratio of the HBD up to 1:5, the solubility of CO_2 increased with increasing the HBD molar ratio i.e. LvAc in this case. However, the effect of the presence of water in the system was not taken into consideration in all the previous cases of these particular DESs. According to our review, the impact of water in this system should be considered in future studies considering that the individual components of these DESs are highly hygroscopic ¹⁸⁷. Furthermore, the CO_2 regeneration process of these particular DESs, the effect of stirring speed on the CO_2 absorption capacity along with the selectivity of ChCl:LvAc must be studied to evaluate the viability of ChCl:LvAc DES for CO_2 capture purposes.

Choline Chloride:phenylacetic (PhoAc) acid-based DES system exhibited impressive characteristics for the CO_2 solubility at different molar ratios ¹⁶⁷. ChCl:PhoAc of (1:2) molar ratio captured 2.1 mol.kg^{-1} at $35 \text{ }^\circ\text{C}$ and 30 bar. The higher molar ratio of the

same system with a higher molar ratio of (1:3) captured 3.35 mol.kg^{-1} under the same conditions of pressure and temperature.

In this recent study conducted by Ren *et al.* ¹⁵⁶ NADES of glycerol (Gly) and hydrophilic L-arginine (L-Arg), DES were prepared at different molar ratios (1:4 – 1:6) and then examined for their CO₂ absorption capacity. The solubility of CO₂ in DES was performed at different conditions of pressure temperatures, the (1:6) molar ratio showed the highest CO₂ absorption capacity of 0.511 mol of CO₂ per mol of DES at 60 °C.

2.8.1 Thermodynamic properties of CO₂ absorption using DESs

2.8.1.1 Henry's Law Constant (HLC)

The thermodynamic driving force behind CO₂ absorption by DESs can be explained by the principles of HLC. The smaller the value of the HLC the higher the solubility of CO₂ in DESs ^{155, 118, 206}. For example, ²⁰³ reported that choline chloride and levulinic acid (1:2) DES have the lowest HLC of $0.145 \text{ MPa kg.mol}^{-1}$ at 40 °C and 0.1 MPa among other studied NADES systems. On the other acetylcholine chloride and levulinic acid has the lowest HLC of $1.79 \text{ MPa kg.mol}^{-1}$ at 30 °C among phosphonium-based DES. Although levulinic acid was the HBD in both cases, and both tests were conducted at the same conditions of temperature and pressure, however, cholinium-based DESs exhibited higher CO₂ uptake although the test was at a higher temperature as compared to the phosphonium-based DESs experiment. This might indicate that cholinium-based DES might have a higher absorption capacity as compared to phosphonium-based DESs.

In Mirza *et al.* work ¹¹⁹, the corresponding HLC of the absorption of CO₂ in choline chloride-based DESs were studied. DESs compositions were composed of choline

chloride as HBA associated with urea (reline) (1:2), with ethylene glycol (1:2) and with malic acid and ethylene glycol (1.3:1:2.2). Experiments were performed under pressures up to 160 kPa and temperature ranges between 36 °C - 56 °C. HLC for these systems was ranging between 3.7 - 6.1 MPa kg.mol⁻¹ determined under the aforementioned conditions of temperature and pressure.

Cholinium-based DES systems associated with ethylene glycol, malic acid, and guanidine carbonate, as hydrogen-bond donors with a molar ratio of (16.3:2:1) were studied¹⁸³. The values of HLC of CO₂ at 40 °C for investigated absorbents indicated that DES composed of 10 wt.% arginine have the smallest HLC value of 1.28 MPa kg.mol⁻¹ and the corresponding highest CO₂ absorption capacity among all investigated sorbents on that study.

2.8.1.2 Enthalpy, Gibbs energy and entropy of DESs-CO₂ systems

The CO₂ absorption enthalpy, Gibbs energy and entropy are very important parameters to predict the interaction between DES absorbent and gas phases. The values of these thermodynamic properties obtained by Rahman .¹¹⁹ for reline, ethaline and malinine exhibited exothermic processes with nonspontaneous solubility of CO₂ in investigated systems. In detail, negative values of the enthalpy indicate a robust intermolecular bond between the DESs and CO₂. While the negative figures of the entropy, show that the dissolution of CO₂ in DES results in a more ordered system. Finally, a positive increase in Gibbs free energy indicates nonspontaneous desorption of CO₂ in DESs. Similar conclusions were deduced by Anderson *et al.*¹¹⁶, Akachuka *et al.*²⁰⁵ and many other studies for other DESs.

On the other hand, the value of the enthalpy physisorption of CO₂ in ILs is approximately -20 kJ·mol⁻¹ while the enthalpy of functionalized amino ILs and CO₂ is about -80 kJ· mol⁻¹¹⁹⁹. Whereas, the enthalpy in the DES-CO₂ systems is much

greater than that of the amine ILs as reported by Marcus *et al.* in their review in ²⁰³. The enthalpy value of (choline chloride: levulinic acid) was found to be much greater than $-15.35 \text{ kJ} \cdot \text{mol}^{-1}$ ²⁰⁵. Therefore, we could confidently conclude that higher CO₂ solubility could be accomplished at high enthalpy values.

2.8.2 The compositional and operating parameters that affect CO₂ solubility in DESs

CO₂ absorption in DESs is subjected to many parameters among which the optimal solubility could be achieved which are

2.8.2.1 HBD to HBA Molar Ratio

DES are prepared at different molar ratios of HBD to HBA, generally, the solubility increases with increasing the molar ratio of the HBD to some specific level (at a constant temperature, pressure, and water content). For example, Li *et al.* ²⁰⁷ found that the molar ratio of choline chloride:urea (1:2) has the highest CO₂ absorption rate compared with (1:1.5 - 1:2.5) molar ratios. Most studies in the literature concluded the same result ^{156, 119, 144, 160, 203, 205}.

2.8.2.2 Operating Pressure

Most studies in the literature proved that high CO₂ solubility is achieved at increased pressure. For example, Leron *et al.* ¹⁵⁵ investigated the absorption of carbon dioxide in a DES system composed of choline chloride and ethylene glycol of (1:2) molar ratio for the temperature up to 70 °C and pressures up to 60 bar. The absorption capacity of the gas in the DES was found to increase with pressure as many other studies were done by ^{156, 119, 144, 160, 203, 207}. This is due to the physical absorption nature of CO₂ in DESs as Henry's laws constant increases steadily with pressure ^{207, 208}. Therefore, higher values of CO₂ absorption capacity of DESs can only be achieved at high pressure which increases the operation cost in this case as compared to the amines

which exhibit high CO₂ absorption capacity under atmospheric pressure due to chemisorption and the physisorption interaction with CO₂.

2.8.2.3 Operating Temperature

The solubility of CO₂ in the sorbent decreases as the temperature increases as reported by many researchers^{155, 118, 119, 133}. For example, CO₂ uptake of choline chloride: ethylene glycol (1:2) DES decreased from 3.13 mol.kg⁻¹ to 2.2 mol.kg⁻¹ when the temperature of absorption increased from 40 to 50 °C respectively at a constant pressure of 6 bar¹³³. The reduction in the CO₂ absorption capacity in DESs with increasing temperature is directly related to the exothermic reaction nature of the dissolution of CO₂ in DESs as explained in section 2.8.1.2 above. Therefore, increasing the temperature of the CO₂ dissolution in DESs reduces the absorption capacity.

Currently, CO₂ capture by monoethanolamine (MEA) takes place at temperatures up to 50 °C and atmospheric pressure¹⁸⁸. Hence, it is highly recommended to investigate CO₂ solubility in DESs within this range of temperature.

2.8.2.4 Water Content

Earlier studies have shown that the viscosity of DES decreases with increasing water content¹⁸⁴, as can be expected, decreasing the viscosity will have an important effect on the capital cost, and on the price of the carbon captured. For example,²⁰⁹ investigated the solubility of CO₂ in butyl methyl imidazolium nitrate ([bmim][NO₃]) and hydroxypropyl methylimidazolium nitrate ([hopmim][NO₃]) which was found to be influenced by water content in the system. The solubility of CO₂ in the bulk solution decreases with increasing the water concentration in the system; however, at very

low water concentrations, the CO₂ solubility is slightly higher compared with the water-free DES.

Similarly, the CO₂ absorption capacity increases (HLC decreases) with increasing water content in choline chloride: glycerol (1:2) DES system at 30 °C¹⁸⁴. However, this behaviour was not detected at temperatures above 35 °C. On the other hand, CO₂ solubility in DESs is directly affected by water content, i.e. for amine-functionalized anion-tethered ILs with tetra-alkyl phosphonium cations in a reversible way. The presence of water in the DES-CO₂ system is considerably reducing the viscosity of both the CO₂-saturated and pure ionic liquids but causes only a small decline in the CO₂ absorbance by ILs²¹⁰.

Interestingly, the aqueous solutions of choline chloride-based DESs have higher CO₂ absorption capacity than choline chloride-based DEs as reported by Zhang *et al.* in their recent review in¹⁴⁰. Many studies did not investigate the impact of the presence of water in the DESs on the CO₂ solubility such as²⁰⁵. Also, the consequences of water on the CO₂ absorption/desorption processes in choline chloride-based DES at elevated pressures have not yet been studied. Therefore, more investigations in this area of research are highly needed.

The optimal water content that gives the highest CO₂ solubility along with the lowest viscosity should always be selected, regarding the other conditions of temperature, pressure and the molar ratios of the CO₂ absorption/desorption system.

2.9 Conclusion

DESs are among the most favourable alternatives to overcome conventional amines and ILs for carbon capture. DESs are greener and more benign sorbents for CO₂ separation than ILs due to their biodegradability, nontoxicity and low price^{135, 140}.

This critical review has distinctive importance to the researchers who look for broad classification, preparation, physicochemical, transport, and greenness characteristics of DESs along with their carbon capture performance. Furthermore, it summarizes the key and optimal parameters that affect CO₂ absorption and desorption processes in DESs. While the available theoretical and experimental investigations are still limited, the available CO₂ solubility data in the DESs are reported along with the limitation of each study by highlighting the gaps in the literature.

Based on our review we would suggest that the selected sorbent shall be green in the first place, whilst equilibrium CO₂ capacity is a key basis of process performance, transport properties (e.g., viscosity) and other thermophysical properties (e.g., thermal stability) have a major effect on the capital and operation costs, and thus on the cost of the carbon captured. The main contribution of this work is the highlight of the minimum set of thermophysical, kinetic parameters and environmental profile of any potential sorbent these must be reported to justify the claim of viability for the current and the proposed sorbents for carbon capture processes.

The compositional and operating parameters that affect CO₂ solubility in DESs have been highlighted in terms of higher HBD to HBA molar ratio to some specific level, increased pressure, decreased temperature, and the optimal water content that gives the highest CO₂ solubility along with the lowest viscosity. Furthermore, the corrosivity, recyclability and selectivity of any potential sorbent must be evaluated and assessed.

All these aspects were extensively investigated in Chapters 3 and 4 respectively to evaluate the viability of choline chloride:levulinic acid-based DESs for carbon capture processes.

Finally, based on our review, it is highly recommended to develop more efficient and greener technologies using DESs and (NADES) for CO₂ capture rather than focusing mainly on developing ionic liquids and conventional amine systems.

Chapter 3: Characterisation of Choline Chloride:Levulinic Acid-Based Deep Eutectic Solvents

3.1 Overview

This chapter presents a comprehensive characterisation of choline chloride: levulinic acid deep eutectic solvents. The chapter contains the description of the techniques employed in the characterisation of the DESs, while the discussion of the results offers insights into the phase behaviour of the DES system and how important properties vary with operating conditions and composition. Supplementary characterisation information and support data are presented in Appendix A.

3.2 Summary

In the present work, DESs were prepared by using choline chloride (ChCl) as a hydrogen bond acceptor (HBA) with levulinic acid (LvAc) as a hydrogen bond donor (HBD). For the first time in the literature, the formation of ChCl:LvAc DESs at was verified by investigating the phase behaviour/diagram of ChCl:LvAc mixtures. The basic physicochemical properties of ChCl:LvAc DESs were measured at different conditions of temperature, HBA:HBD molar ratio, and water content. The prepared DESs were characterised via density and viscosity measurements, thermogravimetric analysis (TGA), FTIR spectrophotometry, and corrosivity tests. ChCl:LvAc DESs showed physicochemical properties comparable to other DESs reported in the literature. The results obtained show that ChCl:LvAc DESs may be useful for engineering applications including but not limited to carbon capture processes.

3.3 Introduction

Despite the potential wide range of applications for DESs that have been reported over the past two decades, the characterisation of DESs is frequently disregarded, making it difficult to comprehend their nature and develop precise and reliable thermodynamic models to describe them, such models are crucial for the conceptual and design phases of new industrial processes²¹¹. The experimental data presented and discussed in this chapter tries to close this gap in the literature for the levulinic acid DES system.

Some researchers^{166,212} prepared and partially characterised choline chloride (ChCl):levulinic acid (LvAc) mixtures with molar ratios of (1:2) and (1:3). Several physicochemical characteristics such as dynamic viscosity, density, and electric conductivity were measured at particular pressure and at a wide range of temperatures. LvAc-based DESs were described as competent sorbents for SO₂ and CO₂ with decent effectiveness^{166,213}. However, the effect of water content was not considered in these studies. Therefore, this chapter covered this gap in the literature by investigating the effect of water content on the physicochemical properties of ChCl:LvAc DESs such as density and viscosity. Furthermore, this work has evaluated the corrosivity behaviour of these compositions in the presence of water in the system.

The phase diagram of the choline chloride: levulinic acid binary system has never been presented before in the literature. Coutinho *et al.*²¹⁴ in their recent review emphasised that the phase diagrams of DES systems should be the first step in the identification and characterisation of DESs. ChCl:LvAc mixtures are liquid at room temperature but that does not automatically qualify them as deep eutectic solvents/mixtures. Therefore, one of the major objectives of the characterisation work

presented in this chapter is to verify, based on the obtained phase diagram, whether specific ChCl:LvAc compositions are eutectic mixtures or deep eutectic mixtures.

The viscosity of DESs decreases with increasing the temperature and water content simultaneously as extensively reported in the literature ^{156,158,183,184}. Whereas, the gas solubility performance is enhanced at low-temperature levels, viscosity increases with decreasing the temperature which might bring major concerns in terms of fluid flow and pump requirements. Ullah *et al.* ¹⁶⁶ and Florindo *et al.* ²¹⁵ have reported the viscosity of ChCl:LvAc (1:2) at different temperatures. On the other hand, the effects of increasing the HBD:HBA molar ratio and the presence of CO₂ on the viscosity of ChCl:LvAc DESs was not reported in their work along with the shear flow behaviour (Newtonian or non-Newtonian). Therefore, to cover this gap in the literature, this chapter has thoroughly studied the effects of increasing the HBD:HBA molar ratio and the presence of CO₂ on the rheological properties of ChCl:LvAc DESs. Furthermore, the rheological model describing the shear flow behaviour of ChCl:LvAc DESs is reported in this work for the first time in the literature.

In the present study, ChCl:LvAc mixtures were prepared with different HBA:HBD molar ratios and water contents to make new DESs. The DESs were characterised in terms of phase behaviour, FTIR spectroscopy, density, viscosity and TGA. The corrosivity of the DESs was investigated under different compositional and operating conditions. The importance of examining the characteristics of such DESs originates from the need to introduce benign sorbents, which are practical for various engineering applications, including but not limited to solvent extraction, catalysis, and carbon capture processes.

3.2 Experimental Methodology

3.2.1 Materials

The main materials used in the characterisation work and presented in Table 3-1. The chemicals were used without any further purification.

Table 3-1 Materials used in the characterisation work

Name	Purity	Supplier	Purpose
Choline Chloride	> 99 % w/w	Fisher Scientific	HBA
Levulinic Acid	> 98 % w/w	Fisher Scientific	HBD
Monoethanolamine	> 99 % w/w	Fisher Scientific	Benchmark absorbent
Mild steel specimen	DC01-CR4	Metals4u	Coupons for corrosion tests
CO ₂	99.99%, research-grade N5.0	BOC company	To examine the effect of CO ₂ on the corrosivity of ChCl:LvAc DESs

3.2.2 Preparation method

In this study, DESs were prepared by the heating method. The two components (ChCl and LvAc) were mixed at different molar ratios of (1:2 and 1:3) and with different water contents up to a water:HBA molar ratio of 5. The mixtures were then heated at 100 °C under constant stirring speed (250 rpm) until a homogeneous liquid is formed. The weight of the chemicals was measured by a MT electronic balance with standard uncertainty of 0.2 mg. The water content of the prepared samples was measured using a Karl Fisher moisture titrator (Kyoto Electronics Ltd. MKH-700).

In this work, the composition of a DES is represented by a label of the type “(HBA:HBD:water molar ratio)”. As an example, a DES with the label “(1:2:2.5)” is a DES with a composition defined by HBA/HBD molar ratio of 1:2 and a water/HBA molar ratio of 2.5. This nomenclature avoids the unnecessary lengthy reference to the water content each time a specific DES composition is mentioned.

3.2.3 Construction of the phase diagram for the choline chloride: levulinic acid binary system

The magnitude of the interaction between the HBD and the HBA is directly related to the difference in the freezing point of the DES to that of a theoretical ideal binary mixture of the HBA:HBD. The larger the freezing point difference ΔT_f the larger the interactions between the individual components as shown in Figure 3-1.

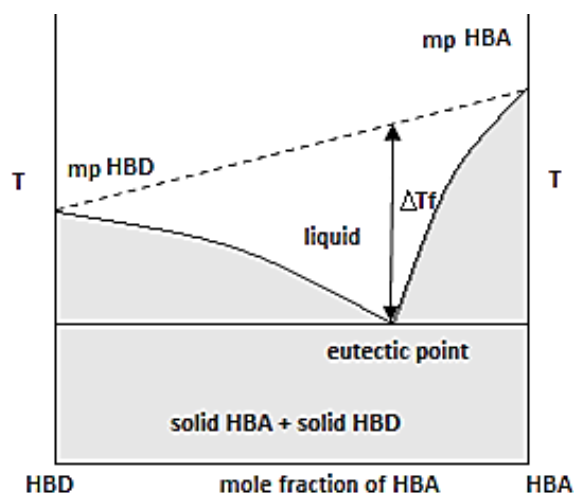


Figure 3-1 Generic binary phase diagram for DES formation

Five different compositions were used to construct the phase diagram of ChCl:LvAc binary mixtures. The mole % of the HBD in these compositions ranged between 50% to 85%. Three samples of the mixtures with 66.67%, 75% and 85% HBD mole % were accurately weighed into aluminium pans and hermetically sealed with aluminium lids. These samples were analysed in a Netzsch Jupiter 449 F1 differential scanning calorimeter. Samples were cooled down at a rate of 20°C/min from 20°C to -100°C, then held isothermally at -100°C for 5 min, before reheating from -100°C to 20°C at a rate of 20°C/min. The glass transition temperature of the samples (T_g) was detected during the heating ramp and analysed using the Netzsch Proteus analysis software version 8.0.2. The DES compositions containing 50% and 55% mole % of HBD are

not liquid at room temperature and the respective melting points were determined using an oven.

The melting temperatures of the HBA: HBD mixtures can be calculated using the simple mixing rule given by Equation 3-1,

$$T_m = x_i T_{mi} + x_j T_{mj} \quad \text{Equation (3-1)}$$

Where T_m is the melting temperature of the HBA: HBD mixture, x_i and x_j are the mole fraction solubility of compounds i and j ($x_i + x_j = 1$), and T_{mi} and T_{mj} are the melting temperatures of the individual components.

To describe the solid-liquid equilibrium curve of each component in eutectic systems, Equation (3-2) was used by many researchers such as Abranches²¹⁶ and Fernandez¹⁷⁶ to construct the ideal solid-liquid curve.

$$\ln(x_i \cdot \gamma_i) = \frac{\Delta H m_i}{R} \cdot \left(\frac{1}{T_{mi}} - \frac{1}{T} \right) + \frac{\Delta C P m_i}{R} \cdot \left(\frac{T_{mi}}{T} - \ln \frac{T_{mi}}{T} - 1 \right) \quad \text{Equation (3-2)}$$

In Equation (3-2) γ_i is the liquid phase activity coefficient, $\Delta H m_i$ is the temperature and enthalpy of melting of the pure component i, T is the absolute temperature, R is the ideal gas constant, and $\Delta C P m_i$ is the change of the heat capacity of compound i upon fusion.

The contribution of the second term of Equation (3-2) tends to be very small for most DES systems as reported by Martins *et al.*¹²⁸ and Coutinho *et al.*²¹⁷. Hence, Equation (3-2) becomes

$$\ln(x_i \cdot \gamma_i) = \frac{\Delta H m_i}{R} \cdot \left(\frac{1}{T_{mi}} - \frac{1}{T} \right) \quad \text{Equation (3-3)}$$

For an ideal system, γ_i equals one, and this assumption has been used in previous works such as the ones mentioned above^{128,217}. Therefore, Equation (3-3) simplifies to:

$$\ln(x_i) = \frac{\Delta H m_i}{R} \cdot \left(\frac{1}{T_{mi}} - \frac{1}{T} \right) \quad \text{Equation (3-4)}$$

Equation (3-4) shows a linear relationship between $\ln(x_i)$ and $1/T$. The fusion properties of the HBA and the HBD were taken from the literature¹⁷⁶. The enthalpy of fusions are 4.3 and 9.2 kJ.mol⁻¹ for the HBA and the HBD, respectively¹⁷⁶. The melting points of the HBA and the HBD are 303 °C and 32 °C, respectively. These values can be used in Equation (3-4) to predict the absolute temperature T at any given mole fraction x_i .

3.2.4 FTIR measurements of the DES

Some researchers in the literature utilised FTIR to study the formation of hydrogen bonds and vibration modes in the deep eutectic solvents^{218, 187, 219}. The formation of hydrogen bonds between the HBA and the HBD directly affects the vibrational stretching of all functional groups of both constituents of the DES. This can be shown by comparing the IR spectra of the individual components with the IR spectrum of the DES²¹⁹. In this work, the FTIR spectra of the HBD, the HBA and the DES compositions were measured with the help of a ABB MB 3000 FTIR spectrophotometer. The number of scans was set to 32 for all samples while the recorded data points were taken every 8 wavenumbers (scan range) from 550 to 4000 cm⁻¹.

3.2.5 Density measurements

The density of the prepared DESs was measured at different HBA:HBD molar ratios and water content at temperatures ranging between 20°C - 65°C using a Densito 30PX which is a portable density meter (Labpro, Oxford, UK). The temperature and density accuracies are ± 0.05 °C \pm and 0.0001 kg.m⁻³ respectively. The density meter was calibrated with water at different temperatures and compared with literature values.

3.2.6 Viscosity measurements

The viscosity of the ChCl: LvAc deep eutectic solvents was measured at different conditions using a TA Instruments Discovery HR-2 rheometer with cone and plate geometry. To understand the effect of different compositional parameters on the viscosity of the DESs, the measurements followed the experimental design presented in Table 3-2.

Table 3-2 Experimental design of the viscosity measurements under different compositional conditions

Run no.	HBA: HBD molar ratio	Water content (water:HBA molar ratio)	Presence/ absence of CO ₂
1	1:2	0	With CO ₂
2	1:2	0	Without CO ₂
3	1:2	5	Without CO ₂
4	1:3	0	With CO ₂
5	1:3	5	With CO ₂
6	1:3	5	Without CO ₂

Runs 1+2 and 5 + 6 are designed to study the effect of CO₂ on viscosity at different concentrations of water. While runs 2 to 5 will show the effect of water content on viscosity in the presence and absence of CO₂. Finally, runs 1+4 and 3 + 6 will show the effect of increasing the HBA:HBD molar ratio on the viscosity of ChCl:LvAc DESs. A controlled shear rate ramp between 0.1 and 1000 s⁻¹ at 25 °C was applied to study the effect of increasing the shear rate on the viscosity of ChCl:LvAc DESs.

A controlled temperature ramp between 20 and 65 °C at a constant shear rate of 100 s⁻¹ was applied to study the effect of increasing temperature on viscosity ChCl:LvAc DESs.

3.2.7 Thermal stability

Thermal stability is an important factor associated with the absorbents utilised for capturing CO₂ from the flue gas at high temperatures. In this study, initial decomposition temperature, half decomposition temperature, and the final residue (wt.%) were analysed on the TGA analyser (NETZSCH STA 449 F1 Jupiter) for all prepared DES compositions. A weight loss curve with temperature was obtained, and the DES was heated from 30 to 500 °C at the rate of 50 °C.min⁻¹ of N₂ gas stream with a flow rate of 50 ml.min⁻¹. The TGA analyser was calibrated periodically with a reference sample of INDIUM by conducting the same procedure mentioned above to verify the reliability of the device.

3.2.8 Corrosivity measurements

The corrosivity analysis of the sorbents used for CO₂ capture is important because corrosion affects the performance of the processing units where metallic plumbing, absorber columns, and other utilities are in direct contact with the absorbent.

Currently, two main corrosion protocols are used to measure the corrosivity of DES, the electrochemical method (EC) which is widely used by many studies such as ^{167, 136, 171}. While the second less used corrosion measurement technique is the weight-loss (WL) method used by Traviedi . ¹⁵⁹ Both methods are summarised in Table 3-3. In the EC method, polarization values indicate the corrosivity of metals in a corrosive environment. It was utilised to conduct a comprehensive corrosivity study dealing with CO₂ saturated choline chloride-based DES with levulinic acid ¹³⁶. The DES system showed high corrosion resistance, the CR value of 0.027 mm.year⁻¹ for the CO₂ saturated DES system, whereas under the same conditions the CR value of 0.54 mm.year⁻¹ was obtained for the CO₂ saturated system containing monoethanolamine. However, the effects of water content, temperature, HBA: HBD molar ratio and presence of CO₂ in the system on the corrosion rate were not considered in the work by Ullah *et al.* ¹³⁶.

Table 3-3 DESs used in corrosion tests, test methods, metals used, standard protocols and specimen areas from the literature

DES system tested (corrosion tests)	Metals /alloys tested	Corrosion tests followed standard protocols	Specimen Area (cm ²)	Reference
Choline chloride + Levulinic acid (1:2)	Carbon steel 1018	Electrochemical method. ASTM G-31 for sample preparation.	1.93	166
Monoethanolamine hydrochloride (MEA.Cl) + Ethylenediamine (EDA)	Stainless steel	Weight loss method. (No standard used for sample preparation)	2.0125	133
Choline chloride + Phenylacetic acid [(1:2), (1:3) and (1:4)]	Low carbon steel	Electrochemical method. ASTM G1-03 for samples preparation.	0.785	167
Choline chloride + Urea (Reline) Choline chloride + Ethylene glycol (Ethaline) Choline chloride + Glycerol (Glyceline) Choline chloride + Oxalic acid (Oxaline)	Mild steel	Electrochemical method. ASTM G 59-97 for calculation corrosion rates.	-	174

In this work, the corrosivity of the prepared DESs system (ChCl:LvAc) was examined at different conditions using the weight-loss method (WL) only.

Four independent parameters are affecting the corrosion process in the CO₂ absorption system using DESs according to the literature ^{133,136}. These parameters are namely: HBA to HBD molar ratio, water content, temperature, and the presence of CO₂. Furthermore, stirring speed has a significant effect on CO₂ absorption by DES as reported by Aboshatta *et al.* in their recent work in ²²⁰. Therefore, in this work, we are going to study the effect of stirring speed on the corrosivity of DESs. The factorial design array requires 4 replicates per run -as per Table 3-4 - This neat experimental design allows us to analyse the obtained results statistically and optimise the corresponding corrosion parameters.

Table 3-4 Factorial design of corrosivity tests

Run Order	No. of replicates	Molar Ratio	Molar Ratio of Water	T (°C)	Stirring Speed (rpm)
1	4	1:2	0	25	0
2	4	1:2	0	25	100
3	4	1:2	5	25	0
4	4	1:3	0	25	0
5	4	1:3	0	25	100
6	4	1:3	5	25	0
7	4	30% (wt.) MEA	70% (wt.)	25	0

Corrosion measurements procedure and method using the weight-loss method according to the standard practice for laboratory immersion corrosion testing of metals ²²¹.

3.2.8.1 Apparatus

A set of beakers with a parafilm closure were used, simple immersion tests were done isothermally at 25 °C, and the thermal incubator (Stuart Scientific S160D) was used to maintain the constant temperature at 25 ± 0.5°C . Whereas the VLE

rig was used to study the effect of stirring speed at 100 rpm on the corrosivity of ChCl:LvAc DESs.

3.2.8.2 Test specimen

- a. Uniform corrosion rates of 4 identical specimens are within $\pm 10\%$ under the same test environment, therefore, tetraplicate specimens are exposed in each test. MEA was used as a benchmark to show the corrosive behaviour of DES under the same test conditions.
- b. The surface-to-mass ratio must be large, while the ratio of edge area to total area is preferred to be small. coupons of 50*25*1.6 mm are preferred for corrosion specimens, both specimen areas in Table 3-5 were chosen arbitrarily. Specimen of 25*12.5*1.2 mm of mild steel DC01-CR4 was used in this test. This brand of mild steel used in this work has poor corrosion resistance. This is necessary for this test, as any changes in weight due to corrosion by the DESs and amines could be observed. The chemical composition of mild steel Coupons is represented in Table 3-5.

Table 3-5 Chemical composition of mild steel specimen ²²²

Element	C	Si	Mn	P	Fe
Wt.%	0.12	0.45	0.6	0.045	98.785

- c. Surface treatment of coupons including finishing with No. 120 abrasive paper usually necessary unless the metal surface is in mill-finished condition.
- d. Wet grinding and polishing of samples were performed using grit SiC papers.
- e. The Coupons should be lastly de-greased by using bleach-free scrubbing powder, if necessary, finally, coupons were rinsed in water-acetone solution (50% vol.), and air-dried.

- f. Towels should be avoided during the final drying of samples which might introduce an error due to contamination of Coupons with grease.
- g. An analytical balance of $\pm 4\text{mg}$ was used for weighing the dried specimens.

3.2.8.3 Specimen support

There are some common supports used to mount the samples such as glass hooks, ceramic rods, fabric strings, and various insulated metallic strings. In our case, plastic wires were used to hang coupons. These wires separated specimens physically and electrically.

3.2.8.4 Control specimen

Four control specimens were weighed before and after chemical cleaning, to measure to which extent weight loss resulting from chemical cleaning, the average lost value (W_c) is then utilised to correct the corrosion weight loss.

3.2.8.5 Duration of test

If corrosion rates are anticipated to be moderate or low, Equation (3-5) should be used:

$$\text{Hours} = \frac{2000}{\text{Corrosion rate in mils per year (mpy)}} \quad \text{Equation (3-5)}$$

The corrosion rate of choline chloride-levulinic acid DES was found to be $0.027 \text{ mm}\cdot\text{year}^{-1}$ (1.08 mpy) as reported by Ullah *et al.*¹⁶⁶. Therefore, the duration of the weight-loss test should be 1851.85 hours (77.16 days) according to Equation (3-5). However, according to the ASTM G1, the most common testing periods are 48 to 168 h (2 to 7 days). Hence, 10 days might give satisfactory results.

3.2.8.6 Cleaning coupons after the test

- a. Cleaning coupons after the test is very important in this method can cause misleading results if not done properly.
- b. The cleaning procedure is divided into two general methods: chemical and mechanical, or electrolytic. Clarke solution – Table 3-6 - used as a chemical method to remove corrosion products from coupons. For the mechanical cleaning method, cleaning with a brush and mild abrasive is the most used technique.

Table 3-6 Clarke solution formula, cleaning duration, the temperature of the test according to the ASTM G1.03 - C.3.5 ²²³

Material	Solution	Time (min)	Temperature (°C)
Mild Steel	500 mL HCl + 3.5 g Hexamethylene tetramine + H ₂ O to make 1 L	10	20 - 25

3.2.8.7 Calculating Corrosion Rates

Based on the weight difference (before and after immersion), the corrosion penetration rate (CPR) in millimetres per year (mm/y) was calculated using Equation (3-6):

$$\text{CPR} = \frac{K \cdot W}{\rho \cdot t \cdot A} \quad \text{Equation (3-6)}$$

Where K is a conversion constant (8.76×10^4), W is the weight loss due to corrosion in g, ρ is the density of stainless steel in $\text{g}\cdot\text{cm}^{-3}$, t is the time of exposure in hours and A is the area of the specimen exposed/immersed (cm^2).

In this study, the PCR values of ChCl:LvAc DESs were calculated at different water contents and CO_2 concentrations.

The weight loss due to corrosion (W) is calculated by Equation (3-7):

$$W = W_T - W_C$$

Equation (3-7)

Where W_T is the total weight loss of specimen due to corrosion and cleaning and W_C is the weight loss of the specimen due to chemical cleaning only.

3.3 Results and discussion

3.3.1 Preparation of ChCl:LvAc DESs compositions

ChCl:LvAc DESs compositions were prepared successfully at different molar ratios and water contents -according to Table 3-2 using the heating preparation method as explained in section 3.2.2 above. Homogeneous DES systems were successfully prepared in molar ratios of (1:2) and (1:3) –as shown in Figure 3-2-. Different DES systems were prepared by altering levulinic acid molar ratios at a constant quantity of choline chloride. Under the same conditions, homogeneous DES systems were successfully prepared in molar ratios of (1:2) and (1:3) under the same conditions, DES compositions with a ChCl:LvAc ratio of (1:1) could not be prepared regardless of the water content and preparation temperature. In this case, the result was the formation of heterogeneous mixtures composed of turbid brown or white solid-liquid mixtures -as shown in Figure 3-3 - indicating that, the DES system did not form throughout the process and after cooling to room temperature. The existence of solid precipitations in the heterogeneous system implies that the ratio of the hydrogen bond donor (LvAc) is fewer as compared to the equivalent hydrogen bond acceptor (ChCl). This resulted in suspending the solid particles of the excess amount of the HBA, these cannot interact with the HBD via hydrogen bonds.



Figure 3-2 ChCl:LvAc DESs prepared at HBA:HBD molar ratios of (1:2) (left) and (1:3) (right)



Figure 3-3 Unsuccessful preparation of ChCl:LvAc DESs at the HBA:HBD molar ratio of (1:1)

The heterogeneous compositions were not considered for further investigation in this study. On the other hand, the homogeneous compositions that have HBD mole ratio above 60 % remained liquid at room temperature. These compositions were selected for further characterisation and physical properties measured in the following sections. The water content of these compositions was measured as per section 3.2.2 and summarized in Table 3-7. DESs compositions exhibited higher water content than expected due to the hygroscopic property of the HBD and the HBA ¹⁸⁷. For example, the composition of (1:2) in which no water was added was found to have a water mole ratio of 1.6 as shown in Table 3-7.

Table 3-7 The water content of ChCl:LvAc DESs compositions

Mole ratio (HBA:HBD)	Measured Water content (water:HBA molar ratio)	Nomenclature in this work
(1:2)	1.6	(1:2:0)
(1:2)	2.56	(1:2:2.5)
(1:2)	4.56	(1:2:5)
(1:3)	1.4	(1:3:0)
(1:3)	4.57	(1:3:2.5)
(1:3)	5.93	(1:3:5)

3.3.2 Choline chloride: levulinic acid binary phase diagram

The solid-liquid equilibrium (phase behaviour plot) of ChCl:LvAc mixtures is constructed and reported for the first time in the literature according to the method explained earlier in section 3.2.3. The glass transition and melting temperatures of ChCl:LvAc mixtures are shown in Figure 3-4 and summarised in Table 3-8.

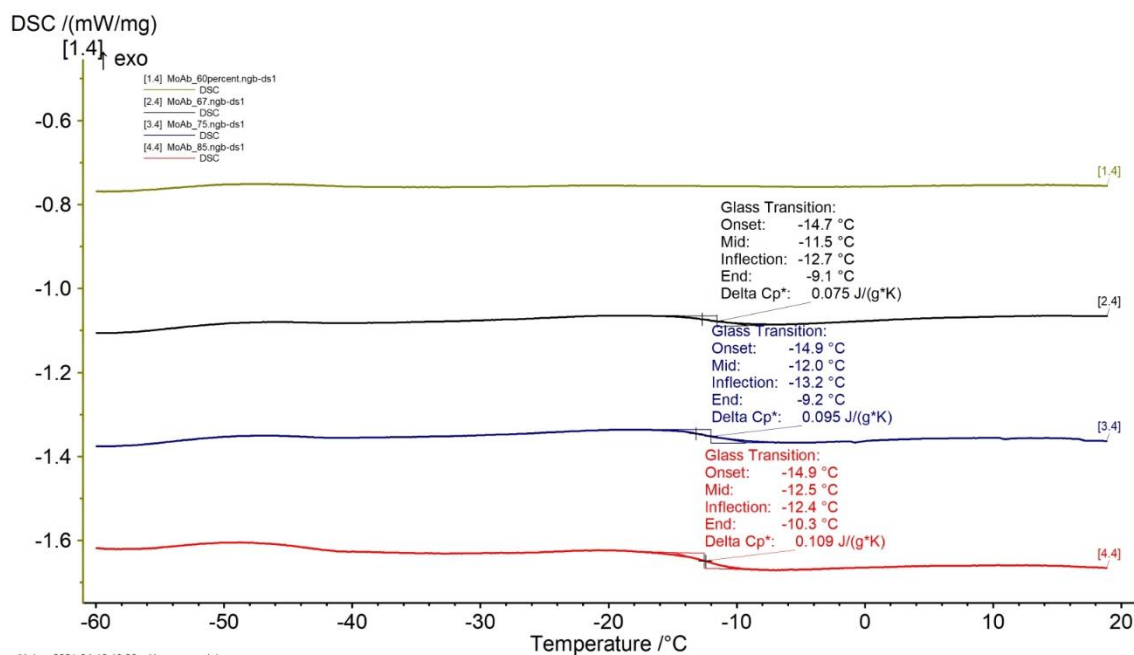


Figure 3-4 DSC plots showing the glass transition temperature of ChCl: LvAc mixtures

Table 3-8 Melting the glass transition temperatures of ChCl:LvAc mixtures

Mole % of the HBD	Melting point (°C)	Tg (°C)
50%	155	
55%	60	
66.67%		-11.5
75%		-12
85%		-12.5

3.3.3 Phase behaviour plot of ChCl:LvAc mixtures

The Tg values prepared above were plotted against the melting points of the HBA:HBD mixtures using a simple mixing rule and the ideal melting points of both components as per Figure 3-5.

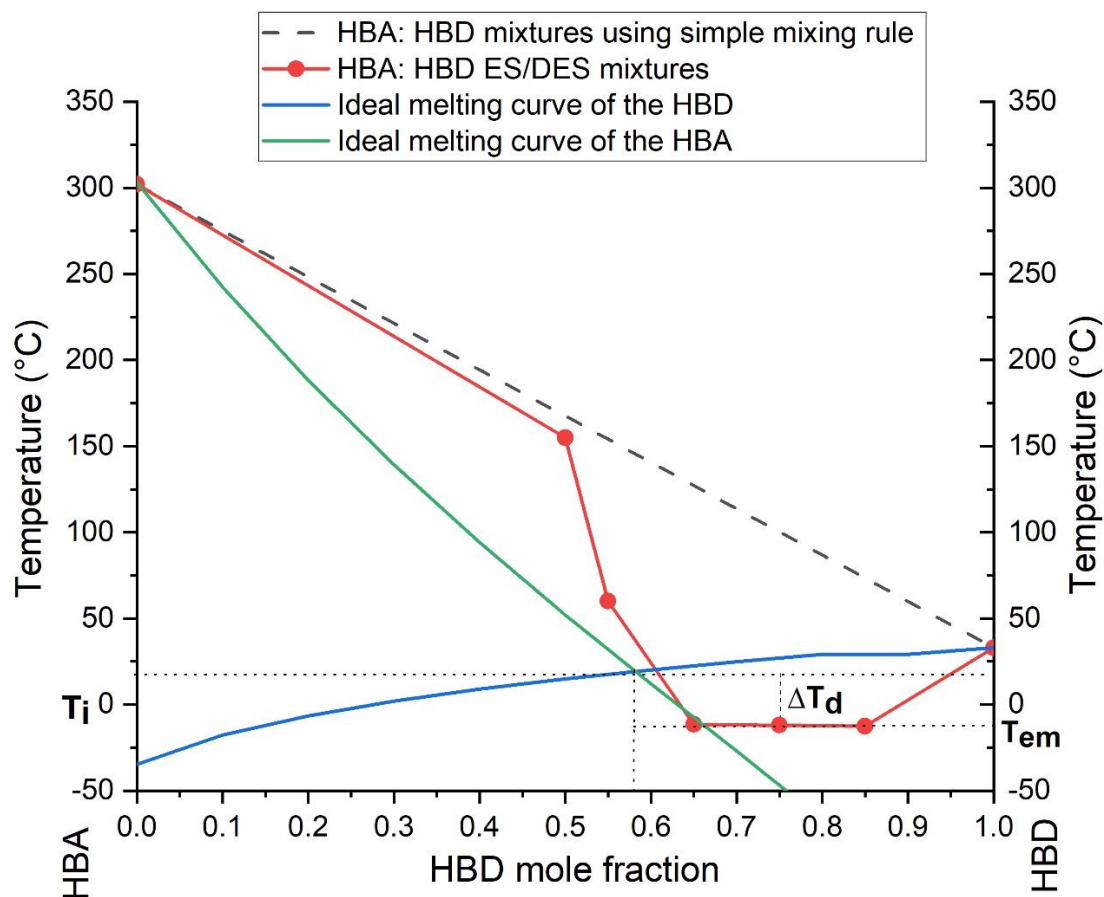


Figure 3-5 Phase behaviour plot of ChCl:LvAc binary mixtures

The temperature depression from the ideality, ΔT_d , is defined as the difference between the ideal mixture melting temperature (T_i) and the deep eutectic temperature (T_{em}) as per Figure 3-5. The values of ΔT_d could only be calculated for ChCl:LvAc mixtures with HBD mole percentage equal or above 66.67% and tabulated in Table 3-9. These mixtures are liquid at room temperature with $\Delta T_d > 0$ thus fulfilling all the criteria for being considered deep eutectic mixtures and, therefore, can be defined as DESs. Whereas mixtures containing 50 and 55 mole% levulinic acid can only be described as eutectic mixtures that show phase separation at room temperature.

Table 3-9 Temperature depression of the DES compositions from ideality

Mole % of the HBD	ΔT_d (°C)
66.67%	24.9
75%	25.4
85%	25.9

3.3.4 FTIR measurements of ChCl:LvAc DESs

FTIR spectra of ChCl:LvAc DESs with molar ratios of (1:2:0) and (1:3:0) were measured and compared –as Table 3-10 - with the work by Mellado . (2) who measured the FTIR of ChCl:LvAc DES of (1:2) molar ratio and its components.

Table 3-10 FTIR peaks for ChCl:LvAc DESs and its pure components

Functional group	Wave number (DES) (cm ⁻¹) (This work)	Wave number (DES) (cm ⁻¹) Mellado . ¹⁸⁷	Wave number (LVAC) (cm ⁻¹) Mellado . ¹⁸⁷	Wave number (CHCL) (cm ⁻¹) Mellado . ¹⁸⁷
Alkyl (-CH ₂ -)	2920	2910	2910	2990
	1480	1485	-	1485
Aliphatic ketone (C=O)	1690-1740	1711	1711	-
	1400	1400	1400	-
	1355	1360	1360	-
	1200-1500	1200-1550	1200-1550	-
	1150-1250	1000-1300	1000-1300	-
N-H	3000-3250	-	-	3220
-OH Stretching	3260	-	-	-
-OH bending	575	-	-	-

Table 3-10 and Figure 3-6 show the FTIR transmittance of ChCl:LvAc DES at molar ratios of (1:2:0) and (1:3:0). The coexistence and shift of some vibrational bands of functional groups in the DES and its components show the formation of the DESs at different molar ratios. For example, the transmittance of the alkyl group in the

DES is $1690\text{--}1740\text{ cm}^{-1}$ which is similar to its value in levulinic acid reported by Mellado *et al.*¹⁸⁷. In addition, the vibrational bands observed at 3320 cm^{-1} represent the symmetric N-H stretching as reported by Mellado *et al.* in¹⁸⁷ for choline chloride only. These peaks were observed in our FTIR measurements for the ChCl:LvAc DESs are related to the formation of hydrogen bonds between ChCl and LvAc.

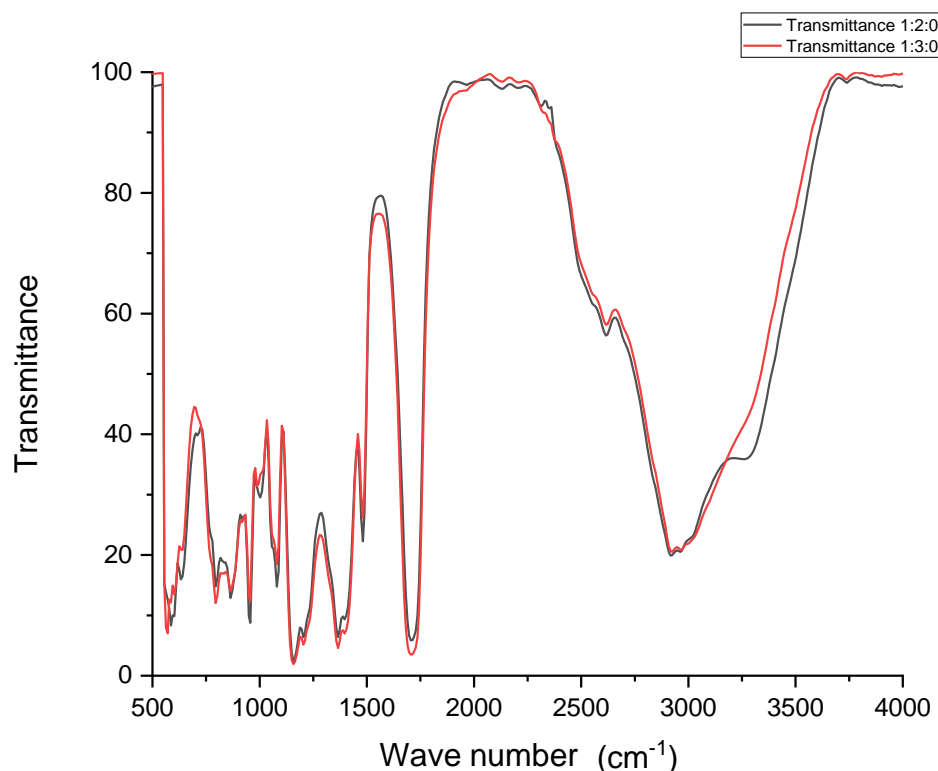


Figure 3-6 FTIR spectra of ChCl:LvAc DESs (1:2:0 and 1:3:0) at 25 °C

3.3.5 The effect of water on FTIR transmittance of ChCl:LvAc DESs

It is highly recommended to study the presence of water in the DESs since the individual components of the DESs are highly hygroscopic particularly for ChCl:LvAc DES systems. Some researchers in the literature i.e. Ullah *et al.*¹⁶⁶ and Mellado *et al.*¹⁸⁷ studied ChCl:LvAc DES, however, the effect of water on the FTIR spectra of ChCl:LvAc DESs have not been considered in the previous works.

In this work, FTIR measurements were utilised to show the effect of water on the DES transmittance. Figure 3-7 displays broad transmittance – approximately 3400 cm^{-1} - of hydroxyl group as compared to the medium transmittance of NH_2 group of 3300 cm^{-1} in the samples of ChCl:LvAc (1:2) with water molar ratio of 2.5 and 5 as compared to the sample without no added water. This transmittance peak of the hydroxyl group is broadening with water content whereas, it narrowed with increasing desorption temperature during the regeneration process. In addition, there is an observable shift in hydroxyl group transmittance from 575 to 600 cm^{-1} when increasing water content from 0 molar ratio to water molar ratios of 2.5 and 5, respectively.

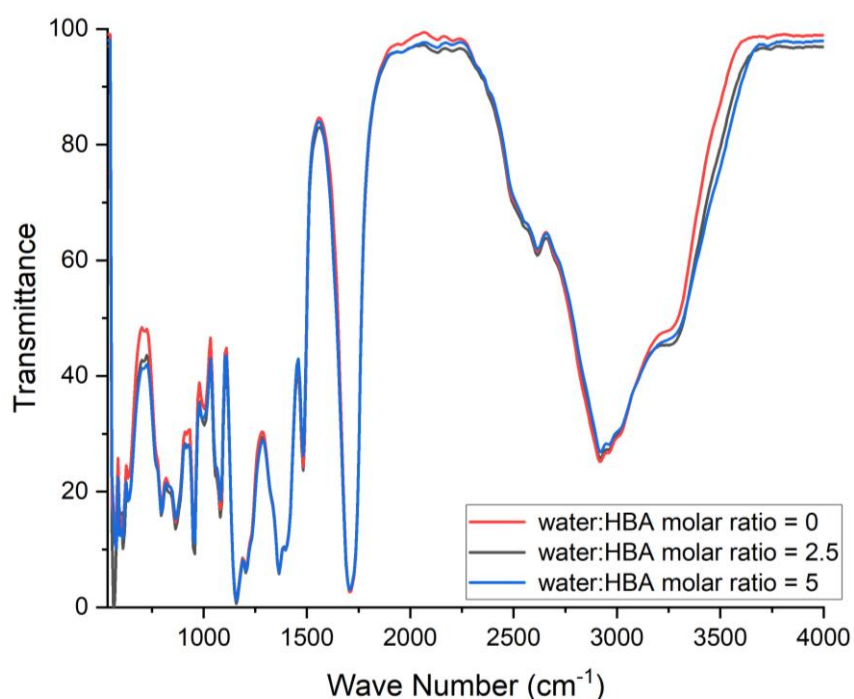


Figure 3-7 FTIR spectra of ChCl:LvAc DESs (1:2) with different water contents at 25 °C

Similar behaviour was detected for ChCl:LvAc (1:3) with water molar ratios of 2.5 and 5, as shown in Figure 3-8. However, for this specific HBA:HBD molar ratio, different water contents showed similar transmittance signatures.

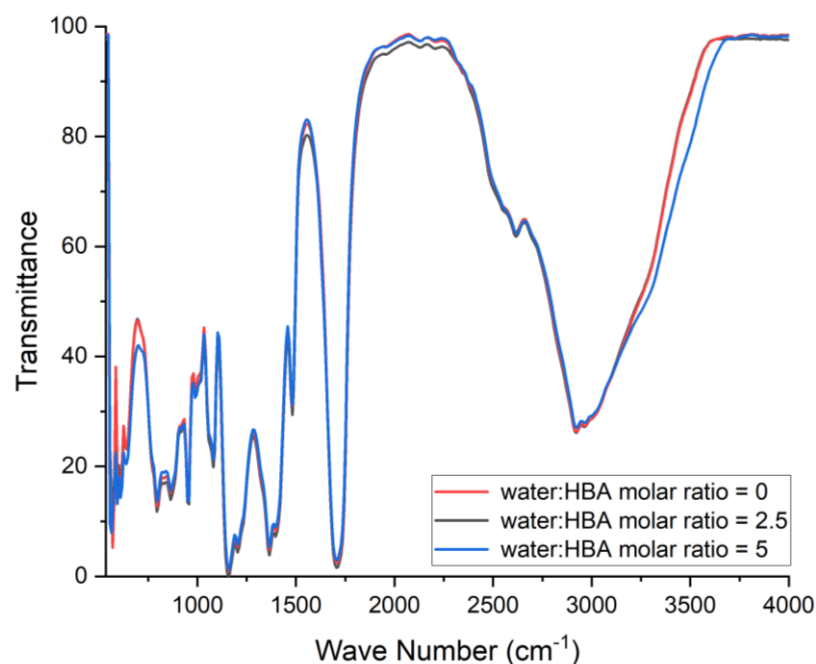


Figure 3-8 FTIR spectra of ChCl:LvAc DESs (1:3) with different water contents at 25 °C

3.3.6 Density measurements

The density of ChCl:LvAc DESs decreases with increasing the temperature according to ^{156,158,183, 184}. However, only a few previous studies in the literature reported the effect of water content and the HBA:HBD molar ratio on the density of DES of ChCl:LvAc DESs ²⁰⁵. For the experimented ChCl:LvAc DES system of (1:2) molar ratio and no added water, density values range between 1.38 –1.1g.cm⁻³ at temperatures ranging between 20 – 65 °C. Figure 3-9 shows that the results are in good agreement with density values reported in the literature for ChCl:LvAc DESs (Ullah *et al.* ¹³⁶ and Lu *et al.* ²⁰⁵). It is worth-mentioning that, the non-linearity of the variation of density with temperature observed in this work, is due to the difference in water content between the ChCl:LvAc DESs used in this work and the DESs used in the works by Ullah *et al.* ¹³⁶ and Lu *et al.* ²⁰⁵.

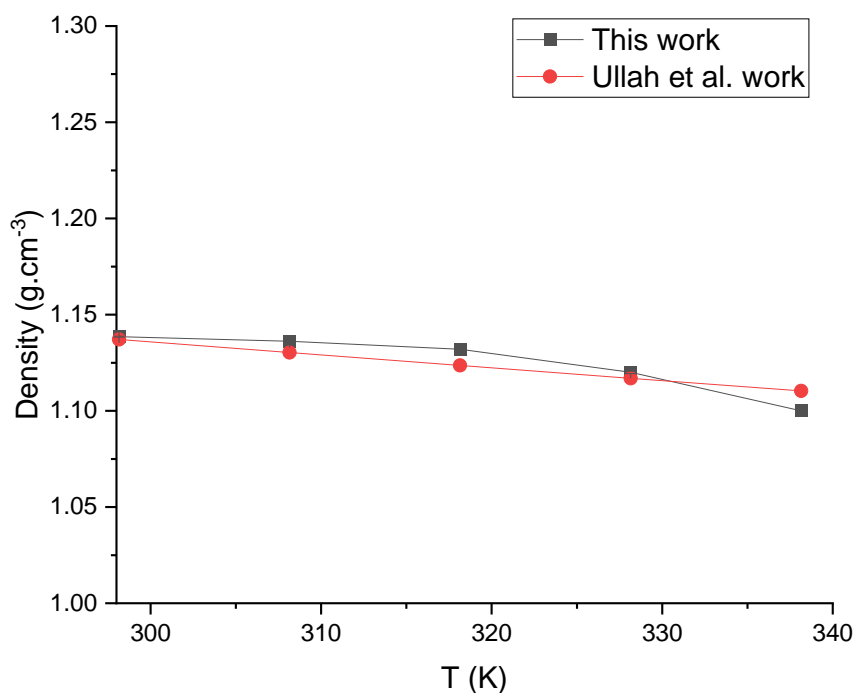


Figure 3-9 Density of ChCl:LvAc DESs (1:2) as a function of temperature

Note: Error bars are not visible as they are smaller than the data point size

The density of investigated ChCl:LvAc DES systems was found to be decreasing with increasing the temperature, HBD molar ratio and water content simultaneously as shown in Figure 3-10.

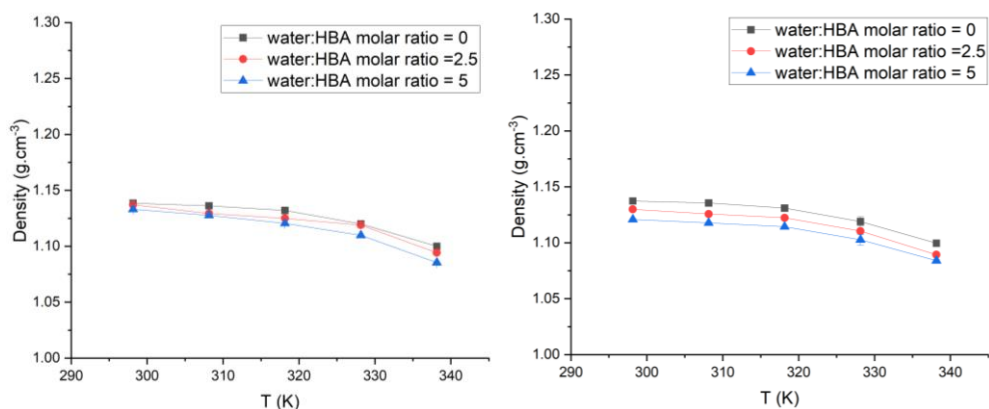


Figure 3-10 Density of ChCl:LvAc DES systems as a function of temperature, water content and HBA:HBD molar ratio 1:2 (left) and 1:3 (right)

Note: Error bars are not visible as they are smaller than the data point size

3.3.7 Viscosity measurements

3.3.7.1 Effect of water content, HBD and temperature on viscosity

A viscosity value of 154.5 mPa.s at 25 °C has been reported in this work for the experimented ChCl:LvAc (1:2:0). While Florindo *et al.*²¹⁵ and Ullah *et al.*¹⁶⁶ have also reported viscosity values of 226.8 mPa.s and 171.3 mPa.s respectively at 25 °C for the same system as per Figure 3-11. The variation among the viscosity values reported by Florindo *et al.*²¹⁵ and Ullah *et al.*¹⁶⁶ and those reported in this work comes from some reasons. Firstly, the difference in water content, as the water content of ChCl:LvAc (1:2) in this work is 7.25 wt% > Ullah *et al.*¹⁶⁶ 1.6 wt% > Florindo *et al.*²¹⁵ 0.23 wt% which justifies the lower values of viscosity stated in this work as compared to the previous ones. This is also confirmed by the viscosity value of 41.9 mPa.s reported for ChCl: LvAc (1:2) water-saturated (9.88 wt%) by Florindo *et al.*²¹⁵. Which is the lowest viscosity value of these DESs reported in the literature.

What is clear from Figure 3-11 is that independently of the HBA:HBD molar ratio (1:2 or 1:3), there is progressive reduction in viscosity with increasing water content. It is also important to point out that the preparation method affects the physical properties of the DESs (including viscosity). This was a major conclusion of the work published by Florindo *et al.*²¹⁵. In the work by Florindo *et al.*²¹⁵ the DESs were prepared using the grinding method, while in this work and in the work published by Ullah *et al.*¹⁶⁶, the DES were prepared by the mixing/heating method. Therefore, while trends in viscosity are expected to follow similar patterns independently of the DES preparation method, direct comparisons between absolute values of viscosity are less reliable and should always take into consideration the experimental variability produced by the preparation method.

Regarding the effect of the HBA:HBD molar ratio, increasing the HBD mole fraction decreases the viscosity of ChCl: LvAc DESs. This reduction in viscosity can be directly related to the formation of more hydrogen bonds when adding more LvAc^{224, 225}.

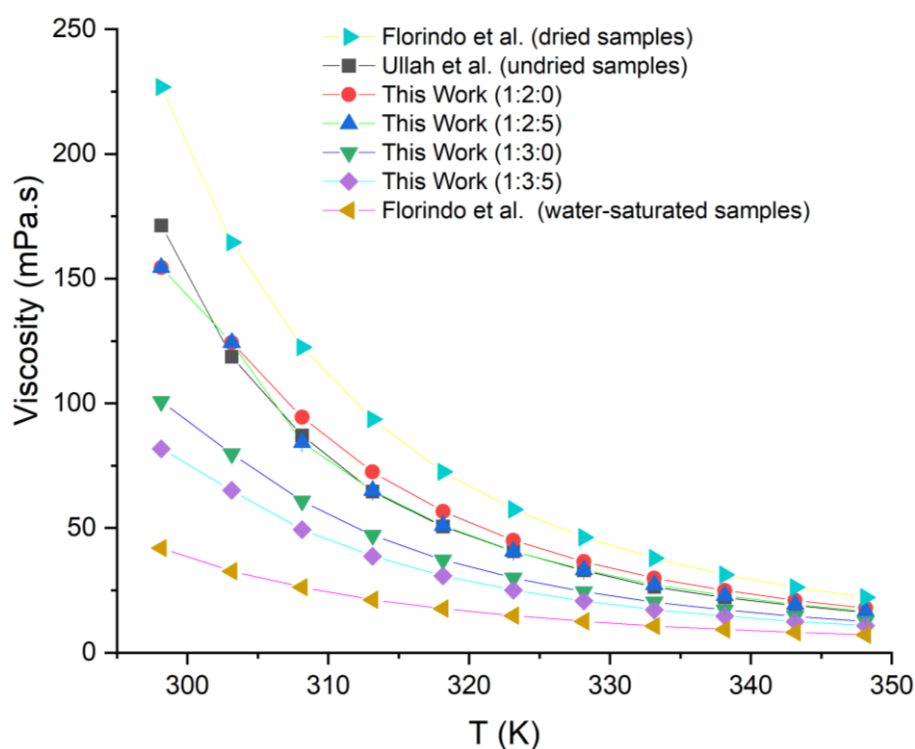


Figure 3-11 Viscosity of ChCl: LvAc DESs as a function of water content and temperature. Measurements carried out at a constant shear rate of 100 s^{-1}

Note: Error bars are not visible as they are smaller than the data point size

The viscosity of all studied ChCl:LvAc DESs compositions decreases with increasing temperature as has been extensively reported in the literature as shown in Figure 3-12. To describe this behaviour, a logarithmic model built on the Arrhenius model correlated was used for correlation as per Equation (3-8).

$$\eta = \eta_{\infty} \exp\left[\frac{E_a}{RT}\right] \quad \text{Equation (3-8)}$$

Where η is the viscosity of ChCl:LvAc in mPa.s, R is the ideal gas constant (8.314 J·K⁻¹·mol⁻¹), E_a is the activation energy in J·mol⁻¹, η_{∞} is a pre-exponential constant in mPa.s and T is the temperature in K.

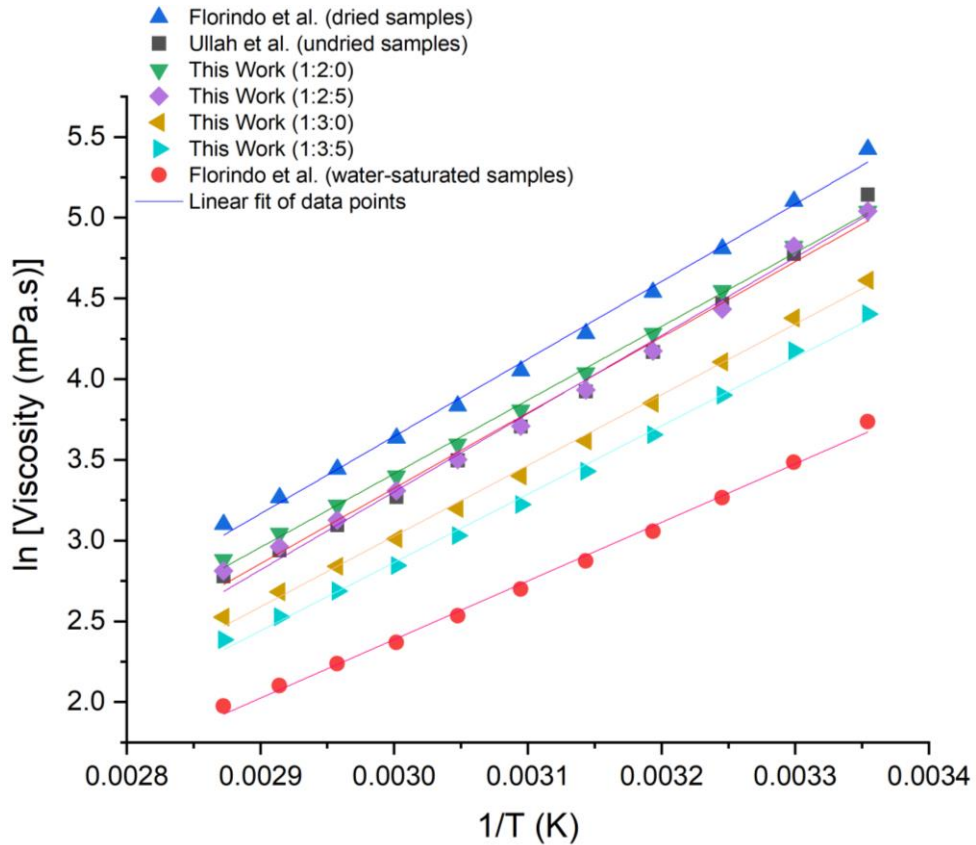


Figure 3-12 Viscosity of ChCl: LvAc DESs as a function of water content and temperature. Measurements carried out at a constant shear rate of 100 s⁻¹

The corresponding values to η_{∞} and E_a , for each DESs compositions were calculated from Equation (3-8) and summarised in Table 3-11.

Table 3-11 The calculated values of the activation energy and the pre-exponential constant

DESs (water content in wt%)	η_{∞} (mPa.s)	E_a (kJ.mol ⁻¹)	Reference
1:2 (0.23)	2.16E-05	39.88	Florindo <i>et al.</i> ²¹⁵
1:2 (1.6)	1.34E-05	40.24	Ullah <i>et al.</i> ¹⁶⁶
1:2 (7.25)	3.46E-05	38.88	This Work
1:2 (9.88)	2.03E-04	30.26	Florindo <i>et al.</i> ²¹⁵
1:2 (18.1)	2.24E-05	37.93	This Work
1:3 (4.91)	4.06E-05	36.42	This Work
1:3 (17.9)	5.33E-05	35.20	This Work

This model allows better analysis and understanding of the viscosity of ChCl:LvAc compositions. The positive activation energy E_a represents the energy impediment of the liquid to the shear stress, the lower the E_a value the easier it is for the particles to flow. This can correspond to the strength of the intermolecular reactions within the fluid or the entanglement or the mass of ions which can be obtained from the molar volume of each composition ²¹⁵.

In this set, the reduction in viscosity with increasing temperature was detected for all ChCl:LvAc compositions. This behaviour is due to the significant reduction in the level of hydrogen bond interactions with increasing temperature ²²⁵.

3.3.7.2 The effect of CO₂ on viscosity

Basically, the viscosity measurements at different temperatures require removing any bubbles from the fluid before any measurements as it responds to the applied shear rate differently than the fluid, hence affecting the accuracy of the experiment. However, in this case, the existence of CO₂ bubbles within ChCl:LvAc compositions is inevitable due to the physical absorption nature of the DESs mechanism to capture

CO₂. At the beginning of the test, the applied shear rate and temperature release CO₂ from the DES samples with a residual CO₂ instead of directly reducing viscosity this explains why the samples with a residual CO₂ showed slightly higher viscosities than the pure sample at the start of the test. However, at higher around 55 °C, when most of the CO₂ is released by heat – as proven previously in our previous work in ²²⁰ - and shear stress, all the compositions with and without CO₂ behave similarly as shown in Figure 3-12.

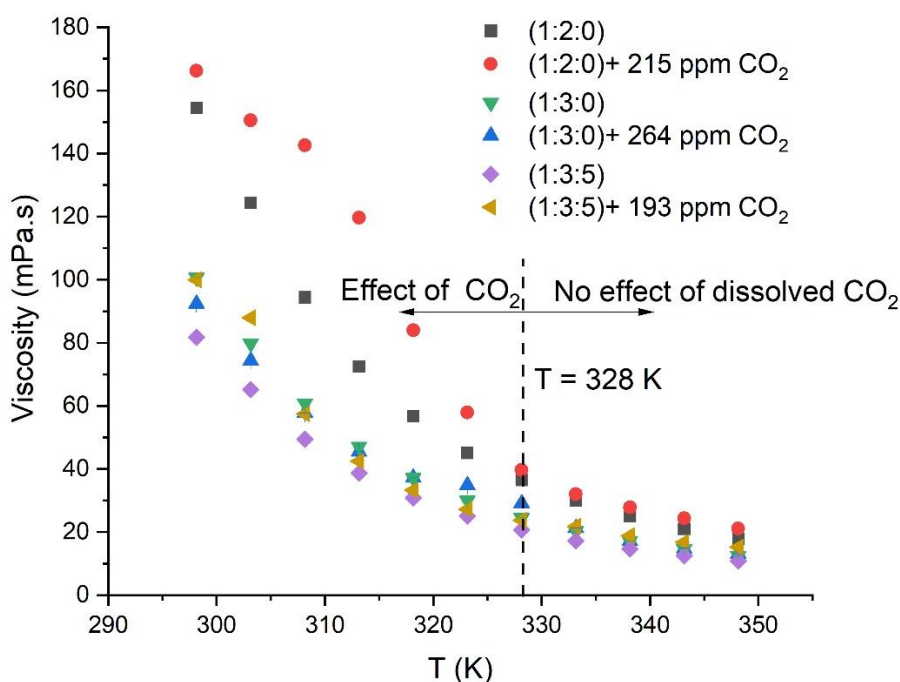


Figure 3-12 Viscosity of ChCl: LvAc DESs as a function of temperature and in the absence or presence of residual CO₂. Measurements carried out at constant shear rate of 100 S⁻¹

3.3.7.3 Steady shear flow behaviour

ChCl:LvAc (1:2:0) and (1:3:0) showed a shear thinning behaviour at shear rates up to 1 s⁻¹. However, the viscosity remains constant between 1 s⁻¹ and 100 s⁻¹ as per Figure 3-13 which makes ChCl:LvAc DESs more suitable for applications within this range of shear rate such as pumping and mixing processes. Another non-Newtonian

behaviour appeared at a shear rate above 100 s^{-1} . Therefore, it is highly recommended to develop a rheological model that can describe this kind of non-Newtonian regions below 1 s^{-1} and above 100 s^{-1} . The model must fit the experimental flow curves of ChCl:LvAc (1:2:0) and (1:3:0) DESs.

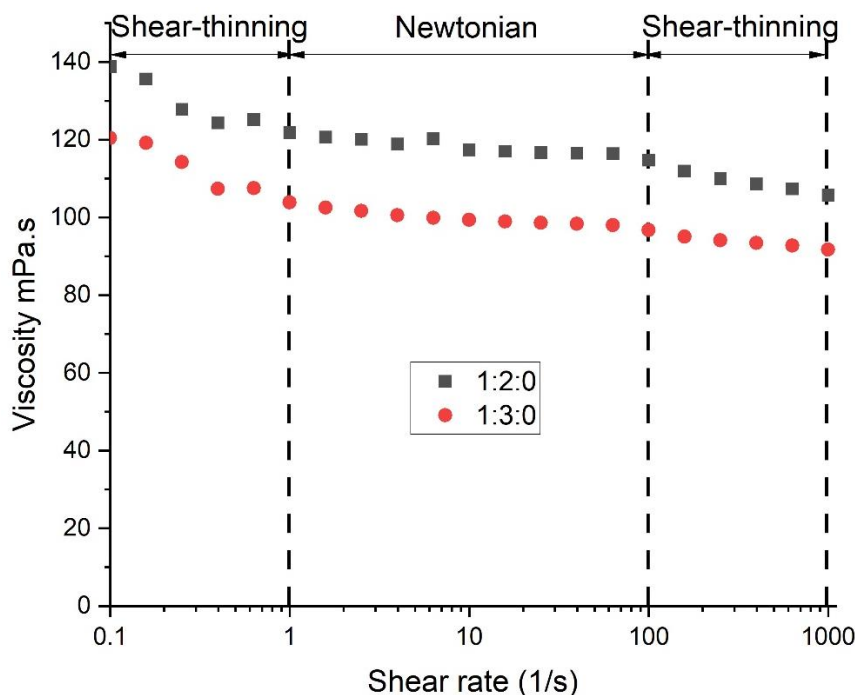


Figure 3-13 Steady shear flow curves of ChCl:LvAc DESs at 25 °C with Newtonian and non-Newtonian regions

3.3.8 TGA measurements of ChCl: LvAc DESs

The thermogravimetric analysis profile of the studied DESs showed single-step thermal degradation behaviour with varying degradation rates. The analysis showed that the ChCl:LvAc (1:2:0) DES is thermally stable up to 196°C as compared to the values of 158°C and 180°C reported in the literature reported in Ullah *et al.*¹⁶⁶ and Mellado *et al.*¹⁸⁷ respectively. The thermal stability of the tested DES compositions was found to be decreasing with increasing the molar ratio and water content simultaneously. Therefore, the minimum decomposition temperature reported is

147°C of ChCl:LvAc (1:3:5). This makes the investigated DESs fit for high-temperature applications including CO₂ capture processes. Figure 3-14 and Table 3-13 show the TGA profile of tested DES systems. Initial decomposition temperature (IDT) of the ChCl:LvAc DESs always lie in between the IDT of individual components of the HBA and HBD as shown in Figure 3-15 follows.

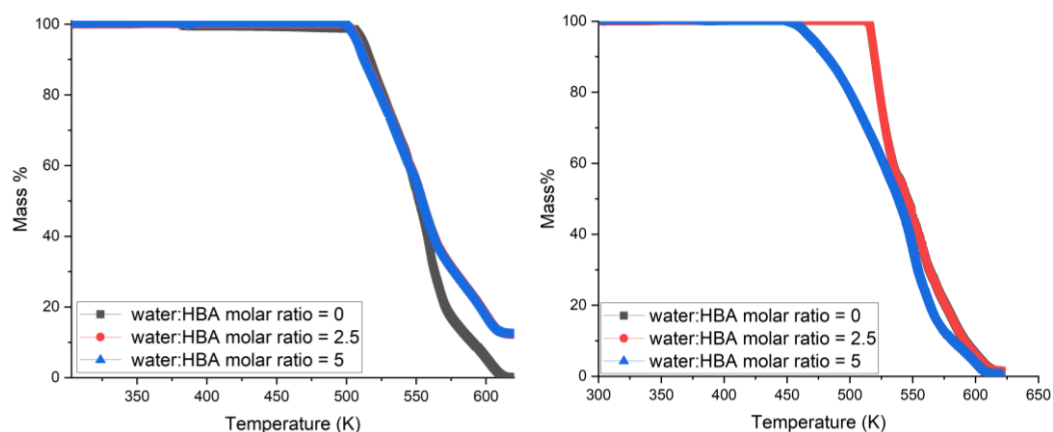


Figure 3-14 Thermal gravimetric analysis of ChCl:LvAc DESs with HBA:HBD molar ratio (1:2) (left) and (1:3) (right)

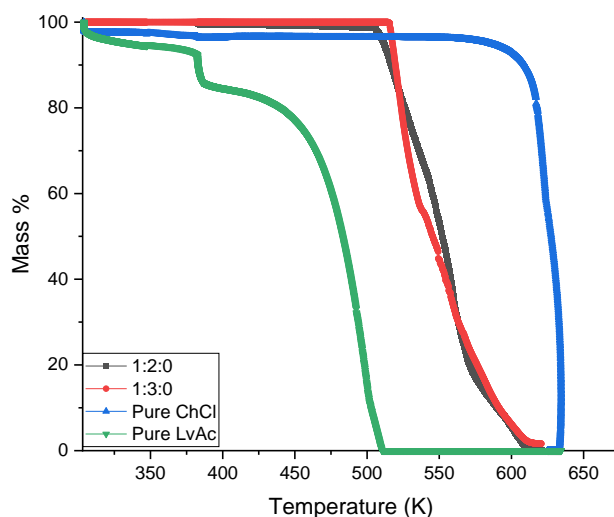


Figure 3-15 Thermal gravimetric analysis of ChCl:LvAc DESs and pure individual components

The thermal stability of ChCl:LvAc DESs declined with increasing the molar ratio and water content simultaneously. Table 3-13 displays IDT, half decomposition and final

residue values of tested DESs. IDT expresses the highest temperature at which DESs remain in a liquid state before decay and consequently their range of application as sorbents. This makes ChCl:LvAc DESs suitable for carbon capture processes or any other high-temperature applications. Half decomposition ($D_{1/2}$): is the temperature at which 50 wt.% of DESs samples of 30 mg is degraded. While final Residue (FR): is the remaining amount of sample at the end of the test.

Table 3-13 Thermal Stability of DESs at a heating rate of 5 °C ·min⁻¹, P = 0.1 MPa

DES composition	Initial decomposition temperature (K)	Half decomposition (K)	Final residue (wt.% at 623.15 K)
1:2:0	469	525	0.2
1:2:2.5	430	523	12.3
1:2:5	430	527	12.3
1:3:0	469	527	0.5
1:3:2.5	458	517	1.3
1:3:5	421	510	0.4

3.3.9 The corrosivity of ChCl:LvAc DESs

The weight loss due to corrosion was calculated according to Equation (3-6) and presented in Figure 3-16. The data presented in Figure 3-16 clearly show that three cleaning cycles are needed to remove all corrosion adherent products from the specimen using Clark solution. No corrosion adherent products were observed after three cleaning cycles while the average weight-loss of specimen increased slightly between the second and the third cleaning cycle as per Figure 3-16. Further cleaning of specimen results in weight loss due to cleaning only not corrosion. It also shows the net weight loss due to the corrosion effect, by deducting total weight loss due to cleaning only which was found to be 4.4 mg from the total weight loss of each specimen. Therefore, the difference between in weight of the baseline –control

specimen- and test specimen represents the net weight loss due to corrosion that is used for CPR calculation.

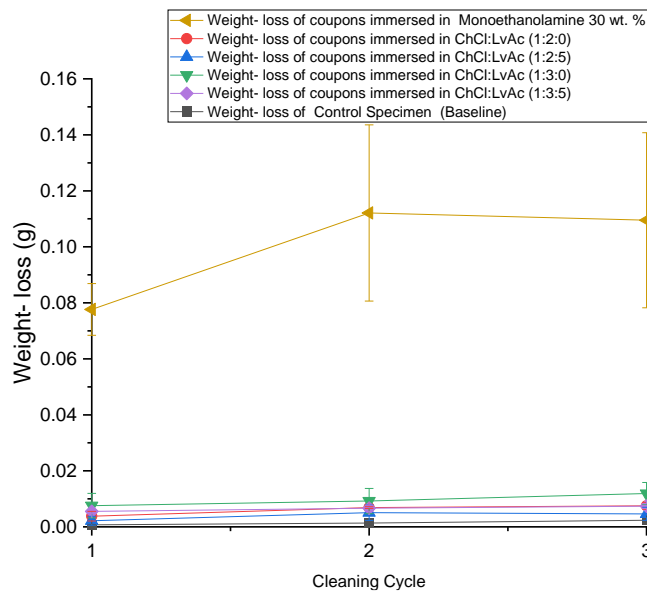


Figure 3-16 (A) Weight-loss of control specimen Vs. weight-loss of experimented specimen

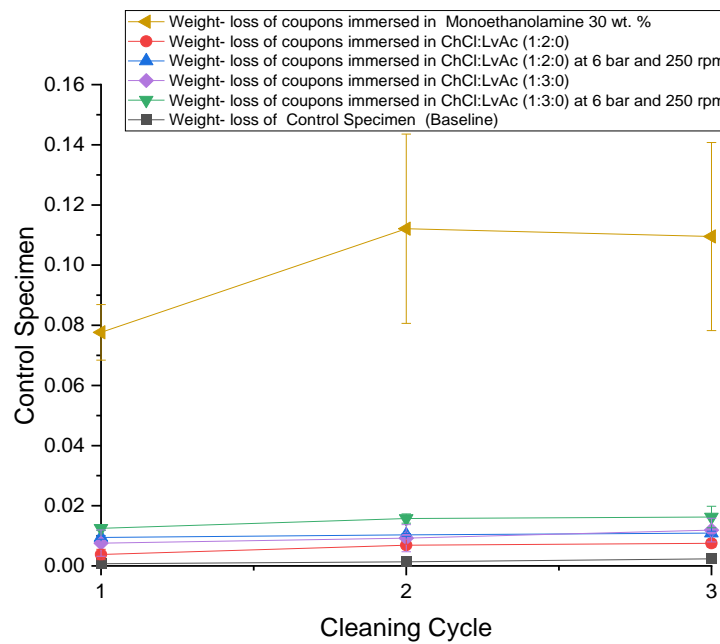


Figure 3-17 (B) Weight-loss of control specimen Vs. weight-loss of experimented specimen

3.3.9.1 Calculation of the corrosion penetration rate (CPR)

The CPR values of ChCl:LvAc DESs are increasing with increasing the molar ratio of the HBD to HBA. The average CPR value of ChCl:LvAc (1:2:0) is 0.023 mm.Y⁻¹ while, the CPR value of ChCl:LvAc (1:3:0) was a bit higher at 0.056 mm.Y⁻¹.

In addition to the effect of increasing the HBD to HBA molar ratios, CPRs figures were found to drop in the presence of water as compared to the ones in the absence of water. ChCl: LvAc (1:2) with a water:HBD molar ratio of 5, exhibited a lower CPR value of 0.015 mm.Y⁻¹ as compared to the CPR value for ChCl: LvAc (1:2) without water. Also, ChCl:LvAc (1:3:) with the largest water content (water:HBA molar ratio of 5) showed a lower CPR value of 0.022 mm.Y⁻¹ as compared to the CPR value obtained for the ChCl: LvAc DES without water (1:3:0) as shown in Figure 3-18.

Finally, CPR values increase with stirring speed and CO₂ concentration simultaneously in the system. The corrosivity of ChCl:LvAc DESs with (1:2:0) and (1:3:0) has increased from 0.023 mm.Y⁻¹ and 0.055 mm.Y⁻¹ at stagnant conditions to 0.04 mm.Y⁻¹ and 0.102 mm.Y⁻¹ respectively at stirring speed of 100 rpm and 6 bar of CO₂ pressure as per Figure 3-18. Prepared CPR values of ChCl: LvAc (1:2:0) at stirring conditions and 6 bar of CO₂ are higher than the ones prepared by Ullah *et al.* in their work ¹³⁶ of 0.027 mm.Y⁻¹.

There are four reasons behind getting a lower value of the same DES system, firstly, Ullah *et al.* in their work ¹³⁶ prepared the CPR's for carbon steel 1018 not mild steel DC01-CR4 as in our case. Secondly, they used the EC, not the WL method. More importantly, they did not consider weight loss due to the chemical cleaning of the specimen (Wc) by utilising the control specimen as per our case and the ASTM G1-03. While Ullah *et al.* ¹³⁶ never showed how they performed chemical cleaning of

coupons after the corrosion test. Finally, Ullah *et al.* in their work ¹³⁶ conducted the test under stagnant conditions; whereas the CO₂ absorption capacity of ChCl:LvAc DESs increases with stirring speed as per our previous analysis. Increasing the concentration of CO₂ due to the stirring effect leads to an increase in the CPR value for the same DESs composition.

We can safely conclude that CPR values for ChCl:LvAc DESs increase with HBD/HBA ratio, stirring speed and CO₂ concentration and pressure simultaneously and decreases with increasing water content in the system as per Figure 3-19. On the other hand, MEA solution at 30 wt.% showed the highest CPR value of 0.7 mm.Y⁻¹ which is higher than the results prepared by Ullah *et al.* in ¹³⁶ since the metal we used in this work DC01-CR4 has poor corrosion resistance as compared to the carbon steel 1018 used by Ullah *et al.* ¹³⁶. Finally, we found out that MEA is more corrosive than ChCl:LvAc DESs even in the absence of water according to the WL method as per Figure 3-18.

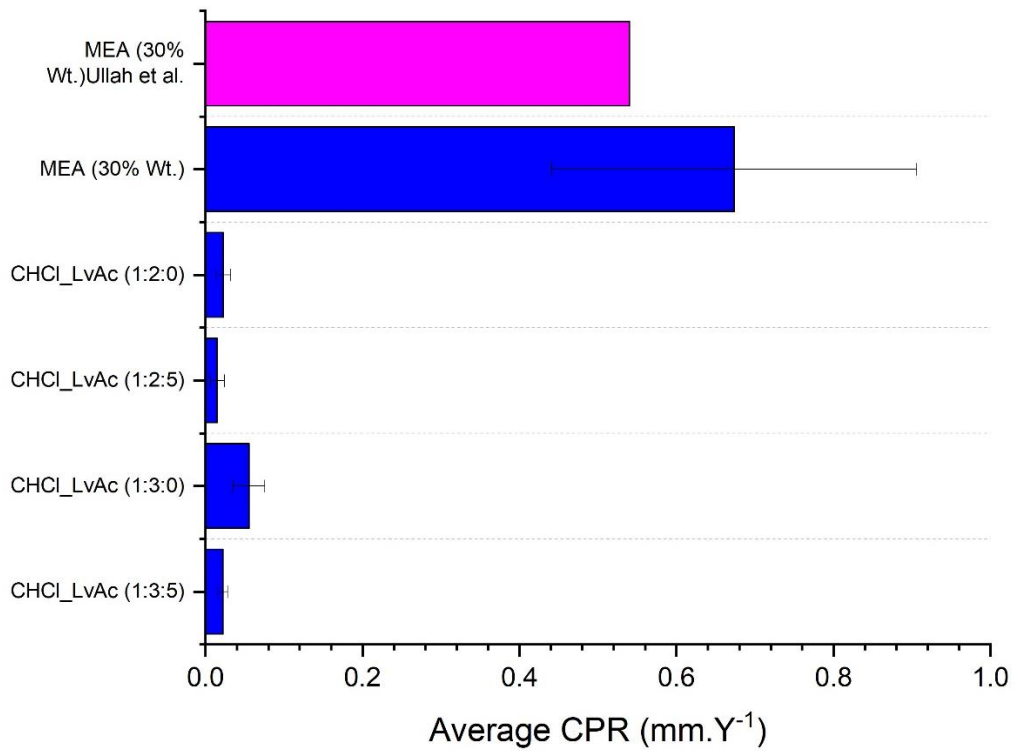


Figure 3-18 CPR values of ChCl:LvAc DESs and MEA on coupons at 25 °C at stagnant conditions

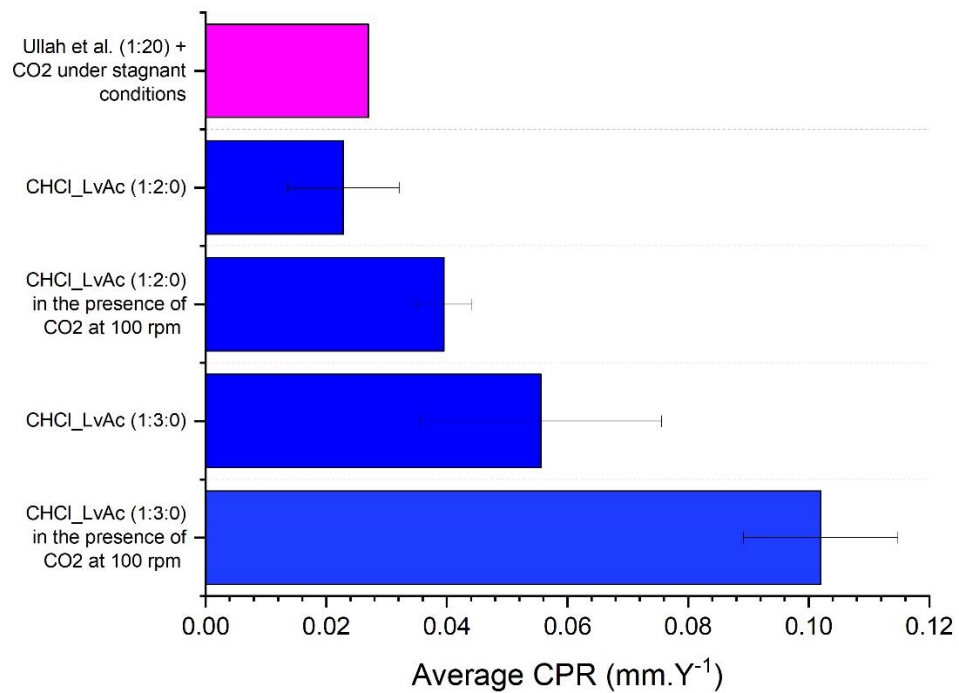


Figure 3-19 Average CPR values of ChCl:LvAc DESs on coupons at stagnant conditions Vs. stirring conditions of 100 rpm and in the presence of CO₂ at. All measurements carried out at 25 °C

Corrosion tests were done at different conditions to simulate the corrosivity scenarios in the actual post-combustion absorption carbon capture plant. For example, investigating the corrosivity of the pure DESs compositions simulate the corrosion behaviour in the raw material tank. While studying the corrosivity under stirring speed and the presence of CO₂ in the absorber and the desorber units. It is recommended to study the effect of temperature on the corrosivity of ChCl:LvAc DESs, also to investigate the corrosion at the micro-level via scanning electron microscope (SEM) as a future recommendation. Statistical analysis of results gained from both methods could also be performed to investigate the significance of the main parameters affecting the corrosivity of DESs and interactions among these parameters.

3.4 Conclusion

Choline chloride:levulinic-based DESs were prepared successfully at different molar ratios and water contents using the heating preparation method as explained in section 3.2.2. Homogeneous DES systems were successfully prepared with HBA:HBD molar ratios of (1:2) and (1:3).

The phase behaviour plot (solid-liquid diagram) of ChCl:LvAc mixtures is constructed and reported for the first time. The temperature depression from ideality, ΔT_d , which is the difference between the ideal mixture melting temperature (T_i) and the deep eutectic temperature (T_{em}) was calculated for ChCl: LvAc mixtures with HBD mole percentage equal to or above 66.7%. These mixtures are liquid at room temperature with $\Delta T_d > 0$ thus fulfilling all the criteria for being considered deep eutectic mixtures and, therefore, can be defined as DESs.

In this work, the FTIR transmittance of ChCl:LvAc DESs was reported at different molar ratios and water contents. The coexistence, stretches and shifts of some

vibrational bands of functional groups in the DES and its components show the formation of the ChCl:LvAc DESs compositions.

The density of prepared ChCl:LvAc DESs was measured at different water content molar and ratios at temperatures ranging between 20 - 65 °C. The density of investigated ChCl:LvAc DESs found to decrease with increasing the temperature and water content simultaneously.

The viscosity values of the prepared ChCl:LvAc DESs are in good agreement with the ones reported in the literature. Increasing the HBD mole fraction decreases the viscosity of the ChCl:LvAc DESs. The viscosity of all studied ChCl:LvAc DESs decreases with increasing temperature as has been extensively reported in the literature. ChCl:LvAc DESs showed a light shear thinning behaviour at shear rates between 0.1 and 1 s⁻¹. However, the viscosity remains constant between 1 s⁻¹ and 100 s⁻¹ which makes ChCl:LvAc DESs Newtonian fluids in this range of shear rates. At shear rate above 100 s⁻¹ the DESs are also slightly shear-thinning.

All ChCl:LvAc DESs showed single-step thermal decomposition behaviour. The TGA analysis demonstrates that the ChCl:LvAc (1:2:0) DES is thermally stable up to temperatures of 196 °C, a temperature higher than reported in the literature of the same. This makes ChCl:LvAc DES system stable at the typical operating temperatures observed in post-combustion CO₂ capture process.

The corrosion penetration rate (CPR) of ChCl:LvAc DESs was found to increase with HBD mole fraction, stirring speed and CO₂ presence and decreases with increasing water content in the system. On the other hand, MEA solution at 30 wt.% showed the highest CPR value of 0.7 mm.Y⁻¹ which is similar to the results obtained by Ullah *et*

al. ¹³⁶. ChCl:LvAc DESs are much less corrosive than MEA even in the absence of water according to the weight loss method.

In this work, several techniques were used to characterise the ChCl:LvAc DESs. This is an essential step to verify the suitability of utilising these DESs for carbon capture processes or any application domain. The magnitude of investigating the properties of such DESs systems comes from the necessity of introducing benign sorbents that are viable for some engineering applications including but not limited to carbon capture processes, catalysis, and solvent extraction. To investigate the viability of these DESs systems, the physicochemical characteristics of such new sorbents of DESs must be evaluated and assessed before being considered for any application.

This chapter has covered the gaps in the literature related to the properties of ChCl:LvAc DESs. In the next chapter, the viability of ChCl:LvAc DESs for carbon capture processes is evaluated under different compositional and operational conditions.

Chapter 4: Experimental study of CO₂ absorption and desorption by choline chloride levulinic acid-based deep eutectic solvents

4.1 Overview

Chapter 3 presented a comprehensive characterisation of choline chloride:levulinic acid-based deep eutectic solvents (ChCl:LvAc) to evaluate their viability for carbon capture processes. Chapter 3 also highlighted the operational and compositional parameters that affect the CO₂ absorption and desorption by the DESs. This chapter presents a work published in *Molecules* journal published by MPDI. The title of the article is “A comprehensive study of CO₂ absorption and desorption by choline chloride levulinic acid-based deep eutectic solvents”, and was published in September 2021 (DOI <https://www.mdpi.com/1420-3049/26/18/5595>). In this chapter, the viability of ChCl:LvAc DESs for carbon capture processes is investigated. To evaluate the carbon capture performance of ChCl:LvAc DESs, the absorption and desorption of CO₂ by ChCl:LvAc DESs with different compositions were investigated thoroughly under different operational conditions and compared with the CO₂ absorption by monoethanolamine (MEA) as the benchmark. Furthermore, the carbon capture performance in terms of the recyclability and the selectivity of ChCl:LvAc DESs was evaluated and reported in this chapter. The supplementary material of this work is presented in Appendix B.

4.2 Summary

In this work, the CO₂ absorption capacity of choline chloride/levulinic acid-based deep eutectic solvents ChCl:LvAc DESs was measured at different temperatures,

pressures and stirring speeds using a vapour liquid equilibrium rig. DESs regeneration (CO₂ desorption) was performed using a heat treatment method. FTIR was used to verify the absorption and desorption of CO₂ by/from ChCl:LvAc DESs at different temperatures for these compositions for the first time in the literature. The molar ratios of ChCl: LvAc were selected as 1:2 and 1:3 with different water contents were used. Thermodynamic properties such as Henry's constants, enthalpy, entropy and Gibbs free energy for CO₂ dissolution were calculated from the solubility data. The experimental results showed that the CO₂ absorption capacity of the ChCl:LvAc DESs is strongly affected by the operating pressure and stirring speed, and minimally affected by the HBA:HBD molar ratio and the water content of the DES. The results also showed that the CO₂ absorption capacity of the DESs decreases with increasing temperature. The regeneration of the DESs was performed at different temperatures, with the optimal regeneration temperature estimated to be 60 °C. In this work, the DESs exhibited good recyclability and good selectivity towards CO₂ over N₂, up to 5.63 at 50% mole CO₂ and 25 °C.

4.3 Introduction

The effect of the water content on CO₂ absorption by a DES (CO₂ solubility) depends on the specific composition of the DES, with researchers reporting different trends for different systems. Several researchers^{155, 226, 178} have studied the CO₂ absorption in choline chloride-based DESs with urea (reline), with the review by Rima¹⁴⁴ showing reline as a promising sorbent for CO₂ capture when compared with ILs. However, CO₂ solubility in reline drops significantly with increasing water content as water acts as an anti-solvent in this system^{227,184}. On the other hand, CO₂ solubility increases with water content in other DES systems. For example, this behaviour is observed in L-arginine:glycerol mixtures with molar ratios ranging between 1:4 and 1:8 as reported

by Ren *et al.* ¹⁵⁶. One potential explanation for this phenomenon is that small increments in water content lead to a significant reduction in the viscosity of the DESs, which enhances CO₂ solubility ¹⁵⁶.

(ChCl:LvAc) DESs are biodegradable, non-toxic and cheap sorbents as reported by Magugeri *et al.* ²⁰⁴. CO₂ absorption into ChCl:LvAc DESs have been studied at a molar ratio of 1:2 at a temperature of 50 °C and pressure up to 30 bar by Ullah *et al.* ¹⁶⁶, while Lu *et al.* in their work in ²⁰⁵ increased the molar ratio of the hydrogen bond donor (levulinic acid) up to 1:5. However, the effect of water on CO₂ solubility in ChCl:LvAc is still unknown; and because both the HBD and the HBA are hygroscopic ¹⁸⁷, studying the effect of water in CO₂ solubility is crucial for practical reasons when dealing with wet flue gas as well. Besides, CO₂ absorption thermodynamics in ChCl:LvAc DESs and sorbent/DES regeneration are still not reported in the literature as concluded by the authors in a recent review of the literature discussed in chapter 2 and submitted as a review paper for publication.

Many studies in the literature have reported on the effect of stirring speed on CO₂ absorption by ethanolamine aqueous solutions ^{228, 229}. For example, Pashaei *et al.* ²³⁰ reported a dramatic increase in the CO₂ absorption capacity of aqueous solutions of diethanolamine (DEA) by increasing the stirring speed of their apparatus from 0 to 600 rpm. On the other hand, no such attention has been given to the effect of stirring speed on CO₂ absorption by deep eutectic solvents (DES). For example, although Ullah *et al.* ¹⁶⁶ and Lu *et al.* ²⁰⁵ have reported the CO₂ absorption of some choline chloride:levulinic acid DESs at different temperatures and pressures, the effect of the stirring speed on the CO₂ absorption capacity was not taken into consideration. For a better assessment of the viability of any sorbent for CO₂ capture purposes, the absorption isotherms should be studied under dynamic conditions as similar as

possible to ones these applied in the industrial plants (i.e. in the absorption columns)²²⁸ rather than studying the absorption capacity of sorbents under stagnant conditions.

Few researchers in the literature have reported on the recyclability of DESs. For example, Ren *et al.*¹⁵⁶ studied the regeneration process of L-arginine:glycerol DESs with a molar ratio 1:6 by bubbling nitrogen gas at 100 °C for 80 min to release the CO₂. The recyclability of choline chloride:levulinic acid DESs is still unknown; therefore, one of the main objectives of this work is to investigate the recyclability of ChCl:LvAc DESs at constant conditions of temperature, pressure and stirring speed.

Most researchers in the literature have reported the solubility of acidic gases²³¹ such as hydrogen sulfide²³², nitrogen dioxide²³³, and CO₂ gas mixtures in the DESs. However, for most DESs the selectivity of DESs towards CO₂ in a mixture of CO₂/N₂ gases is not commonly tested, including the CO₂/N₂ selectivity of choline chloride:levulinic acid-based DESs. Therefore, it is essential to investigate the selectivity of chloride:levulinic acid-based DESs towards CO₂ among other gases.

The major objective of this chapter is to investigate the CO₂ absorption and desorption at different operating conditions and thereby optimise some key operating parameters of the process. Experimental parameters such as molar ratio, pressure, temperature, stirring speed, and water content were selected as input factors and their effect was investigated. Different experiments were conducted using a parametric study to investigate the effectiveness of different types of DESs for carbon dioxide capture and were used to calculate the thermodynamic properties of CO₂ absorption in ChCl:LvAc DESs. Additionally, this work aims to study the recyclability of ChCl:LvAc DESs and

their selectivity towards CO₂ at specific conditions of temperature, pressure and stirring speed.

4.4 Materials and methods

4.4.1 Preparation of the DESs

All chemicals used in this work have been reported in section 3.2.1 of the previous chapter. In this work, the DESs were prepared as per section 3.2.2 described in Chapter 3. The heating method has been commonly used in literature ^{155, 157, 154, 134, 158, 159, 160, 156}.

In this chapter, the composition of DESs is represented by a label of the type “(HBA:HBD:water molar ratio)”. The nomenclature used to label DESs compositions has been summarized in section 3.1.1 of the previous chapter. Again, this nomenclature avoids the unnecessary lengthy reference to the water content each time a specific DES composition is mentioned.

4.4.2 CO₂ absorption measurements

A vapour-liquid equilibrium (VLE) absorption rig was used to conduct the CO₂ absorption experiments – see Figure 4-1 below. The VLE rig consists of a buffer vessel and a VLE measurement vessel (Millipore pressure vessels, model XX6700P120). Both vessels were fitted with pressure gages and valves to monitor and control the pressure. An incubation chamber was used to control the temperature of the system with a precision of ± 0.5 °C. The pressure and temperature inside the absorption vessel were monitored by a GS4200-USB digital pressure-temperature transducer and software purchased from ESI Technology Ltd. (UK).

The CO₂ absorption capacity of different ChCl:LvAc DESs was measured at different temperatures, pressures and stirring speeds. In the absorption measurement runs, a known mass of DES (40 g) was loaded into the VLE measurement vessel. After thermal equilibrium was reached –normally within 2 hours – the pure CO₂ (or pure N₂ and CO₂/N₂ mixtures in the case of the selectivity tests) was quickly transferred from the buffer vessel into the VLE measurement vessel until the desired pressure level was reached. The system was maintained under test conditions (temperature and stirring rate) until equilibrium was reached.

To ensure the validity of results, baseline and calibration runs were carried out before conducting any absorption measurements. The baseline runs were “leakage detection runs” and consisted in charging the rig with CO₂ in the absence of DES at a constant temperature, and in monitoring the pressure drop in the system until equilibrium was reached. Baseline runs were necessary to ensure that the pressure drop in the system during the measurement runs was only due to gas absorption by the DESs and not due to residual leakages. The calibration runs consisted in charging the rig with an aqueous solution of MEA 30 wt% (instead of a DES) and by running CO₂ absorption experiments at 25 °C and pressures up to 6 bar. The results of the baseline and calibration runs are available in table B-1 in Appendix B.

Generally, DESs have low vapour pressures²³⁴; therefore it was assumed that the total pressure in the system is equal to the pressure of the pure gas or gas mixture charged into the rig. The CO₂ absorption capacity by the ChCl:LvAc DES was calculated based on the absolute pressure drop due to absorption only as per equation 4-1 and equation 4-2 below and then expressed in terms of moles of CO₂ per kg of DES (mol.kg⁻¹). The pressure drop due to CO₂ absorption only, ΔP , is given by:

$$\Delta P = (P_{CO_2}^{\circ} - P_{CO_2}^{equil}) - (P_{baseline}^{\circ} - P_{baseline}^{equil}) \quad \text{Equation (4-1)}$$

The first term of equation 4-1 represents the pressure drop in the system during the CO₂ absorption runs (measurement runs) whereas the second term accounts for the pressure drop in the system due to leakages (baseline runs). In equation 4-1, $P_{CO_2}^{\circ}$ is the CO₂ pressure at the start of the absorption/measurement run, $P_{CO_2}^{equil}$ is the CO₂ pressure when the system reaches equilibrium during the measurement run, $P_{baseline}^{\circ}$ is the pressure at the start of the baseline run and $P_{baseline}^{equil}$ is the pressure when the system reaches equilibrium during the baseline run. The experimental results (raw data) are available in Tale B-2 Appendix B.

The values of pressure drop were then used to calculate the number of moles of CO₂ absorbed by 40g of the DES according to:

$$n = \frac{V * \Delta P}{R * T} \quad \text{Equation (4-2)}$$

where n is the number of CO₂ moles absorbed by the DES, V is the volume of the measurement vessel in m³, ΔP is the absolute pressure drop due to absorption calculated using Equation (4-1) (in Pa), T is the absorption temperature in Kelvin and R is the universal gas constant in J.mol⁻¹ K⁻¹.

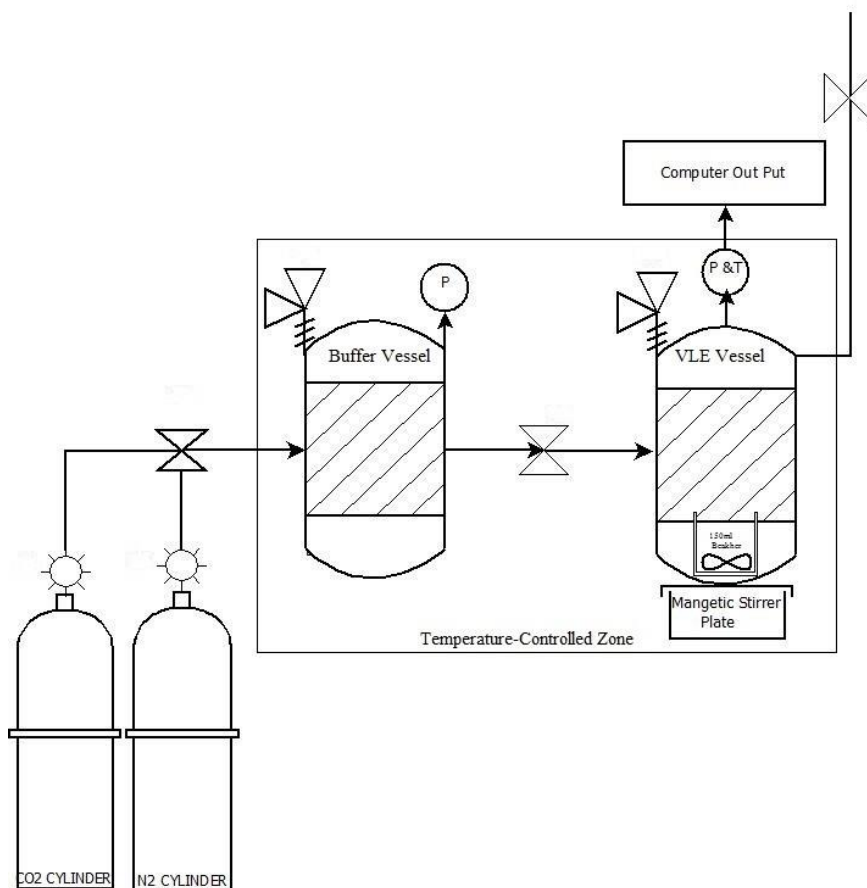


Figure 4-1 Schematic diagram of the VLE absorption rig to measure CO₂ absorption by DES systems. Adopted with modification from ¹¹⁹

4.4.3 Thermodynamics analysis of CO₂ absorption

The solubility of CO₂ in the DESs can be expressed in terms of Henry's law constant (HLC). The smaller the value of the HLC, the higher the solubility in the liquid ^{155, 118} and ²⁰⁶. The HLC based on mass fractions, H_x , was calculated using equation B-1 in Appendix B. Additionally, the enthalpy (ΔH), Gibbs free energy (ΔG) and entropy (ΔS) of absorption were calculated using the Van't Hoff equations (B-5, B-6 and B-7 in Appendix B).

4.4.4 Sorbent regeneration measurements

Sorbent regeneration starts once the rig is depressurised, with the spontaneous release of part of the absorbed gas. To release the residual CO₂ still absorbed in the DES samples after depressurisation (CO₂ not-spontaneously released), a heat treatment was used. CO₂ desorption tests were performed in an oven by heating 10g aliquots of the DESs samples with residual CO₂ at temperatures of 60°C, 80 °C and 100 °C for 60 minutes. The weight-loss method was used, with the weight-loss of the aliquots measured by a Mettler Toledo AM100 electronic balance with an accuracy of 2×10⁻⁴ g.

4.4.5 FTIR spectra measurements

To determine the CO₂ released after thermal treatment at each desorption temperature, FTIR spectra of the DES samples were measured before CO₂ absorption, after CO₂ absorption and after thermal treatment. The FTIR spectra were measured using an ABB MB 3000 FTIR spectrophotometer (Clairet Scientific Ltd., Northampton, UK). The device was calibrated with air before measuring the transmittance of the samples. The CO₂ released was determined using the Beer-Lambert law²³⁵ as per Equation 4-3 below:

$$A = \epsilon L C \quad \text{Equation 4-3}$$

where A is the absorbance of samples before and after CO₂ absorption and after desorption at different temperatures, ϵ is the molar absorptivity of the CO₂ in (L.mol⁻¹.cm⁻³) is the path length of the sample in cm and C is the concentration of CO₂ in the sample in mol.L⁻¹.

4.4.6 Recyclability of the DESs

Two replicate samples of ChCl:LvAc (1:2:0) were selected for this purpose. The DES samples were subjected to 5 sequential absorption/desorption cycles under the following experimental conditions: a) constant temperature of 25 °C; b) CO₂ pressures up to 300 kPa during the absorption step; c) 250 rpm stirring speed during the absorption step; and d) desorption (heat treatment) temperature of 80 °C.

All samples were cooled down to room temperature before starting the next absorption/desorption cycle. Weight-gain and weight-loss measurements were taken before and after each CO₂ absorption and desorption step, respectively.

4.4.7 Selectivity of the DESs towards CO₂

Samples of ChCl:LvAc DES with composition 1:3:2.5 were used in the CO₂ selectivity tests. The tests were performed using N₂/CO₂ gases mixtures with different molar ratios of CO₂ (100%, 50%, 15% and 0%, respectively). All tests were carried out under constant temperature of 25 °C, pressures up to 300 kPa and stirring speed 250 rpm. The total pressure inside the buffer vessel is equal to the summation of the partial pressures of the two gases. The partial pressures of CO₂ and N₂ before the absorption measurements and at the start of the absorption measurements are given in Table 4-1 below.

Table 4-1 Partial pressures of CO₂ and N₂ and the total pressure applied in the selectivity tests.

Run	Before measurements: pressure in buffer tank only (during temperature equilibration)		At the start of the measurements: pressure in the buffer and measuring tanks	
	p _{CO2} (bar)	p _{N2} (bar)	p _{CO2} (bar)	p _{N2} (bar)
Pure CO ₂	6	0	3	0
50% CO ₂ / 50% N ₂	3	3	1.5	1.5
15% CO ₂ / 85% N ₂	0.9	5.1	0.45	2.55
Pure N ₂	0	6	0	3

The absorption of the pure CO₂ is taken as the baseline in this case. The selectivity of absorbing CO₂ over N₂ of the DESs is defined as (S_{CO_2/N_2}) as per Equation 4-4 and Equation 4-5 below.

Selectivity based on the absorption of pure gases in the DES:

$$S_{CO_2/N_2} = \frac{x_{CO_2}}{x_{N_2}} \quad \text{Equation 4-4}$$

Selectivity based on the absorption of mixtures of gases in the DES:

$$S_{CO_2/N_2} = \frac{x_{CO_2}}{x_{N_2}} \times \frac{y_{N_2}}{y_{CO_2}} \quad \text{Equation 4-5}$$

where x is the mole fraction of CO₂ or N₂ absorbed by the DESs, and y is the mole fraction of CO₂ or N₂ in the gas phase.

4.5 Results and discussion

4.5.1 CO₂ absorption

In the first set of experiments, the CO₂ absorption capacity of different ChCl:LvAc DESs was measured at different pressures and temperatures, with the DESs under a constant stirring speed of 250 rpm. The results obtained are presented in Figure 2, which shows quite similar values of absorption capacity and trends for all DES compositions. A visual inspection of Figure 4-2 seems to indicate that, overall, the HBA:HBD molar ratio and the water content both have a small effect on the CO₂ absorption capacity in ChCl:LvAc DESs. The only obvious trend observed concerns the effect of temperature, with the CO₂ absorption capacity decreasing with increasing temperature for all compositions. The temperature trend observed for the ChCl:LvAc DESs agrees with the results reported in the literature for other DESs ^{155, 118, 119, 133}.

The CO₂ absorption capacities measured for the ChCl:LvAc DESs are clearly lower than the CO₂ absorption capacity reported in the literature for aqueous solutions of MEA at 30 wt% ²³⁶ as shown in Figure 4-3 below. This might be due to the fact that the CO₂ absorption mechanism is different in both cases: CO₂ absorption in MEA solutions is a combination of chemisorption and physisorption ^{237, 85}, whereas the CO₂ absorption in the DESs studied in this work is limited to physisorption only ²³⁸. The values of CO₂ absorption capacity reported in this work are higher than the values reported in the literature by Ullah *et al.* in ¹⁶⁶ and Lu *et al.* in ²⁰⁵ for ChCl:LvAc DESs at pressures between 1 and 6 bar. The justification for the higher values presented in this work seems to be related with the use of “flow”/dynamic conditions. While the results reported by Ullah *et al.* in ¹⁶⁶ and Lu *et al.* in ²⁰⁵ seem to have been measured under stagnant conditions, the results presented in Figure 4-2 below were all obtained under strong stirring (250 rpm). To support this hypothesis, the effect of stirring speed

on the CO₂ absorption capacity of ChCl:LvAc DESs was studied and the results are presented in Section 4-3.

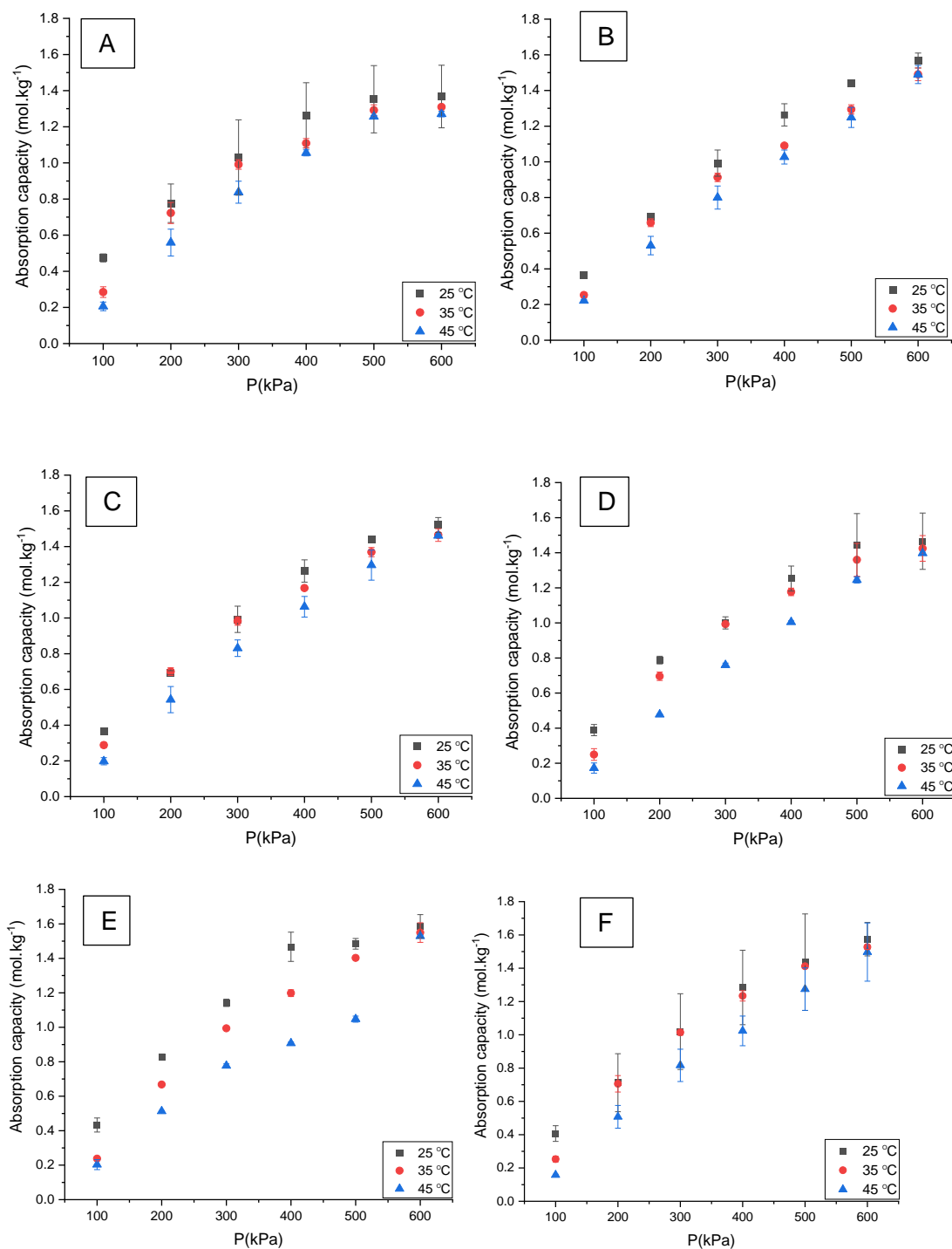


Figure 4-2 CO₂ absorption capacity of ChCl:LvAc DESs with different compositions at temperatures ranging from 25 °C to 45 °C at a stirring speed of 250 rpm: A – 1:2:0; B – 1:2:2.5; C – 1:2:5; D – 1:3:0; E – 1:3:2.5; F – 1:3:5.

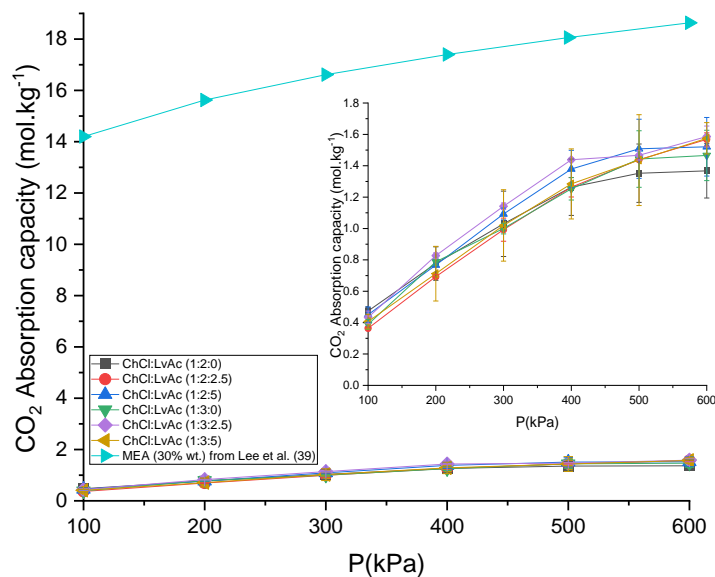


Figure 4-3 The CO₂ absorption capacity of ChCl: LvAc Vs. MEA 30% wt. at 25 °C

4.5.2 Thermodynamics analysis of CO₂ absorption

According to the literature, the absorption of CO₂ in DESs made of choline chloride and carboxylic acids is only due to physisorption^{119, 238}. The thermodynamic properties of CO₂ absorption in ChCl:LvAc DESs were estimated at 1 bar. Henry's law constant (H_x), the change in enthalpy (ΔH), the change in entropy (ΔS) and the change in Gibbs free energy (ΔG) were calculated and are presented in Table 4-2 below.

As expected based on the experimental results presented in Section 4.5.2 below, the values of H_x tabulated in Table 4-2 are very consistent and similar for all DES compositions. The values of H_x represents the driving force of the dissolution of CO₂ in ChCl:LvAc compositions. H_x increase with increasing temperature for all ChCl:LvAc

compositions and the data are well fitted by a $\ln(Hx)$ versus $1/T$ correlation as exemplified by the Arrhenius plot in Figure 4-4 below.

CO₂ absorption in ChCl:LvAc DESs is exothermic ($\Delta H < 0$); therefore, increasing the temperature decreases CO₂ uptake as reported in the literature by other researchers^{116, 205}. It is worth-mentioning that, the heat of CO₂ absorption in ChCl:LvAc DESs is higher than those reported in the wider literature due to the stirring effect at which these data were generated^{229, 239}.

On the other hand, the negative change of entropy ($\Delta S < 0$) for CO₂ absorption in ChCl:LvAc DESs indicates a more ordered system after absorption takes place. Additionally, the ΔG values for the CO₂ absorption in ChCl:LvAc DESs were found to be positive, signifying that the absorption process is not thermodynamically spontaneous²⁴⁰. The results obtained are aligned with results reported in the literature for other DESs. For example, Mirza *et al.*¹¹⁹ analysed the thermodynamics of CO₂ absorption in reline, ethaline and malinine, and showed that the absorption process was also exothermic and nonspontaneous.

Table 4-2 Calculated values of Henry's law constant, changes in enthalpy, entropy and Gibbs free energy of CO₂-DESs at 1 bar

CO ₂ -DESs	T (K)	Hx (MPa)	$-\Delta H$ (kJ.mol ⁻¹)	ΔG (kJ.mol ⁻¹)	$-\Delta S$ (J.mol ⁻¹ .K ⁻¹)
CO ₂ -ChCl:LvAc (1:2:0)	298.15	5.34	41.5	9.86	172.4
	308.15	6.92	49.6	10.9	196.1
	318.15	12.1	65.9	12.7	246.8
CO ₂ -ChCl:LvAc (1:2:2.5)	298.15	6.14	45.0	10.2	185.2
	308.15	8.88	56.0	11.5	218.9
	318.15	10.5	62.2	12.3	234.4
CO ₂ -ChCl:LvAc (1:2:5)	298.15	5.47	42.1	9.92	174.6
	308.15	8.17	53.8	11.3	211.3
	318.15	10.3	61.8	12.3	232.8
CO ₂ -ChCl:LvAc (1:3:0)	298.15	5.60	42.7	9.97	176.8
	308.15	10.1	59.3	11.8	230.7
	318.15	10.8	63.0	12.4	237.1

CO ₂ -ChCl:LvAc (1:3:2.5)	298.15	4.61	37.9	9.49	159.0
	308.15	9.25	57.0	11.6	222.6
	318.15	10.8	63.0	12.4	237.1
CO ₂ -ChCl:LvAc (1:3:5)	298.15	4.96	39.7	9.67	165.7
	308.15	9.29	57.1	11.6	223.0
	318.15	14.2	70.3	13.1	262.0

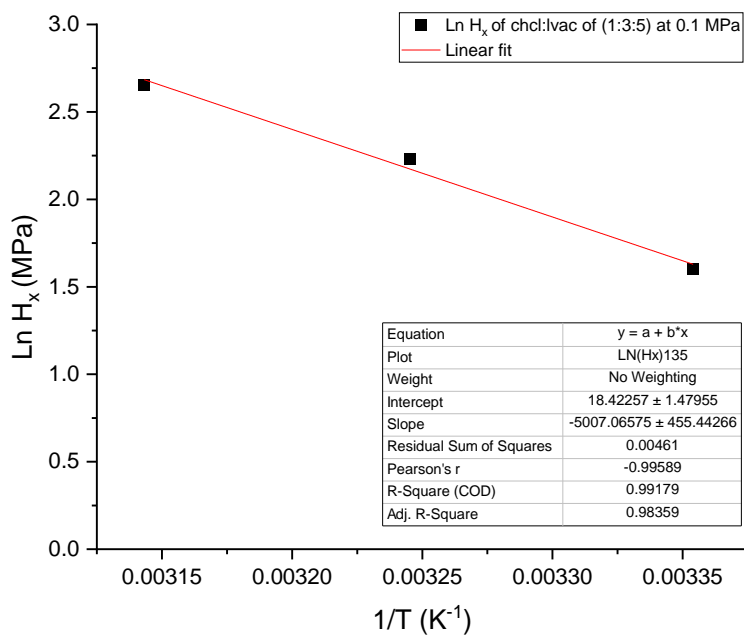


Figure 4-4 Arrhenius plot of Henry's law constant for the absorption of CO₂ in ChCl:LvAc (1:3:5)

4.5.3 The effect of stirring speed on the CO₂ absorption capacity of the DESs

The CO₂ absorption capacity by ChCl:LvAc of (1:2:0) mole ratio at 25 °C increases steadily with stirring speed as shown in Figure 4-5. below. The raw data are available in table B-3 in appendix B.

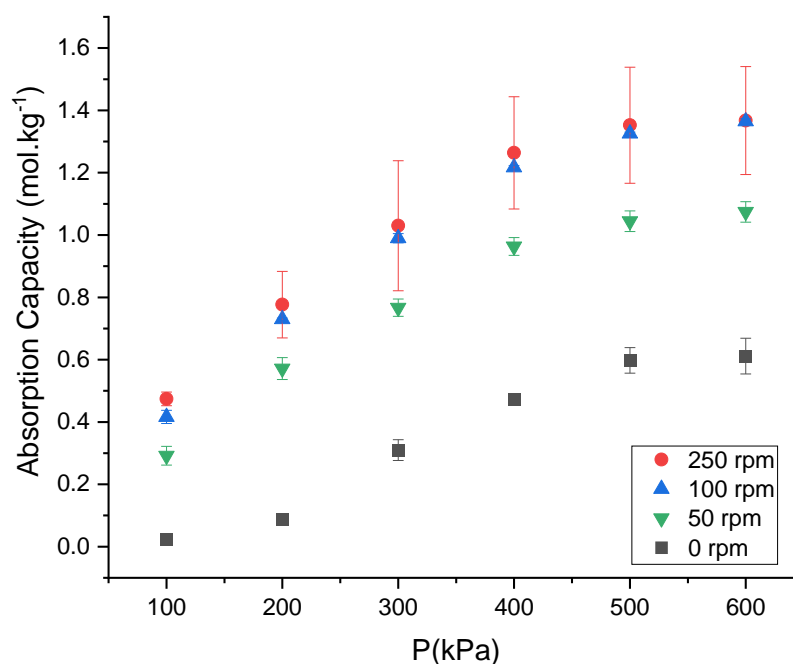


Figure 4-5 CO₂ absorption capacity of ChCl: LvAc (1:2:0) at 0 ,50, 100 & 250 rpm at 25 °C

At 6 bar and 25 °C, the CO₂ absorption capacity of ChCl:LvAc (1:2:0) increased from 0.61 mol.kg⁻¹ under stagnant conditions up to 1.37 mol.kg⁻¹ under strong (max) stirring at 250 rpm. The CO₂ absorption capacity increases strongly with increasing stirring speeds up to 100 rpm. An increase in stirring speed to a value beyond 100 rpm did not have a significant effect on the CO₂ absorption capacity. Stirring can affect the CO₂ absorption capacity of DESs in different ways. Firstly, a cylindrical beaker was used to hold the DES samples, and above a certain stirring speed, it was observed that the interface DES/gas suffered a gradual change from a circular shape (stagnant conditions) to a conical shape as the vortex in the fluid grew with increasing stirring speed. Hence, increments in stirring speed lead to larger surface areas for CO₂ absorption when compared to stagnant conditions. Secondly, in the case of stagnant conditions, CO₂ mass transfer occurs via the dissolution of CO₂ at the surface of the DESs and via the transport of the CO₂ molecules from the surface to

the bulk of the liquid solely by molecular diffusion. When the DES is stirred, convection becomes a relevant factor and facilitates/boosts the transport of CO₂ molecules from the interface to the bulk of the liquid. The facilitated mass transfer can be understood based on the two-film theory^{228,229}, and by understanding that stirring reduces the thickness of the stagnant liquid film that the CO₂ molecules must cross by molecular diffusion before reaching well-mixed zones of the fluid.

The values of CO₂ absorption capacity measured under stagnant conditions in this work are approximately similar to the ones reported by Ullah *et al.*¹⁶⁶ at low pressures as per Figure 4-6. However, the values presented in this work are slightly higher at higher pressures, with the difference reaching approximately 0.16 mol.kg⁻¹ at a pressure of 6 bar. The such difference should be at least partially due to differences in the equipment used.

On the other hand, Lu *et al.*¹⁰ reported that ChCl:LvAc DESs of higher HDB molar ratios (1:3 , 1:4, 1:5) exhibited lower CO₂ absorption capacities as compared to this work and to Ullah *et al.*¹⁶⁶ as well. This could be explained due to the following reasons : a) the water content of ChCl:LvAc DESs reported by Lu *et al.*¹⁰ is extremely low (less than 9.6×10^{-4}) as compared to this/Ullah *et al.*¹⁶⁶ work, b) the CO₂ absorption measurements done by Lu *et al.*¹⁰ these are shown in Figure 4-6 were conducted at temperatures ≥ 30 °C and slightly lower pressures as compared to this work/Ullah .¹⁶⁶ works. Furthermore, when it comes to the CO₂ absorption capacity by ChCl:LvAc DESs, pressure with temperature interaction is the most significant second order interaction as seen in section 4.5.4.7. On the other hand, increasing the molar ratio of the HBD has a minimal effect on the CO₂ absorption capacity by ChCl:LvAc DESs. This explains why the the CO₂ absorption capacity of this work as lower than the ones reported by Lu *et al.*¹⁰ considering the difference of molar ratios used of both works.

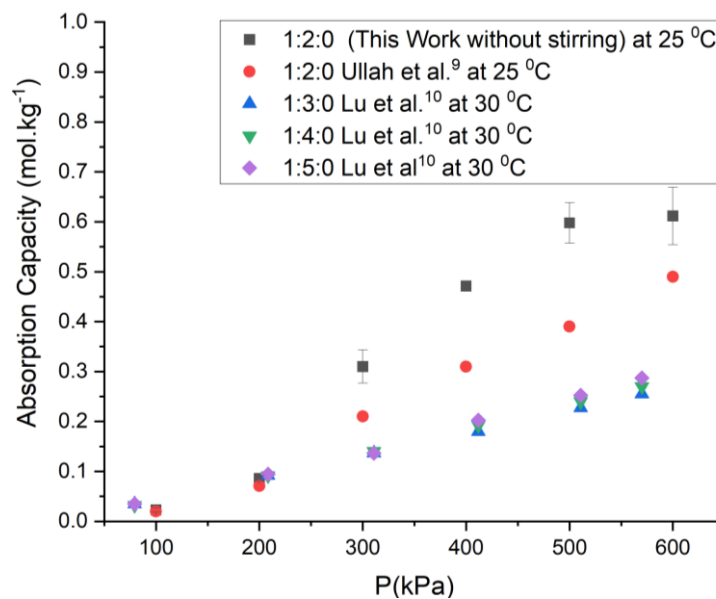


Figure 4-6 CO₂ absorption capacity of ChCl:LvAc DESs compositions at stagnant conditions

4.5.4 Statistical analysis of CO₂ absorption results

The experimental design of experiments allows determining the operating parameters at which the maximum absorption capacity could be achieved. However, it does not allow studying the interactions among controlled parameters or the optimal operating parameters. Therefore, statistical analysis of results is crucial; the optimal water content that gives the highest absorption capacity could be confirmed statistically. Also, the interactions among these parameters might give a deeper understanding of the CO₂ absorption behaviour in ChCl:LvAc DESs.

4.5.4.1 Design of experiment (DOE)

The following factorial design shown in Table 4-3 was used to conduct the experiments of CO₂ absorption in ChCl:LvAc DESs. This neat factorial design allows studying the effect of each parameter on the CO₂ absorption in ChCl:LvAc DESs. It also allows studying the second order interactions among these parameters:

Table 4-3 Factorial design factors, levels and values

Parameter	Number of levels	Values
Molar ratio	2	0.67, 0.75
Stirring speed	4	0, 50, 100, 250
Pressure	6	1, 2, 3, 4, 5, 6
Temperature	3	25, 35, 45
Water content (water:HBA ratio)	3	0, 2.5, 5

4.5.4.2 Model equation

The full factorial design was analyzed by considering all input factors and their interactions that form the following model equation described below in Equation (4-6).

$$Y = \beta_0 + \beta_1x_1 + \beta_2x_2 + \beta_3x_3 + \beta_4x_4 + \beta_5x_5 + \beta_{12}x_1x_2 + \beta_{13}x_1x_3 + \dots + \varepsilon \quad \text{Equation (4-6)}$$

Where Y is the response (CO_2 absorption capacity), the β 's are parameters whose values are to be determined, x_i represents the compositional and the operational input factors in terms of molar ratio, stirring speed, pressure, temperature and water content in the uncoded form and ε is a random error term. The developed model found to be highly accurate with $R^2 > 99\%$.

4.5.4.3 Analysis of variance

Analysis of variance of the full factorial design - table B-4 in Appendix B- shows the effect of each controlled parameter (molar ratio, stirring speed, water content, pressure and temperature) and the second and third-order interactions among the parameters on the response in terms of the CO_2 absorption capacity via ChCl:LvAc DESs.

As can be seen from table B-4, all controlled parameters were found to be significant (with P-value < 0.05), and some of the second and interactions among the factors were found to be significant as will be demonstrated in the following sections. Only one third-order interaction among the parameters was found to be significant in this model equation. Coefficients of the parameters (the β 's) of the model are presented in Table B-4.

4.5.4.4 Residual's analysis

The residual plot for the data shows a normal distribution of the residuals with equal variance and independent distribution as shown below in Figure 4-7. Which validates that the fitted model is highly accurate with $R^2 > 99\%$ as shown in section B-6 in Appendix B.

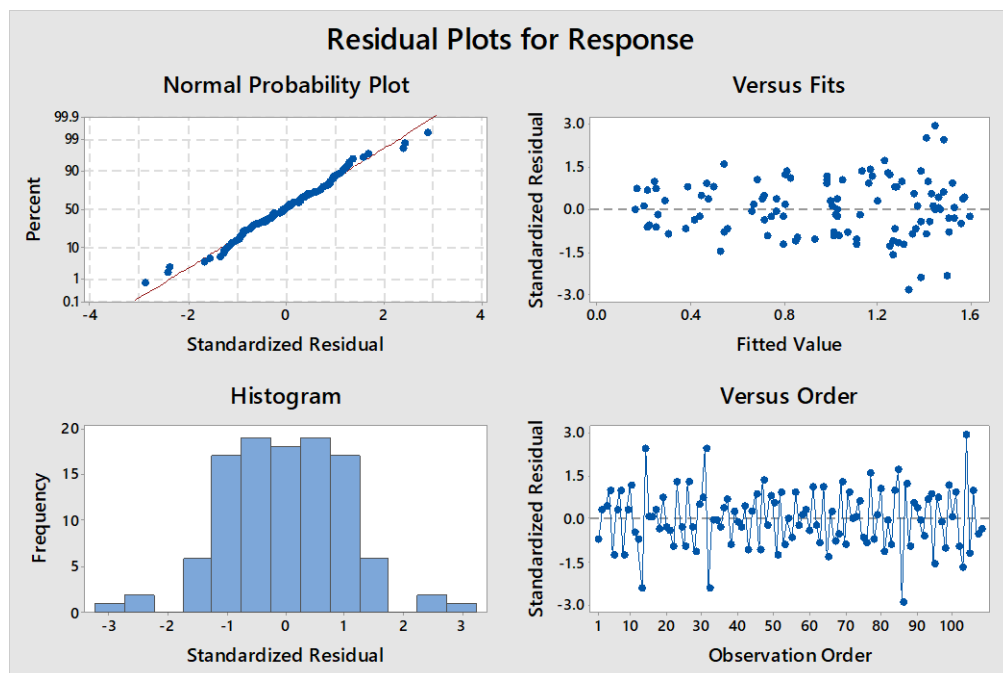


Figure 4-7 Residual plots for response

4.5.4.5 Main effects plot

All controlled factors have statistically relevant effects on the CO₂ absorption in ChCl:LvAc DESs with p-values < 0.05. Figure 6 presents the main effects plot with the mean response for each factor. The pressure is the most significant factor with a contribution of 79.31% to the model describing CO₂ absorption in ChCl:LvAc DESs, followed by the stirring speed with 14%, temperature with 2.8%, water content with 0.39% and finally the HBA:HBD molar ratio with a contribution of 0.79% as shown in table B-5 in appendix B and Figure 4-8 below. We can conclude that CO₂ absorption in ChCl:LvAc DESs increases strongly with increasing the pressure and stirring speed, decreases moderately with increasing temperature and is minimally affected by the HBA:HBD molar ratio and by the water content in the DES.

The second-order and higher interactions of parameters have a very small contribution to the model. More details are available in section B-6.3 in appendix B.

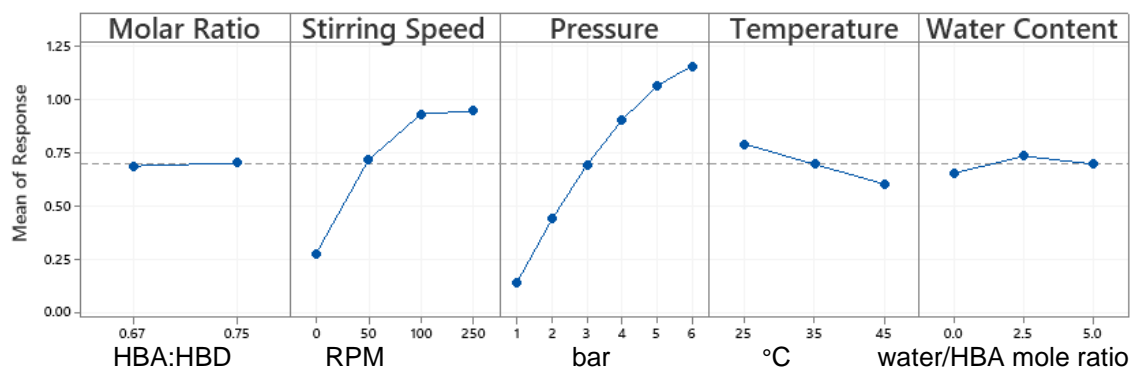


Figure 4-8 Main effects plot for CO₂ absorption in ChCl:LvAc DESs

4.5.4.6 Refining the model

Figure B-6 in the supplementary information document reveals many insignificant interactions of different orders, therefore; it is essential to remove all the insignificant interactions from the model as per figure B-6. The refined model equation – equation B-8 – is available in appendix B whereas, the refined model adjusted R² is 99.72.

4.5.4.7 Interaction's plot

The second-order interactions of parameters have a non-considerable total contribution in the model with 2.53 %. However, in terms of significance, pressure with temperature interaction is the most significant interaction ($P\text{-value} = 0.001 < 0.05$) followed by stirring speed with pressure interactions and pressure with molar ratio interactions respectively among second-way interactions as per figure B-8 in appendix B. The interactions among molar ratio, temperature and water content are the only significant third-order interaction. Whereas the rest of the second-order and third-order interactions are insignificant ($P\text{-values} > 0.05$) along with the fourth-order interactions as per figure B-8. In detail, for any DESs composition CO_2 solubility in ChCl:LvAc DESs increases with increasing pressure, stirring speed, water content and molar ratio respectively. However, CO_2 solubility declines with increasing temperature as per Figure 4-9 below.

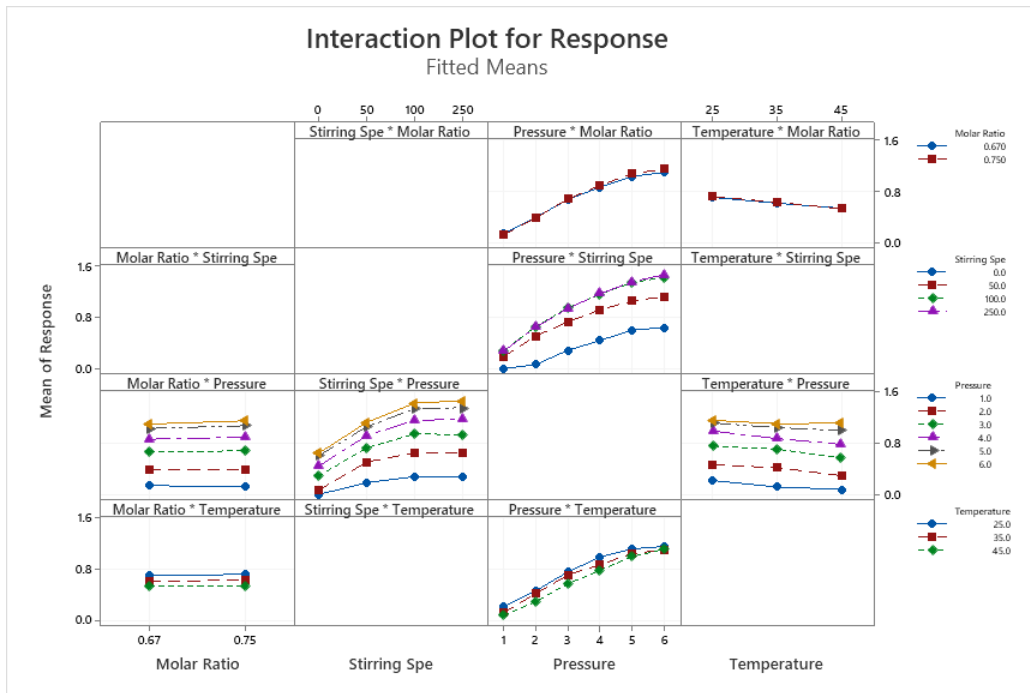


Figure 4-9 The second-order interactions plots

4.5.4.8 Optimization of controlled parameters

The optimal operating parameters that give the highest CO₂ absorption by the DESs were prepared using Minitab optimizer as per below. The optimal parameters of HBA: HBD molar ratio, pressure, and water content were found to be (1:3), 6 bar, 250 rpm and water:HBA molar ratio of 2.5, respectively. Optimized values are consistent with the experimental results mentioned in the experimental section above and with the similar work reported in the literature for other DESs ¹¹⁹.

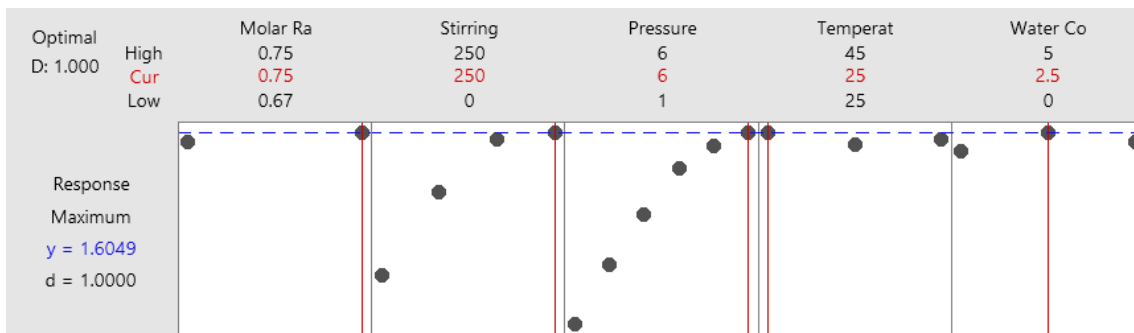


Figure 4-10 Optimization of controlled parameters

4.5.4.9 Prediction of CO₂ absorption by DESs using the statistical model

This model allows predicting the corresponding response of CO₂ absorption by the ChCl:LvAc DESs at any given controlled parameters including high-pressure values these are unfeasible in the laboratory, or operating parameters from pilot/industrial plants. Therefore, it would be beneficial to use this statistical model to estimate the performance of these sorbents when scaling up the process.

4.5.4.10 Model applicability

The CO₂ absorption data in ChCl:LvAc DESs were prepared isothermally at temperatures up to 45 °C with different levels of other factors according to equation B-8 in appendix B. To apply this model, the CO₂ absorption data should be prepared within these ranges of temperature, pressure, stirring speed, molar ratio and water content.

4.5.5 The effect of water content on the CO₂ absorption by DESs

ChCl:LvAc DESs are highly hygroscopic, as reported by Delgado *et al.* in their work in ¹⁸⁷. Therefore, even the DES compositions in which no water was added (i.e., 1:2:0 and 1:3:0) will always contain some residual water. Therefore, although the statistical

analysis of the results shows the effect of each experimental parameter on the CO₂ absorption in ChCl:LvAc DESs, the result obtained for the effect of the water content should be treated cautiously and deserves a more accurate analysis. Such analysis can only be carried out if the “real” water content of the DESs is accurately known, therefore, Karl Fisher titration was used for this purpose and the results are shown in Figure 4-11 and Figure 4-12 below.

For both HBD:HBA molar ratios, the CO₂ absorption capacity first increases with increasing water content but then decreases above a certain value of water content Figure 4-11. This effect is more pronounced for ChCl:LvAc (1:2) than for ChCl:LvAc (1:3). We hypothesise that the addition of some water reduces the viscosity of the DES, thus facilitating the diffusivity of CO₂ molecules in the liquid film. However, adding excessive water reduces CO₂ absorption due to the reduced CO₂ solubility in water^{227, 184}.

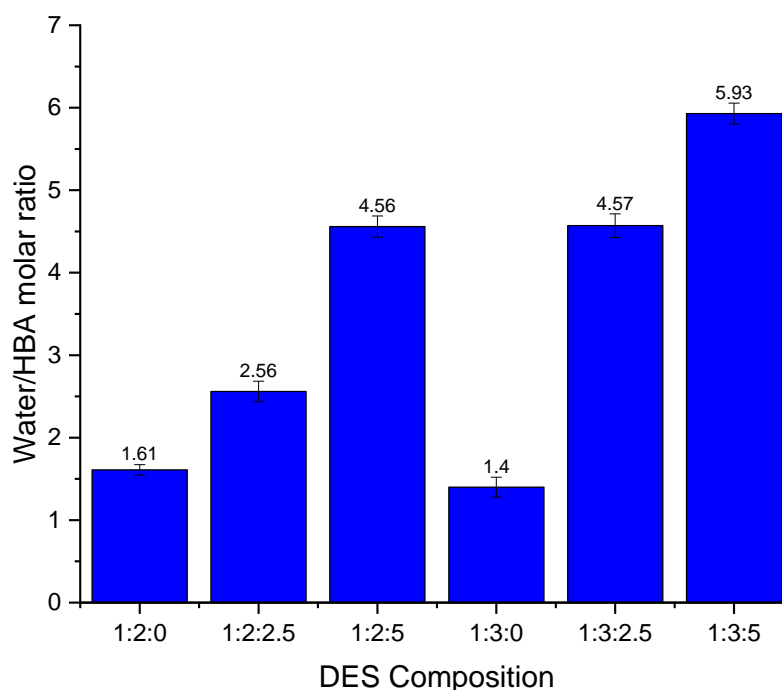


Figure 4-11 Water content (water:HBA molar ratio) in different ChCl:LvAc DES compositions

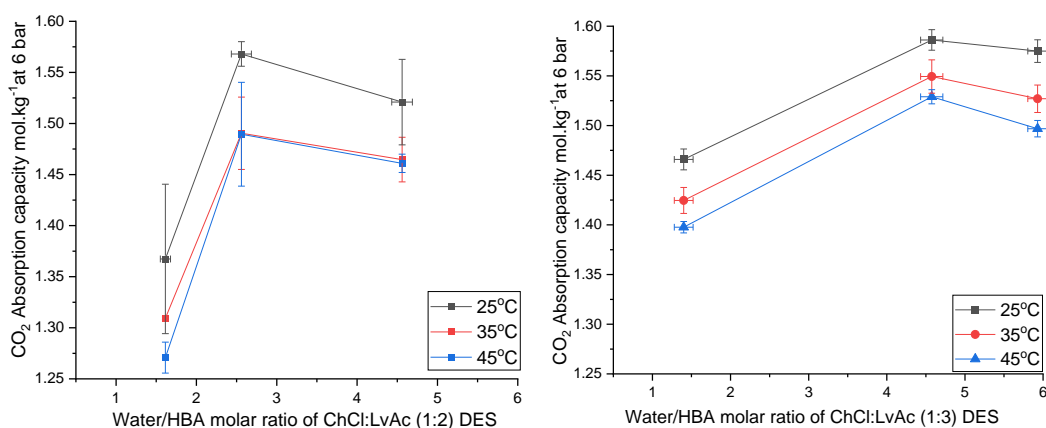


Figure 4-12 The effect of water content on the CO₂ absorption capacity of ChCl: LvAc DESs (1:2) (left) and (1:3) (right) at 6 bar and different temperatures

4.5.6 CO₂ desorption results

4.5.6.1 Indication of Nonspontaneous Released (Residual) CO₂ by Weight Gain Measurements

The absolute pressure drop in the system indicates the absorption of CO₂ by the DES under investigation. The amount of CO₂ absorbed is calculated using the ideal gas law as per Equation (4-2). The thermodynamics of the absorption process (discussed in Section 4.3.2 shows that CO₂ absorption by the DESs is a nonspontaneous phenomenon. Therefore, the spontaneous release of most of the absorbed CO₂ is expected (and indeed observed) once the VLE rig is depressurised. The weighing of the DES samples before and after the absorption test allows for the determination of the CO₂ that remains in the DES after depressurisation (residual CO₂) and must be released by other methods (e.g., heat treatment of the DESs). The difference between the CO₂ content according to pressure drop calculations and the CO₂ content after depressurising corresponds to the CO₂ that is released spontaneously. As an example, this information is presented in Figure 4-13 for ChCl:LvAc (1:3:0).

Figure 4-13 shows that the absorption capacity of ChCl:LvAc DES (1:3:0) decreases with increasing temperature. Similar behaviour was observed for all the other ChCl:LvAc compositions.

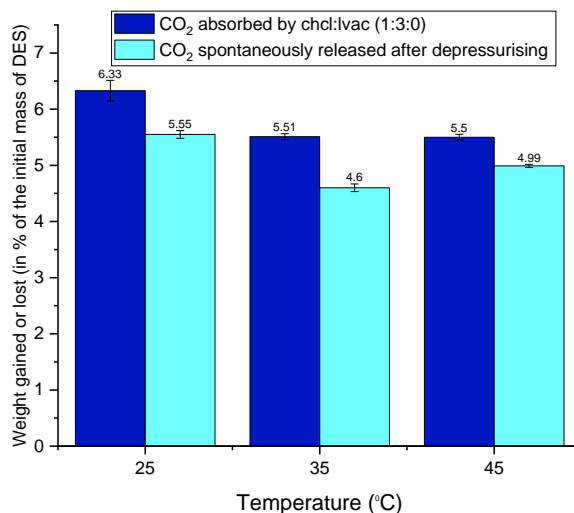


Figure 4-13 Weight gained by ChCl:LvAc (1:3:0) after CO₂ absorption at 25 °C, 35 °C and 45 °C and lost by CO₂ released spontaneously after depressurisation

4.5.6.2 Quantitative Use of FTIR to Follow the Desorption of Nonspontaneous Released (Residual) CO₂

Figure 4-14 displays the FTIR spectra of ChCl:LvAc (1:3:0) before and after CO₂ absorption and desorption at different temperatures. The FTIR transmittance peak associated with the double carbonyl O=C=O functional group (visible at 2340 cm⁻¹) was only detected after the CO₂ absorption tests. Similar behaviour was observed for all the other ChCl:LvAc compositions.

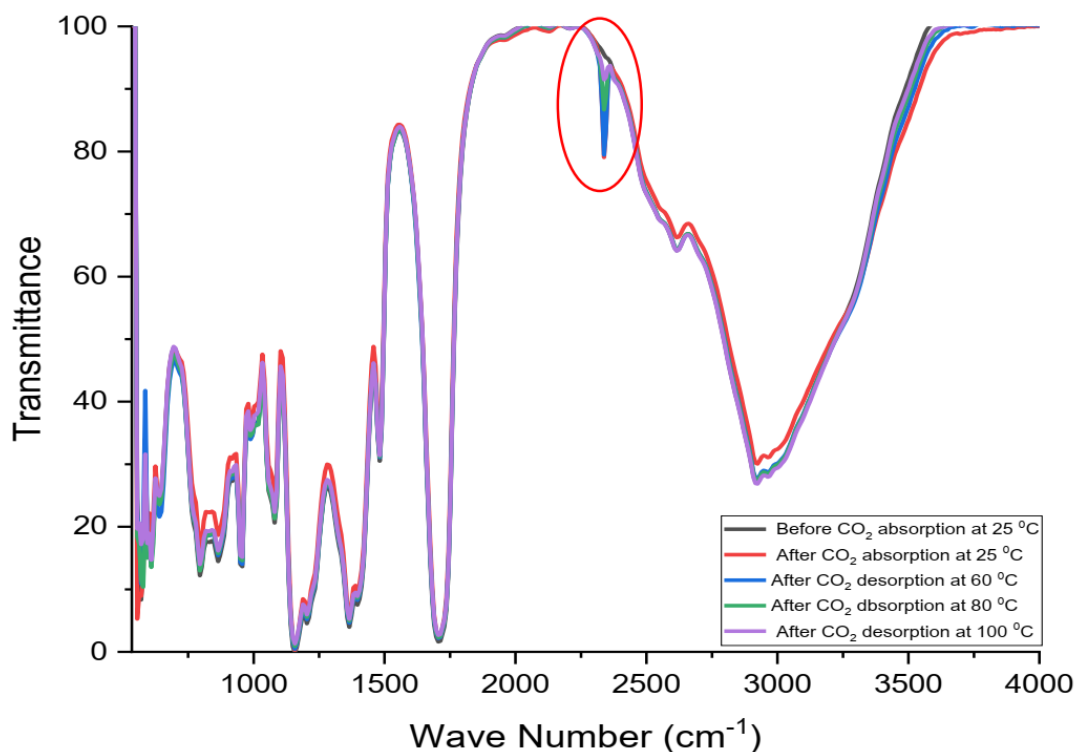


Figure 4-14 The FTIR spectra of ChCl:LvAc (1:3:0) before and after CO₂ absorption at 25 °C and CO₂ desorption at different temperatures

Increasing the regeneration temperature results in a progressive release of CO₂ from DES samples with residual CO₂ as shown in Figure 4-14 above. The FTIR transmittance peak associated with the double carbonyl O=C=O functional group ($\approx 2340 \text{ cm}^{-1}$) decreases when the DES containing CO₂ is heated at a temperature of 60 °C or above .

4.5.6.3 Indication of CO₂ absorption by weight-gain measurements

The absolute pressure drop in the system indicates the solubility of CO₂ in the DESs under investigation, the amount of CO₂ absorbed is calculated using the ideal gas law as per Equation (4-2) above. However, the weight-gain method was also used to verify CO₂ absorption. Figure 4-13 below shows that the absorption capacity of ChCl:LvAc DESs with a molar ratio of (1:3:0) decreases with increasing temperature. Similar behaviour was observed for all the other ChCl: LvAc compositions.

The difference between the CO₂ content according to pressure drop calculations and the CO₂ content after depressurising is corresponding to the CO₂ that is released spontaneously. Whereas the residual CO₂ in the DESs is released by heat treatments as per Figure 4-13.

4.5.6.4 Indication of CO₂ desorption by weight-loss measurements

The weight loss method was also used to verify the CO₂ desorption at different temperatures. It also compares the weight gained by the DESs after CO₂ absorption with the total weight reduction due to the heat treatment (regeneration) process. Figure 4-15, Figure 4-16, Figure 4-17 below show that the weight of DES samples with residual CO₂ decreases with increasing absorption and desorption temperatures simultaneously.

Weight loss due to the regeneration process is always higher than the weight of CO₂ in the DES before the start of the regeneration (heat treatment) process. In short, the weight loss is not limited to CO₂ desorption during the regeneration process but also due to the partial evaporation of the water contained in the DES.

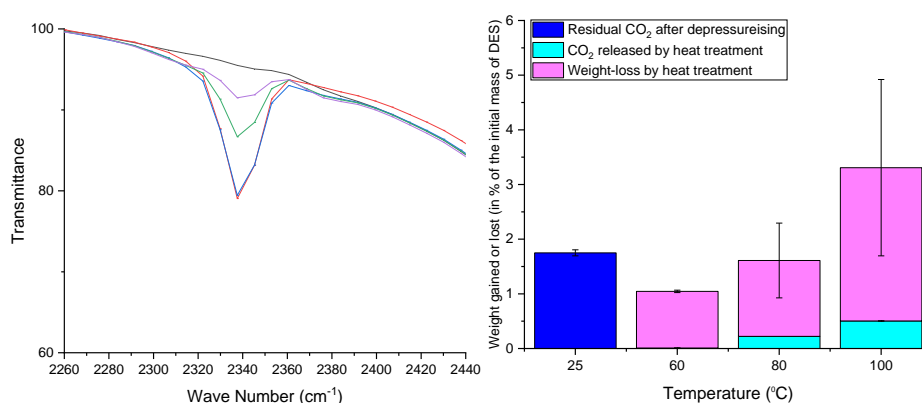


Figure 4-15 Regeneration of ChCl:LvAc (1:3:0) after CO₂ absorption at 25 °C. A) Reduction in FTIR transmittance peak associated with the double carbonyl group with increasing regeneration temperature; B) residual CO₂ after

depressurisation, CO₂ released by heat treatment and weight loss after regeneration at different temperatures

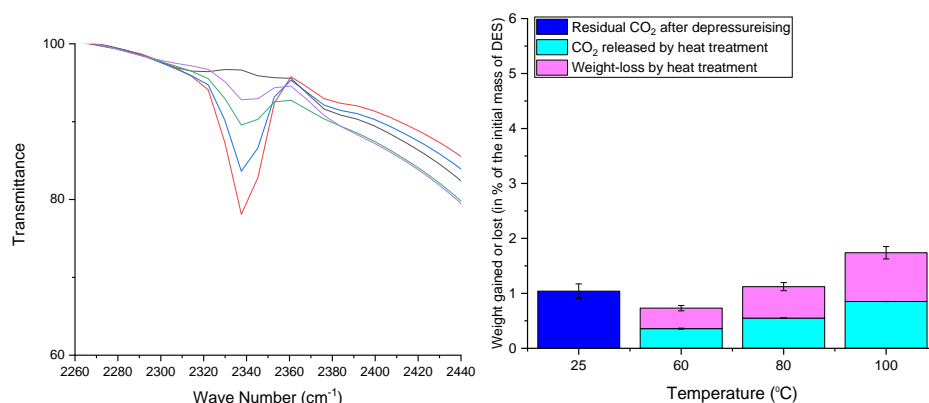


Figure 4-16 Regeneration of ChCl:LvAc (1:3:0) after CO₂ absorption at 35 °C. A) Reduction in FTIR transmittance peak associated with the double carbonyl group with increasing regeneration temperature; B) residual CO₂ after depressurisation, CO₂ released by heat treatment and weight loss after regeneration at different temperatures

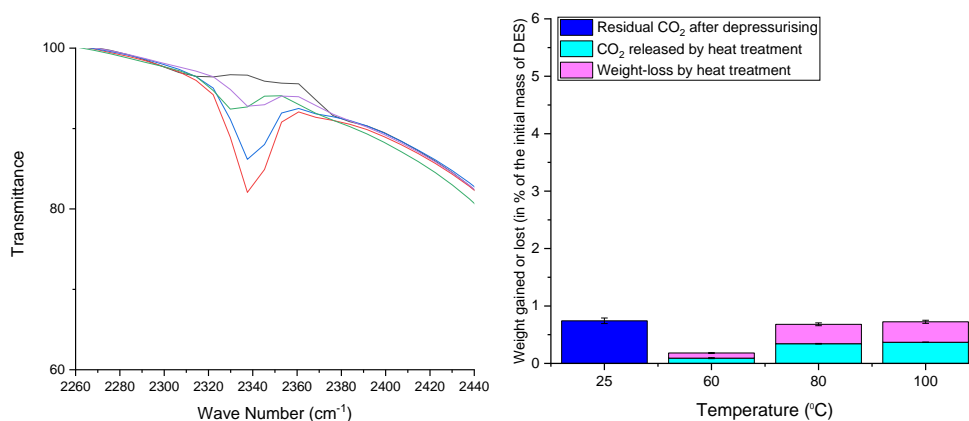


Figure 4-17 Regeneration of ChCl:LvAc (1:3:0) after CO₂ absorption at 45 °C. A) Reduction in FTIR transmittance peak associated with the double carbonyl group with increasing regeneration temperature; B) residual CO₂ after depressurisation, CO₂ released by heat treatment and weight loss after regeneration at different temperatures.

4.5.7 Total CO₂ released

The total amount of CO₂ released from the DES sample is the combination of the CO₂ amount released spontaneously after depressurisation and the amount released by heat treatment as per Figure 4-18. The results presented in Figure 4-18 clearly show

that, more than 97% of CO₂ can be released from the DES samples within this range of temperature 60 °C to 100°C. The Y axis on Figure 4-18 starts from 95% just to show the fact that there is no significant difference between applying the minimum and maximum desorption temperatures. Therefore, from energy optimisation perspective, the minimum regeneration temperature of 60 °C can be considered as the optimal regeneration temperature of ChCl:LvAc DESs. On the other hand, at 60 °C most CO₂ is released with a minimal reduction in DES weight according to weight loss measurements. Furthermore, at 60 °C, the transmittance peak associated with the double carbonyl group of the CO₂ molecule is minimal, indicating that most of the initial CO₂ was released. because of these three reasons, 60 °C might be considered as the optimal regeneration temperature for ChCl:LvAc DESs.

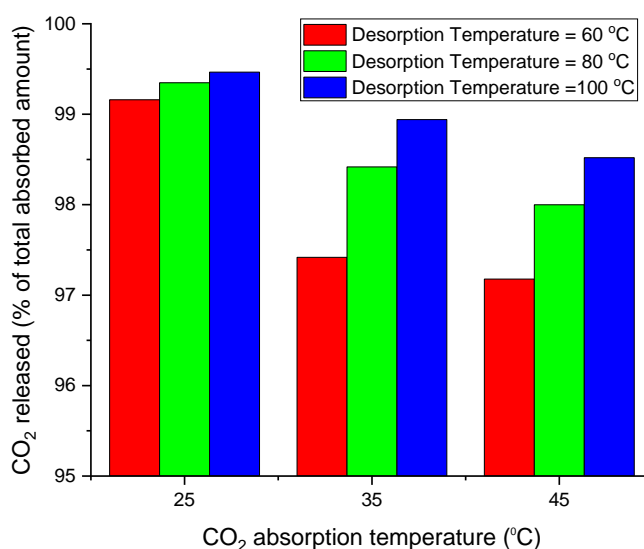


Figure 4-18 The total CO₂ released from ChCl:LvAc (1:3:0) samples absorbed CO₂ at 25 °C, 35 °C & 45 °C and released CO₂ at 60 °C, 80 °C & 100 °C

Note: Error bars are not visible as they are smaller than the data point size

4.5.8 The recyclability of the DESs

The The CO₂ absorption capacity of ChCl:LvAc (1:2:0) slightly decreases with the recycling of the sorbent at 80 °C and 250 rpm as shown as shown in Figure 4-19 below.

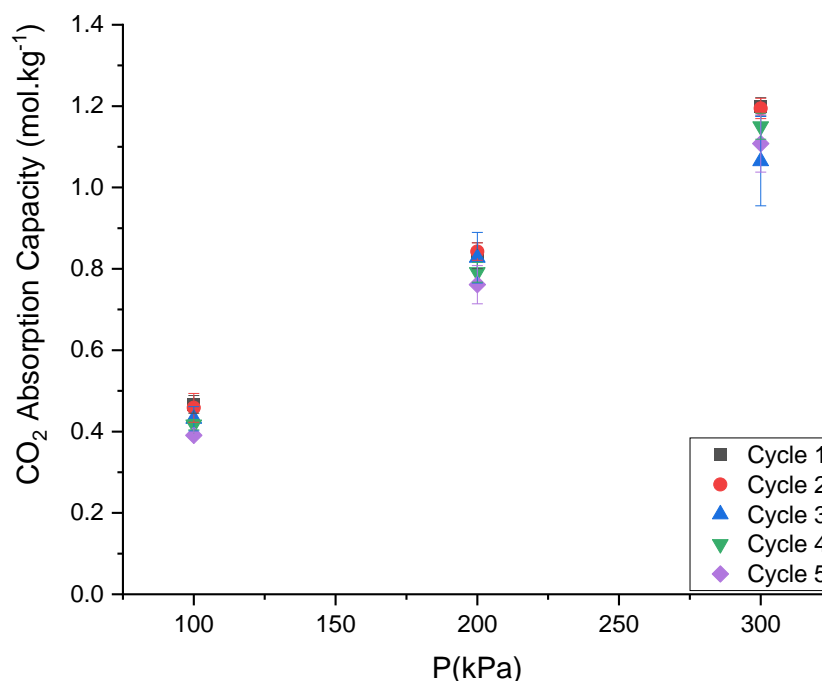


Figure 4-19 Variation of the CO₂ absorption capacity of ChCl:LvAc (1:2:0) over five consecutive absorption/desorption cycles: values measured at 25 °C and 250 rpm

The CO₂ absorption capacity of ChCl:LvAc (1:2:0) slightly decreased from 1.2 mol.kg⁻¹ in the first absorption cycle to 1.11 mol.kg⁻¹ in the fifth cycle, at the same operating conditions (25 °C, 3 bar and stirring rate of 250 rpm).

Figure 4-20 shows that the absorption capacity of choline ChCl:LvAc of (1:2:0) molar ratio slightly decreases with reusing the sorbent. It also shows that, for the same DES composition and operating conditions, the amount of CO₂ that is released spontaneously after the depressurisation of the system can vary from cycle to cycle. The difference between the CO₂ content according to pressure drop calculations and

the CO₂ content after depressurising is corresponding to the CO₂ that is released spontaneously.

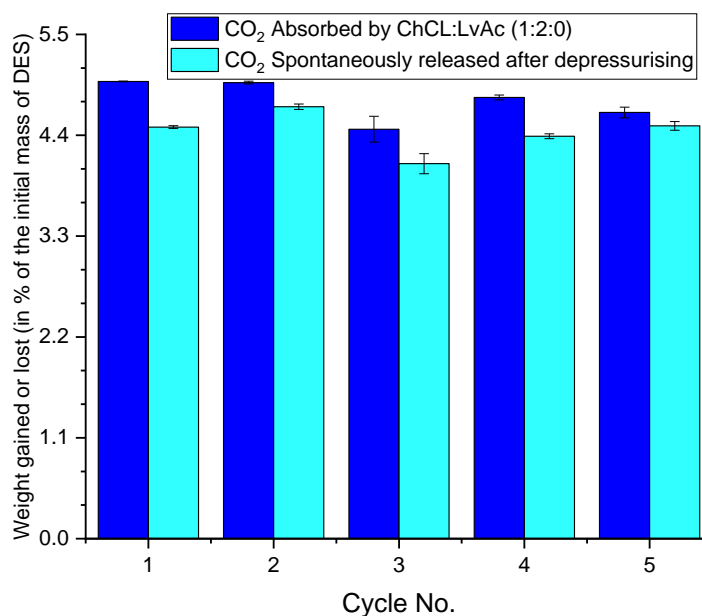


Figure 4-20 Weight gained through CO₂ absorption for 5 cycles at 25 °C and CO₂ released spontaneously after depressurisation. Experiments carried out with ChCl:LvAc (1:2:0) at 25 °C and 250 rpm

One of the major disadvantages of utilising the MEA for carbon capture processes is the huge loss of the sorbent during the regeneration process due to the formation of carbamates during the absorption process²⁴¹. Additionally, the regeneration of the MEA is costly as it must be performed at high temperatures^{242, 243}. On the other hand, in this work DESs samples have lost only 0.48% of their initial weight after five consecutive cycles of CO₂ absorption at 25 °C and desorption/regeneration at 80 °C. We could conclude that ChCl:LvAc DESs are recyclable under the conditions aforementioned which make these DESs a good candidate for CO₂ absorption processes.

4.5.9 The selectivity of the DESs towards CO₂

The CO₂ absorption capacity by ChCl: LvAc of (1:3:2.5) molar ratio decreases with decreasing the molar ratio of CO₂ in the gas phase at 25 °C and 250 rpm as shown in Figure 4-21.

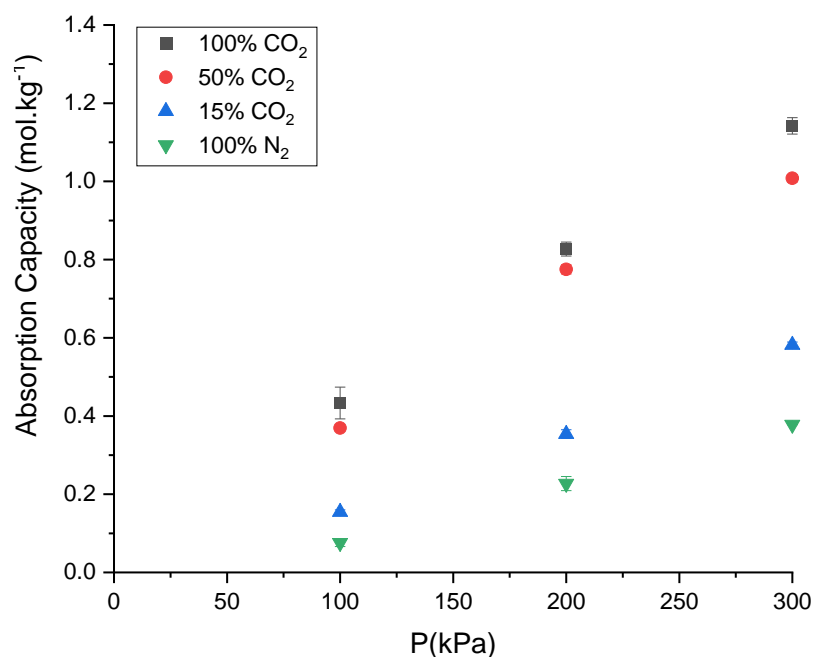


Figure 4-21 Absorption capacity of ChCl:LvAc (1:3:2.5) for different gas mixtures of CO₂ and N₂. Experiments carried out at 25 °C and 250 rpm

The absorption capacity of ChCl:LvAc (1:3:2.5) at 3 bar decreases from 1.14 mol.kg⁻¹ for pure CO₂ to 1.0 mol.kg⁻¹ for gas mixtures with 50% CO₂, and finally to 0.58 mol.kg⁻¹ for gas mixtures with 15% CO₂. The reduction in the absorption capacity of ChCl:LvAc (1:3:2.5) is proportional to the molar fraction of the CO₂ in the (feed) gas mixtures as per Figure 4-22 and as reported by Blauwhoff *et al.*²⁴⁴. Nitrogen has more limited solubility in the DES (0.37 mol.kg⁻¹) under the same conditions and is all completely released from the DES after depressurisation.

As a result of the selectivity Figures in Figure 4-20, ChCl:LvAc DESs are more suitable when the concentration of CO₂ in the flue gas is greater than 15%, such as in the cement industry ²⁴⁵.

On the other hand, ChCl:LvAc (1:3:2.5) seems to be more selective towards CO₂ over N₂ at lower pressures as seen in Figure 4-23. The selectivity towards CO₂ seems to decline asymptotically as pressure increases.

On the other hand, ChCl: LvAc (1:3:2.5) tend to intake more CO₂ over N₂ at low pressures as per Figure 4-23 below. Figure 4-23 also shows the CO₂ selectivity based on pure gases solubilities in ChCl:LvAc (1:3:2.5) as per Equation 4-5 above. Now, we can take the solubility of pure gases in ChCl:LvAc (1:3:2.5) as a base to estimate the solubility of each gas – from a mixture of gases- into the DES as per Table 4-4 below.

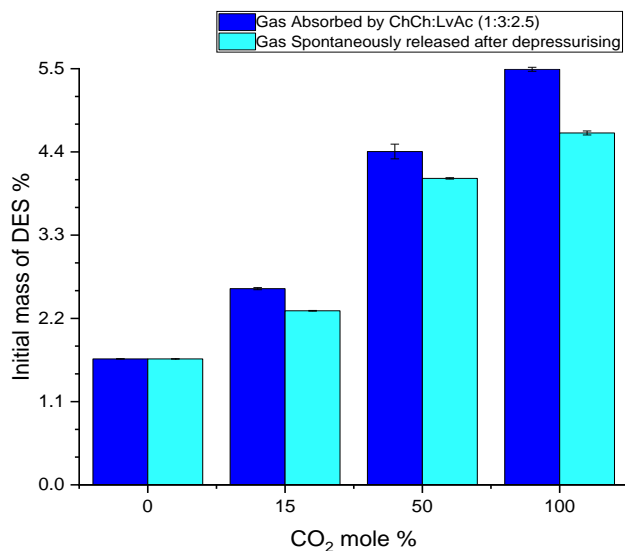


Figure 4-22 Weight gained by ChCl:LvAc (1:3:2.5) after gas absorption at 25 °C and 250 rpm, and lost by the spontaneous release of gas after depressurisation

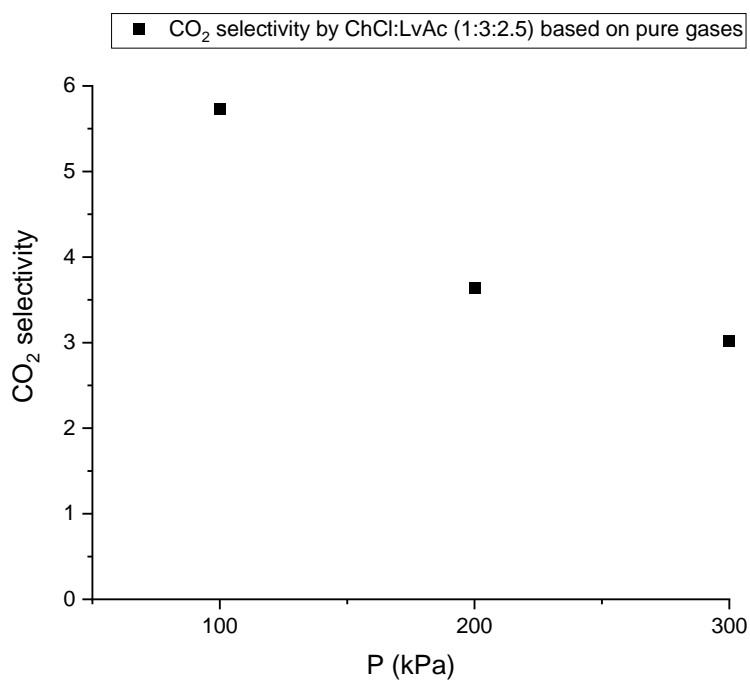


Figure 4-23 CO₂ selectivity based on the absorption of pure gases by ChCl:LvAc (1:3:2.5) at 25 °C and 250 rpm

The selectivity towards CO₂ in a mixture of gases in ChCl:LvAc (1:3:2.5) was calculated and compared to the selectivity of ionic liquids taken from the literature

(see Table 4-4). Compared to ionic liquids, the ChCl:LvAc DES exhibits lower CO₂/N₂ selectivities.

It is highly recommended to investigate the selectivity of any candidate sorbent - including DESs- towards CO₂ in a mixture of gases to simulate the industrial scenario where the flue gas is composed of different gases including CO₂.

Table 4-4 The selectivity of some adsorbents at 100 kPa and 25 °C

Material	Description	Molar % of gases (CO ₂ /N ₂)	Selectivity (S)	Reference
DES	ChCl:LvAc (1:3:2.5)	50 / 50	5.63	This work
		15 / 85	4.94	
IL	bmim[BF ₄]		28.7*	²⁴⁶
IL	bmim[PF ₆]		22.6*	²⁴⁷

* selectivity values were calculated based on pure components, measurements were done at 30 °C

4.6 Conclusion

Choline-chloride:levulinic-acid-based DESs were prepared successfully at different molar ratios and water contents. The CO₂ absorption in ChCl:LvAc DESs was obtained at different molar ratios, pressures, water content, stirring speeds and temperatures. Thermodynamic properties (ΔH , ΔS and ΔG) of CO₂ absorption in ChCl:LvAc DESs showed that CO₂ absorption is exothermic and nonspontaneous.

In this study, FTIR spectrophotometry was utilised as a secondary method to identify the absorption and desorption of CO₂ by ChCl:LvAc DESs at different conditions of temperature pressures. The FTIR transmittance peak associated with the double carbonyl O=C=O functional group (visible at 2340 cm⁻¹) was only detected after the CO₂ absorption tests, while this transmittance peak decreases with increasing DES regeneration temperature.

The regeneration process at 60 °C is a temperature at which most CO₂ is released with a minimal reduction in DES weight according to weight loss measurements. The residual amount of CO₂ in the DES that cannot be released by heat treatment was calculated using the Beer–Lambert law.

All the main input factors (pressure, stirring speed, temperature, water content and molar ratio) have statistical significance on the CO₂ absorption by ChCl:LvAc DESs. The pressure is found to be the most significant factor, followed by stirring speed, temperature and finally water content and HBA:HBD molar ratio.

In this work, ChCl:LvAc DESs exhibited good recyclability as samples lost only 0.48% of their initial weight after five consecutive cycles of CO₂ absorption at 25 °C and desorption at 80 °C. Finally, ChCl:LvAc DESs showed moderate selectivity towards CO₂ over N₂, with up to 5.63 at 50% CO₂.

This is the first work in the literature investigating these aspects of utilising ChCl:LvAc DESs for CO₂ absorption and desorption processes. Techniques and methods used in this work are highly recommended being utilized for future studies of any DESs besides full characterization of any candidate sorbent -including DESs- to ensure its suitability for any application domain including the CO₂ absorption and desorption processes.

Chapter 5 : Conclusions

5.1 Overview

Deep eutectic solvents have been utilised in several engineering domains as benign substitutes for traditional chemicals. Recent studies^{143,43} have shown that DESs have many advantages as compared to monoethanolamine in the area of carbon capture. As a result, this work has evaluated the application of ChCl:LvAc DESs for carbon capture processes. Within the work, ChCl:LvAc DESs compositions were investigated extensively for their potential use as sorbents. The impact of the composition of the DESs on their physicochemical characteristics was evaluated and discussed in depth. Also, the CO₂ absorption and desorption studies were performed to assess the ChCl:LvAc composition's potential for utilisation in carbon capture processes. During the DESs preparation processes, the changes that appeared within the DESs compositions' inherent characteristics enhanced their properties and their CO₂ absorption capacity as well as their regeneration process.

The composition of the DESs namely, the HBA:HBD molar ratio and the water content, are the key parameters that determine the physicochemical properties of each composition. ChCl:LvAc DESs also showed some characteristic tendency (i.e. high thermal stability, low corrosivity and viscosity) as a potential sorbent for CO₂ capture.

The phase behaviour plots showed that some ChCl:LvAc compositions can be considered as DESs while some others can only be defined as simple eutectic mixtures. ChCl:LvAc DESs exhibited high thermal stability, less corrosivity and better recyclability as compared to some conventional sorbents which qualify them to be potential candidates for carbon capture processes.

This work has investigated the CO₂ absorption capacity at different compositional and operational conditions these not yet considered before in the literature as summarised previously in chapters 3 and 4 of this work. Therefore, the CO₂ absorption capacities obtained for ChCl:LvAc DES compositions are higher than those of the same DESs that have been reported in other studies within the literature by Ullah *et al.* in their work in ¹³⁶. Furthermore, most published work on the use of DESs for carbon capture, focused only on reporting the CO₂ absorption capacity of the candidate sorbents without considering the regeneration process of these sorbents. Therefore, to give a comprehensive evaluation of their CO₂ absorption and desorption performance, it is worth mentioning to note that, this is the first work in the literature to study the CO₂ regeneration process of ChCl:LvAc DESs ²²⁰.

5.2 Overall conclusions

Referring to the research questions and the knowledge gaps stated in chapter 1, this work has successfully answered all the 8 research questions in chapters 3 and 4, and filled an important gap in the literature as summarised in this section.

The first research question of this work was about the nature of ChCl:LvAc mixtures, and whether they can be considered deep eutectic solvents or not. In chapter 3, the experimental results have proven that some ChCl:LvAc compositions can be considered as deep eutectic solvents required conditions, namely they meet the definition of being DESs, as the melting points of these mixtures are lower than the ideal melting temperatures of the individual components. The range at which ChCl:LvAc compositions are considered as deep eutectic mixtures is where the molar ratio of the levulinic acid (HBD) is ≥ 2 as compared to the choline chloride (HBA)

molar ratio. On the other hand, compositions formulated with HBA:HBD molar ratios lower than 1:2 can only be considered as simple mixtures.

The key physicochemical properties of the proposed DESs were studied extensively in chapter 3 to fulfil the second objective of this research “*What are the key thermophysical properties of the proposed DESs?*”. The physicochemical characteristic of ChCl:LvAc DESs in terms of density, viscosity, thermal stability, and the chemical fingerprint (FTIR spectra) of the proposed DESs have been reported and compared to other DESs reported in the literature. The values of these properties proved that ChCl:LvAc DESs may be used in other engineering applications including but not limited to carbon capture processes.

The third question of this work was “*What is the corrosivity of the proposed ChCl:LvAc DESs as compared to the corrosivity of amines (benchmark sorbents) in different corrosion scenarios?*”. To answer this question, the corrosivity of ChCl:LvAc DESs was investigated in terms of corrosion penetration rate (CPR) at different conditions simulating the corrosion scenarios in the actual carbon capture plant. The results clearly show that these DESs are much less corrosive than MEA solutions, with the maximum CPR observed being 92% smaller than the one exhibited by MEA 30 wt.% aqueous solution. Compared to the currently used amines, this aspect qualifies ChCl:LvAc DESs to be friendlier to the construction materials typically used in carbon capture equipment.

The fourth question of this work was about “*The performance of proposed DESs on the CO₂ absorption and desorption as compared to the MEA as a benchmark*” and was fully answered in chapter 4. The performance of proposed DESs systems on CO₂ absorption and desorption was investigated at different operational and compositional

conditions and compared to the MEA as a benchmark. Although, ChCl:LvAc showed lower CO₂ absorption capacity than MEA, these chemicals can be recycled and regenerated with less energy-intensive processes, are far less corrosive and possess better environmental credentials when compared to MEA.

The mechanism of CO₂ absorption by the experimented DESs was the fifth question in this work. The experiments demonstrated that the CO₂ absorption by ChCl:LvAc DESs is limited only to physisorption which is similar to the mechanism exhibited by ChCl:LvAc in the work by Ullah *et al.*¹⁶⁶ and exhibited by other choline-based DESs reported in the literature^{140, 43}. The experimental FTIR results showed that the transmittance peak related to the double carbonyl group that solely existed in the CO₂ molecule only appears after the CO₂ absorption by ChCl:LvAc DESs. This peak also reduces with increasing temperature during the CO₂ desorption process. The physical absorption of CO₂ by ChCl:LvAc DESs was formulated in terms of Henry's law constant. This also explains why the proposed systems exhibited lower CO₂ absorption capacity as compared to the MEA, as the CO₂ absorption in the second case is composed of both physisorption and chemisorption unlike the CO₂ absorption by the proposed DESs which is limited to physisorption alone as explained above¹⁴⁰.

The sixth question of this research was *"What are the optimal key operating parameters of the process of CO₂ absorption and desorption?"*. To determine the optimal key operating parameters for the absorption and desorption of CO₂ by ChCl:LvAc DESs. All tested parameters (stirring speed, pressure, HBA:HBD molar ratio, water content and temperature) are statistically significant (P-values < 0.05) and influence the CO₂ absorption capacity by ChCl:LvAc DESs. Statistical analysis revealed that the most significant factor is the pressure (expected) followed by stirring speed, temperature, water content and finally the HBA:HBD molar ratio. We can

safely conclude that CO₂ absorption in ChCl:LvAc DESs increases significantly with pressure and stirring speed but only increases slightly with the water content and, with the HBD:HBA molar ratio. On the other hand, the CO₂ absorption in ChCl:LvAc DESs is an exothermic process^{166, 248} according to the thermodynamics analysis results in²²⁰, therefore, the CO₂ absorption capacity of ChCl:LvAc DESs decreases with increasing temperature.

The statistical model describing the CO₂ absorption in ChCl:LvAc DESs under experimented conditions was generated and discussed. The model can only be applicable under these ranges of compositional and operational conditions aforementioned in Chapter 4. Also, this model can be used to estimate the CO₂ solubility in ChCl:LvAc DESs within these limits of the compositional and operational parameters. The optimal CO₂ absorption conditions that are giving the highest CO₂ absorption capacity have been investigated experimentally and have been represented statistically in Chapter 4.

While up to 95% of the CO₂ absorbed by ChCl:LvAc DESs is spontaneously released during the depressurizing process, the remaining CO₂ was released from the DESs by a heat treatment. According to weight-loss measurements and FTIR analysis, 80 °C is the temperature at which most of the remaining CO₂ is released with a minimal reduction in DESs weight. Therefore, 60 °C can be considered the optimal CO₂ desorption temperature for the studied DESs. This is lower than the regeneration temperature of amines which is higher than 100 °C^{242, 243} making the regeneration of amines a more energy-intensive process. The regeneration process of the MEA absorbent (30 %wt.) accounts for up to 80% of the total energy consumption of industrial CO₂ capture processes^{249, 250}, and is also associated with the thermal degradation of carbamates, thus adding more burden to the process due to the

environmental complications of disposing the waste produced from amines regeneration ^{251, 241}.

The seventh question of this research was related to the recyclability of the studied DESs. In this work, the ChCl:LvAc DESs displayed decent recyclability as DESs samples lost less than 0.50% of their initial weight after five consecutive cycles of CO₂ absorption at 25 °C and desorption at 80 °C. This result reinforces the sustainability credentials of the ChCl:LvAc DESs.

The eighth (final) question of this work was “*To which extent ChCl:LvAc DESs are recyclable?*”, which was fully answered by investigating the selectivity of ChCl:LvAc DESs towards CO₂ absorption. ChCl:LvAc DESs displayed a considerable selectivity towards CO₂ over N₂ with values up to 5.63 at 50% CO₂, which makes these compositions suitable for CO₂ from a gas stream composed of different gases. Hence, This aspect has not been considered in any previous work in the literature that investigated the viability of ChCl:LvAc DESs for carbon capture processes.

This is the first work in the literature investigating these aspects of utilising ChCl:LvAc DESs for CO₂ absorption and desorption processes. The initial framework of this research was to study the viability of ChCl:LvAc DESs for post-combustion carbon capture processes. This would have offered a benign sorbent to replace the currently used amines. Unfortunately, this aspect of the original research plan could not be realised due to limitations within the investigated DESs; hence, an understanding of the applicability of the ChCl:LvAc DESs would require a high CO₂ absorption capacity similar to the amines under the same operating conditions. However, the experimental

results have revealed that the maximum CO₂ absorption capacity by ChCl:LvAc DESs is lower by 70% than the ones offered by the MEA (30 %wt.) under the same conditions of temperature and pressure.

Techniques and methods used in this work are highly recommended to be utilised for future studies of any potential sorbents including DESs. Furthermore, candidate sorbents must be fully characterized to ensure their viability for any application domain including carbon capture processes.

5.3 Research limitations

As discussed and concluded in this work, the proposed DESs compositions might not represent a competitive alternative to the currently used amine sorbents if the comparison is based only in terms of the CO₂ absorption capacity. On the other hand, the environmental profile of ChCl:LvAc DESs in terms of, corrosivity, toxicity, biodegradability and recyclability, is in many ways better than the amines. Hence, all these factors must be taken into consideration before considering replacing the amines with ChCl:LvAc DESs.

One of the major experimental obstacles faced during this work was a limitation related to the vapour-liquid equilibrium (VLE) rig that was used to study the carbon capture performance of ChCl:LvAc DESs and MEA (30 wt.%). The time required for the rig to reach the thermodynamic equilibrium during calibration and measurements is 8 hours per data point. Therefore, it took more than 9 months to generate the data reported and analysed in chapter 4 only. On the other hand, the VLE rig allowed studying the carbon capture performance of ChCl:LvAc DESs under dynamic conditions which is considered the major advantage of utilising this method.

The outbreak of the Coronavirus COVID-19 in February 2020 was also one of the major incidents that hugely affected every aspect of my PhD life, as the laboratories were closed for 6 months due to the national lockdown. Then, access to the laboratories was limited upon following many strict procedures that were introduced to control the spread of the virus. Since I was given only 3 months as an extension to finish my experimental work, I had to adjust and reprioritise my PhD experimental plans to cope with these changes and try to finish my experimental work within the given time.

Aside from the above, other criteria for assessing carbon capture performance by ChCl:LvAc DESs such as investigating the characteristics and the CO₂ absorption capacity of blends composed of ChCl:LvAc DESs and amines would have offered a more detailed analysis of the possibility of enhancing the CO₂ absorption capacity of ChCl:LvAc DESs by adding amines to the system. However, the timeline to conduct these analyses was impacted by universities' lockdown for several months due to the outbreak of the COVID-19 global pandemic. As a result, the results reported in this work could serve as a groundwork for future studies on the utilisation of ChCl:LvAc DESs for carbon capture processes, based on the optimum compositional and operational conditions of performance established using these compositions.

The binary phase diagram of the ChCl:LvAc DES compositions reported in this work was constructed and explained in detail. However, it should be emphasised that the studied ChCl:LvAc DESs are a ternary mixture composed of (choline chloride, levulinic acid, and water) due to the hygroscopic nature of the DESs as shown by the Karl Fischer results. Therefore, having this in mind, the binary phase diagram presented in this work is in fact a pseudo-binary phase diagram because the presence of water in the system is neglected. This realisation is of most relevance for practical

use, as water content affects both the properties of ChCl:LvAc DESs and their carbon capture performance as explained in the previous sections in chapters 3 and 4 respectively.

Still on the pseudo-binary phase diagram, this diagram was plotted using the melting points of the individual components and the ideal melting curves against the glass transition temperatures of the DESs. Ideally, this diagram should be plotted using the melting points only. However, ChCl:LvAc DESs are considered glass-formers that have glass transition temperatures instead of melting points. Although, this phenomenon of having glass transition temperature only has been explained in the literature^{252, 131} due to the Van Der Waals forces and the hydrogen bond between the HBA and the HBD forming supramolecular complexes. As a result, the free energy of the solid phase is changed as compared to the liquid phase which prevents these mixtures to have melting points^{253,254}. Therefore, the diagram was plotted using the melting points of the individual components against the glass-transition temperatures of DESs. It is essential to understand the chemistry beyond the fact that these DESs as glass-formers, the building principles and interactions of these supramolecular complexes are directly affecting their characteristics and hence their potential applications.

In the following last chapter, we are going to summarise our future recommendations based on the limitations stated in this chapter and the previous chapters as well.

Chapter 6: Future Work

6.1 Overview

The previous chapter summarised the overall findings of the thesis regarding the utilisation of ChCl:LvAc DESs for carbon capture processes. Given the limitations encountered in this work, there is no doubt that additional work is needed to fully justify the utilisation of ChCl:LvAc DESs for the post-combustion CO₂ capture processes. In the present chapter, some open questions that can be tackled with these findings are discussed. Some of the suggested future work for the utilisation of ChCl:LvAc DESs for carbon capture purposes is summarised as follows.

One of the interesting questions to discuss is what the CO₂ capture performance of blends composed of ChCl:LvAc DESs and amines? This situation is quite distinct from employing the pure DESs for CO₂ capture as considered in this work. Based on the work by Xia *et al* in ¹²², we know that ILs can be functionalised by adding functional groups such as amines to the pure ILs. Functionalised ILs showed a CO₂ absorption capacity higher than the traditional ones. Furthermore, the blend showed high thermal stability and can be regenerated much easier when compared to amines ¹²². Recently, Li *et al.* ²⁵⁵ studied the performance of ethanolamine-based DESs for carbon capture processes, these blends exhibited higher and faster CO₂ absorption as compared to the pure DESs. On the other hand, these blends were found highly thermally stable as compared to the pure ethanolamine solutions. Therefore, the same approach could be applied with ChCl:LvAc DESs to see whether functionalization with amines would increase their CO₂ absorption capacity and improve its properties.

Another interesting scenario is to use DESs as additives for existing amine sorbents, in order to enhance their properties such as reducing their corrosivity, enhancing

recyclability and improving thermal stability. Some DESs, particularly choline chloride and glycerol, were proven to be efficient corrosion inhibitors¹⁷⁴. These DESs revealed very low corrosion penetration rates with aluminium, nickel and steel, even when the compositions are mixed with water^{174, 256}. Therefore, investigating the possibility of applying ChCl:LvAc DESs as corrosion inhibitors would be an interesting gap in the literature to fill. We also know from this work and previous works¹⁸⁷ that, ChCl:LvAc DESs show high thermal stability, hence, perhaps they can be used to reduce the thermal degradation of amine sorbents, especially during the regeneration process. In this work, ChCl:LvAc DESs were recycled up to 5 times without any degradation problem, as samples lost only 0.48% of their initial weight after 5 consecutive absorption and desorption cycles²²⁰. Therefore, it would be interesting to test whether employing these benign chemicals as additives to amine-based sorbents would enhance their characteristics and recyclability while maintaining the high CO₂ absorption capacity inherently associated to amine-based sorbents.

As this study focused on a single carboxylic acid-based DES system and therefore, it is recommended that other carboxylic acid-based DES systems and other families of DESs such as sugar-based DESs (e.g. ChCl:Xylose DESs)¹⁸⁵ are considered and assess their viability for carbon capture purposes considering all aspects highlighted by this work. For example ChCl:Xylose DESs were characterised and recommended to be used for carbon capture processes, hence more DESs systems need to be investigated to enable comparison of their carbon capture performances.

The chemicals used in this work have a decent environmental profile, ChCl:LvAc DESs are considered non-toxic and fully biodegradable²⁰⁴. Yet, it is highly recommended to perform a comprehensive life cycle assessment (LCA) of the utilisation of ChCl:LvAc DESs for carbon capture processes. Recently, Lovell *et al.* in

their work in life cycle assessment of the separation and recycling of the fluorinated ionic liquids. LCA is a method applied to define the possible environmental consequences of a particular material over its entire life cycle ²⁵⁷. It involves all the energy and material inputs, as well as the environmental impacts of outputs during production, utilisation, and waste disposal along with emissions to the atmosphere, soil, and water. These activities have direct consequences of environmental impact issues such as global warming which represents a considerable issue to all industrial applications in recent decades. Therefore, understanding the significance of the environmental impacts and impending issues associated with the utilisation of ChCl:LvAc DESs for carbon capture processes requires focusing on the development of methods to recognise and tackle their impacts before being considered for commercial scales. To achieve this purpose it is recommended the application of the latest versions of the ISO 14040 and ISO 14044 standards, which contain the methodological framework to perform the LCA of any product according to the International Organisation of Standardisation (ISO) ²⁵⁸.

In this work, the binary phase diagram of the ChCl:LvAc system was constructed and discussed in detail. However, the effect of water content as a third component was neglected in this work and in all the works published in the literature. Since, most Choline Chloride-based DESs are highly hygroscopic ¹⁸⁷, the presence of water is, in practice, unavoidable. Therefore, it is highly recommended to consider the effect of water content when constructing the phase diagram of DES systems, and therefore, the DES has ternary systems represented by a ternary phase diagram where water is the third component (see Figure 6-1 below).

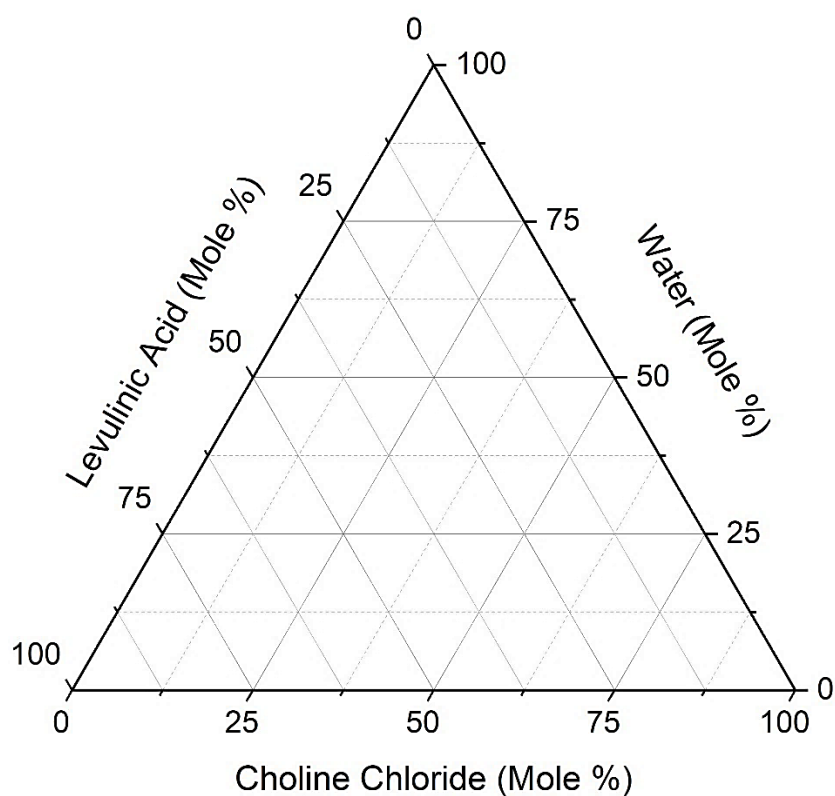


Figure 6-1 Ternary Phase Diagram of ChCl:LvAc:Water

This work has fully investigated the carbon capture performance by ChCl:LvAc DESs by studying the CO₂ absorption capacity of these DESs compositions along with their regeneration process. While the majority of previous work in the literature has been only focusing on measuring the CO₂ absorption capacity of DESs without evaluating their regeneration process, recyclability of selectivity. Therefore, it is highly recommended to consider all these aspects when evaluating any sorbent for carbon capture processes. In addition, most of the published work focused on measuring the CO₂ absorption capacity only under stagnant conditions, which does not provide much information about their potential from a practical point of view. Thus, it is essential to study the carbon capture performance under dynamic flow conditions to simulate the actual scenarios in carbon capture plants.

In this work, the corrosivity of ChCl:LvAc DESs was investigated experimentally at different conditions (stagnant versus stirred conditions and in the presence and absence of CO₂), in order to “imitate” the corrosion scenarios in the CO₂ absorption and desorption processes. Although, the experimental results clearly show that these DESs are much less corrosive than MEA much lower corrosion penetration rates. Yet it is recommended to investigate the corrosion of metals by DESs at a fundamental level. Many techniques can be employed for this purpose such as but not limited to the scanning electron microscope (SEM) to identify the elemental composition and surface morphology of pristine and corroded samples while X-ray diffraction (XRD) could be used to identify corrosion products ²⁵⁹.

Finally, it is also important to point out that any complete framework to develop DES systems for carbon capture processes must take into consideration scalability (scale-up).

Future researchers, in addition to pursuing the development of DESs that perform very well in terms of CO₂ absorption, regeneration, corrosion minimisation, recyclability and selectivity, must also consider scalability as an additional complexity. That is, DESs that perform very well in lab conditions must still be tested at larger scales before being considered as real alternative sorbents for commercial applications in actual post-combustion carbon capture plants.

Appendix A

Supplementary material of Chapter 3:

A comprehensive characterization of choline chloride levulinic acid-based deep eutectic solvents

A.1 Phase behaviour plot data

Table A - 1 Ideal melting curve data of the HBA and the HBD

Ideal melting curve for ChCl		Ideal melting curve for LvAc	
Mole fraction (x)	T (K)	Mole fraction (x)	T (K)
1.00	576.15	1.00	306.15
0.90	515.63	0.90	297.50
0.80	461.45	0.80	288.38
0.70	412.32	0.70	278.71
0.60	367.20	0.60	268.31
0.50	325.11	0.50	256.98
0.40	285.12	0.40	244.34
0.30	246.09	0.30	229.78
0.20	206.29	0.20	211.97
0.10	161.61	0.10	187.17

A.2 Density measurement data

Table A - 2 Density of water in kg.cm⁻³ at different temperatures

T (°C)	Density of water (kg.m ⁻³) (This Work)	Density of water (kg.m ⁻³) as reported in Ref. 1 in ²⁶⁰	Density of water (kg.m ⁻³) as reported in Ref. 2 in ²⁶¹	10 × Relative Deviation
25	997.0413	997.047	997.05	0.01
35	994.0247	994.0326	994.03	0.01
45	990.1767		990.21	0.03
55	985.62		985.69	0.07
65	980.48		980.55	0.07

Table A - 3 Density of ChCl:LvAc DESs in g.cm⁻³ at different temperatures

T (K)	ChCl:LvAc Composition					
	1:2:0	1:2:2.5	1:2:5	1:3:0	1:3:2.5	1:3:5
298.15	1.13853	1.13713	1.133	1.1374	1.1299	1.12077
308.15	1.13617	1.1293	1.1277	1.1356	1.1257	1.11783
318.15	1.132	1.125	1.121	1.131	1.1223	1.11437
328.15	1.12	1.119	1.1098	1.119	1.1104	1.1026
338.15	1.1	1.0943	1.0854	1.0995	1.08933	1.08407

A.3 Viscosity measurement data

Table A - 4 Viscosity of ChCl:LvAc Compositions in mPa.s

T (K)	ChCl:LvAc Composition						
	1:2:0	1:2:5	1:2:0+CO ₂	1:3:0	1:3:0+CO ₂	1:3:5	1:3:5+CO ₂
298.13	154.478	154.3380	166.2027	100.6940	92.4356	81.7791	99.9451
303.13	124.303	124.21	150.5513	79.7586	74.3740	65.1127	87.9313
308.13	94.4295	84.3414	142.6167	60.8065	57.7438	49.4252	57.3991
313.13	72.4889	64.9948	119.6165	47.0382	45.5216	38.6983	42.4376
318.13	56.7047	51.0518	84.0390	37.2129	37.2431	30.8360	33.2573
323.13	45.0943	40.7769	57.9010	29.9963	34.7776	25.1080	27.1982
328.13	36.5316	33.1817	39.6605	24.4974	29.1140	20.7082	23.7183
333.13	29.9377	27.3475	32.0575	20.3037	21.3114	17.2056	21.8222
338.13	24.977	22.8296	27.8621	17.1162	17.2142	14.6907	18.8524
343.13	21.0145	19.3404	24.3591	14.6243	14.8894	12.5299	16.7473
348.13	17.8615	16.6591	21.0802	12.4911	13.1620	10.8547	15.2545

A.4 Corrosivity measurement data

Table A - 5 Average CPR values of ChCl:LvAc Compositions in mm.Y⁻³

T (K)	ChCl:LvAc Composition						
	1:2:0	1:2:0+CO ₂ + 250 rpm	1:2:5	1:3:0	1:3:0+CO ₂ + 250 rpm	1:3:5	MEA 30%
298.15	0.02288	0.03953	0.01506	0.05561	0.10202	0.02213	0.67365

Appendix B

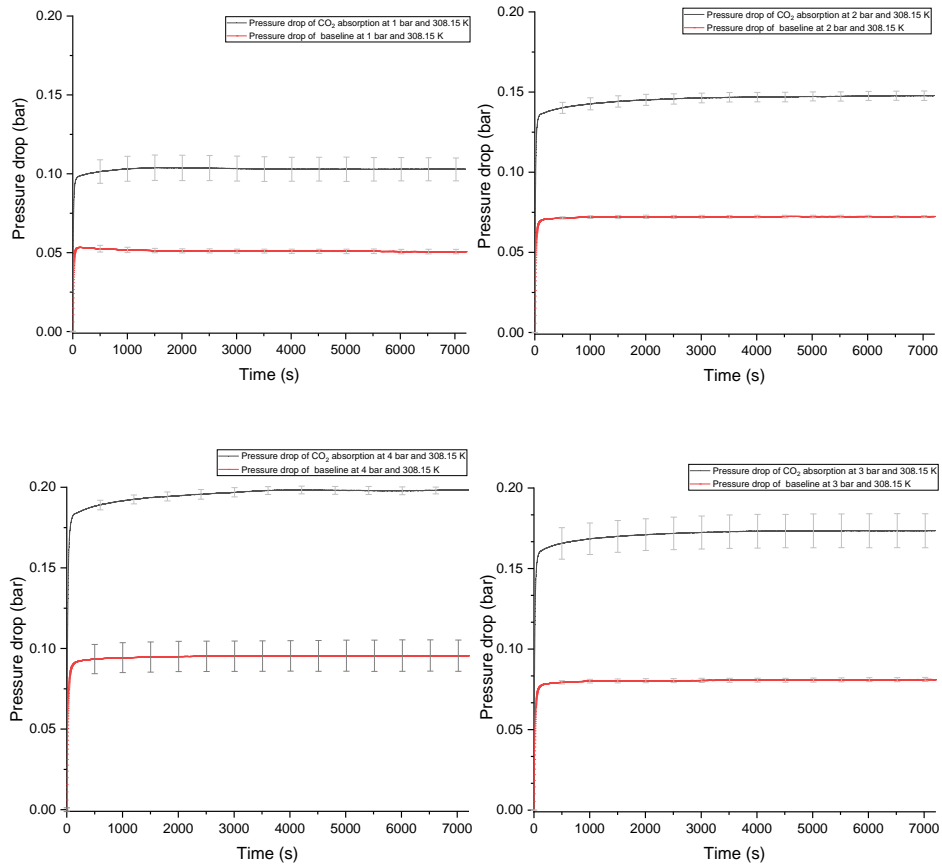
Supplementary material of Chapter 4:

**The CO₂ absorption and desorption data by
choline chloride levulinic acid-based deep
eutectic solvents**

B.1 Determination of baselines.

B.1.1 Baselines VS. absorption measurements at 298.15 K of ChCl: LvAc (1:3:0)

The VLE rig reaches equilibrium at 298.15 K within 2 hours as shown in below. The absolute pressure drop due to the CO₂ absorption only is the difference between the two isotherms pressure drop curves in Figure B-1 below.



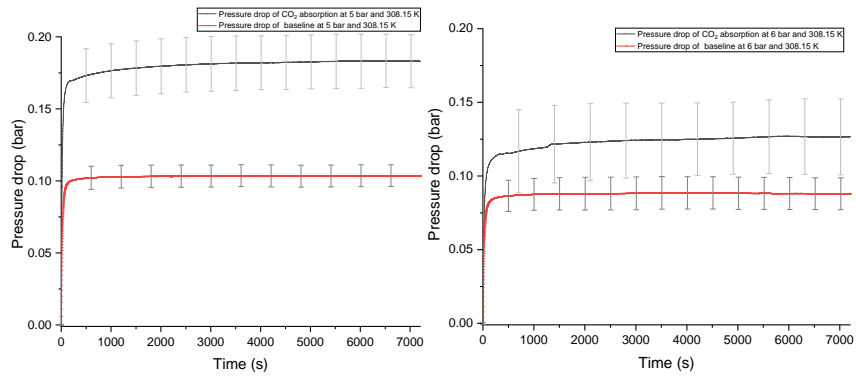
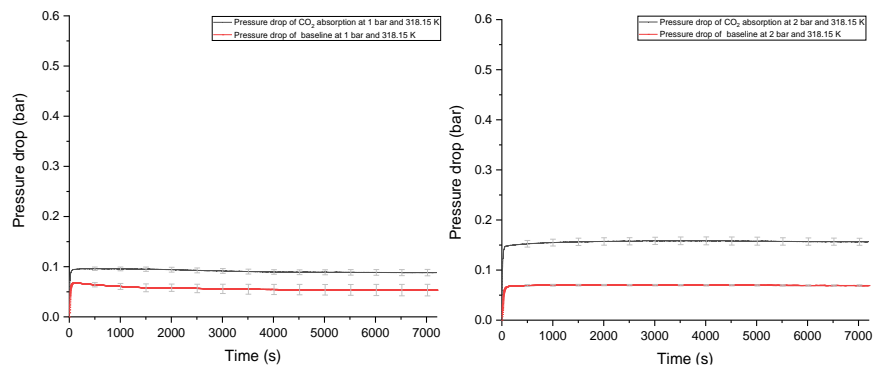


Figure B - 1 Pressure drop values of the absolute pressure drop in the rig due to CO₂ absorption by ChCl: LvAc (1:3:0) at 308.15 K Vs. pressure drop at the baselines

B.2 Baselines VS. absorption measurements at 318.15 K of ChCl: LvAc (1:3:0)



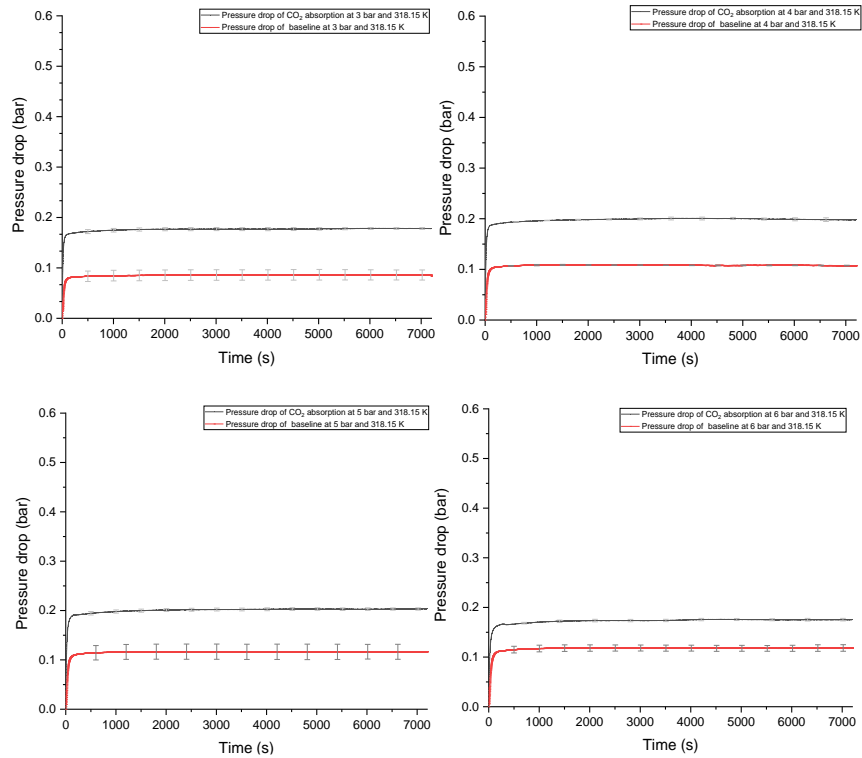
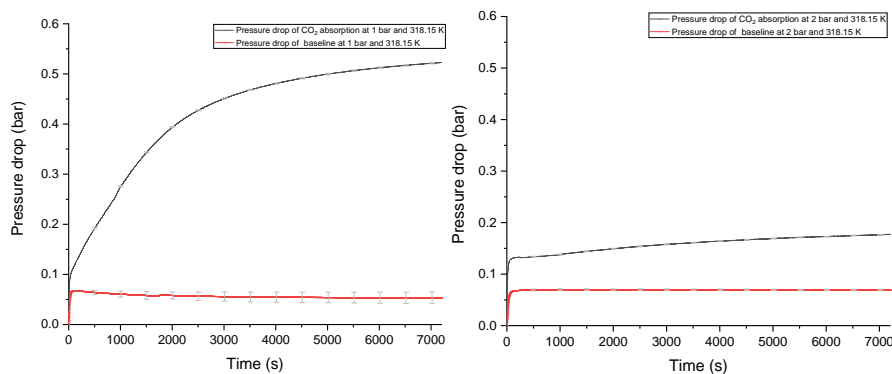


Figure B -2 Pressure drop values of the absolute pressure drop in the rig due to CO₂ absorption by ChCl: LvAc (1:3:0) at 318.15 K Vs. pressure drop at the baselines

B.3 Calibration of the VLE rig using Monoethanolamine at 45 °C

B.3.1 Thermodynamic Equilibrium

The VLE rig reaches equilibrium within 2 hours as shown in Figure B-3, the pressure drop in the system decreases with increasing the pressure at a constant temperature of 45 °C



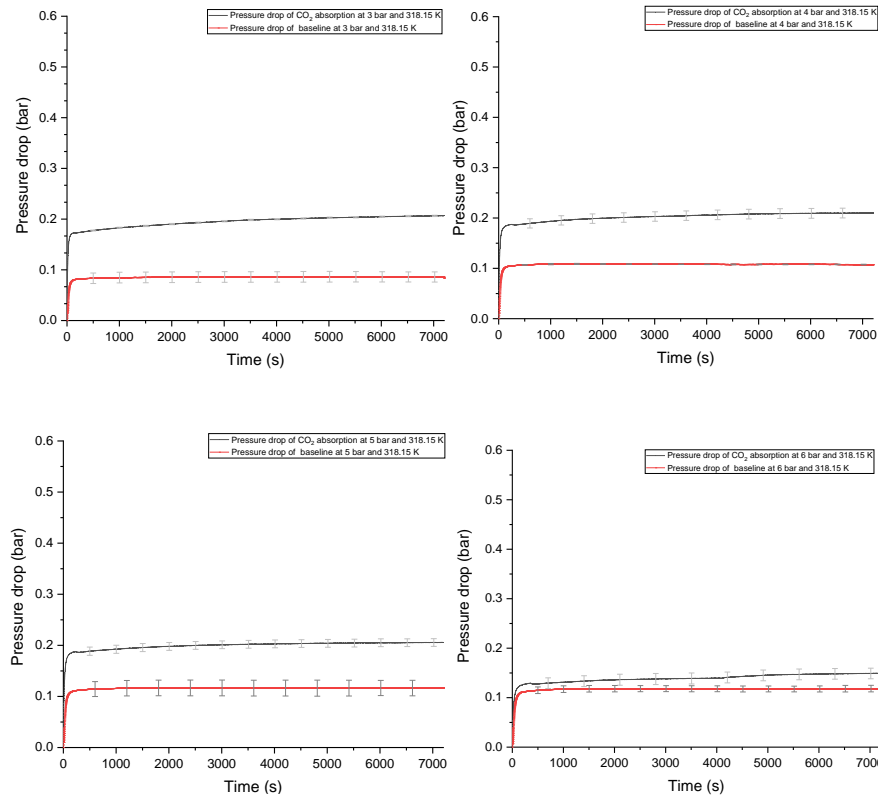


Figure B -3 Pressure drop values of the absolute pressure drop in the rig due to CO₂ absorption by MEA Vs. pressure drop at the baselines

B.4 CO₂ load calculation

CO₂ load increases with increasing the pressure in the system as extensively reported in the literature ²³⁶. Lee *et al.* in their work in ²³⁶ reported the CO₂ load absorbed by MEA (30% wt.) at pressures ranging between 0.1 – 1000 kPa as shown in table B1 and figure 2 below. However, we have estimated CO₂ load absorbed by MEA (30% wt.) at pressures of 100, 200, 300, 400, 500 and 600 kPa at 318.15 K by fitting a nonlinear power-law fit to the raw data reported by Lee *et al.* ²³⁶. The fitted model is highly precise of R² value of 100%. Then, we compared our calculated values against estimated values at certain pressures as per Figure B-4:

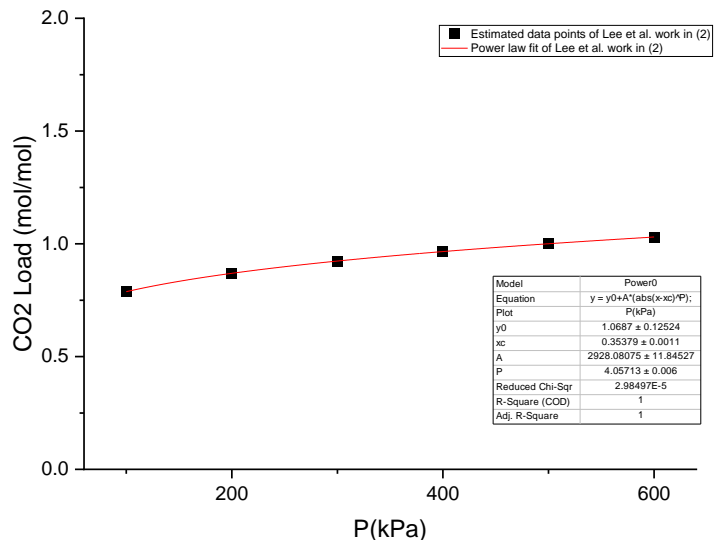


Figure B-4 CO₂ load at 318.15 from the estimated data from Lee *et al.* work in (1) with a nonlinear fitting

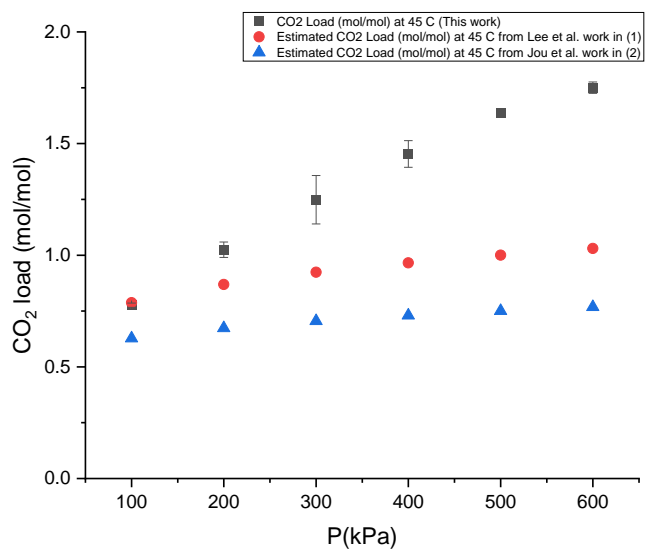


Figure B-5 CO₂ load at 318.15 K of this work Vs. Lee *et al.* work in (1) and Jou *et al.* work in (2)

Table B-8-1 Calculated correction factors at 318.15 K

Estimated values of CO ₂ Load at given pressures from using nonlinear fitting from Lee <i>et al.</i> work in ²³⁶		This work		Correction Factor (CF)
CO ₂ Load (mol/mol) at 318.15 K	P(kPa)	CO ₂ Load (mol/mol) at 318.15 K	P(kPa)	
0.7877	100	0.7759	100	1.0152
0.8692	200	1.0247	200	0.8482
0.9236	300	1.2484	300	0.7398
0.9656	400	1.4535	400	0.6643
1.0003	500	1.6384	500	0.6105
1.0301	600	1.7504	600	0.5885

B.5 Correction factors

Figure B-5 above shows a clear deviation between the calculated values of CO₂ load in MEA (30% wt.) at 318.15 K from the rig equilibrium data and the ones reported in the literature under the same conditions. Therefore, correction factors (CFs) must be estimated and applied to compensate for the deviation. CF is applicable only for systematic errors, hence to ensure that the error is a systematic one we need to check how calculated values gained from the rig fit with the nonlinear power-law model that fitted with the raw data from the literature²³⁶ as per Figure B-5 above. The calculated values fit well with the nonlinear model of R² value of 99.77% as per Figure B-6 below. Therefore, it is justifiable to generate a linear CFs between gained results and the ones reported in the literature as per table B-2 below.

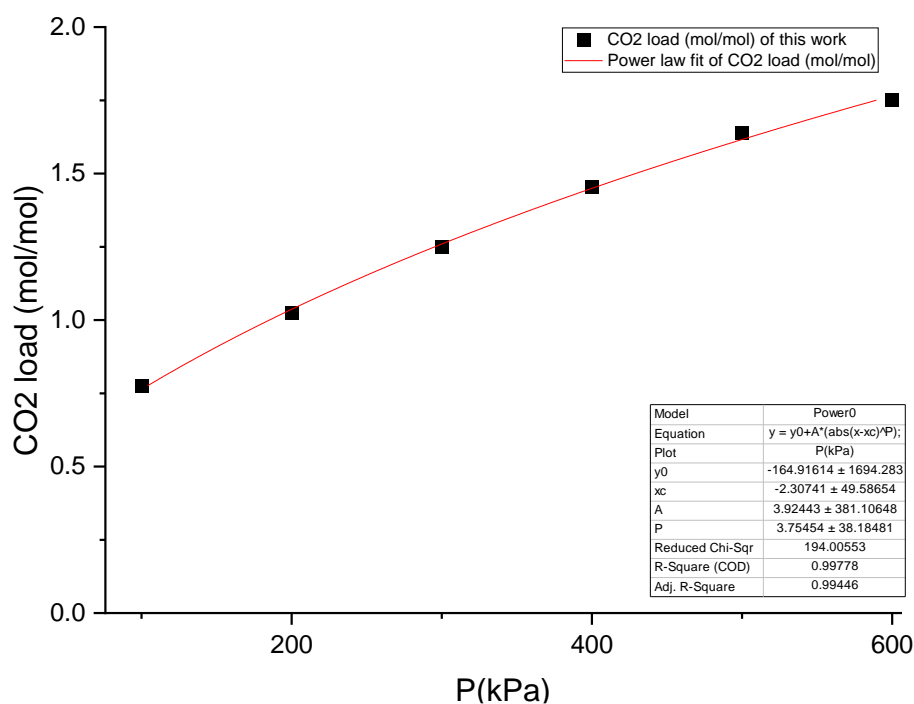


Figure B -6 Power-law fitting CO₂ load at 318.15 of this work

Table 8-2 Factors and levels of the factorial design at different temperatures

HBA:HBD molar ratio	Water content (water:HBA molar ratio)	Temperature (°C)	Pressure (bar)	CO ₂ Absorption (mol.kg ⁻¹)
1:2	0	25	1	0.4741
1:2	0	25	2	0.7767
1:2	0	25	3	1.02991
1:2	0	25	4	1.26366
1:2	0	25	5	1.3525
1:2	0	25	6	1.36739
1:2	2.5	25	1	0.36352
1:2	2.5	25	2	0.69315
1:2	2.5	25	3	0.9926
1:2	2.5	25	4	1.26322
1:2	2.5	25	5	1.43897
1:2	2.5	25	6	1.56806
1:2	5	25	1	0.45091
1:2	5	25	2	0.76693
1:2	5	25	3	1.09265
1:2	5	25	4	1.37936
1:2	5	25	5	1.50813
1:2	5	25	6	1.52095
1:3	0	25	1	0.38898
1:3	0	25	2	0.78817
1:3	0	25	3	1.0001
1:3	0	25	4	1.25297
1:3	0	25	5	1.44295
1:3	0	25	6	1.46589
1:3	2.5	25	1	0.43321
1:3	2.5	25	2	0.82708
1:3	2.5	25	3	1.14201
1:3	2.5	25	4	1.43815
1:3	2.5	25	5	1.46695
1:3	2.5	25	6	1.58618
1:3	5	25	1	0.40692
1:3	5	25	2	0.71202
1:3	5	25	3	1.01957
1:3	5	25	4	1.28441
1:3	5	25	5	1.43618
1:3	5	25	6	1.57494

HBA:HBD molar ratio	Water content (water:HBA molar ratio)	Temperature (°C)	Pressure (bar)	CO ₂ Absorption (mol.kg ⁻¹)
1:2	0	35	1	0.2856
1:2	0	35	2	0.73661
1:2	0	35	3	0.99646
1:2	0	35	4	1.12232
1:2	0	35	5	1.28709
1:2	0	35	6	1.30934
1:2	2.5	35	1	0.25299
1:2	2.5	35	2	0.65864
1:2	2.5	35	3	0.91296
1:2	2.5	35	4	1.09089
1:2	2.5	35	5	1.29432
1:2	2.5	35	6	1.49044
1:2	5	35	1	0.28944
1:2	5	35	2	0.71323
1:2	5	35	3	0.98762
1:2	5	35	4	1.18212
1:2	5	35	5	1.36429
1:2	5	35	6	1.46463
1:3	0	35	1	0.25059
1:3	0	35	2	0.70921
1:3	0	35	3	0.9976
1:3	0	35	4	1.19119
1:3	0	35	5	1.35511
1:3	0	35	6	1.42458
1:3	2.5	35	1	0.23812
1:3	2.5	35	2	0.66805
1:3	2.5	35	3	0.99417
1:3	2.5	35	4	1.19821
1:3	2.5	35	5	1.40254
1:3	2.5	35	6	1.54939
1:3	5	35	1	0.25323
1:3	5	35	2	0.70565
1:3	5	35	3	1.0143
1:3	5	35	4	1.23403
1:3	5	35	5	1.41172
1:3	5	35	6	1.52696
1:2	0	45	1	0.20586
1:2	0	45	2	0.55889
1:2	0	45	3	0.83784

HBA:HBD molar ratio	Water content (water:HBA molar ratio)	Temperature (°C)	Pressure (bar)	CO ₂ Absorption (mol.kg ⁻¹)
1:2	0	45	4	1.05581
1:2	0	45	5	1.25663
1:2	0	45	6	1.27078
1:2	2.5	45	1	0.22173
1:2	2.5	45	2	0.53081
1:2	2.5	45	3	0.79991
1:2	2.5	45	4	1.02709
1:2	2.5	45	5	1.24891
1:2	2.5	45	6	1.48952
1:2	5	45	1	0.19792
1:2	5	45	2	0.5431
1:2	5	45	3	0.83104
1:2	5	45	4	1.06314
1:2	5	45	5	1.29621
1:2	5	45	6	1.46098
1:3	0	45	1	0.17272
1:3	0	45	2	0.47796
1:3	0	45	3	0.7596
1:3	0	45	4	1.00449
1:3	0	45	5	1.24484
1:3	0	45	6	1.39762
1:3	2.5	45	1	0.20866
1:3	2.5	45	2	0.5039
1:3	2.5	45	3	0.84396
1:3	2.5	45	4	1.17127
1:3	2.5	45	5	1.47713
1:3	2.5	45	6	1.52899
1:3	5	45	1	0.15801
1:3	5	45	2	0.50721
1:3	5	45	3	0.81658
1:3	5	45	4	1.02373
1:3	5	45	5	1.27446
1:3	5	45	6	1.49683

B.6 The effect of stirring speed on the CO₂ absorption capacity

Table 8-3 The effect of stirring speed on CO₂ absorption capacity of ChCl:LvAc (1:2:0) at 298.15 K

Pressure (kPa)	Stirring Speed (rpm)			
	0	50	100	250
100	0.02295	0.29192	0.41624	0.4741
200	0.08609	0.57144	0.73008	0.7767
300	0.31007	0.76677	0.98967	1.02991
400	0.47134	0.96334	1.21714	1.26366
500	0.59781	1.04431	1.32556	1.3525
600	0.61153	1.07413	1.36501	1.36739

B.7 Thermodynamics analysis of CO₂ absorption

B.7.1 Henry's law constant (H_x)

The solubility of CO₂ in the DESs could be expressed in terms of HLC. The smaller the value of the HLC the higher the solubility^{155, 118} and²⁰⁶. H_x is defined as HLC based on mass fraction, could be expressed in Equation (8-1) as follows

$$H_x(T, P) = \lim_{x_{CO_2} \rightarrow 0} f_{CO_2}^{Liq} \left[\frac{(T, P, x_{CO_2})}{x_{CO_2}} \right] \quad \text{Equation (8-1)} \\ \text{HLC}$$

Where:

$H_x(T, P)$: Henry's constant based on the mass fraction

x_{CO_2} : mass fraction of CO₂ in DES

$f_{CO_2}^{Liq}(T, P, x_{CO_2})$: fugacity of CO₂ in the DESs

When vapour-liquid equilibrium reached, the fugacity of CO₂ in the vapour phase is equal to that in the liquid phase as per Equation (8-2) below, hence:

$$\begin{aligned} f_{CO_2}^{Liq}(T, P, x_{CO_2}) &= f_{CO_2}^{Vap}(T, P, y_{CO_2}) \\ &= y_{CO_2} P \phi_{CO_2}(T, P, y_{CO_2}) \end{aligned} \quad \begin{array}{l} \text{Equation (8-2)} \\ \text{VLE} \end{array}$$

Where:

$f_{CO_2}^{Vap}(T, P, y_{CO_2})$: fugacity of CO₂ in the vapour phase

y_{CO_2} : mole fraction of CO₂

ϕ_{CO_2} : fugacity coefficient of CO₂ in the vapour phase, could be calculated using the three-term virial equation as per ²⁶².

Since the vapour pressure of the DESs is very small as compared to the vapour pressure of CO₂ ²³⁴. Hence, the vapour phase is composed of pure CO₂. In this case, Henry's law constant based on the mass fraction (H_x) can be expressed as per Equation (8-3) & Equation (B-8-4) below:

$$H_x(T, P) = \lim_{x_{CO_2} \rightarrow 0} f \left[\frac{(T, P, x_{CO_2})}{x_{CO_2}} \right] = \lim_{y_{CO_2} \rightarrow 0} f \left[\frac{(T, P, y_{CO_2})}{y_{CO_2}} \right] \quad \begin{array}{l} \text{Equation (8-3) HLC} \\ \text{based on mass} \\ \text{fraction} \end{array}$$

$$H_x(T, P) = \frac{P \phi_{CO_2}(T, P)}{x_{CO_2}} \quad \begin{array}{l} \text{Equation (B-8-4)} \\ \text{HLCx} \end{array}$$

B.7.2 Changes in enthalpy (ΔH), entropy (ΔS) and Gibbs free energy (ΔG)

Changes in enthalpy, Gibbs energy and entropy can be calculated from using Van't Hoff equations Equation (B-8-5), Equation (8-6), and Equation (B-8-7) below:

$$\Delta G = R T \ln \left[\frac{H(T,P)}{P_0} \right]$$

Equation
(B-8-5) Changes
in Gibbs free
energy

$$\Delta H = -R \left\{ \frac{\delta \ln \left[\frac{H(T,P)}{P_0} \right]}{\delta \left(\frac{1}{T} \right)} \right\}$$

Equation (8-6)
Changes in
Enthalpy

$$\Delta S = \left[\frac{\Delta H - \Delta G}{T} \right]$$

Equation
(B-8-7) Changes
in Entropy

Where: $P_0 = 1 \text{ bar}$

B.8 Analysis of variance

Analysis of variance of the full factorial design - Table 8-4 below- shows the effect of each controlled parameter (molar ratio, stirring speed, water content, pressure and temperature) and the second and third-order interactions among the parameters on the response (CO_2 absorption capacity).

B.9 Refining the quadratic model

The refined model summary is presented the refined model summary in Table 8-4 below

B.9.1 Analysis of variance of the factorial designs

Table 8-4 Analysis of variance

Analysis of Variance for Transformed Response

Source	DF	Seq SS	Contribution	Adj SS	Adj MS
Model	55	3.34196	99.86%	3.34196	0.060763
Linear	13	3.25625	97.29%	1.04282	0.080217
Molar Ratio	1	0.02646	0.79%	0.00015	0.000148
Stirring Speed	3	0.46903	14.01%	0.37933	0.126445
Pressure	5	2.65425	79.31%	0.56519	0.113038
Temperature	2	0.09330	2.79%	0.09330	0.046650
Water Content	2	0.01320	0.39%	0.01320	0.006601
2-Way Interactions	38	0.08477	2.53%	0.08477	0.002231
Molar Ratio*Pressure	5	0.00436	0.13%	0.00360	0.000720
Molar Ratio*Temperature	2	0.00051	0.02%	0.00051	0.000254
Molar Ratio*Water Content	2	0.00016	0.00%	0.00016	0.000080
Stirring Speed*Pressure	15	0.03490	1.04%	0.03904	0.002603
Pressure*Temperature	10	0.04419	1.32%	0.04419	0.004419
Temperature*Water Content	4	0.00065	0.02%	0.00065	0.000162
3-Way Interactions	4	0.00095	0.03%	0.00095	0.000237
Molar Ratio*Temperature*Water Content	4	0.00095	0.03%	0.00095	0.000237
Error	70	0.00485	0.14%	0.00485	0.000069
Total	125	3.34681	100.00%		

Source	F-Value	P-Value
Model	877.48	0.000
Linear	1158.41	0.000
Molar Ratio	2.13	0.149
Stirring Speed	1825.99	0.000
Pressure	1632.37	0.000
Temperature	673.67	0.000
Water Content	95.33	0.000
2-Way Interactions	32.21	0.000
Molar Ratio*Pressure	10.40	0.000
Molar Ratio*Temperature	3.66	0.031
Molar Ratio*Water Content	1.15	0.323
Stirring Speed*Pressure	37.58	0.000
Pressure*Temperature	63.82	0.000
Temperature*Water Content	2.33	0.064
3-Way Interactions	3.42	0.013
Molar Ratio*Temperature*Water Content	3.42	0.013
Error		
Total		

B.9.2 Pareto charts of standardized and refined models

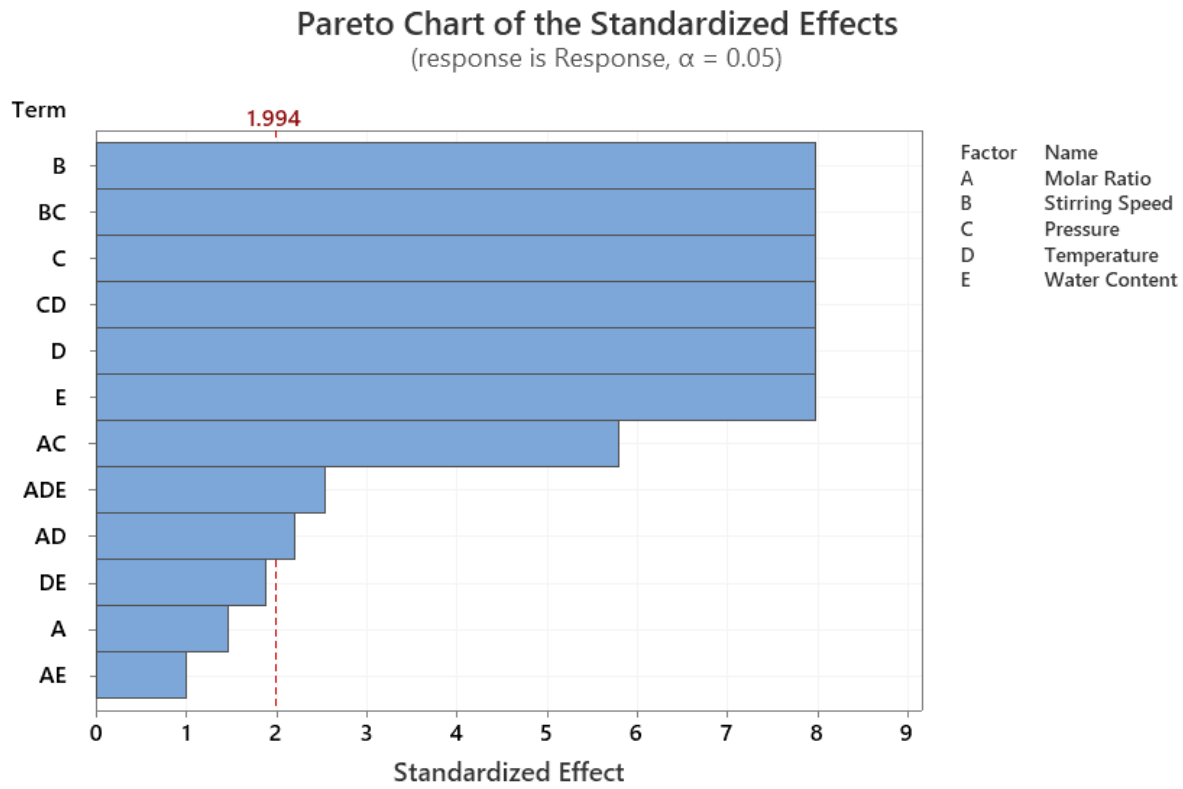


Figure B-7 Pareto chart of the standardized effects

Pareto Chart of the Standardized Effects
(response is Response, $\alpha = 0.05$)

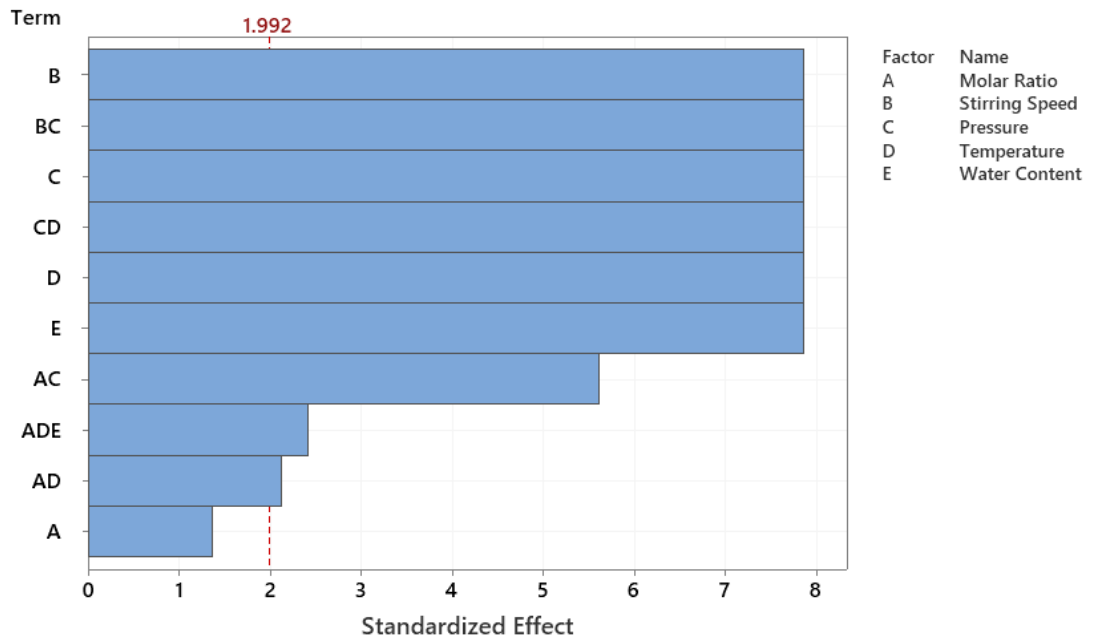


Figure B-8 Pareto chart of the standardized effects after removing the insignificant terms

B.10 Refined model equation is presented as per Equation B-8 below

Equation B-8 Refined model equation

Response^0.279157 = 0.87842 - 0.001098 Molar Ratio_0.67 + 0.001098 Molar Ratio_0.75
- 0.20823 Stirring Speed_0 + 0.02383 Stirring Speed_50
+ 0.09216 Stirring Speed_100 + 0.09224 Stirring Speed_250
- 0.29990 Pressure_1 - 0.10561 Pressure_2 + 0.02151 Pressure_3
+ 0.08885 Pressure_4 + 0.13812 Pressure_5 + 0.15702 Pressure_6
+ 0.03453 Temperature_25 + 0.00087 Temperature_35
- 0.03540 Temperature_45 - 0.01349 Water Content_0.0
+ 0.01270 Water Content_2.5 + 0.00079 Water Content_5.0
+ 0.01063 Molar Ratio*Pressure_0.67 1 + 0.00348 Molar Ratio*Pressure_0.67
2 - 0.00040 Molar Ratio*Pressure_0.67 3
- 0.00364 Molar Ratio*Pressure_0.67 4 - 0.00469 Molar Ratio*Pressure_0.67
5 - 0.00537 Molar Ratio*Pressure_0.67 6
- 0.01063 Molar Ratio*Pressure_0.75 1 - 0.00348 Molar Ratio*Pressure_0.75
2 + 0.00040 Molar Ratio*Pressure_0.75 3
+ 0.00364 Molar Ratio*Pressure_0.75 4 + 0.00469 Molar Ratio*Pressure_0.75
5 + 0.00537 Molar Ratio*Pressure_0.75 6
- 0.00101 Molar Ratio*Temperature_0.67 25
- 0.00193 Molar Ratio*Temperature_0.67 35
+ 0.00294 Molar Ratio*Temperature_0.67 45
+ 0.00101 Molar Ratio*Temperature_0.75 25
+ 0.00193 Molar Ratio*Temperature_0.75 35
- 0.00294 Molar Ratio*Temperature_0.75 45
- 0.09758 Stirring Speed*Pressure_0 1 - 0.08438 Stirring Speed*Pressure_0
2 + 0.01909 Stirring Speed*Pressure_0 3
+ 0.04028 Stirring Speed*Pressure_0 4 + 0.06315 Stirring Speed*Pressure_0
5 + 0.05943 Stirring Speed*Pressure_0 6
+ 0.03083 Stirring Speed*Pressure_50 1
+ 0.03464 Stirring Speed*Pressure_50 2
- 0.00559 Stirring Speed*Pressure_50 3
- 0.01275 Stirring Speed*Pressure_50 4
- 0.02295 Stirring Speed*Pressure_50 5
- 0.02419 Stirring Speed*Pressure_50 6
+ 0.03634 Stirring Speed*Pressure_100 1
+ 0.02687 Stirring Speed*Pressure_100 2
- 0.00536 Stirring Speed*Pressure_100 3
- 0.01432 Stirring Speed*Pressure_100 4
- 0.02160 Stirring Speed*Pressure_100 5
- 0.02193 Stirring Speed*Pressure_100 6
+ 0.03041 Stirring Speed*Pressure_250 1
+ 0.02287 Stirring Speed*Pressure_250 2
- 0.00815 Stirring Speed*Pressure_250 3
- 0.01322 Stirring Speed*Pressure_250 4
- 0.01860 Stirring Speed*Pressure_250 5
- 0.01331 Stirring Speed*Pressure_250 6 + 0.04840 Pressure*Temperature_1
25 - 0.01460 Pressure*Temperature_1 35 - 0.03379 Pressure*Temperature_1
45 + 0.00369 Pressure*Temperature_2 25 + 0.01577 Pressure*Temperature_2
35 - 0.01947 Pressure*Temperature_2 45 - 0.00614 Pressure*Temperature_3
25 + 0.01045 Pressure*Temperature_3 35 - 0.00431 Pressure*Temperature_3
45 - 0.00200 Pressure*Temperature_4 25 - 0.00260 Pressure*Temperature_4
35 + 0.00460 Pressure*Temperature_4 45 - 0.01748 Pressure*Temperature_5
25 - 0.00325 Pressure*Temperature_5 35 + 0.02073 Pressure*Temperature_5
45 - 0.02647 Pressure*Temperature_6 25 - 0.00577 Pressure*Temperature_6
35 + 0.03224 Pressure*Temperature_6 45
- 0.00201 Molar Ratio*Temperature*Water Content_0.67 25 0.0
+ 0.00143 Molar Ratio*Temperature*Water Content_0.67 25 2.5
+ 0.00058 Molar Ratio*Temperature*Water Content_0.67 25 5.0
- 0.00241 Molar Ratio*Temperature*Water Content_0.67 35 0.0
+ 0.00371 Molar Ratio*Temperature*Water Content_0.67 35 2.5
- 0.00130 Molar Ratio*Temperature*Water Content_0.67 35 5.0
+ 0.00442 Molar Ratio*Temperature*Water Content_0.67 45 0.0
- 0.00514 Molar Ratio*Temperature*Water Content_0.67 45 2.5
+ 0.00072 Molar Ratio*Temperature*Water Content_0.67 45 5.0
+ 0.00201 Molar Ratio*Temperature*Water Content_0.75 25 0.0
- 0.00143 Molar Ratio*Temperature*Water Content_0.75 25 2.5
- 0.00058 Molar Ratio*Temperature*Water Content_0.75 25 5.0
+ 0.00241 Molar Ratio*Temperature*Water Content_0.75 35 0.0
- 0.00371 Molar Ratio*Temperature*Water Content_0.75 35 2.5
+ 0.00130 Molar Ratio*Temperature*Water Content_0.75 35 5.0
- 0.00442 Molar Ratio*Temperature*Water Content_0.75 45 0.0
+ 0.00514 Molar Ratio*Temperature*Water Content_0.75 45 2.5
- 0.00072 Molar Ratio*Temperature*Water Content_0.75 45 5.0

B.11 Factorial design array

Table B-8-5 Factorial design array

Factor Information

Factor	Levels Values
Molar Ratio	2 0.67, 0.75
Stirring Speed	4 0, 50, 100, 250
Pressure	6 1, 2, 3, 4, 5, 6
Temperature	3 25, 35, 45
Water Content	3 0.0, 2.5, 5.0

B.12 Recyclability measurements data

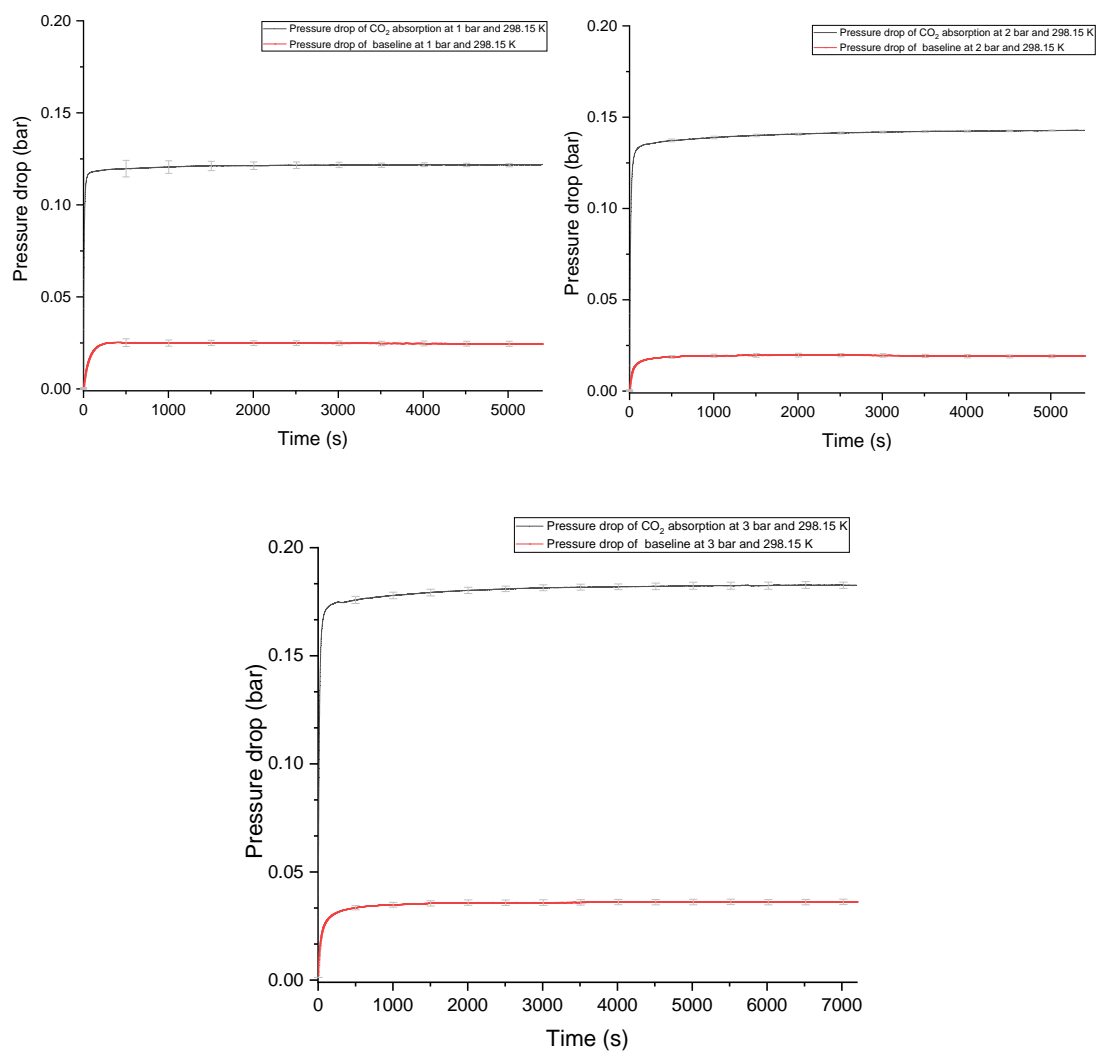


Figure B-9 Pressure drop values of the absolute pressure drop in the rig due to CO₂ absorption by ChCl:LvAc of (1:2:0) molar ratio at 25 °C and 250 rpm of the first cycle Vs. the pressure drop of the baselines

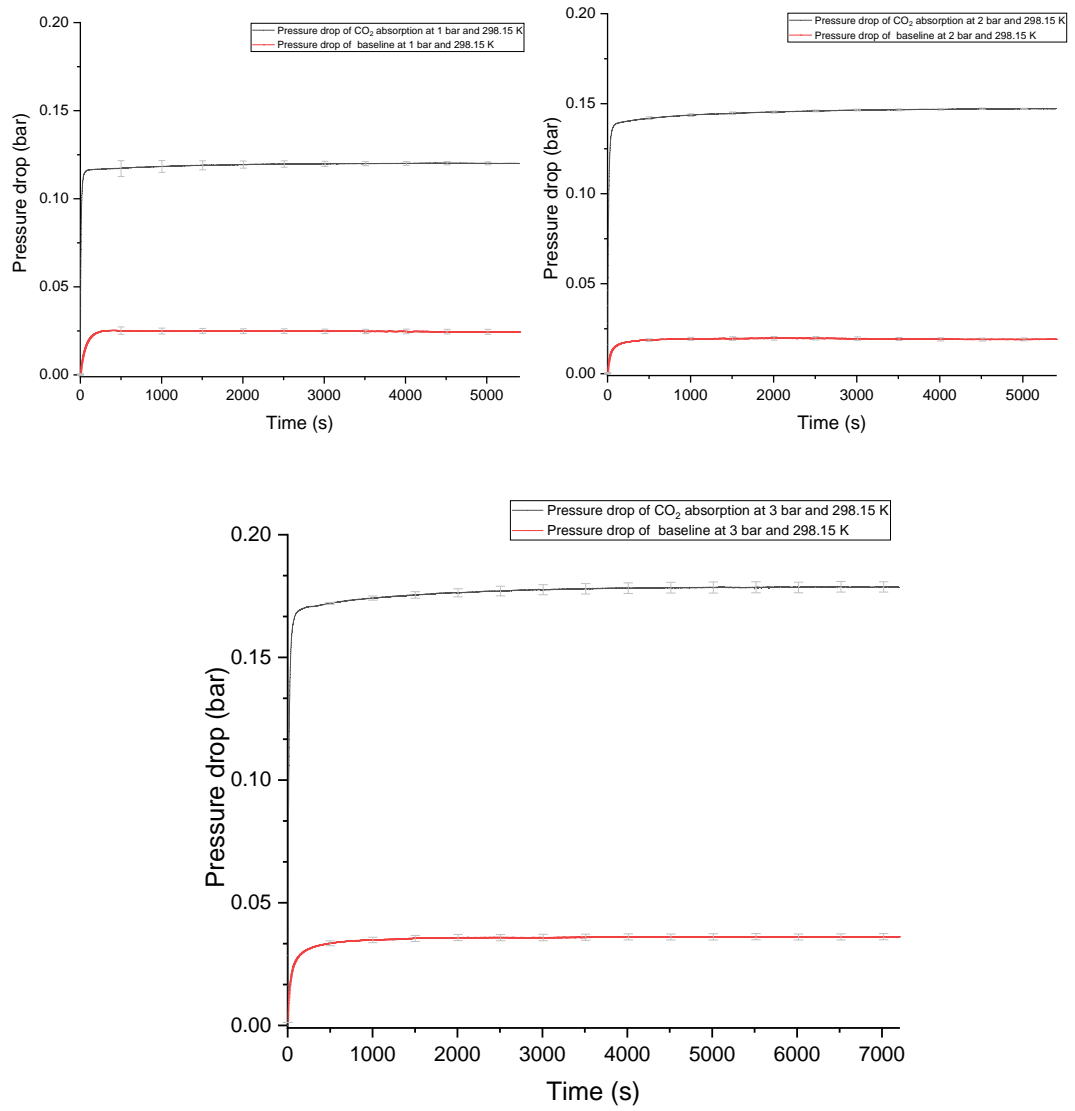


Figure B -10 Pressure drop values of the absolute pressure drop in the rig due to CO₂ absorption by ChCl:LvAc of (1:2:0) molar ratio at 25 °C and 250 rpm of the second cycle Vs. the pressure drop of the baselines

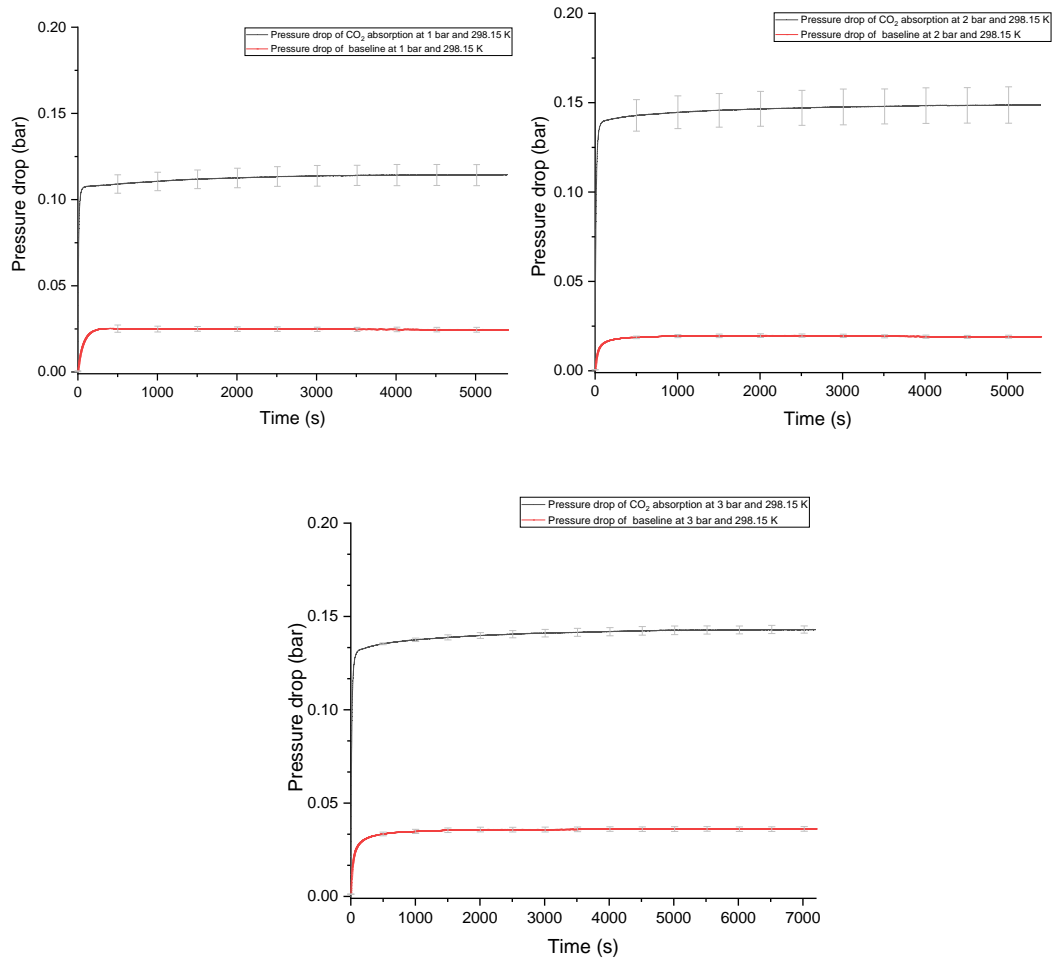
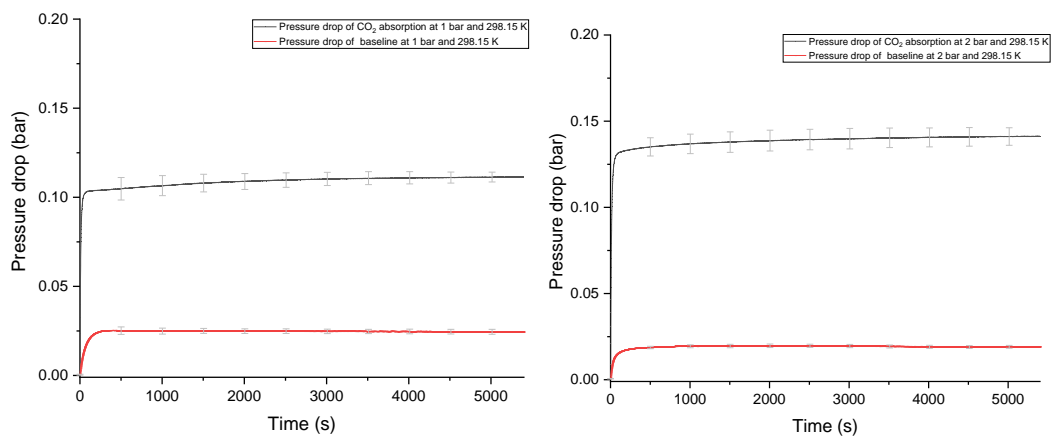


Figure B -11 Pressure drop values of the absolute pressure drop in the rig due to CO₂ absorption by ChCl:LvAc of (1:2:0) molar ratio at 25 °C and 250 rpm of the third cycle Vs. the pressure drop of the baselines



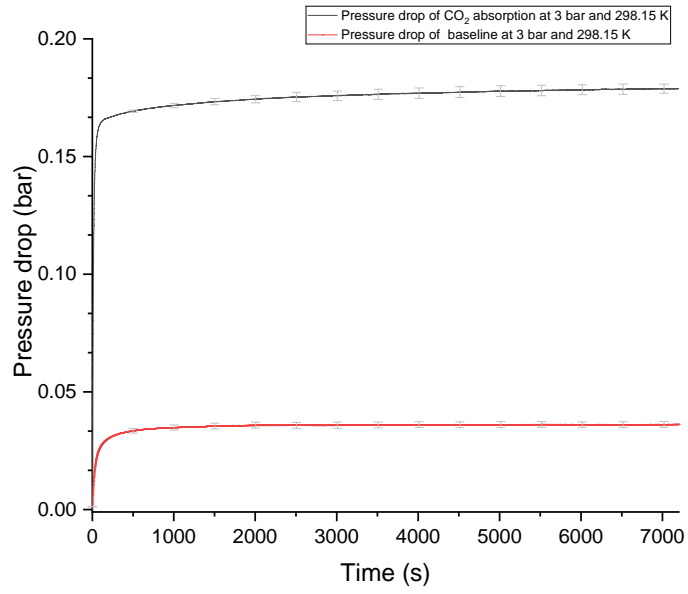
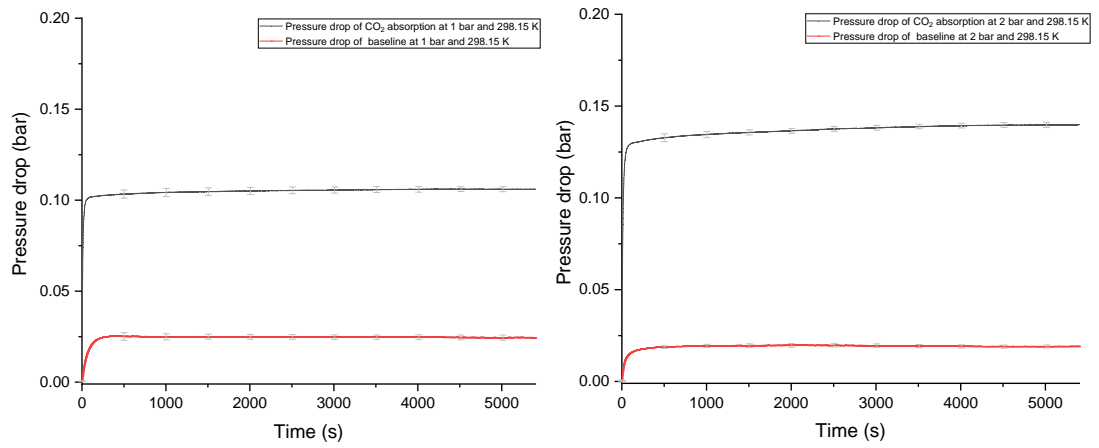


Figure B -12 Pressure drop values of the absolute pressure drop in the rig due to CO₂ absorption by ChCl:LvAc of (1:2:0) molar ratio at 25 °C and 250 rpm of the fourth cycle Vs. the pressure drop of the baselines



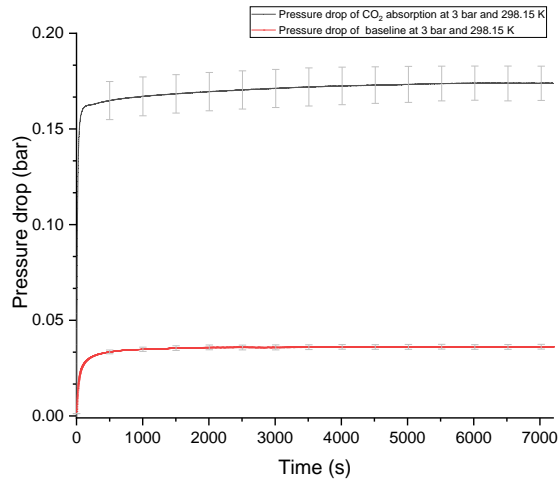
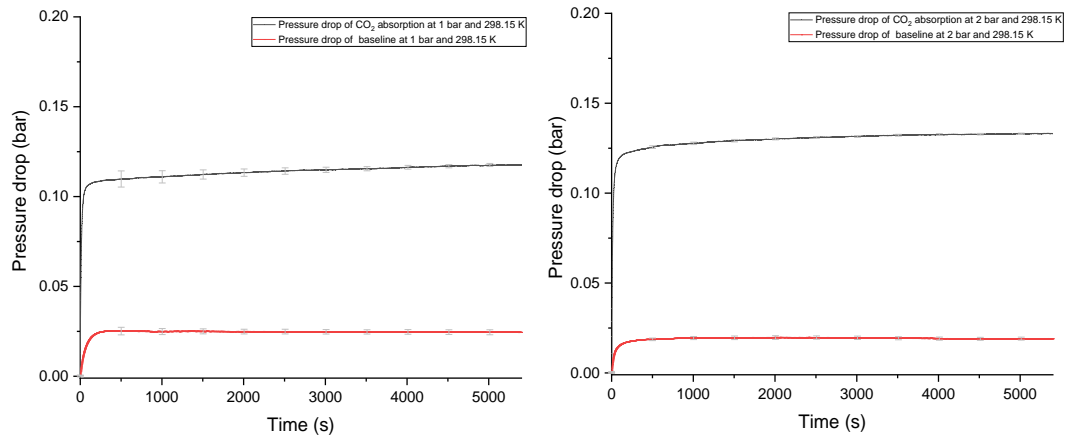


Figure B -13 Pressure drop values of the absolute pressure drop in the rig due to CO₂ absorption by ChCl:LvAc of (1:2:0) molar ratio at 25 °C and 250 rpm of the fifth cycle Vs. the pressure drop of the baselines

B.13 Selectivity measurements data

The VLE rig reaches equilibrium within 2 hours as shown in Figure B -13 below. The absolute pressure drop due to the CO₂/N₂ absorption only is the difference between the two isotherms pressure drop curves in Figure B - 13 below.



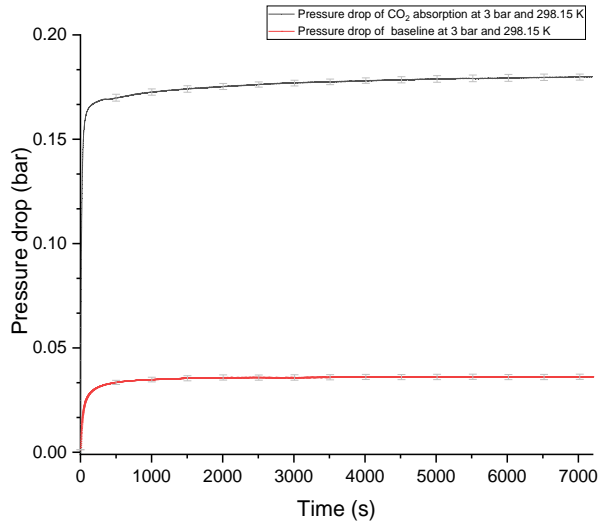
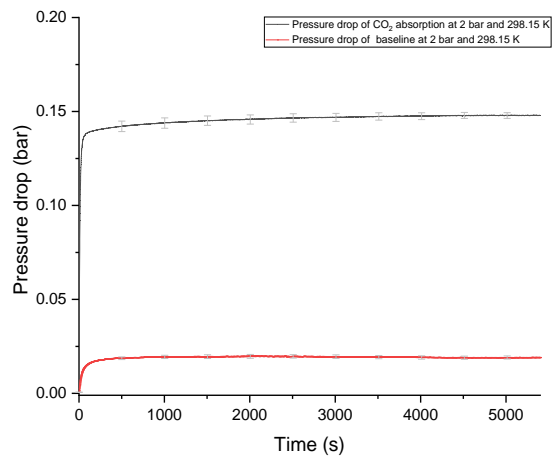
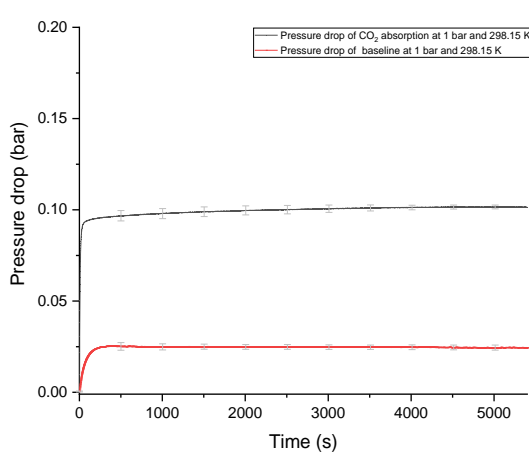


Figure B -14 CO₂ absorption raw data for tests carried out with a ChCl:LvAc DES with molar ratio (1:3:2.5) and a gas mixture with 100% CO₂ and 0% N₂, tests carried out at 25 °C and stirring speed of 250 rpm



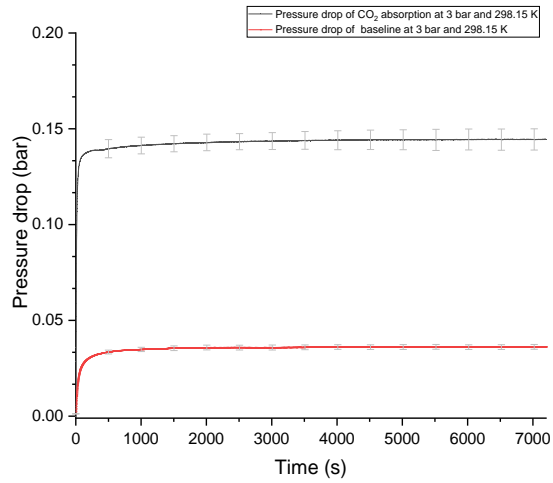
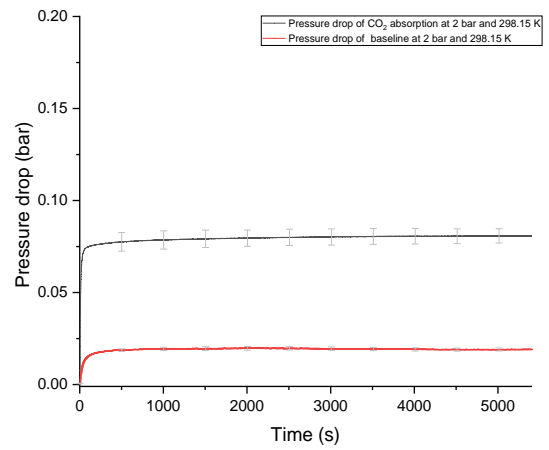
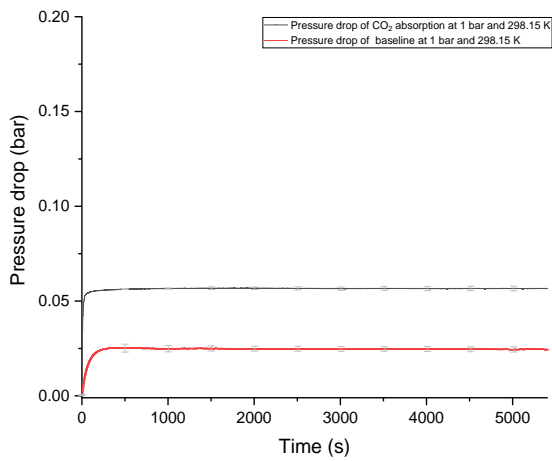


Figure B -15 CO₂ absorption raw data for tests carried out with a ChCl:LvAc DES with molar ratio (1:3:2.5) and a gas mixture with 50% CO₂ and 50% N₂ , tests carried out at 25 °C and stirring speed of 250



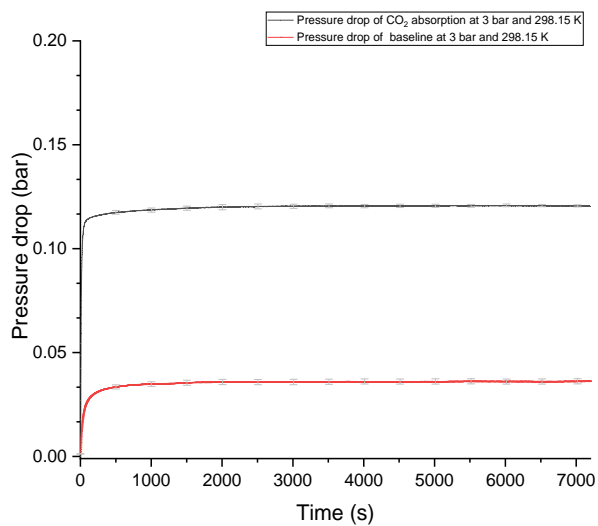


Figure B -16 CO₂ absorption raw data for tests carried out with ChCl:LvAc DES with molar ratio (1:3:2.5) and a gas mixture with 15% CO₂ and 85% N₂, tests carried out at 25 °C and stirring speed of 250 rpm

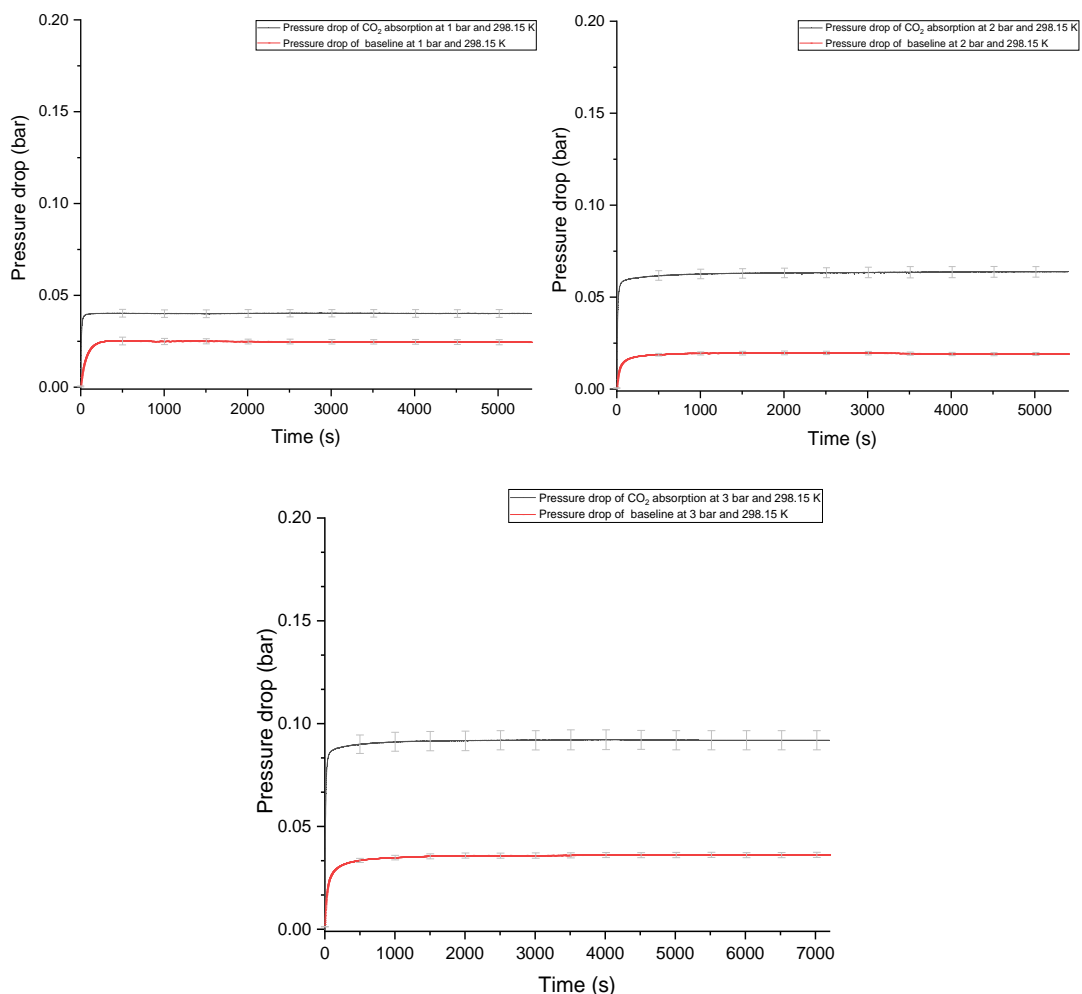


Figure B -17 CO₂ absorption raw data for tests carried out with a ChCl:LvAc DES with molar ratio (1:3:2.5) and a gas mixture with 0% CO₂ and 100% N₂, tests carried out at 25 °C and stirring speed of 250 rpm

B.14 References

- (1) IPCC. *Climate Change 2021: The Physical Science Basis - Summary for the Policymakers (Working Group I)*; 2021.
- (2) Oceanography SI. *The Scripps CO₂ measurements at Mauna Loa*. The Scripps CO₂ measurements at Mauna Loa. <https://scripps.ucsd.edu/programs/keelingcurve/>.
- (3) West, J. B. Joseph Black , Carbon Dioxide , Latent Heat , and the Beginnings of the Discovery of the Respiratory Gases. *Am. Physiol. Soc.* **2014**, 306, 1057–1063. <https://doi.org/10.1152/ajplung.00020.2014>.
- (4) Weibel, G. L.; Ober, C. K. A n Overview of Supercritical CO₂ Applications in Microelectronics Processing. **2003**, 65, 145–152.

- (5) Span, R.; Wagner, W. A New Equation of State for Carbon Dioxide Covering the Fluid Region from the Triple-Point Temperature to 1100 K at Pressures up to 800 MPa. *Lehrstuhl fur Thermodyn.* **1996**, 25 (6).
- (6) Sparavigna, A. C. Freezers , Dry Ice and Phase-Change Materials for Cold Chain Equipment in Ultra Low Temperature Logistics. **2021**, 1–7.
- (7) Ahangari, H.; King, J. W.; Ehsani, A.; Yousefi, M. Trends in Food Science & Technology Supercritical Fluid Extraction of Seed Oils – A Short Review of Current Trends. *Trends Food Sci. Technol.* **2021**, 111 (March), 249–260. <https://doi.org/10.1016/j.tifs.2021.02.066>.
- (8) Special Report on Carbon Capture Utilisation and Storage CCUS. Energy Technology Perspectives Energy Technology Perspectives. *IEA* **2020**.
- (9) Lenntech. *Properties of carbon dioxide*. <https://www.lenntech.com/carbon-dioxide.htm>.
- (10) Huang, J.; Mendoza, B.; Daniel, J. S.; Nielsen, C. J.; Rotstayn, L.; Wild, O. Anthropogenic and Natural Radiative Forcing. *Anthropog. Nat. Radiat. Forcing* **2013**.
- (11) Pincus, R.; Buehler, S. A.; Brath, M.; Crevoisier, C.; Jamil, O.; Evans, K. F.; Manners, J.; Menzel, R. L.; Mlawer, E. J. Benchmark Calculations of Radiative Forcing by Greenhouse Gases. *J. Geophys. Res. Atmos.* **2020**, 125 (e2020JD033483), 15. <https://doi.org/10.1029/2020JD033483>.
- (12) Arrhenius . Svante. On the Influence of Carbonic Acid in the Air upon the Temperature of the Ground. *London, Edinburgh, Dublin Philos. Mag. J. Sci.* **1896**, 120 (1–3), 27–42. <https://doi.org/10.1080/14786449608620846>.
- (13) Hulburt, E. O. The Temperature of the Lower Atmosphere of the Earth. *Phys. Rev.* **1931**, 38 (10), 1876–1890. <https://doi.org/10.1103/PhysRev.38.1876>.
- (14) WORLD ENERGY BALANCES 2020 EDITION. 2020 EDITION. *Int. Energy Agence.* **2020**.
- (15) International Energy Agency (IEA). World Energy Outlook 2022. **2022**, 1–524.
- (16) BP Statistical Review of World Energy 7 th edition Renewable energy. BP Statistical Review of World Energy. **2020**, 67 (7).
- (17) Friedlingstein, Pierre, O’Sullivan, Michael, Jones, Matthew W., Andrew, Robbie M., Hauck, Judith, Olsen, Are, Peters, Glen P., Peters, Wouter, Pongratz, Julia, Sitch, Stephen, Le Quéré, Corinne, Canadell, Josep G., Ciais, Philippe, Jackson, Robert B., Ali, S. Global Carbon Project. *Suppl. data Glob. Carbon Budg.* **2020**, 3269–3340 (12).
- (18) B.P. Statistical Review. BP Statistical Review of World Energy. *Rep. Stat. Rev. World Energy Glob. consistent data world energy Mark.* **2022**, 60.

- (19) Seneviratne, S. I.; Rogelj, J.; S  ferian, R.; Wartenburger, R.; Allen, M. R.; Cain, M.; Millar, R. J.; Ebi, K. L.; Ellis, N.; Hoegh-guldberg, O.; Payne, A. J.; Schleussner, C.; Agreement, P. The Many Possible Climates from the Paris Agreement's Aim of 1.5   C Warming. *Nature* **2018**, 1–9. <https://doi.org/10.1038/s41586-018-0181-4>.
- (20) Finkenrath, M. Carbon Dioxide Capture from Power Generation - Status of Cost and Performance. *Chem. Eng. Technol.* **2012**, 35 (3), 482–488. <https://doi.org/10.1002/ceat.201100444>.
- (21) Ra, A.; Rajab, K.; Milani, D.; Panahi, M. Journal of Environmental Chemical Engineering Trends in CO 2 Conversion and Utilization : A Review from Process Systems Perspective. **2018**, 6 (August), 5771–5794. <https://doi.org/10.1016/j.jece.2018.08.065>.
- (22) Hepburn, C.; Adlen, E.; Beddington, J.; Carter, E. A.; Fuss, S.; Mac Dowell, N.; Minx, J. C.; Smith, P.; Williams, C. K. The Technological and Economic Prospects for CO2 Utilization and Removal. *Nature* **2019**, 575 (7781), 87–97. <https://doi.org/10.1038/s41586-019-1681-6>.
- (23) Wilberforce, T.; Olabi, A. G.; Taha, E.; Elsaid, K.; Ali, M. Science of the Total Environment Progress in Carbon Capture Technologies. *Sci. Total Environ.* **2021**, 761, 143203. <https://doi.org/10.1016/j.scitotenv.2020.143203>.
- (24) Wilberforce, T.; Baroutaji, A.; Soudan, B.; Al-Alami, A. H.; Olabi, A. G. Outlook of Carbon Capture Technology and Challenges. *Sci. Total Environ.* **2019**, 657, 56–72. <https://doi.org/10.1016/j.scitotenv.2018.11.424>.
- (25) Global CCS institute. Global Status of CCS 2020. **2020**.
- (26) Zanco, S. E.; Jos, P.; Gas, A.; Cordiano, B.; Becattini, V.; Mazzotti, M. Postcombustion CO 2 Capture : A Comparative Techno-Economic Assessment of Three Technologies Using a Solvent , an Adsorbent , and a Membrane. *Am. Chem. Soc.* **2021**. <https://doi.org/10.1021/acseengineeringau.1c00002>.
- (27) Al-hamed, K. H. M.; Dincer, I. A Comparative Review of Potential Ammonia-Based Carbon Capture Systems. *J. Environ. Manage.* **2021**, 287 (March), 112357. <https://doi.org/10.1016/j.jenvman.2021.112357>.
- (28) Plaza, M. G.; Pevida, C. *Current Status of CO2 Capture from Coal Facilities*; Elsevier, 2018. <https://doi.org/10.1016/B978-0-08-102201-6.00002-9>.
- (29) Porter, R. T. J.; Fairweather, M.; Kolster, C.; Mac, N.; Shah, N.; Woolley, R. M. International Journal of Greenhouse Gas Control Cost and Performance of Some Carbon Capture Technology Options for Producing Different Quality CO 2 Product Streams. *Int. J. Greenh. Gas Control* **2017**, 57, 185–195. <https://doi.org/10.1016/j.ijggc.2016.11.020>.
- (30) Ishida, M.; Jin, H. A NEW ADVANCED POWER-GENERATION SYSTEM

USING CHEMICAL-LOOPING COMBUSTION. *Pergamon* **1994**, 19 (4), 415–422.

- (31) Saghafifar, M.; Gabra, S. A Critical Overview of Solar Assisted Carbon Capture Systems: Is Solar Always the Solution? *Int. J. Greenh. Gas Control* **2020**, 92 (October 2019), 102852. <https://doi.org/10.1016/j.ijggc.2019.102852>.
- (32) Hong, H.; Jin, H. A Novel Solar Thermal Cycle with Chemical Looping Combustion. *Int. J. Green Energy ISSN* **2005**, 5075. <https://doi.org/10.1080/01971520500288022>.
- (33) GLOBAL CCS INSTITUTE. CO₂ CAPTURE TECHNOLOGIES POST COMBUSTION CAPTURE (PCC). *Glob. CCS Inst.* **2012**, No. January.
- (34) Drage, T. C.; Snape, C. E.; Stevens, L. A.; Wood, J.; Wang, J.; Cooper, A. I.; Dawson, R.; Guo, X.; Satterley, C.; Irons, R. Materials Challenges for the Development of Solid Sorbents for Post-Combustion Carbon Capture. *J. Mater. Chem.* **2012**, 22 (7), 2815–2823. <https://doi.org/10.1039/c2jm12592g>.
- (35) Leeson, D.; Mac Dowell, N.; Shah, N.; Petit, C.; Fennell, P. S. A Techno-Economic Analysis and Systematic Review of Carbon Capture and Storage (CCS) Applied to the Iron and Steel, Cement, Oil Refining and Pulp and Paper Industries, as Well as Other High Purity Sources. *Int. J. Greenh. Gas Control* **2017**, 61, 71–84. <https://doi.org/10.1016/j.ijggc.2017.03.020>.
- (36) Sodiq, A.; Abdullatif, Y.; Aissa, B.; Ostovar, A.; Nassar, N.; El-Naas, M.; Amhamed, A. A Review on Progress Made in Direct Air Capture of CO₂. *Environ. Technol. Innov.* **2023**, 29, 102991. <https://doi.org/10.1016/j.eti.2022.102991>.
- (37) Custelcean, R. Direct Air Capture of CO₂ Using Solvents. *Ann. Rev.* **2022**.
- (38) Samari, M.; Ridha, F.; Manovic, V.; Macchi, A. Direct Capture of Carbon Dioxide from Air via Lime-Based Sorbents. *Mitig. Adapt. Strateg. Glob. Chang.* **2020**, 25–41.
- (39) McQueen, N.; Gomes, K. V.; McCormick, C.; Blumanthal, K.; Pisciotta, M.; Wilcox, J. A Review of Direct Air Capture (DAC): Scaling up Commercial Technologies and Innovating for the Future. *Prog. Energy* **2021**, 3 (3). <https://doi.org/10.1088/2516-1083/abf1ce>.
- (40) Young, J.; McQueen, N.; Charalambous, C.; Foteinis, S.; Hawrot, O.; Ojeda, M.; Pilorgé, H.; Andresen, J.; Psarras, P.; Renforth, P.; Garcia, S.; van der Spek, M. The Cost of Direct Air Capture and Storage Can Be Reduced via Strategic Deployment but Is Unlikely to Fall below Stated Cost Targets. *One Earth* **2023**, 6 (7), 899–917. <https://doi.org/10.1016/j.oneear.2023.06.004>.
- (41) Desport, L.; Gurgel, A.; Morris, J.; Herzog, H.; Chen, Y. H. H.; Selosse, S.; Paltsev, S. Deploying Direct Air Capture at Scale: How Close to Reality? *Energy Econ.* **2024**, 129 (December 2023), 107244.

<https://doi.org/10.1016/j.eneco.2023.107244>.

- (42) Kárászová, M.; Zach, B.; Petrusová, Z.; Bobák, M.; Michal, Š.; Izák, P. Separation and Purification Technology Post-Combustion Carbon Capture by Membrane Separation. *Sep. Purif. Technol.* **2020**, *238* (December 2019). <https://doi.org/10.1016/j.seppur.2019.116448>.
- (43) Ochedi, F. O.; Yu, J.; Yu, H.; Liu, Y.; Hussain, A. *Carbon Dioxide Capture Using Liquid Absorption Methods : A Review*; Springer International Publishing, 2021; Vol. 19. <https://doi.org/10.1007/s10311-020-01093-8>.
- (44) Yu, C.; Huang, C.; Tan, C. A Review of CO₂ Capture by Absorption and Adsorption. *Aerosol Air Qual. Res.* **2012**, *12*, 745–769. <https://doi.org/10.4209/aaqr.2012.05.0132>.
- (45) He, B.; Liu, J.; Zhang, Y.; Zhang, S.; Wang, P.; Xu, H. Separation and Purification Technology Comparison of Structured Activated Carbon and Traditional Adsorbents for Purification of H₂. *Sep. Purif. Technol.* **2020**, *239* (August 2019), 116529. <https://doi.org/10.1016/j.seppur.2020.116529>.
- (46) Theo, W. L.; Lim, J. S.; Hashim, H.; Mustaffa, A. A.; Ho, W. S. Review of Pre-Combustion Capture and Ionic Liquid in Carbon Capture and Storage. *Appl. Energy* **2016**, *183*, 1633–1663. <https://doi.org/10.1016/j.apenergy.2016.09.103>.
- (47) Songolzadeh, M.; Soleimani, M.; Ravanchi, M. T.; Songolzadeh, R. Carbon Dioxide Separation from Flue Gases : A Technological Review Emphasizing Reduction in Greenhouse Gas Emissions. **2014**, *2014* (Figure 1).
- (48) Sher, F.; Zafar, S.; Albazzaz, S.; Ali, U.; Andresa, D.; Rashid, T. Development of Biomass Derived Highly Porous Fast Adsorbents for Post- Combustion CO₂ Capture. *Fuel* **2020**, *282* (June), 118506. <https://doi.org/10.1016/j.fuel.2020.118506>.
- (49) Bedia, J.; Peñas-garz, M.; Almudena, G.; Rodriguez, J. J.; Belver, C. Review on Activated Carbons by Chemical Activation with FeCl₃. *J. Carbon Res. Rev.* **2020**, No. 1, 1–25.
- (50) Riboldi, L.; Bolland, O. Overview on Pressure Swing Adsorption (PSA) as CO₂ Capture Technology : State-of-the-Art , Limits and Potentials. *Energy Procedia* **2017**, *114* (1876), 2390–2400. <https://doi.org/10.1016/j.egypro.2017.03.1385>.
- (51) Wang, Y.; Levan, M. D. Adsorption Equilibrium of Carbon Dioxide and Water Vapor on Zeolites 5A and 13X and Silica Gel : Pure Components. *J. Chem. Eng. Data* **2009**, *54* (2009), 2839–2844.
- (52) Millward, A. R.; Yaghi, O. M. Metal - Organic Frameworks with Exceptionally High Capacity for Storage of Carbon Dioxide at Room Temperature. *JACS* **2005**, 17998–17999.

- (53) Lin, Y.; Kong, C.; Chen, L. Direct Synthesis of Amine-Functionalized MIL-101(Cr) Nanoparticles and Application for CO₂ Capture. *RSC Adv.* **2012**, *2* (16), 6417–6419. <https://doi.org/10.1039/c2ra20641b>.
- (54) Serra-Crespo, P.; Ramos-Fernandez, E. V.; Gascon, J.; Kapteijn, F. Synthesis and Characterization of an Amino Functionalized MIL-101(Al): Separation and Catalytic Properties. *Chem. Mater.* **2011**, *23* (10), 2565–2572. <https://doi.org/10.1021/cm103644b>.
- (55) Kumar, S.; Srivastava, R.; Koh, J. Utilization of Zeolites as CO₂ capturing Agents: Advances and Future Perspectives. *J. CO₂ Util.* **2020**, *41* (June), 101251. <https://doi.org/10.1016/j.jcou.2020.101251>.
- (56) Haoran Wei, S. D. Granular Bamboo-Derived Activated Carbon for High CO₂ Adsorption: The Dominant Role of Narrow Micropores. CHEMSUSCHEM 2012.
- (57) Vaidhyanathan, R.; Iremonger, S. S.; Dawson, K. W.; Shimizu, G. K. H. An Amine-Functionalized Metal Organic Framework for Preferential CO₂ Adsorption at Low Pressures. *Chem. Commun.* **2009**, No. 35, 5230–5232. <https://doi.org/10.1039/b911481e>.
- (58) Valizadeh, B.; Nguyen, T. N.; Stylianou, K. C. Shape Engineering of Metal–Organic Frameworks. *Polyhedron* **2018**, *145*, 1–15. <https://doi.org/10.1016/j.poly.2018.01.004>.
- (59) Mondal, M. K.; Balsora, H. K.; Varshney, P. Progress and Trends in CO₂ Capture / Separation Technologies : A Review. *Energy* **2012**, *46* (1), 431–441. <https://doi.org/10.1016/j.energy.2012.08.006>.
- (60) Burt, S.; Baxter, A.; Baxter, L. Cryogenic CO₂ Capture to Control Climate Change Emissions. In *The 34th International Technical Conference on Clean Coal & Fuel Systems*; 2009.
- (61) Press, C. U. *IPCC Special Report on Carbon Dioxide Capture and Storage*; Cambridge University Press, 2005.
- (62) Leung, D. Y. C.; Caramanna, G.; Maroto-valer, M. M. An Overview of Current Status of Carbon Dioxide Capture and Storage Technologies. *Renew. Sustain. Energy Rev.* **2014**, *39*, 426–443. <https://doi.org/10.1016/j.rser.2014.07.093>.
- (63) Gao, L. A Novel Coal-Based Hydrogen Production System With Low CO₂. *J. Eng. Gas Turbines Power* **2010**, *132* (March), 1–9. <https://doi.org/10.1115/1.3159369>.
- (64) Xu, G.; Liang, F.; Yang, Y.; Hu, Y.; Zhang, K.; Liu, W. An Improved CO₂ Separation and Purification System Based on Cryogenic Separation and Distillation Theory. *energies MDPI* **2014**, *7*, 3484–3502. <https://doi.org/10.3390/en7053484>.

- (65) Tuinier, M. J.; Hamers, H. P.; Annaland, M. V. S. Techno-Economic Evaluation of Cryogenic CO₂ Capture — A Comparison with Absorption and Membrane Technology. *Int. J. Greenh. Gas Control* **2011**, *5*, 1559–1565. <https://doi.org/10.1016/j.ijggc.2011.08.013>.
- (66) Zhao, M. Membrane Separation Technology in Carbon Capture. In *Membrane Separation Technology in Carbon Capture*; 2017; p 34. <https://doi.org/10.5772/65723>.
- (67) Sullivan, J. M. Carbon Capture in Vehicles : A Review of General Support , Available MECHANISMS, AND CONSUMER-ACCEPTANCE ISSUES. *Univ. Michigan Transp. Res. Inst. Ann Arbor, Michigan 48109-2150* **2015**, No. January.
- (68) Fu, Y.; Jiang, Y. B.; Dunphy, D.; Xiong, H.; Coker, E.; Chou, S.; Zhang, H.; Vanegas, J. M.; Croissant, J. G.; Cecchi, J. L.; Rempe, S. B.; Brinker, C. J. Ultra-Thin Enzymatic Liquid Membrane for CO₂ Separation and Capture. *Nat. Commun.* **2018**, *9* (1), 1–12. <https://doi.org/10.1038/s41467-018-03285-x>.
- (69) Böcking, A.; Koleva, V.; Wind, J.; Thiermeyer, Y.; Blumenschein, S.; Goebel, R.; Skiborowski, M.; Wessling, M. Can the Variance in Membrane Performance Influence the Design of Organic Solvent Nanofiltration Processes? *J. Memb. Sci.* **2019**, *575* (August 2018), 217–228. <https://doi.org/10.1016/j.memsci.2018.12.077>.
- (70) Magueijo, V. M.; Anderson, L. G.; Fletcher, A. J.; Shilton, S. J. Polysulfone Mixed Matrix Gas Separation Hollow Fibre Membranes Filled with Polymer and Carbon Xerogels. *Chem. Eng. Sci.* **2013**, *92*, 13–20. <https://doi.org/10.1016/j.ces.2013.01.043>.
- (71) Khalilpour, R.; Mumford, K.; Zhai, H.; Abbas, A.; Stevens, G.; Rubin, E. S. Membrane-Based Carbon Capture from Flue Gas : A Review. *J. Clean. Prod.* **2015**, *103*, 286–300. <https://doi.org/10.1016/j.jclepro.2014.10.050>.
- (72) Moradi, M. R.; Pihlajamäki, A.; Hesampour, M.; Ahlgren, J.; Mänttari, M. End-of-Life RO Membranes Recycling: Reuse as NF Membranes by Polyelectrolyte Layer-by-Layer Deposition. *J. Memb. Sci.* **2019**, *584* (March), 300–308. <https://doi.org/10.1016/j.memsci.2019.04.060>.
- (73) Lawler, W.; Alvarez-Gaitan, J.; Leslie, G.; Le-Clech, P. Comparative Life Cycle Assessment of End-of-Life Options for Reverse Osmosis Membranes. *Desalination* **2015**, *357*, 45–54. <https://doi.org/10.1016/j.desal.2014.10.013>.
- (74) Wang, M.; Wang, Z.; Zhao, S.; Wang, J.; Wang, S. Chinese Journal of Chemical Engineering Recent Advances on Mixed Matrix Membranes for CO₂ Separation ☆. *Chinese J. of Chemical Eng.* **2017**, *25*, 1581–1597.
- (75) Das, S.; Das, S.; Das, I.; Ghangrekar, M. M. Application of Bioelectrochemical Systems for Carbon Dioxide Sequestration and Concomitant Valuable Recovery: A Review. *Mater. Sci. Energy Technol.* **2019**, *2* (3), 687–696.

<https://doi.org/10.1016/j.mset.2019.08.003>.

- (76) Kassim, M. A.; Meng, T. K. Carbon Dioxide Bio Fixation by Microalgae and Its Potential for Bioremediation and Biofuel Production. *Sci. Total Environ.* **2017**, *585*, 1121–1129. <https://doi.org/10.1016/j.scitotenv.2017.01.172>.
- (77) Zhang, S.; Jiang, J.; Wang, H.; Li, F.; Hua, T. A Review of Microbial Electrosynthesis Applied to Carbon Dioxide Capture and Conversion: The Basic Principles, Electrode Materials, and Bioproducts. *J. CO₂ Util.* **2021**, *51* (June), 101640. <https://doi.org/10.1016/j.jcou.2021.101640>.
- (78) Halim, R.; Gladman, B.; Danquah, M. K.; Webley, P. A. Oil Extraction from Microalgae for Biodiesel Production. *Bioresour. Technol.* **2011**, *102* (1), 178–185. <https://doi.org/10.1016/j.biortech.2010.06.136>.
- (79) Zeng, X.; Danquah, M. K.; Zhang, S.; Zhang, X.; Wu, M.; Dong, X.; Ng, I.; Jing, K.; Lu, Y. Autotrophic Cultivation of *Spirulina Platensis* for CO₂ Fixation and Phycocyanin Production. *Chem. Eng. J.* **2012**, *183*, 192–197. <https://doi.org/10.1016/j.cej.2011.12.062>.
- (80) Lu, L.; Huang, Z.; Rau, G. H.; Ren, Z. J. Microbial Electrolytic Carbon Capture for Carbon Negative and Energy Positive Wastewater Treatment. *Am. Chem. Soc.* **2015**, *8193–8201* (49). <https://doi.org/10.1021/acs.est.5b00875>.
- (81) Neethu, B.; Bhowmick, G. D.; Ghangrekar, M. M. Enhancement of Bioelectricity Generation and Algal Productivity in Microbial Carbon-Capture Cell Using Low Cost Coconut Shell as Membrane Separator. *Biochem. Eng. J.* **2018**, *133*, 205–213. <https://doi.org/10.1016/j.bej.2018.02.014>.
- (82) Bui, M.; Gunawan, I.; Verheyen, V.; Artanto, Y.; Meuleman, E. Dynamic Modeling and Validation of Post-Combustion CO₂ Capture Plants in Australian Coal-Fired Power Stations. *Energy Procedia* **2013**, *37*, 2694–2702. <https://doi.org/10.1016/j.egypro.2013.06.154>.
- (83) Bishnoi, S.; Rochelle, G. T. Absorption of Carbon Dioxide into Aqueous Piperazine: Reaction Kinetics, Mass Transfer and Solubility. *Chem. Eng. Sci.* **2000**, *55*.
- (84) Mirzaei, S.; Shamiri, A.; Aroua, M. K. CO₂ absorption/Desorption in Aqueous Single and Novel Hybrid Solvents of Glycerol and Monoethanolamine in a Pilot-Scale Packed Bed Column. *Energy and Fuels* **2020**, *34* (7), 8503–8515. <https://doi.org/10.1021/acs.energyfuels.8b04389>.
- (85) Huertas, J. I.; Gomez, M. D.; Giraldo, N.; Garzón, J. CO₂ Absorbing Capacity of MEA. *J. Chem.* **2015**, *2015* (2). <https://doi.org/10.1155/2015/965015>.
- (86) Jou, F.; Mather, A. E.; Otto, F. D. The Solubility of CO₂ in a 30 Mass Percent MEA Solution. *Can. J. CHEM. ENG. VOL. 73 1995* **1995**, *73*.
- (87) Karimi, M.; Hillestad, M.; Svendsen, H. F. Capital Costs and Energy

Considerations of Different Alternative Stripper Configurations for Post Combustion CO₂ Capture. *Chem. Eng. Res. Des.* **2011**, 89 (8), 1229–1236. <https://doi.org/10.1016/j.cherd.2011.03.005>.

- (88) Caplow, M. Kinetics of Carbamate Formation and Breakdown. *J. Am. Chem. Soc.* **1968**, 1968 (5), 6795–6803.
- (89) Crooks, J. E.; Donnellan, J. P. Kinetics and Mechanism of the Reaction between Carbon Dioxide and Amines in Aqueous Solution. *J. Chem. Soc.* **1989**, 2 (331–333), 2–4.
- (90) Silva, E. F.; Svendsen, H. F. Ab Initio Study of the Reaction of Carbamate Formation from CO₂ and Alkanolamines. *Ind. Eng. Chem. Res.* **2004**, 13 (43), 3413–3418.
- (91) Said, R. Ben; Kolle, J. M.; Essalah, K.; Tangour, B.; Sayari, A. A Unified Approach to CO₂ – Amine Reaction Mechanisms. *Am. Chem. Soc.* **2020**, 5 (26125–26144). <https://doi.org/10.1021/acsomega.0c03727>.
- (92) Voldsund, M.; Gardarsdottir, S. O.; Lena, E. De; Jos, P.; Jamali, A.; Berstad, D.; Fu, C.; Romano, M.; Roussanaly, S.; Anantharaman, R.; Hoppe, H.; Sutter, D.; Mazzotti, M.; Gazzani, M.; Cinti, G.; Jordal, K. Comparison of Technologies for CO₂ Capture from Cement Production — Part 1: Technical Evaluation. *energies MDPI* **2019**, 12 (559). <https://doi.org/10.3390/en12030559>.
- (93) Li, X.; Zhou, X.; Wei, J.; Fan, Y.; Liao, L.; Wang, H. Reducing the Energy Penalty and Corrosion of Carbon Dioxide Capture Using a Novel Nonaqueous Monoethanolamine-Based Biphasic Solvent. *Sep. Purif. Technol.* **2021**, 265 (February), 118481. <https://doi.org/10.1016/j.seppur.2021.118481>.
- (94) Li, W.; Landon, J.; Irvin, B.; Zheng, L.; Ruh, K.; Kong, L.; Pelgen, J.; Link, D.; Figueroa, J. D.; Thompson, J.; Nikolic, H.; Liu, K. Use of Carbon Steel for Construction of Post-Combustion CO₂ Capture Facilities: A Pilot-Scale Corrosion Study. *Ind. Eng. Chem. Res.* **2017**, 56 (16), 4792–4803. <https://doi.org/10.1021/acs.iecr.7b00697>.
- (95) Gouedard, C.; Picq, D.; Launay, F.; Carrette, P. International Journal of Greenhouse Gas Control Amine Degradation in CO₂ Capture . I . A Review. *Int. J. Greenh. Gas Control* **2012**, 10, 244–270. <https://doi.org/10.1016/j.ijggc.2012.06.015>.
- (96) Saeed, I. M.; Lee, V. S.; Mazari, S. A.; Ali, B. S.; Basirun, W. J.; Asghar, A.; Ghalib, L.; Jan, B. M. Thermal Degradation of Aqueous 2 - Aminoethylethanolamine in CO₂ Capture ; Identification of Degradation Products , Reaction Mechanisms and Computational Studies. *Chem. Cent. J.* **2017**, 1–12. <https://doi.org/10.1186/s13065-016-0231-7>.
- (97) Sexton, A. J.; Rochelle, G. T. Reaction Products from the Oxidative Degradation of Monoethanolamine. *Ind. Eng. Chem. Res.* **2011**, 50, 667–673.

- (98) Davis, J.; Rochelle, G. Energy Procedia Thermal Degradation of Monoethanolamine at Stripper Conditions. *Energy Procedia* **2009**, 1 (1), 327–333. <https://doi.org/10.1016/j.egypro.2009.01.045>.
- (99) Mohamed, I.; Alaba, P.; Ali, S.; Jeffrey, W.; Sanghiran, V.; Sabzoi, N. Opportunities and Challenges in the Development of Monoethanolamine and Its Blends for Post-Combustion CO₂ Capture. *Int. J. Greenh. Gas Control* **2018**, 79 (May), 212–233. <https://doi.org/10.1016/j.ijggc.2018.11.002>.
- (100) Pathamaporn Wattanaphan. STUDIES AND PREVENTION OF CARBON STEEL CORROSION AND SOLVENT DEGRADATION DURING AMINE-BASED CO₂ CAPTURE FROM INDUSTRIAL GAS STREAMS, 2012.
- (101) Borhani, T. N. G.; Azarpour, A.; Akbari, V.; Wan Alwi, S. R.; Manan, Z. A. CO₂ Capture with Potassium Carbonate Solutions: A State-of-the-Art Review. *Int. J. Greenh. Gas Control* **2015**, 41, 142–162. <https://doi.org/10.1016/j.ijggc.2015.06.026>.
- (102) Benson, H E; Field, J H; Jameson, R. M. CO₂ Absorption: Employing Hot Potassium Carbonate Solutions. *Chem. Eng. Prog.* **1954**, 50 (1).
- (103) Hu, G.; Nicholas, N. J.; Smith, K. H.; Mumford, K. A.; Kentish, S. E.; Stevens, G. W. Carbon Dioxide Absorption into Promoted Potassium Carbonate Solutions: A Review. *Int. J. Greenh. Gas Control* **2016**, 53, 28–40. <https://doi.org/10.1016/j.ijggc.2016.07.020>.
- (104) Rahimpour, M. R.; Kashkooli, A. Z. Enhanced Carbon Dioxide Removal by Promoted Hot Potassium Carbonate in a Split-Flow Absorber. *Chem. Eng. Process. Process Intensif.* **2004**, 43 (7), 857–865. [https://doi.org/10.1016/S0255-2701\(03\)00106-5](https://doi.org/10.1016/S0255-2701(03)00106-5).
- (105) Smith, K. H.; Anderson, C. J.; Tao, W.; Endo, K.; Mumford, K. A.; Kentish, S. E.; Qader, A.; Hooper, B.; Stevens, G. W. Pre-Combustion Capture of CO₂-Results from Solvent Absorption Pilot Plant Trials Using 30wt% Potassium Carbonate and Boric Acid Promoted Potassium Carbonate Solvent. *Int. J. Greenh. Gas Control* **2012**, 10, 64–73. <https://doi.org/10.1016/j.ijggc.2012.05.018>.
- (106) Fosbøl, P. L.; Maribo-Mogensen, B.; Thomsen, K. Solids Modelling and Capture Simulation of Piperazine in Potassium Solvents. *Energy Procedia* **2013**, 37, 844–859. <https://doi.org/10.1016/j.egypro.2013.05.177>.
- (107) Jansen, D.; Gazzani, M.; Manzolini, G.; Dijk, E. Van. International Journal of Greenhouse Gas Control Pre-Combustion CO₂ Capture. *Int. J. Greenh. Gas Control* **2015**, 40, 167–187. <https://doi.org/10.1016/j.ijggc.2015.05.028>.
- (108) Burr, Barry and Lyddon, L. A COMPARISON OF PHYSICAL SOLVENTS FOR ACID GAS REMOVAL Barry Burr and Lili Lyddon Bryan Research & Engineering, Inc. Bryan, Texas, U.S.A. *Bryan Res. Eng.* **2008**, 87.

- (109) Aidid, F. Optimization of Amine Base CO₂ Removal Process i REMOVAL OF CARBON DIOXIDE FROM NATURAL GAS FOR LNG PRODUCTION ... *Inst. Pet. Technol. Nor. Univ. Sci. Technol.* **2005**, December.
- (110) Austen Angell, C.; Ansari, Y.; Zhao, Z. Ionic Liquids: Past, Present and Future. *Faraday Discuss.* **2012**, *154* (1), 9–27. <https://doi.org/10.1039/c1fd00112d>.
- (111) American Chemical Society. Ionic Liquids. *Acc. Chem. Res.* **2007**, *40* (11), 1077.
- (112) Gao, J.; Cao, L.; Dong, H.; Zhang, X.; Zhang, S. Ionic Liquids Tailored Amine Aqueous Solution for Pre-Combustion CO₂ Capture: Role of Imidazolium-Based Ionic Liquids. *Appl. Energy* **2015**, *154*, 771–780. <https://doi.org/10.1016/j.apenergy.2015.05.073>.
- (113) Blanchard, L. A.; Hancu, D. Green Processing Using Ionic Liquids and CO₂. *Nature* **1999**, *399* (May), 28–29.
- (114) Baltus, R. E.; Counce, R. M.; Culbertson, B. H.; Luo, H.; DePaoli, D. W.; Dai, S.; Duckworth, D. C. Examination of the Potential of Ionic Liquids for Gas Separations. *Sep. Sci. Technol.* **2005**, *40* (1–3), 525–541. <https://doi.org/10.1081/SS-200042513>.
- (115) Bates, E. D.; Mayton, R. D.; Ntai, I.; Davis, J. H. CO₂ capture by a Task-Specific Ionic Liquid. *J. Am. Chem. Soc.* **2002**, *124* (6), 926–927. <https://doi.org/10.1021/ja017593d>.
- (116) Anderson, J. L.; Dixon, J. K.; Brennecke, J. F. Solubility of CO₂, CH₄, C₂H₆, Bis (Trifluoromethylsulfonyl) Imide: Comparison to Other Ionic Liquids. **2008**, *40* (11), 1208–1216.
- (117) Bara, J. E.; Carlisle, T. K.; Gabriel, C. J.; Camper, D.; Finotello, A.; Gin, D. L.; Noble, R. D. Guide to CO₂ Separations in Imidazolium-Based Room-Temperature Ionic Liquids. *Ind. Eng. Chem. Res.* **2009**, *48* (6), 2739–2751. <https://doi.org/10.1021/ie8016237>.
- (118) Hasib-ur-Rahman, M.; Siaj, M.; Larachi, F. Ionic Liquids for CO₂ capture-Development and Progress. *Chem. Eng. Process. Process Intensif.* **2010**, *49* (4), 313–322. <https://doi.org/10.1016/j.cep.2010.03.008>.
- (119) Mirza, N. R.; Nicholas, N. J.; Wu, Y.; Mumford, K. A.; Kentish, S. E.; Stevens, G. W. Experiments and Thermodynamic Modeling of the Solubility of Carbon Dioxide in Three Different Deep Eutectic Solvents (DESs). *J. Chem. Eng. Data* **2015**, *60* (11), 3246–3252. <https://doi.org/10.1021/acs.jced.5b00492>.
- (120) Ramdin, M.; De Loos, T. W.; Vlucht, T. J. H. State-of-the-Art of CO₂ capture with Ionic Liquids. *Ind. Eng. Chem. Res.* **2012**, *51* (24), 8149–8177. <https://doi.org/10.1021/ie3003705>.
- (121) Yuan, S.; Chen, Y.; Ji, X.; Yang, Z.; Lu, X. Experimental Study of CO₂

Absorption in Aqueous Cholinium-Based Ionic Liquids. *Fluid Phase Equilib.* **2017**, *445*, 14–24. <https://doi.org/10.1016/j.fluid.2017.04.001>.

- (122) Lv, B.; Xia, Y.; Shi, Y.; Liu, N.; Li, W.; Li, S. A Novel Hydrophilic Amino Acid Ionic Liquid [C2 OHmim][Gly] as Aqueous Sorbent for CO₂ Capture. *Int. J. Greenh. Gas Control* **2016**, *46*, 1–6. <https://doi.org/10.1016/j.ijggc.2015.12.029>.
- (123) Zhang, J.; Yu, L.; Gong, R.; Li, M.; Ren, H.; Duan, E. Role of Hydrophilic Ammonium-Based Deep Eutectic Solvents in SO₂ Absorption. *ACS Energy Fuels* **2020**, *34*, 74–81. <https://doi.org/10.1021/acs.energyfuels.9b02194>.
- (124) Navarro, P.; García, J.; Rodríguez, F.; Carvalho, P. J.; Coutinho, J. A. P. Impact of Water on the [C4 C1 Im][Ac] Ability for the CO₂/ CH₄ Separation. *J. CO₂ Util.* **2019**, *31* (February), 115–123. <https://doi.org/10.1016/j.jcou.2019.02.021>.
- (125) Ma, T.; Wang, J.; Du, Z.; Abdeltawab, A. A.; Al-enizi, A. M.; Chen, X.; Yu, G. A Process Simulation Study of CO₂ Capture by Ionic Liquids. *Int. J. Greenh. Gas Control* **2017**, *58*, 223–231. <https://doi.org/10.1016/j.ijggc.2017.01.017>.
- (126) Lian, S.; Song, C.; Liu, Q.; Duan, E.; Ren, H.; Kitamura, Y. Recent Advances in Ionic Liquids-Based Hybrid Processes for CO₂ Capture and Utilization. *J. Environ. Sci.* **2021**, *99*, 281–295. <https://doi.org/10.1016/j.jes.2020.06.034>.
- (127) Ma, C.; Sarmad, S.; Mikkola, J. P.; Ji, X. Development of Low-Cost Deep Eutectic Solvents for CO₂ Capture. *Energy Procedia* **2017**, *142*, 3320–3325. <https://doi.org/10.1016/j.egypro.2017.12.464>.
- (128) Martins, M. A. R.; Pinho, S. P.; Coutinho, J. A. P. Insights into the Nature of Eutectic and Deep Eutectic Mixtures. *J. Solution Chem.* **2019**, *48* (7), 962–982. <https://doi.org/10.1007/s10953-018-0793-1>.
- (129) Tomé, L. I. N.; Baião, V.; da Silva, W.; Brett, C. M. A. Deep Eutectic Solvents for the Production and Application of New Materials. *Appl. Mater. Today* **2018**, *10*, 30–50. <https://doi.org/10.1016/j.apmt.2017.11.005>.
- (130) Chemat, F.; Anjum, H.; Shariff, A.; Kumar, P.; Murugesan, T. Thermal and Physical Properties of (Choline Chloride + Urea + L -Arginine) Deep Eutectic Solvents. *J. Mol. Liq.* **2016**, *218*, 301–308. <https://doi.org/10.1016/j.molliq.2016.02.062>.
- (131) Kroon, M. C.; Francisco, M.; Bruinhorst, A. Van Den; Kroon, M. C. Low-Transition-Temperature Mixtures (LTTMs): A New Generation of Designer Solvents. **2013**, *2012* (October 2012), 3074–3085. <https://doi.org/10.1002/anie.201207548>.
- (132) Abbott, A. P.; Boothby, D.; Capper, G.; Davies, D. L.; Rasheed, R. K. Deep Eutectic Solvents Formed between Choline Chloride and Carboxylic Acids: Versatile Alternatives to Ionic Liquids. *J. Am. Chem. Soc.* **2004**, *126* (29), 9142–9147. <https://doi.org/10.1021/ja048266j>.

- (133) Trivedi, T. J.; Lee, J. H.; Lee, H. J.; Jeong, Y. K.; Choi, J. W. Deep Eutectic Solvents as Attractive Media for CO₂capture. *Green Chem.* **2016**, *18* (9), 2834–2842. <https://doi.org/10.1039/c5gc02319j>.
- (134) Sze, L. L.; Pandey, S.; Ravula, S.; Pandey, S.; Zhao, H.; Baker, G. A.; Baker, S. N. Ternary Deep Eutectic Solvents Tasked for Carbon Dioxide Capture. *ACS Sustain. Chem. Eng.* **2014**, *2* (9), 2117–2123. <https://doi.org/10.1021/sc5001594>.
- (135) Paiva, A.; Craveiro, R.; Aroso, I.; Martins, M.; Reis, R. L.; Duarte, A. R. C. Natural Deep Eutectic Solvents - Solvents for the 21st Century. *ACS Sustain. Chem. Eng.* **2014**, *2* (5), 1063–1071. <https://doi.org/10.1021/sc500096j>.
- (136) Ullah, R.; Atilhan, M.; Anaya, B.; Khraisheh, M.; García, G.; Elkhattat, A.; Tariq, M.; Aparicio, S. A Detailed Study of Cholinium Chloride and Levulinic Acid Deep Eutectic Solvent System for CO₂capture via Experimental and Molecular Simulation Approaches. *Phys. Chem. Chem. Phys.* **2015**, *17* (32), 20941–20960. <https://doi.org/10.1039/c5cp03364k>.
- (137) Kozlovasky, R. A.; Shvets, V. F.; Makarov, M. G. Technical Notes A Kinetic Model of the Choline Chloride Synthesis Abstract: *Org. Process Res. Dev.* **1999**, *3* (5), 357–362.
- (138) Yao, L.; Qiu, Y.; Zhao, Y.; Tang, C.; Shen, J. Separation and Purification Technology A Continuous Mode Operation of Bipolar Membrane Electrodialysis (BMED) for the Production of High-Pure Choline Hydroxide from Choline Chloride. *Sep. Purif. Technol.* **2020**, *233* (July 2019), 116054. <https://doi.org/10.1016/j.seppur.2019.116054>.
- (139) Hayyan, M.; Hashim, M. A.; Hayyan, A.; Al-Saadi, M. A.; AlNashef, I. M.; Mirghani, M. E. S.; Saheed, O. K. Are Deep Eutectic Solvents Benign or Toxic? *Chemosphere* **2013**, *90* (7), 2193–2195. <https://doi.org/10.1016/j.chemosphere.2012.11.004>.
- (140) Zhang, Y.; Ji, X.; Lu, X. Choline-Based Deep Eutectic Solvents for CO₂separation: Review and Thermodynamic Analysis. *Renew. Sustain. Energy Rev.* **2018**, *97* (July), 436–455. <https://doi.org/10.1016/j.rser.2018.08.007>.
- (141) Nhien, L. C.; Long, N. V. D.; Lee, M. Chemical Engineering Research and Design Design and Optimization of the Levulinic Acid Recovery Process from Lignocellulosic Biomass. *Chem. Eng. Res. Des.* **2020**, *107*, 126–136. <https://doi.org/10.1016/j.cherd.2015.09.013>.
- (142) Jeong, G. Production of Levulinic Acid from Glucosamine by Dilute-Acid Catalyzed Hydrothermal Process. *Ind. Crop. Prod.* **2014**, *62*, 77–83. <https://doi.org/10.1016/j.indcrop.2014.08.006>.
- (143) Foorginezhad, S.; Yu, G.; Ji, X. Reviewing and Screening Ionic Liquids and Deep Eutectic Solvents for Effective CO₂ Capture. *Front. Chem.* **2022**, *10*

(August). <https://doi.org/10.3389/fchem.2022.951951>.

- (144) Isaifan, R. J.; Amhamed, A. Review on Carbon Dioxide Absorption by Choline Chloride/Urea Deep Eutectic Solvents. *Adv. Chem.* **2018**, 2018. <https://doi.org/10.1155/2018/2675659>.
- (145) SDD. *Science Direct Database*. [https://www.sciencedirect.com/search?date=2004-2022&qs=deep eutectic solvents carbon capture&lastSelectedFacet=years&years=2014%2C2022](https://www.sciencedirect.com/search?date=2004-2022&qs=deep+eutectic+solvents+carbon+capture&lastSelectedFacet=years&years=2014%2C2022) (accessed 2023-02-06).
- (146) Mota-Martinez, M. T.; Hallett, J. P.; Mac Dowell, N. Solvent Selection and Design for CO₂ Capture – How We Might Have Been Missing the Point. *Sustain. Energy Fuels* **2017**. <https://doi.org/10.1039/C7SE00404D>.
- (147) Abbott, A. P.; Capper, G.; Davies, D. L.; Rasheed, R. K.; Tambyrajah, V. Novel Solvent Properties of Choline Chloride Urea Mixtures_Supplementaryinfo. **2003**, No. October 2002, 70–71.
- (148) Achkar, T. El; Greige, H.; Sophie, G. Basics and Properties of Deep Eutectic Solvents: A Review. *Environ. Chem. Lett.* **2021**, No. 0123456789. <https://doi.org/10.1007/s10311-021-01225-8>.
- (149) Andrew P. Abbott, John C. Barron, Karl S. Ryder, and D. W. Eutectic-Based Ionic Liquids with Metal-Containing Anions and Cations. 2007.
- (150) Choi, Y. H.; van Spronsen, J.; Dai, Y.; Verberne, M.; Hollmann, F.; Arends, I. W. C. E.; Witkamp, G. J.; Verpoorte, R. Are Natural Deep Eutectic Solvents the Missing Link in Understanding Cellular Metabolism and Physiology? *Plant Physiol.* **2011**, 156 (4), 1701–1705. <https://doi.org/10.1104/pp.111.178426>.
- (151) El Achkar, T.; Moufawad, T.; Ruellan, S.; Landy, D.; Greige-Gerges, H.; Fourmentin, S. Cyclodextrins: From Solute to Solvent. *Chem. Commun.* **2020**, 56 (23), 3385–3388. <https://doi.org/10.1039/d0cc00460j>.
- (152) Martins, M. A. R.; Pinho, S. P.; Coutinho, J. A. P. Insights into the Nature of Eutectic and Deep Eutectic Mixtures. *J. Solution Chem.* **2019**, 48 (7), 962–982. <https://doi.org/10.1007/s10953-018-0793-1>.
- (153) Medicine, U. S. N. L. of; Information, N. C. for B. U.S. National Library of Medicine. **2018**.
- (154) Florindo, C.; Oliveira, F. S.; Rebelo, L. P. N.; Fernandes, A. M.; Marrucho, I. M. Insights into the Synthesis and Properties of Deep Eutectic Solvents Based on Cholinium Chloride and Carboxylic Acids. *ACS Sustain. Chem. Eng.* **2014**, 2 (10), 2416–2425. <https://doi.org/10.1021/sc500439w>.
- (155) Leron, R. B.; Li, M. H. Solubility of Carbon Dioxide in a Choline Chloride-Ethylene Glycol Based Deep Eutectic Solvent. *Thermochim. Acta* **2013**, 551, 14–19. <https://doi.org/10.1016/j.tca.2012.09.041>.

- (156) Ren, H.; Lian, S.; Wang, X.; Zhang, Y.; Duan, E. Exploiting the Hydrophilic Role of Natural Deep Eutectic Solvents for Greening CO₂capture. *J. Clean. Prod.* **2018**, *193*, 802–810. <https://doi.org/10.1016/j.jclepro.2018.05.051>.
- (157) Hayyan, A.; Hashim, M. A.; Hayyan, M.; Mjalli, F. S.; Alnashef, I. M. A New Processing Route for Cleaner Production of Biodiesel Fuel Using a Choline Chloride Based Deep Eutectic Solvent. *J. Clean. Prod.* **2014**, *65*, 246–251. <https://doi.org/10.1016/j.jclepro.2013.08.031>.
- (158) Cao, L.; Huang, J.; Zhang, X.; Zhang, S.; Gao, J.; Zeng, S. Imidazole Tailored Deep Eutectic Solvents for CO₂capture Enhanced by Hydrogen Bonds. *Phys. Chem. Chem. Phys.* **2015**, *17* (41), 27306–27316. <https://doi.org/10.1039/c5cp04050g>.
- (159) Trivedi, T. J.; Lee, J. H.; Lee, H. J.; Jeong, Y. K.; Choi, J. W. Deep Eutectic Solvents as Attractive Media for CO₂capture. *Green Chem.* **2016**, *18* (9), 2834–2842. <https://doi.org/10.1039/c5gc02319j>.
- (160) Ghaedi, H.; Ayoub, M.; Sufian, S.; Murshid, G.; Farrukh, S.; Shariff, A. M. Investigation of Various Process Parameters on the Solubility of Carbon Dioxide in Phosphonium-Based Deep Eutectic Solvents and Their Aqueous Mixtures: Experimental and Modeling. *Int. J. Greenh. Gas Control* **2017**, *66* (October), 147–158. <https://doi.org/10.1016/j.ijggc.2017.09.020>.
- (161) Kudlak, B.; Owczarek, K.; Namieśnik, J. Selected Issues Related to the Toxicity of Ionic Liquids and Deep Eutectic Solvents—a Review. *Environ. Sci. Pollut. Res.* **2015**, *22* (16), 11975–11992. <https://doi.org/10.1007/s11356-015-4794-y>.
- (162) Dai, Y.; van Spronsen, J.; Witkamp, G. J.; Verpoorte, R.; Choi, Y. H. Natural Deep Eutectic Solvents as New Potential Media for Green Technology. *Anal. Chim. Acta* **2013**, *766*, 61–68. <https://doi.org/10.1016/j.aca.2012.12.019>.
- (163) Wen, Q.; Chen, J. X.; Tang, Y. L.; Wang, J.; Yang, Z. Assessing the Toxicity and Biodegradability of Deep Eutectic Solvents. *Chemosphere* **2015**, *132*, 63–69. <https://doi.org/10.1016/j.chemosphere.2015.02.061>.
- (164) Hayyan, M.; Hashim, M. A.; Al-Saadi, M. A.; Hayyan, A.; AlNashef, I. M.; Mirghani, M. E. S. Assessment of Cytotoxicity and Toxicity for Phosphonium-Based Deep Eutectic Solvents. *Chemosphere* **2013**, *93* (2), 455–459. <https://doi.org/10.1016/j.chemosphere.2013.05.013>.
- (165) Radošević, K.; Cvjetko Bubalo, M.; Gaurina Srček, V.; Grgas, D.; Landeka Dragičević, T.; Redovniković, R. I. Evaluation of Toxicity and Biodegradability of Choline Chloride Based Deep Eutectic Solvents. *Ecotoxicol. Environ. Saf.* **2015**, *112*, 46–53. <https://doi.org/10.1016/j.ecoenv.2014.09.034>.
- (166) Ullah, R.; Atilhan, M.; Anaya, B.; Khraisheh, M.; García, G.; Elkhattat, A.; Tariq, M.; Aparicio, S. A Detailed Study of Cholinium Chloride and Levulinic Acid Deep Eutectic Solvent System for CO₂capture via Experimental and Molecular Simulation Approaches. *Phys. Chem. Chem. Phys.* **2015**, *17* (32), 20941–

20960. <https://doi.org/10.1039/c5cp03364k>.

- (167) Altamash, T.; Atilhan, M.; Aliyan, A.; Ullah, R.; Nasser, M.; Aparicio, S. Rheological, Thermodynamic, and Gas Solubility Properties of Phenylacetic Acid-Based Deep Eutectic Solvents. *Chem. Eng. Technol.* **2017**, *40* (4), 778–790. <https://doi.org/10.1002/ceat.201600475>.
- (168) Eustaquio-Rincón, R.; Rebolledo-Libreros, M. E.; Trejo, A.; Molnar, R. Corrosion in Aqueous Solution of Two Alkanolamines with CO₂ and H₂S: N-Methyldiethanolamine + Diethanolamine at 393 K. *Ind. Eng. Chem. Res.* **2008**, *47* (14), 4726–4735. <https://doi.org/10.1021/ie071557r>.
- (169) Campbell, K. L. S.; Zhao, Y.; Hall, J. J.; Williams, D. R. The Effect of CO₂-Loaded Amine Solvents on the Corrosion of a Carbon Steel Stripper. *Int. J. Greenh. Gas Control* **2016**, *47*, 376–385. <https://doi.org/10.1016/j.ijggc.2016.02.011>.
- (170) Power, R.; North, P. CO₂ Capture and Storage VGB Report on the State of the Art PowerTech PowerTech. **2018**.
- (171) Kowsari, E.; Payami, M.; Amini, R.; Ramezanzadeh, B.; Javanbakht, M. Task-Specific Ionic Liquid as a New Green Inhibitor of Mild Steel Corrosion. *Appl. Surf. Sci.* **2014**, *289*, 478–486. <https://doi.org/10.1016/j.apsusc.2013.11.017>.
- (172) Tüken, T.; Demir, F.; Kicir, N.; Siğircik, G.; Erbil, M. Inhibition Effect of 1-Ethyl-3-Methylimidazolium Dicyanamide against Steel Corrosion. *Corros. Sci.* **2012**, *59*, 110–118. <https://doi.org/10.1016/j.corsci.2012.02.021>.
- (173) Zhang, Q. B.; Hua, Y. X. Corrosion Inhibition of Mild Steel by Alkylimidazolium Ionic Liquids in Hydrochloric Acid. *Electrochim. Acta* **2009**, *54* (6), 1881–1887. <https://doi.org/10.1016/j.electacta.2008.10.025>.
- (174) Abbott, A. P.; Ahmed, E. I.; Harris, R. C.; Ryder, K. S. Evaluating Water Miscible Deep Eutectic Solvents (DESS) and Ionic Liquids as Potential Lubricants. *Green Chem.* **2014**, *16* (9), 4156–4161. <https://doi.org/10.1039/c4gc00952e>.
- (175) Rodriguez Rodriguez, N.; Van Den Bruinhorst, A.; Kollau, L. J. B. M.; Kroon, M. C.; Binnemans, K. Degradation of Deep-Eutectic Solvents Based on Choline Chloride and Carboxylic Acids. *ACS Sustain. Chem. Eng.* **2019**, *7* (13), 11521–11528. <https://doi.org/10.1021/acssuschemeng.9b01378>.
- (176) Fernandez, L.; Silva, L. P.; Martins, M. A. R.; Ferreira, O.; Ortega, J.; Pinho, S. P.; Coutinho, J. A. P. Indirect Assessment of the Fusion Properties of Choline Chloride from Solid-Liquid Equilibria Data. *Fluid Phase Equilib.* **2017**, *448*, 9–14. <https://doi.org/10.1016/j.fluid.2017.03.015>.
- (177) Leron, R. B.; Li, M. H. High-Pressure Density Measurements for Choline Chloride: Urea Deep Eutectic Solvent and Its Aqueous Mixtures at T = (298.15 to 323.15) K and up to 50 MPa. *J. Chem. Thermodyn.* **2012**, *54*, 293–301.

<https://doi.org/10.1016/j.jct.2012.05.008>.

- (178) Yadav, A.; Pandey, S. Densities and Viscosities of (Choline Chloride + Urea) Deep Eutectic Solvent and Its Aqueous Mixtures in the Temperature Range 293.15 K to 363.15 K. *J. Chem. Eng. Data* **2014**, *59* (7), 2221–2229. <https://doi.org/10.1021/je5001796>.
- (179) Altamash, T.; Nasser, M. S.; Elhamarnah, Y.; Magzoub, M.; Ullah, R.; Qiblawey, H.; Aparicio, S.; Atilhan, M. Gas Solubility and Rheological Behavior Study of Betaine and Alanine Based Natural Deep Eutectic Solvents (NADES). *J. Mol. Liq.* **2018**, *256*, 286–295. <https://doi.org/10.1016/j.molliq.2018.02.049>.
- (180) Maham, Y.; Teng, T. T.; Hepler, L. G.; Mather, A. E. Densities, Excess Molar Volumes, and Partial Molar Volumes for Binary Mixtures of Water with Monoethanolamine, Diethanolamine, and Triethanolamine from 25 to 80°C. *J. Solution Chem.* **1994**, *23* (2), 195–205. <https://doi.org/10.1007/BF00973546>.
- (181) Rebolledo-Libreros, M. E.; Trejo, A. Density and Viscosity of Aqueous Blends of Three Alkanolamines: N-Methyldiethanolamine, Diethanolamine, and 2-Amino-2-Methyl-1-Propanol in the Range of (303 to 343) K. *J. Chem. Eng. Data* **2006**, *51* (2), 702–707. <https://doi.org/10.1021/je050462y>.
- (182) Welsh, L. M.; Davis, R. A. Density and Viscosity of Aqueous Blends of N-Methyldiethanolamine and 2-Amino-2-Methyl-1-Propanol. *J. Chem. Eng. Data* **1995**, *40* (1), 257–259. <https://doi.org/10.1021/je00017a055>.
- (183) Mirza, N.; Mumford, K.; Wu, Y.; Mazhar, S.; Kentish, S.; Stevens, G. Improved Eutectic Based Solvents for Capturing Carbon Dioxide (CO₂). *Energy Procedia* **2017**, *114* (November 2016), 827–833. <https://doi.org/10.1016/j.egypro.2017.03.1909>.
- (184) Xie, Y.; Dong, H.; Zhang, S.; Lu, X.; Ji, X. Effect of Water on the Density, Viscosity, and CO₂ Solubility in Choline Chloride / Urea. **2014**. <https://doi.org/10.1021/je500320c>.
- (185) Aroso, I. M.; Paiva, A.; Reis, R. L.; Duarte, A. R. C. Natural Deep Eutectic Solvents from Choline Chloride and Betaine – Physicochemical Properties. *J. Mol. Liq.* **2017**, *241*, 654–661. <https://doi.org/10.1016/j.molliq.2017.06.051>.
- (186) Arachchige, U. S. P. R.; Aryal, N.; Eimer, D. A.; Melaaen, M. C. Viscosities of Pure and Aqueous Solutions of Monoethanolamine (MEA), Diethanolamine (DEA) and N-Methyldiethanolamine (MDEA). *Annu. Trans. Nord. Rheol. Soc.* **2013**, *21*, 299–306.
- (187) Delgado-Mellado, N.; Larriba, M.; Navarro, P.; Rigual, V.; Ayuso, M.; García, J.; Rodríguez, F. Thermal Stability of Choline Chloride Deep Eutectic Solvents by TGA/FTIR-ATR Analysis. *J. Mol. Liq.* **2018**, *260*, 37–43. <https://doi.org/10.1016/j.molliq.2018.03.076>.
- (188) Kothandaraman, A. Carbon Dioxide Capture by Chemical Absorption: A

Solvent Comparison Study. *PhD thesis* **2010**, 144–184.

- (189) Aouini, I.; Ledoux, A.; Estel, L.; Mary, S. Pilot Plant Studies for CO₂ Capture from Waste Incinerator Flue Gas Using MEA Based Solvent. *Oil Gas Sci. Technol. – Rev. d'IFP Energies Nouv.* **2014**, *69* (6), 1091–1104. <https://doi.org/10.2516/ogst/2013205>.
- (190) Herzog, H.; Hatton, A. Advanced Post-Combustion CO₂ Capture Prepared for the Doris Duke Foundation. **2015**, No. January 2009.
- (191) Dugas, R.; Rochelle, G. Absorption and Desorption Rates of Carbon Dioxide with Monoethanolamine and Piperazine. *Energy Procedia* **2009**, *1* (1), 1163–1169. <https://doi.org/10.1016/j.egypro.2009.01.153>.
- (192) Hojniak. Highly Selective Separation of Carbon Dioxide from Nitrogen and Methane by Nitrile/Glycol-Difunctionalized Ionic Liquids in Supported Ionic Liquid Membranes (SILMs). *J. Phys. Chem. B* **2014**, *118* (26), 7440–7449. <https://doi.org/10.1021/jp503259b>.
- (193) Pereira, M. M.; Kurnia, K. A.; Sousa, F. L.; Silva, N. J. O.; Lopes-Da-Silva, J. A.; Coutinho, J. A. P.; Freire, M. G. Contact Angles and Wettability of Ionic Liquids on Polar and Non-Polar Surfaces. *Phys. Chem. Chem. Phys.* **2015**, *17* (47), 31653–31661. <https://doi.org/10.1039/c5cp05873b>.
- (194) Gao, L.; McCarthy, T. J. Ionic Liquids Are Useful Contact Angle Probe Fluids. *J. Am. Chem. Soc.* **2007**, *129* (13), 3804–3805. <https://doi.org/10.1021/ja070169d>.
- (195) Carrera, G. V. S. M.; Afonso, C. A. M.; Branco, L. C. Interfacial Properties, Densities, and Contact Angles of Task Specific Ionic Liquids. *J. Chem. Eng. Data* **2010**, *55* (2), 609–615. <https://doi.org/10.1021/je900502s>.
- (196) Blanco, D.; Viesca, J. L.; Mallada, M. T.; Ramajo, B.; González, R.; Battez, A. H. Wettability and Corrosion of [NTf₂] Anion-Based Ionic Liquids on Steel and PVD (TiN, CrN, ZrN) Coatings. *Surf. Coatings Technol.* **2016**, *302*, 13–21. <https://doi.org/10.1016/j.surfcoat.2016.05.051>.
- (197) Soriano, A. N.; Doma, B. T.; Li, M. Solubility of Carbon Dioxide in 1-Ethyl-3-Methylimidazolium Tetrafluoroborate. **2008**, 2550–2555.
- (198) Zhang, Q.; Yuan, H. Y.; Fukaya, N.; Yasuda, H.; Choi, J. C. Direct Synthesis of Carbamate from CO₂ using a Task-Specific Ionic Liquid Catalyst. *Green Chem.* **2017**, *19* (23), 5614–5624. <https://doi.org/10.1039/c7gc02666h>.
- (199) Zeng, S.; Zhang, X.; Bai, L.; Zhang, X.; Wang, H.; Wang, J.; Bao, D.; Li, M.; Liu, X.; Zhang, S. Ionic-Liquid-Based CO₂ Capture Systems: Structure, Interaction and Process. *Chem. Rev.* **2017**, *117* (14), 9625–9673. <https://doi.org/10.1021/acs.chemrev.7b00072>.
- (200) Akachuku, A.; Osei, P. A.; Decardi-Nelson, B.; Srisang, W.; Pouryousefi, F.;

- Ibrahim, H.; Idem, R. Experimental and Kinetic Study of the Catalytic Desorption of CO₂ from CO₂-Loaded Monoethanolamine (MEA) and Blended Monoethanolamine – Methyl-Diethanolamine (MEA-MDEA) Solutions. *Energy* **2019**, *179*, 475–489. <https://doi.org/10.1016/j.energy.2019.04.174>.
- (201) Deng, D.; Deng, X.; Duan, X.; Gong, L. Protic Guanidine Isothiocyanate plus Acetamide Deep Eutectic Solvents with Low Viscosity for Efficient NH₃ Capture and NH₃/CO₂ Separation. *J. Mol. Liq.* **2021**, *324*, 114719. <https://doi.org/10.1016/j.molliq.2020.114719>.
- (202) Yan, M.; Huan, Q.; Zhang, Y.; Fang, W.; Chen, F.; Pariatamby, A.; Kanchanapip, E.; Wibowo, H. Effect of Operating Parameters on CO₂ Capture from Biogas with Choline Chloride—Monoethanolamine Deep Eutectic Solvent and Its Aqueous Solution. *Biomass Convers. Biorefinery* **2022**, No. 0123456789. <https://doi.org/10.1007/s13399-021-02246-7>.
- (203) Marcus, Y. Gas Solubilities in Deep Eutectic Solvents. *Monatshefte fur Chemie* **2017**, *149* (2), 211–217. <https://doi.org/10.1007/s00706-017-2031-8>.
- (204) Maugeri, Z.; Domínguez De María, P. Novel Choline-Chloride-Based Deep-Eutectic-Solvents with Renewable Hydrogen Bond Donors: Levulinic Acid and Sugar-Based Polyols. *RSC Adv.* **2012**, *2* (2), 421–425. <https://doi.org/10.1039/c1ra00630d>.
- (205) Lu, M.; Han, G.; Jiang, Y.; Zhang, X.; Deng, D.; Ai, N. Solubilities of Carbon Dioxide in the Eutectic Mixture of Levulinic Acid (or Furfuryl Alcohol) and Choline Chloride. *J. Chem. Thermodyn.* **2015**, *88*, 72–77. <https://doi.org/10.1016/j.jct.2015.04.021>.
- (206) Li, G.; Deng, D.; Chen, Y.; Shan, H.; Ai, N. Solubilities and Thermodynamic Properties of CO₂ in Choline-Chloride Based Deep Eutectic Solvents. *J. Chem. Thermodyn.* **2014**, *75*, 58–62. <https://doi.org/10.1016/j.jct.2014.04.012>.
- (207) Li, X.; Hou, M.; Han, B.; Wang, X.; Zou, L. Solubility of CO₂ in a Choline Chloride + Urea Eutectic Mixture. **2008**, 548–550.
- (208) Pelaquim, F. P.; Marinho, A.; Neto, B.; Angela, I.; Dalmolin, L.; Conceic, M. Gas Solubility Using Deep Eutectic Solvents : Review and Analysis. *Am. Chem. Soc.* **2021**, *60* (8607–8620). <https://doi.org/10.1021/acs.iecr.1c00947>.
- (209) Gomes, C.; Influence, M. F. Influence of Water on the Carbon Dioxide Absorption by 1-Ethyl-3- Methylimidazolium Bis (Trifluoromethylsulfonyl) Amide. *Fluid Phase Equilib.* **2010**, *294* (1–2), 98–104. <https://doi.org/10.1016/j.fluid.2010.02.021>.
- (210) Goodrich, B. F.; Fuente, J. C. De; Gurkan, B. E.; Lopez, Z. K.; Price, E. A.; Huang, Y.; Brennecke, J. F. Effect of Water and Temperature on Absorption of CO₂ by Amine-Functionalized Anion-Tethered Ionic Liquids. **2011**, 9140–9150. <https://doi.org/10.1021/jp2015534>.

- (211) Crespo, E. A.; Costa, J. M. L.; Palma, A. M.; Soares, B.; Martín, M. C.; Segovia, J. J.; Carvalho, P. J.; Coutinho, J. A. P. Thermodynamic Characterization of Deep Eutectic Solvents at High Pressures. *Fluid Phase Equilib.* **2019**. <https://doi.org/10.1016/j.fluid.2019.112249>.
- (212) Li, G.; Jiang, Y.; Liu, X.; Deng, D. New Levulinic Acid-Based Deep Eutectic Solvents: Synthesis and Physicochemical Property Determination. *J. Mol. Liq.* **2016**. <https://doi.org/10.1016/j.molliq.2016.07.039>.
- (213) Lu, M.; Han, G.; Jiang, Y.; Zhang, X.; Deng, D.; Ai, N. Solubilities of Carbon Dioxide in the Eutectic Mixture of Levulinic Acid (or Furfuryl Alcohol) and Choline Chloride. *J. Chem. Thermodyn.* **2015**, *88*, 72–77. <https://doi.org/10.1016/j.jct.2015.04.021>.
- (214) Martins, M. A. R.; Pinho, S. P.; Coutinho, J. A. P. Insights into the Nature of Eutectic and Deep Eutectic Mixtures. *J. Solution Chem.* **2018**, No. October. <https://doi.org/10.1007/s10953-018-0793-1>.
- (215) Florindo, C.; Oliveira, F. S.; Rebelo, L. P. N.; Fernandes, A. M.; Marrucho, I. M. Insights into the Synthesis and Properties of Deep Eutectic Solvents Based on Cholinium Chloride and Carboxylic Acids. *ACS Sustain. Chem. Eng.* **2014**, *2* (10), 2416–2425. <https://doi.org/10.1021/sc500439w>.
- (216) Abranches, D. O.; Larriba, M.; Silva, L. P.; Melle-franco, M.; José, F.; Pinho, S. P.; Coutinho, J. A. P. Using COSMO-RS to Design Choline Chloride Pharmaceutical Eutectic Solvents. 1–9.
- (217) Coutinho, J. A. P.; Andersen, S. I.; Stenby, E. H. Evaluation of Activity Coefficient Models in Prediction of Alkane Solid-Liquid Equilibria. *Fluid Phase Equilib.* **1995**, *103* (1), 23–39. [https://doi.org/10.1016/0378-3812\(94\)02600-6](https://doi.org/10.1016/0378-3812(94)02600-6).
- (218) Ghaedi, H.; Ayoub, M.; Sufian, S.; Lal, B.; Uemura, Y. Thermal Stability and FT-IR Analysis of Phosphonium-Based Deep Eutectic Solvents with Different Hydrogen Bond Donors. *J. Mol. Liq.* **2017**, *242*, 395–403. <https://doi.org/10.1016/j.molliq.2017.07.016>.
- (219) Alomar, M. K.; Hayyan, M.; Alsaadi, M. A.; Akib, S.; Hayyan, A.; Hashim, M. A. Glycerol-Based Deep Eutectic Solvents: Physical Properties. *J. Mol. Liq.* **2016**, *215*, 98–103. <https://doi.org/10.1016/j.molliq.2015.11.032>.
- (220) Aboshatta, M.; Magueijo, V. A Comprehensive Study of CO₂ Absorption and Desorption by Choline-Chloride/Levulinic-Acid-Based Deep Eutectic Solvents. *Mol. MDPI* **2021**, *26* (5595).
- (221) ASTM Standard G-31. Standard Practice for Laboratory Immersion Corrosion Testing of Metals, Annual Book of ASTM Standards. *ASTM Int. West Conshohocken, USA.* **1999**, 3.02 (Reapproved), 101.
- (222) Metal4u. *Chemical Composition of DC01-CR4.* <https://www.metals4u.co.uk/blog/en8-mild-steel> (accessed 2019-03-01).

- (223) ASTM International. Standard Practice for Preparing , Cleaning , and Evaluating Corrosion Test. *Significance* **2017**, *90* (Reapproved 2011), 1–9. <https://doi.org/10.1520/G0001-03R11.2>.
- (224) Cotroneo-figueroa, V. P.; Aravena, P.; Vesovic, V.; Canales, R. I. Viscosity of Choline Chloride-Based Deep Eutectic Solvents : Experiments and Modeling. *J. Chem. Eng. Data* **2020**, *65* (5581–5592). <https://doi.org/10.1021/acs.jced.0c00715>.
- (225) Agieienko, V.; Buchner, R. A Comprehensive Study of Density, Viscosity, and Electrical Conductivity of (Choline Chloride + Glycerol) Deep Eutectic Solvent and Its Mixtures with Dimethyl Sulfoxide. *J. Chem. Eng. Data* **2021**, *66*, 780–792. <https://doi.org/10.1021/acs.jced.0c00869>.
- (226) Haider, M. B.; Jha, D.; Marriyappan Sivagnanam, B.; Kumar, R. Modelling and Simulation of CO₂ Removal from Shale Gas Using Deep Eutectic Solvents. *J. Environ. Chem. Eng.* **2019**, *7* (1), 102747. <https://doi.org/10.1016/j.jece.2018.10.061>.
- (227) Lin, C. M.; Leron, R. B.; Caparanga, A. R.; Li, M. H. Henry's Constant of Carbon Dioxide-Aqueous Deep Eutectic Solvent (Choline Chloride/Ethylene Glycol, Choline Chloride/Glycerol, Choline Chloride/Malonic Acid) Systems. *J. Chem. Thermodyn.* **2014**, *68*, 216–220. <https://doi.org/10.1016/j.jct.2013.08.029>.
- (228) Pashaei, H.; Ghaemi, A.; Nasiri, M. Modeling and Experimental Study on the Solubility and Mass Transfer of CO₂ into Aqueous DEA Solution Using a Stirrer Bubble Column. *RSC Adv.* **2016**, *6* (109), 108075–108092. <https://doi.org/10.1039/c6ra22589f>.
- (229) Kim, Y. E.; Lim, J. A.; Jeong, S. K.; Yoon, Y. Il; Bae, S. T.; Nam, S. C. Comparison of Carbon Dioxide Absorption in Aqueous MEA, DEA, TEA, and AMP Solutions. *Bull. Korean Chem. Soc.* **2013**, *34* (3), 783–787. <https://doi.org/10.5012/bkcs.2013.34.3.783>.
- (230) Pashaei, H.; Zarandi, M. N.; Ghaemi, A. Experimental Study and Modeling of CO₂ Absorption into Diethanolamine Solutions Using Stirrer Bubble Column. *Chem. Eng. Res. Des.* **2017**, *121*, 32–43. <https://doi.org/10.1016/j.cherd.2017.03.001>.
- (231) Chen, Y.; Han, X.; Liu, Z.; Yu, D.; Guo, W.; Mu, T. Capture of Toxic Gases by Deep Eutectic Solvents. *ACS Sustain. Chem. Eng.* **2020**, *8* (14), 5410–5430. <https://doi.org/10.1021/acssuschemeng.0c01493>.
- (232) Liu, F.; Chen, W.; Mi, J.; Xun, J. Z.; Kuan, F. Z.; Zheng, H. A.; Jiang, L. Thermodynamic and Molecular Insights into the Absorption of H₂S, CO₂, and CH₄ in Choline Chloride plus Urea Mixtures. **2019**, No. September 2018, 1–10. <https://doi.org/10.1002/aic.16574>.
- (233) Deng, D.; Deng, X.; Duan, X.; Gong, L. Protic Guanidine Isothiocyanate plus Acetamide Deep Eutectic Solvents with Low Viscosity for Efficient NH₃ Capture

and NH₃/CO₂ Separation. *J. Mol. Liq.* **2020**, *324*, 114719. <https://doi.org/10.1016/j.molliq.2020.114719>.

- (234) Wu, S. H.; Caparanga, A. R.; Leron, R. B.; Li, M. H. Vapor Pressure of Aqueous Choline Chloride-Based Deep Eutectic Solvents (Ethaline, Glyceline, Maline and Reline) at 30-70 °c. *Thermochim. Acta* **2012**, *544*, 1–5. <https://doi.org/10.1016/j.tca.2012.05.031>.
- (235) Swinehart, D. F. The Beer-Lambert Law. *J. Chem. Educ.* **1962**, *39* (7), 333–335. <https://doi.org/10.1021/ed039p333>.
- (236) Lee, J. I.; Otto, F. D.; Mather, A. E. Equilibrium Between Carbon Dioxide and Aqueous Monoethanolamine Solutions. *J Appl Chem Biotechnol* **1976**, *26* (10), 541–549. <https://doi.org/10.1002/jctb.5020260177>.
- (237) Akachuku, A.; Osei, P. A.; Decardi-Nelson, B.; Srisang, W.; Pouryousefi, F.; Ibrahim, H.; Idem, R. Experimental and Kinetic Study of the Catalytic Desorption of CO₂ from CO₂-Loaded Monoethanolamine (MEA) and Blended Monoethanolamine – Methyl-Diethanolamine (MEA-MDEA) Solutions. *Energy* **2019**. <https://doi.org/10.1016/j.energy.2019.04.174>.
- (238) Chen, Y.; Ai, N.; Li, G.; Shan, H.; Cui, Y.; Deng, D. Solubilities of Carbon Dioxide in Eutectic Mixtures of Choline Chloride and Dihydric Alcohols. *J. Chem. Eng. Data* **2014**, *59* (4), 1247–1253. <https://doi.org/10.1021/je400884v>.
- (239) Kierzkowska-Pawlak, H.; Sobala, K. Heat of Absorption of CO₂ in Aqueous Solutions of DEEA and DEEA + MAPA Blends—A New Approach to Measurement Methodology. *Int. J. Greenh. Gas Control* **2020**, *100* (July), 103102. <https://doi.org/10.1016/j.ijggc.2020.103102>.
- (240) Smith, J. M.; Van Ness, H. C.; Abbott, M. M.; Swihart, M. T. *Introduction To Chemical Engineering Thermodynamics Eighth Edition*; 2018.
- (241) Luis, P. Use of Monoethanolamine (MEA) for CO₂ Capture in a Global Scenario: Consequences and Alternatives. *Desalination* **2016**, *380*, 93–99. <https://doi.org/10.1016/j.desal.2015.08.004>.
- (242) Moiola, S.; Pellegrini, L. A. Regeneration Section of CO₂ Capture Plant by MEA Scrubbing with a Rate-Based Model. *Chem. Eng. Trans.* **2013**, *32*, 1849–1854. <https://doi.org/10.3303/CET1332309>.
- (243) Fan, W.; Liu, Y.; Wang, K. Detailed Experimental Study on the Performance of Monoethanolamine, Diethanolamine, and Diethylenetriamine at Absorption/Regeneration Conditions. *J. Clean. Prod.* **2016**, *125*, 296–308. <https://doi.org/10.1016/j.jclepro.2016.03.144>.
- (244) Blauwhoff, P. M. M.; Van Swaaij, W. P. M. Selective Absorption of Hydrogen Sulfide from Natural Gas. *I2 - Procestechol.* **1986**, *No. 7-8*, 13–18.
- (245) Wang, X.; Song, C. Carbon Capture From Flue Gas and the Atmosphere: A

Perspective. *Front. Energy Res.* **2020**, 8 (December 2019).
<https://doi.org/10.3389/fenrg.2020.560849>.

- (246) Jacquemin, J.; Costa Gomes, M. F.; Husson, P.; Majer, V. Solubility of Carbon Dioxide, Ethane, Methane, Oxygen, Nitrogen, Hydrogen, Argon, and Carbon Monoxide in 1-Butyl-3-Methylimidazolium Tetrafluoroborate between Temperatures 283 K and 343 K and at Pressures Close to Atmospheric. *J. Chem. Thermodyn.* **2006**, 38 (4), 490–502. <https://doi.org/10.1016/j.jct.2005.07.002>.
- (247) Jacquemin, J.; Husson, P.; Majer, V.; Gomes, M. F. C. Low-Pressure Solubilities and Thermodynamics of Solvation of Eight Gases in 1-Butyl-3-Methylimidazolium Hexafluorophosphate. *Fluid Phase Equilib.* **2006**, 240 (1), 87–95. <https://doi.org/10.1016/j.fluid.2005.12.003>.
- (248) Ali, E.; Hadj-Kali, M. K.; Mulyono, S.; Alnashef, I.; Fakeeha, A.; Mjalli, F.; Hayyan, A. Solubility of CO₂ in Deep Eutectic Solvents: Experiments and Modelling Using the Peng-Robinson Equation of State. *Chem. Eng. Res. Des.* **2014**, 92 (10), 1898–1906. <https://doi.org/10.1016/j.cherd.2014.02.004>.
- (249) Wang, L.; Liu, S.; Wang, R.; Li, Q.; Zhang, S. Regulating Phase Separation Behavior of a DEEA – TETA Biphasic Solvent Using Sulfolane for Energy-Saving CO₂ Capture. *Environ. Sci. Technol* **2019**, 53, 12873–12881. <https://doi.org/10.1021/acs.est.9b02787>.
- (250) Jiang, C.; Chen, H.; Wang, J.; Shen, Y.; Ye, J.; Zhang, S.; Wang, L.; Chen, J. Phase Splitting Agent Regulated Biphasic Solvent for Efficient CO₂ Capture with a Low Heat Duty. *Environ. Sci. Technol.* **2020**, 54, 7601–7610. <https://doi.org/10.1021/acs.est.9b07923>.
- (251) Kim, H.; Hwang, S. J.; Lee, K. S. Novel Shortcut Estimation Method for Regeneration Energy of Amine Solvents in an Absorption-Based Carbon Capture Process. *Environ. Sci. Technol.* **2015**, 49, 1478–1485. <https://doi.org/10.1021/es504684x>.
- (252) Wang, B.; Sui, J.; Yu, B.; Yuan, C.; Guo, L.; El-aty, A. M. A. Phase Behavior of Aqueous Solutions of Ethaline Deep Eutectic Solvent. *Carbohydr. Polym.* **2020**, No. 304, 117314.
- (253) Morrison, H. G.; Sun, C. C.; Neervannan, S. Characterization of Thermal Behavior of Deep Eutectic Solvents and Their Potential as Drug Solubilization Vehicles. *Int. J. Pharm.* **2009**, 378, 136–139. <https://doi.org/10.1016/j.ijpharm.2009.05.039>.
- (254) Florindo, C.; Fernandes, A. M.; Marrucho, I. M. Insights into the Synthesis and Properties of Deep Eutectic Solvents Based on Cholinium Chloride and Carboxylic Acids. *ACS Sustain. Chem. Eng.* **2014**, 2 (2014), 2416–2425. <https://doi.org/10.1021/sc500439w>.
- (255) Li, Z.; Wang, L.; Li, C.; Cui, Y.; Li, S.; Yang, G.; Shen, Y. Absorption of Carbon

Dioxide Using Ethanolamine-Based Deep Eutectic Solvents. *ACS Sustain. Chem. Eng.* **2019**, *7* (2019), 10403–10414. <https://doi.org/10.1021/acssuschemeng.9b00555>.

- (256) Smith, E. L.; Abbott, A. P.; Ryder, K. S. Deep Eutectic Solvents (DESs) and Their Applications. *Chem. Rev.* **2014**, *114* (21), 11060–11082. <https://doi.org/10.1021/cr300162p>.
- (257) Finkbeiner, M.; Inaba, A.; Tan, R. B. H.; Christiansen, K.; Klüppel, H. The New International Standards for Life Cycle Assessment : ISO 14040 and ISO 14044. *Commentaries* **2006**, *11* (2), 80–85.
- (258) Finkbeiner, M. The International Standards as the Constitution of Life Cycle Assessment: The ISO 14040 Series and Its Offspring. In *Background and Future Prospects in Life Cycle Assessment*; Klöpffer, W., Ed.; Springer Netherlands: Dordrecht, 2014; pp 85–106. https://doi.org/10.1007/978-94-017-8697-3_3.
- (259) Fytianos, G.; Ucar, S.; Grimstvedt, A.; Hyldbakk, A.; Svendsen, H. F.; Knuutila, H. K. International Journal of Greenhouse Gas Control Corrosion and Degradation in MEA Based Post-Combustion CO₂ Capture. *Int. J. Greenh. Gas Control* **2016**, *46*, 48–56. <https://doi.org/10.1016/j.ijggc.2015.12.028>.
- (260) Tanaka, M.; Girard, G.; Davis, R.; Peuto, A. Recommended Table for the Density of Water between 0 ° C and 40 ° C Based on Recent Experimental Reports. *Metrologia* **2001**, *38* (301).
- (261) Engineering ToolBox. *Water - Density, Specific Weight and Thermal Expansion Coefficients*. Online. https://www.engineeringtoolbox.com/water-density-specific-weight-d_595.html.
- (262) (CDIAC), C. D. I. A. C. Calculation of the Fugacity of Carbon Dioxide in the Pure Gas or in Air. *Carbon Dioxide Inf. Anal. Cent.* **1997**, No. 3, 1–5.